

MOUNTAIN-PLAINS CONSORTIUM

MPC 20-423 | D. Turner, J. van de Lindt, and B. Senior

Reducing Flood
Vulnerability of
Communities with Limited
Road Access by Optimizing
Bridge Elevation



A University Transportation Center sponsored by the U.S. Department of Transportation serving the Mountain-Plains Region. Consortium members:

Colorado State University
North Dakota State University
South Dakota State University

University of Colorado Denver
University of Denver
University of Utah

Utah State University
University of Wyoming

Reducing Flood Vulnerability of Communities with Limited Road Access by Optimizing Bridge Elevation

David Turner

John W. van de Lindt

Bolivar Senior

Civil & Environmental Engineering
Colorado State University
Fort Collins, CO

October 2020

Acknowledgements

I would like to thank Dr. van de Lindt and Dr. Senior for giving me the opportunity to work on this project. This thesis would not have been possible without the help and guidance of my advisor and co-advisor. Thank you to my thesis committee member, Dr. Atadero, for your time and support, which played an essential role in the success of this project and my master's degree.

Bob Jarrett is appreciated for his time and for helping me understand the hydrology aspect of my thesis. The author is also thankful to Steven Griffin for providing the construction drawings and helping define a criterion for elevation adjustments.

The utmost appreciation is given to Mohammad Amini. I would not have made it without his help and support. Last but not least, I would like to thank my parents for their encouragement throughout this project.

Disclaimer

The contents of this report reflect the views of the authors, who are responsible for the facts and accuracy of the data presented herein. The contents do not necessarily reflect the official views of the Mountain Plains Consortium. This report does not constitute a standard, specification, or regulation. Any information contained herein should be used at the users own risk.

NDSU does not discriminate in its programs and activities on the basis of age, color, gender expression/identity, genetic information, marital status, national origin, participation in lawful off-campus activity, physical or mental disability, pregnancy, public assistance status, race, religion, sex, sexual orientation, spousal relationship to current employee, or veteran status, as applicable. Direct inquiries to: Vice Provost, Title IX/ADA Coordinator, Old Main 201, 701-231-7708, ndsueoaa@ndsu.edu.

ABSTRACT

On September 11-17, 2013, Colorado suffered devastating and widespread flash flooding over 150 miles from Colorado Springs north to Fort Collins, impacting 24 counties. The flood damaged several bridges and over 400 miles of state roads. As a result of the transportation damage, residents of Drake, Colorado, were isolated and had to be evacuated via helicopter. This thesis aims to determine the failure risk associated with the inundation of bridge superstructures.

A linear network of eight bridges near Drake, Colorado, was selected for analysis, which includes three unique structural configurations. Flood analysis was performed using the design equations presented by Kerenyi et al. (2009), which follows the same equation format listed in AASHTO. Fragilities were developed for the most critical internal and external composite girders for each bridge. The results obtained from fragility analysis were then used to determine the elevation adjustments needed to reach a target beta value of 3.5. Based on the analysis conducted in this thesis, it was found that the forces associated with bridge deck inundation, more specifically, in fast-moving mountain rivers is substantial and must be considered in design. Currently, bridge superstructures are designed based on the 100-year flood, which in the case of the bridges in this study, would not have resulted in any inundation of the bridge deck at the time of construction based on the knowledge at that time. To counter this, bridge superstructures should be designed based on the 500-year flood, which would incorporate inundation forces in the initial design. The methodology presented in this thesis can be used to assess and improve the flood vulnerability for any communities' bridge network.

TABLE OF CONTENTS

1. INTRODUCTION.....	1
1.1 Literature Review	5
2. FRAGILITY MODELING	11
2.1 Fragility Analysis	11
2.2 Limit States.....	12
2.3 Resistance Statistics.....	13
2.4 Hydraulic Modeling.....	14
2.5 Flood Frequency Analysis	18
2.6 Finite Element Modeling	21
2.7 Procedure	25
3. RESULTS AND DISCUSSION	27
3.1 Bridge C-15-AM results	27
3.2 Bridge C-15-AL results	36
3.3 Bridge C-15-O results.....	44
3.4 Bridge C-15-U results.....	51
3.5 Bridge C-15-Y results.....	58
3.6 Bridge C-15-C results	64
3.7 Bridge C-15-AN results	69
3.8 Bridge C-16-DI Results	75
4. CONCLUSIONS, CONTRIBUTIONS AND RECOMMENDATIONS	82
REFERENCES.....	85
APPENDIX A. CONSTRUCTION DRAWINGS	87
APPENDIX B. LOGNORMAL PARAMETERS FOR NEGATIVE MOMENT FRAGILITIES..	143

LIST OF TABLES

Table 1.1	Estimate of September 2013 peak discharge return interval (Generated from Jacobs, 2014)	2
Table 1.2	Reliability index and probability of failure values	10
Table 2.1	Statistical information for the variables used in the monte carlo simulation	13
Table 2.2	Log Pearson type III distribution fitted parameters used for the hazard probabilities.....	19

LIST OF FIGURES

Figure 1.1	Precipitable water data from the weather balloon in Denver as collected from 1948-2012 ..3
Figure 1.2	Topography the Big Thompson Canyon with elevations ranging from 8100-7150 feet located slightly downstream from Estes Park at bridge C-15-AM 4
Figure 1.3	Plan view of the Big Thompson canyon with bridges and other key features labeled..... 4
Figure 1.4	Scaled six-girder bridge deck used in the development of the force coefficients with the dimensions and forces labeled (Kerenyi et al. 2009) 6
Figure 1.5	Drag coefficient vs. inundation ratio for the six-girder bridge (Kerenyi et al. 2009) 7
Figure 1.6	Lift coefficient vs. inundation ratio for the six-girder bridge (Kerenyi et al. 2009) 8
Figure 1.7	Moment coefficient vs. inundation ratio for the six-girder bridge (Kerenyi et al. 2009)..... 8
Figure 1.8	An example of the applied net lift force on the bridge superstructures 15
Figure 1.9	Failure locations for the girders in this study..... 15
Figure 2.1	Example fragilities for illustration 12
Figure 2.2	Nominal moment capacity for an external girder for bridge C-15-Y..... 14
Figure 2.3	Cross section locations at a bridge (excerpted from Brunner, 2010).. 15
Figure 2.4	Geometric data plan view of HEC-RAS model for bridge C-15-AM..... 16
Figure 2.5	An example of the cross sections pulled from ArcMap with LiDAR data obtained from Colorado GeoData at bridge C-15-AM 17
Figure 2.6	The profile graph of the elevation data pulled from cross section 1 (the furthest right line on Figure 2.4.3) 17
Figure 2.7	Applied negative moment for an external girder on bridge C-15-Y 20
Figure 2.8	Peak discharge profile for the Big Thompson River (Excerpted from Jacobs, 2014)..... 21
Figure 2.9	Shell stresses for the modeling procedure check 22
Figure 2.10	Labeled example of SAP2000 elements used 23
Figure 2.11	Extruded view of bridge C-15-Y under the loading for $h^*=0.3$ 24
Figure 2.12	Negative plastic moment capacity for an internal girder on bridge C-15-C 24
Figure 2.13	Flow chart of the procedure followed for calculating the beta values 26
Figure 3.1	Longitudinal view of C-15-AM (CDOT see Appendix A) 27
Figure 3.2	Cross sectional view of C-15-AM (CDOT see Appendix A) 27
Figure 3.3	Typical integral abutment layout (CDOT see Appendix A) 28
Figure 3.4	Cross sections generated in ArcMap for C-15-AM 29
Figure 3.5	HEC-RAS geometric plan view for C-15-AM..... 29
Figure 3.6	Plan rating curve for C-15-AM (CDOT see Appendix A)..... 30
Figure 3.7	HEC-RAS generated rating curve for C-15-AM..... 30
Figure 3.8	SAP2000 model for C-15-AM..... 31
Figure 3.9	Plan view of C-15-AM (CDOT see Appendix A)..... 31
Figure 3.10	Applied negative moment felt by girder G7 for C-15-AM 32
Figure 3.11	Negative nominal moment capacity for an external girder for C-15-AM..... 33
Figure 3.12	Fitted lognormal CDF function to the fragility values for C-15-AM..... 34
Figure 3.13	Hazard probabilities used to generate the probability of failure curve for C-15-AM 35
Figure 3.14	Probability of failure curve for C-15-AM 36
Figure 3.15	Longitudinal section of C-15-AL (CDOT see Appendix A)..... 37
Figure 3.16	Cross sections generated in ArcMap for C-15-AL..... 37

Figure 3.17	HEC-RAS geometric plan view for C-15-AL.....	38
Figure 3.18	HEC-RAS rating curve for C-15-AL	39
Figure 3.19	SAP2000 model for C-15-AL	39
Figure 3.20	Plan view of the bridge deck for C-15-AL (CDOT see Appendix A)	40
Figure 3.21	Applied negative moment felt by girder G1 for C-15-AL	40
Figure 3.22	Negative nominal moment capacity for an external girder for C-15-AL.....	41
Figure 3.23	Fitted lognormal CDF function to the fragility values for C-15-AL.....	42
Figure 3.24	Hazard probabilities used to generate the probability of failure curve for C-15-AL	43
Figure 3.25	Probability of failure values for C-15-AL.....	43
Figure 3.26	Cross sections generated in ArcMap for C-15-O	44
Figure 3.27	HEC-RAS geometric plan view for C-15-O	45
Figure 3.28	Plan rating curve for C-15-O (CDOT see Appendix A)	46
Figure 3.29	HEC-RAS rating curve for C-15-O.....	46
Figure 3.30	SAP2000 model for C-15-O.....	47
Figure 3.31	Plan view of the bridge deck of C-15-O (CDOT see Appendix A)	47
Figure 3.32	Applied negative moment felt by G1 span 2 for C-15-O.....	48
Figure 3.33	Negative nominal moment capacity for an external girder for C-15-AL.....	49
Figure 3.34	Fitted lognormal CDF function to the fragility values for C-15-AM.....	49
Figure 3.35	Hazard probabilities used to generate the probability of failure curve for C-15-O.....	50
Figure 3.36	Probability of failure values for C-15-O	51
Figure 3.37	Cross sections generated in ArcMap for C-15-U	52
Figure 3.38	HEC-RAS geometric plan view for C-15-U	52
Figure 3.39	Plan rating curve for C-15-U (CDOT see Appendix A)	53
Figure 3.40	HEC-RAS rating curve for C-15-U.....	53
Figure 3.41	AP2000 model for C-15-U.....	54
Figure 3.42	Plan view of the bridge deck of C-15-U (CDOT see Appendix A)	54
Figure 3.43	Applied negative moment felt by G1 for C-15-U	55
Figure 3.44	Negative nominal moment capacity for an external girder for C-15-U	56
Figure 3.45	Fitted lognormal CDF function to the fragility values for C-15-U	56
Figure 3.46	Hazard probabilities used to generate the probability of failure curve for C-15-U.....	57
Figure 3.47	Probability of failure values for C-15-U	57
Figure 3.48	Cross sections generated in ArcMap for C-15-Y	58
Figure 3.49	HES-RAS geometric plan view for C-15-Y.....	59
Figure 3.50	Plan rating curve for C-15-Y (CDOT see Appendix A)	60
Figure 3.51	HEC-RAS rating curve for C-15-Y.....	60
Figure 3.52	SAP2000 model for C-15-Y.....	61
Figure 3.53	Plan view of the bridge deck of C-15-Y (CDOT see Appendix A)	61
Figure 3.54	Applied negative moment felt by G1/4 for C-15-Y	61
Figure 3.55	Negative nominal moment capacity for an external girder for C-15-Y	62
Figure 3.56	Fitted lognormal CDF function to the fragility values for C-15-Y	62
Figure 3.57	Hazard probabilities used to generate the probability of failure curve for C-15-Y.....	63
Figure 3.58	Probability of failure values for C-15-Y	63
Figure 3.59	Cross sections generated in ArcMap for C-15- C	64
Figure 3.60	HEC-RAS geometric plan view for C-15- C	65

Figure 3.61	HEC-RAS rating curve for C-15- C.....	65
Figure 3.62	SAP2000 model for C-15- C.....	66
Figure 3.63	Plan view of the bridge deck of C-15- C (CDOT see Appendix A)	66
Figure 3.64	Applied negative moment felt by G6 for C-15- C	67
Figure 3.65	Negative nominal moment capacity for an external girder for C-15- C	67
Figure 3.66	Fitted lognormal CDF function to the fragility values for C-15- C	68
Figure 3.67	Hazard probabilities used to generate the probability of failure curve for C-15- C.....	68
Figure 3.68	Probability of failure values for C-15- C	69
Figure 3.69	Cross sections generated in ArcMap for C-15- AN	70
Figure 3.70	HEC-RAS geometric plan view for C-15- AN	70
Figure 3.71	Plan rating curve for C-15- AN (CDOT see Appendix A).....	71
Figure 3.72	HEC-RAS rating curve for C-15- AN.....	71
Figure 3.73	SAP2000 model for C-15- AN.....	72
Figure 3.74	Plan view of the bridge deck of C-15- AN (CDOT see Appendix A)	72
Figure 3.75	Applied negative moment felt by G1 for C-15- AN	73
Figure 3.76	Negative nominal moment capacity for an external girder for C-15- AN	73
Figure 3.77	Fitted lognormal CDF function to the fragility values for C-15- AN	74
Figure 3.78	Hazard probabilities used to generate the probability of failure curve for C-15- AN.....	74
Figure 3.79	Probability of failure values for C-15- AN	75
Figure 3.80	Cross sections generated in ArcMap for C-16-DI.....	76
Figure 3.81	HEC-RAS rating curve for C-16-DI	76
Figure 3.82	Plan rating curve for C-16-DI (CDOT see Appendix A)	77
Figure 3.83	HEC-RAS rating curve for C-16-DI	77
Figure 3.84	SAP2000 model for C-16-DI	78
Figure 3.85	Plan view of the bridge deck of C-16-DI (CDOT see Appendix A).....	78
Figure 3.86	Applied negative moment felt by G6 span 2 for C-16-DI.....	79
Figure 3.87	Negative nominal moment capacity for an external girder for C-16-DI.....	79
Figure 3.88	Fitted lognormal CDF function to the fragility values for C-16-DI.....	80
Figure 3.89	Hazard probabilities used to generate the probability of failure curve for C-16-DI	80
Figure 3.90	Probability of failure values for C-16-DI.....	81
Figure 4.1	100 year flood beta values for all bridges	82
Figure 4.2	500 year flood beta values for all bridges	83

LIST OF SYMBOLS

A_{ps}	Area of prestressing steel
A_s	Area of mild steel
C_D	Drag coefficient
C_L	Lift coefficient
C_M	Moment coefficient
F_B	Buoyancy force
f'_c	Compressive strength of concrete
F_D	Drag force
F_L	Lift force
f_{ps}	yield stress of prestressing steel
f_y	yield stress of mild steel
g	gravity
h^*	Inundation ratio
M_{CG}	Moment about the center of gravity
R_n	Nominal capacity of a member
s	Deck thickness
W	Width of the bridge deck
V	Velocity
Vol_{dis}	Displaced volume of water
ρ	Density of water
ϕ	Resistance factor that takes into account material strength variability
γ	Load factor that takes into account the uncertainties in the load
$\Phi(.)$	Standard normal cumulative distribution function
λ_R	Logarithmic mean of capacity R
ξ_R	Logarithmic standard deviation of capacity R

1. INTRODUCTION

During September 11–17, 2013, Colorado suffered devastating and widespread flash flooding, which spread 150 miles from Colorado Springs north to Fort Collins, impacting 24 counties. The flooding resulted in considerable erosion, realigning of stream channels, transport of rock and debris, failures of dams and impact to several residential and commercial structures (Jacobs, 2014). High-velocity floodwater resulted in 10 lives lost (Jacobs, 2014) and more than 18,000 people evacuated (Ulccellini, 2014). Approximately 19,000 homes and commercial buildings were damaged and more than 1,500 destroyed (Ulccellini, 2014). Also, an estimated 485 miles of roads and 50 bridges were damaged or destroyed in the impacted counties (Ulccellini, 2014).

The focus of this thesis is on the community of Drake, Colorado, located in Larimer County with a population of a little more than 1,000 people. Drake is located in the Big Thompson Canyon west of Loveland, Colorado. This flood isolated the community due to copious road and bridge damage along US 34 and County Road 43. As a result of the damage, the residents had to be evacuated via helicopter. This scenario led to the current research, focusing on what would be required to make the bridges along US 34 from Estes Park to the mouth of the canyon more resistant to flood damage, thereby improving the resiliency of Drake. The concept and approach used herein is focused on a specific community but could be applied to other similar small communities that rely on bridges in a series system.

The most recent flood frequency analysis for the Big Thompson River was completed in August 2014 by Jacobs Engineering Group. Based on the drainage basin characteristics, rainfall amounts and intensities measured during the storm, the discharge estimates provided by Jacobs are greater than expected (Jacobs, 2014). This post assessment by Jacobs and field observations by Bob Jarrett led to the conclusion that dam failures, which include woody debris dams, road-embankments, beaver dams, stock ponds, and landslides played a large role in the September 2013 flood (Jacobs, 2014). This assessment was verified by post-flood aerial imagery. The images showed evidence of dam failures, mostly from debris flow, but there were also signs of releasing of groundwater caused by landslides (Jacobs, 2014).

The Intergovernmental Panel on Climate Change (IPCC) found that the intensity of rain events, specifically the proportion of total precipitation that falls during lower probability events, has increased, and it is plausible that the proportion will continue to rise in the future (Solomon et al. 2007). The IPCC concluded that higher precipitation intensity could also increase the risk of flooding (Parry et al. 2007). In 1981, effective regulatory flow rates documented by the Federal Emergency Management Agency (FEMA) in the 2013 Flood Insurance Study (FIS) were developed (Jacobs, 2014). These discharges were used for Larimer County to designate the 100-year floodplain and informed bridge construction decisions. A 100-year event is described as having a 1 in 100 or 1% chance of occurring in any given year. The most recent hydrologic evaluation of the Big Thompson watershed, completed in August 2014, produced larger discharges for the 100- and 500-year flood on the order of 1,400 to 8,000 cubic feet per second (cfs) respectively (Jacobs, 2014). However, for the 10- and 50-year storms, the discharges were lower than the FIS values. Over a span of 33 years, the discharge values for the lower probability events increased by 13.5% for the 100-year flood discharge and 46.7% for the 500-year discharge. If this trend continues to increase, it will have catastrophic effects on the current infrastructure.

An analysis by Wright et al. (2012) found that approximately one-fourth of the more than 500,000 bridges in the National Bridge Database are currently deficient and therefore are more vulnerable to climate change than other bridges (Wright et al., 2012). The total cost for adjusting bridges in response to the threats from climate change throughout the course of the 21st century vary from approximately \$140 billion to \$250 billion (Wright et al., 2012). The large range of cost is attributed to the emissions scenario and assumptions about adaption. Only rainfall amounts were allowed to change in the analysis. Consequently, no land use changes were altered, and all other hydrologic conditions were assumed to

remain unchanged (Wright et al., 2012). There were several assumptions made in the estimate, which leads to the numbers provided being quite conservative. Nonetheless, the estimate provides an implication of the potential effect of climate change to bridges in the United States.

This region of Colorado is no stranger to destructive flash floods. The 1976 Big Thompson Canyon flood resulted in discharge values at the mouth of the canyon on the order of a 500-year flood event. In comparison, the 2013 flood resulted in discharge values at the mouth of the canyon around the 100-year flood event. However, the 2013 flood did result in discharge values close to a 500-year flood in some locations along the Big Thompson, as shown below in Table 1.1. The fact that two low probability flood events occurred within 37 years of one another demonstrates the importance of having infrastructure that can withstand the forces associated with floods.

Table 1.1 Estimate of September 2013 peak discharge return interval (Generated from Jacobs, 2014)

Location	Estimated Discharge (cfs)	Annual Change Peak Discharge (cfs)					Estimated Recurrence Interval (yr)
		10%	4%	2%	1%	0.2%	
Lake Estes	5,330	850	1,980	3,420	5,550	13,370	≈100
Big Thompson at Loveland Heights	9,300	940	2,180	3,750	6,060	14,520	100 to 500
Big Thompson above Drake	12,500	960	2,280	3,960	6,450	15,690	100 to 500
Big Thompson below Drake	14,800	2,120	4,540	7,500	11,800	26,990	100 to 500
Big Thompson at Mouth of Canyon	15,500	3,040	6,250	10,050	15,450	34,000	≈100
North Fort Big Thompson 4.5 miles above Drake	18,400	1,100	2,090	3,200	4,640	9,500	> 500
North Fork Big Thompson at Drake	5,900	1,540	2,870	4,340	6,240	12,600	≈100

The total sum of the flood-related damages is approximately \$2.9 billion (Aguilar, J., 2014). The majority of structure losses were uninsured due to damage being done outside of designated flood zones. Flood zones are denoted as areas that become inundated by a 100-year flood. Historically, the portion of homeowners who purchase flood insurance outside of designated flood zones is small. The total sum includes damage done to housing, infrastructure and economic sectors. Due to the scale of the flooding, the United States Department of Housing and Urban Development (HUD) issued notice of a \$62,800,000 allocation of federal recovery funds to the State of Colorado in December 2013 (Disaster Recovery, n.d.). These funds were allocated to assist recovery in the most impacted counties. FEMA designated 11 counties as Presidential Disaster Areas, which were to receive the funds. Boulder, Larimer, and Weld County were three of the hardest hit counties and received 80% of the funds (Disaster Recovery, n.d.). Floods rank second behind hurricanes in insurance-based loss estimates with \$7.97 billion per year (Hydrologic Information Center - Flood Loss Data, 2015). Loss estimates exclude damage done by coastal flooding caused by tropical cyclones and the monetary values are adjusted for inflation.

This flash flood event in northern Colorado came together through a collection of ingredients. The ground was saturated with heavy rainfall, there was a deep moisture source, a slow-moving pressure system was present and there was instability and lift in the atmosphere. On September 9 and 10, radar showed that parts of the Front Range picked up over one inch of rain both afternoons and evenings. This saturation prevented any further infiltration by ensuing rainstorms. Moisture present in the atmosphere is measured by the observed precipitable water (PW) values. These values represent the depth of water in the atmosphere that could condense and fall as rain. Values between 1.2 and 1.4 inches during the peak of the heavy rainfall events exceeded the all-time maximum values for September, as illustrated by Figure 1.1 (Ulccellini, 2014). The atmospheric state involved an upper-level low pressure center above the Great Basin, which due to a large dome of high pressure over the Pacific Northwest and southwest Canada was blocked from moving east or north (Erdman, J. 2013). This setup allowed moist air to be transported northward and westward from the Gulf of Mexico and the tropical east Pacific Ocean (Ulccellini, 2014). The presence of a stationary cold front brought about the initial instability. The combination of the stagnate low pressure center and the cold front generated the upslope flow along the foothills (Bolinger, 2013). This lift, instability and moisture combination lead to the 1,000-year rainstorm event starting from the higher elevations east of the Continental Divide, across the foothills and into the Front Range. It should be noted that a 1,000-year rainstorm event doesn't directly correlate to a 1,000-year flood event.

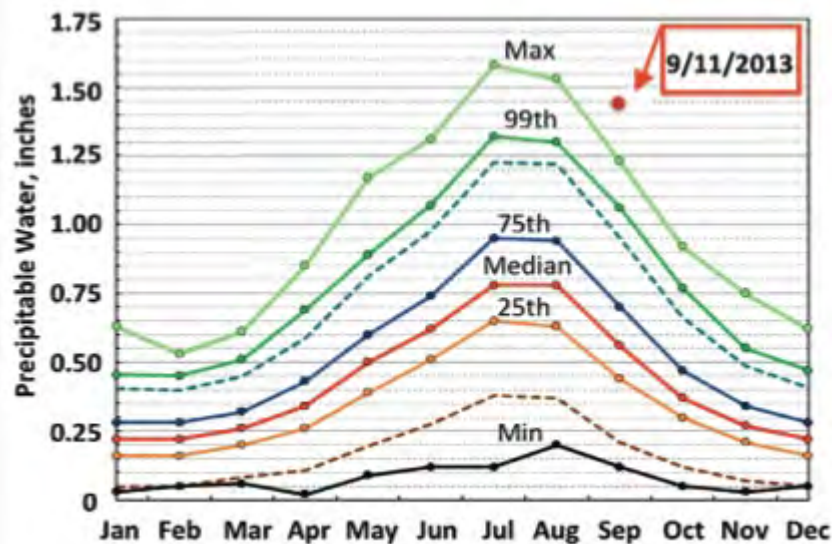


Figure 1.1 Precipitable water data from the weather balloon in Denver as collected from 1948-2012. The seasonal fluctuations are attributed to warm air being able to contain more water vapor (Excerpted from Colorado Climate Center, Bolinger, 2013).

The topography of the Drake is one of the most important factors as to why the community is so vulnerable to flooding. It is characterized by narrow valleys bordered by side slopes generally ranging from 10 to 80 percent (Figure 1.2). Rugged rock faces of even steeper slope occur at many locations along the canyon floors, which is most noticeable at the mouth of the canyon with near vertical faces. Soils are shallow, consisting of coarse material resulting from colluvial and alluvial processes (McCain et al., 1979). Soil grade varies from gravelly near the ridges to sandy gravel near stream levels. The Big Thompson River headwaters are located on the Continental Divide at an altitude of about 11,000 feet. The altitude of the area of interest from Estes Park to the mouth of the canyon ranges from 7,500 feet to 5,200 feet. Tributaries in the Big Thompson River basin west of Drake range in altitude from 7,000 feet to 9,000 feet with extremely steep gradients on the order of 700 feet per mile or a 13.2% slope (McCain et

al., 1979). The Big Thompson River streambed has gradients ranging from 31 feet per mile at Estes Park to 100 feet per mile at the mouth of the canyon, which is 0.6% to 1.8% slope. On the North Fork Big Thompson River, the average streambed gradient is 128 feet per mile in the reach between Glen Haven and Drake, which is a 2.4% slope (McCain et al., 1979). Combining the steep streambed with the lack of an escape for excessive flows leads to a community with high vulnerability to flooding.



Figure 1.2 Topography the Big Thompson Canyon with elevations ranging from 8100-7150 feet located slightly downstream from Estes Park at bridge C-15-AM. This was generated via ArcMap in combination with LiDAR data provided by Colorado GeoData.



Figure 1.3 Plan view of the Big Thompson canyon with bridges and other key features labeled

Figure 1.3 presents a plan view of Drake, Colorado, which is centralized at bridge C-15-Y, but the residents live along US 34 from Estes Park to the mouth of the canyon. The end goal of this research was to identify what elevations the most critical bridges would need to be raised to such that all eight bridges in the canyon along US 34 meet a target reliability criterion. While such an approach may not be cost effective or practical for an existing bridge network, it would prevent a future low probability flood from causing isolation of the residents of Drake, which serves as an example for future planning. Providing a uniform hazard for the bridges would ensure that the post flood construction be minimized and therefore not disrupt the flow of traffic due to closures. Cost would also be lowered due to the bridge components that would be undamaged. As shown from the figure, the residents only avenue of escape is via US 34 eastbound toward Loveland or westbound toward Estes Park. County road 43 running along the North

Fork Big Thompson River would potentially be an escape route; however, the damage suffered due to the September flood was catastrophic, which led to US 34 being the most flood resilient route available.

1.1 Literature Review

Bridges are vulnerable to water forces associated with extreme storms. These storms can cause mild to sometimes catastrophic damage to the bridge sub or superstructure. Many state departments of transportation have recognized this and ended numerous research efforts over the years to quantify said forces. This literature review will be divided into two sections: work related to flood forces on inundated bridge decks, and an overview on structural reliability.

Research into flood loads on bridge superstructures, more specifically bridge girders, was first conducted by Tainsh (1965). Tainsh (1965) analyzed the force on the girders of three and four girder bridges under the condition of partially submerged and totally submerged. The bridge deck elevation was adjusted such that the influence of the channel floor was negligible. Forces were calculated by measuring the pressure distribution on the girders located at the middle of the flume. Shear stresses along the surface of the bridge deck were not included. Testing was done on a scale model and the results were scaled up to the parent bridge using Froude similarity, with the assumption that the Reynolds number, R , was within the range of 4×10^4 to 5×10^5 .

Denson (1982) was the first to conduct an experimental study of the lift, drag, and moment coefficients on three different types of bridge decks under the condition of partially and fully submerged. Denson studied the force coefficients dependence on a bridge relative inundation depth, h/l , Froude number, $\frac{V}{\sqrt{gl}}$, and relative thickness of the bridge, s/l . Where V is the average upstream velocity, s is the total bridge thickness, g is gravity, h is the inundation ratio and l is the bridge length. The moment, drag and lift coefficients were evaluated using l^2 , s , and l respectfully. Even though several data sets were given, no evaluation of the physical meaning of the dependencies was presented in this study. Tainsh (1965) and Denson (1982) assumed the parameters were independent of the Reynolds number.

Naudashcer and Medlarz (1983) used a dynamometer to measure the drag acting on bridge girders. They analyzed effects of the elevation of the bridge, angle between the flow and the bridge, and the number and length of the girders. They observed that the flow through bridge girders generates an unsteady vortex formation that gives rise to a variation in the dynamic force acting on the bridge. A relationship between the drag coefficient, C_D , and the governing parameters was also presented.

Matsuda et al. (2001) determined that the value of the drag, lift, and moment coefficients was independent of the scale of the model. Three different bridge deck scale models were analyzed in a wind tunnel at different angles of attack in the low Reynolds number range of $1.1 \times 10^4 < R < 1.5 \times 10^6$. When comparing different angles of attack, there was variation in the coefficients; however, at the same angle of attack there was no variation in C_D , C_L and C_M between the different models.

Okajima et al. (1997) analyzed the effect of the blockage ratio on the drag coefficient for a rectangular bridge deck. The blockage ratio is defined as the ratio between the upstream area of the bridge deck that is inundated by the free surface stream and the total area of the free surface stream measured at a reference section located upstream of the bridge. They concluded that there is a linear relationship between the blockage ratio and the drag coefficient.

Tainsh (1965) and Denson (1982) investigated the effects of free surface flow on specific bridge deck structures. Whereas Malavasi and Guadagnini (2003) modeled the bridge deck as a rectangular cylinder in their study. Evidence was provided on the nature of the dependence of the time-averaged force

coefficients (lift, drag, and moment coefficients) on a normalized cylinder submersion, $h^* = (h - h_b) / s$ and the Froude number. Where h is the water depth upstream of the bridge deck h^* is the inundation ratio and h_b is the elevation of the low chord of the bridge girder relative to the channel floor. They deduced that the values of the mean force coefficients were much different when in free surface flow versus an unbounded domain. The presence of a free surface changed the coefficients by a factor of 2 or even lower than the values of an unbounded domain. They found that the worst situation for bridge stability occurs when the bridge's inundation ratio is slightly greater than 1.0, which is a common and realistic situation. The authors established drag coefficient values up to 3.4 and lift coefficient values up to -10.

Kerenyi et al. (2009) developed experimental tests and Computational Fluid Dynamics (CFD) models to develop force coefficients for different bridge deck geometries that can be used in design. The project was funded by the U.S. Department of Transportation and was conducted at the Federal Highway Administration (FHWA) labs in McLean, VA. They tested three different bridge types, which included a six-girder, three-girder and prototype streamlined deck shapes designed to reduce the force associated with inundation. The equations developed for the lift, drag and moment forces were used in the assessment of the bridges along US 34 in this thesis. Below are the design equations and the nomenclature used herein.

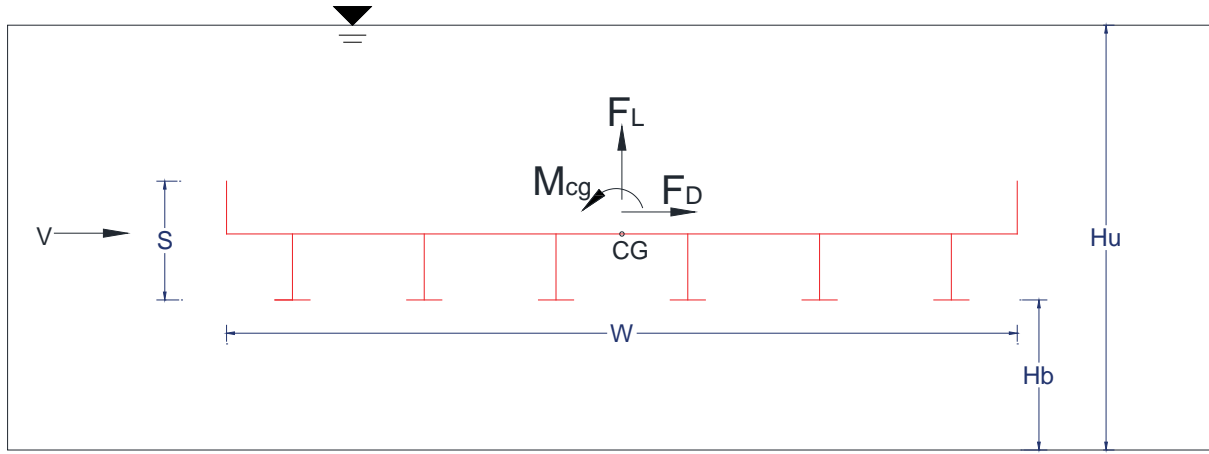


Figure 1.4 Scaled six-girder bridge deck used in the development of the force coefficients with the dimensions and forces labeled (Kerenyi et al. 2009)

$$\frac{F_L}{L} = 0.5 C_L \rho W V^2 \quad (1.1.1)$$

$$\frac{F_D}{L} = 0.5 C_D \rho s V^2 \quad (1.1.2)$$

$$\frac{M_{cg}}{L} = 0.5 C_M \rho W^2 V^2 \quad (1.1.3)$$

The forces are expressed as a force per length in the units of lb/ft and lb-ft/ft. Values of the coefficients are driven by the inundation ratio and the Froude number (F_r). For the experimental setup, all three models were tested in the same flume to minimize the experimental error. They were tested under four approach velocities ranging from 0.82 to 1.64 ft/s (0.25 to 0.5 m/s) and a constant flow depth, h_u , of 0.82 ft or 0.25 m. Under these settings, the F_r varied from 0.16 to 0.32. The bridge deck model was mounted on a bracket, which was then attached to a platform via four ball-bearing pendulums. The pendulums

movement was resisted by two pairs of flat springs in each direction. The tension in the springs was measured by strain gauges, which gave the forces associated with the drag and lift forces. Unevenly distributed forces on the bridge decks lead to moments about the center of gravity about the bridge deck. The values of the drag, lift and moment coefficient obtained by Kerenyi et al. (2009) are presented in the Figures 1.1, 1.3 and 1.4, respectively. For this research, the fitting equation that corresponded to a higher Froude number was used in developing the bridge forces. This is due to the bridges' hydraulic models Froude number output being greater than 0.32, which is the highest Froude number tested in the study.

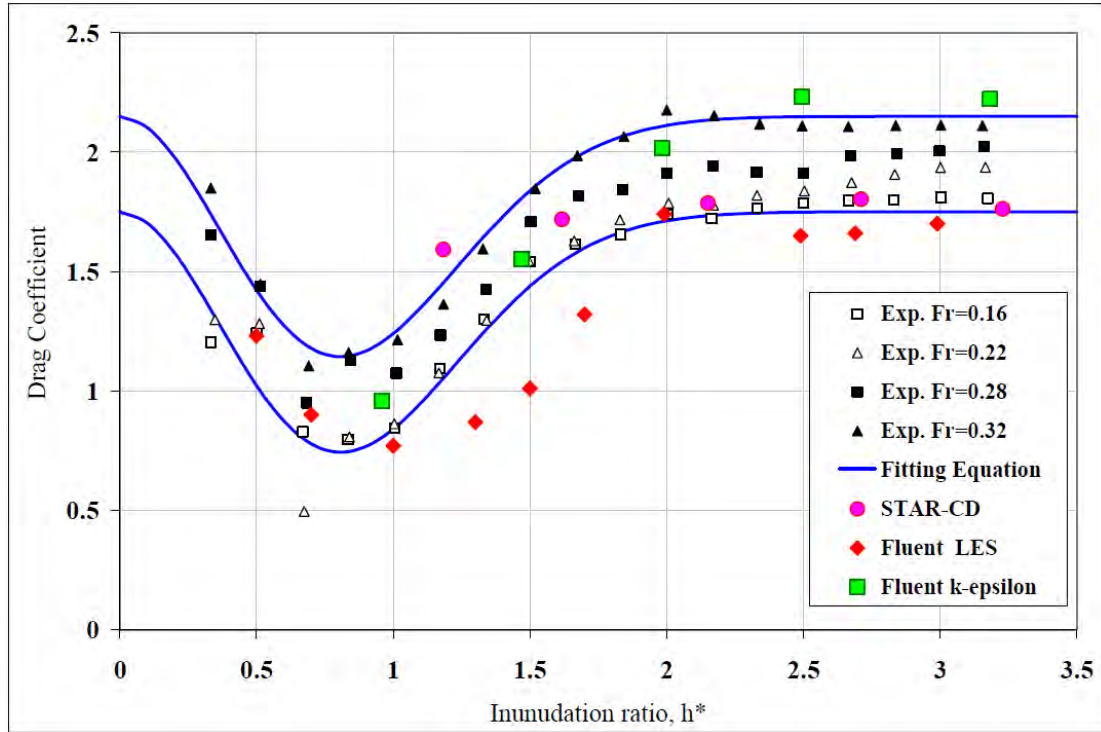


Figure 1.5 Drag coefficient vs. inundation ratio for the six-girder bridge (Kerenyi et al. 2009)

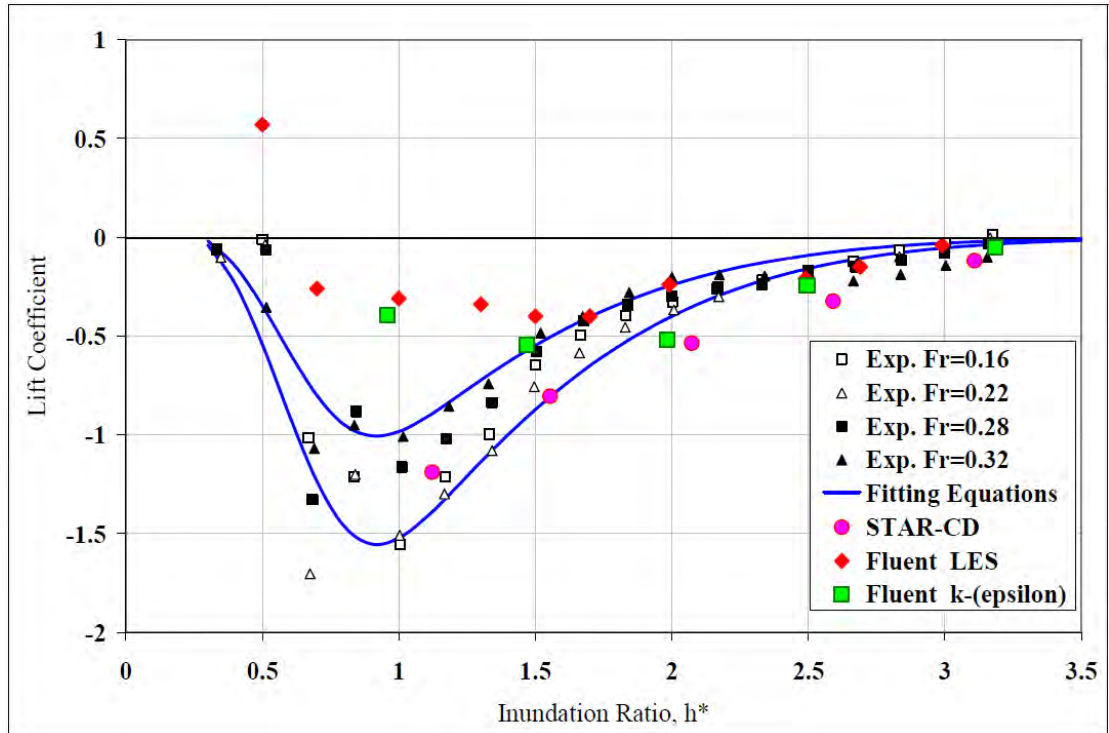


Figure 1.6 Lift coefficient vs. inundation ratio for the six-girder bridge (Kerenyi et al. 2009)

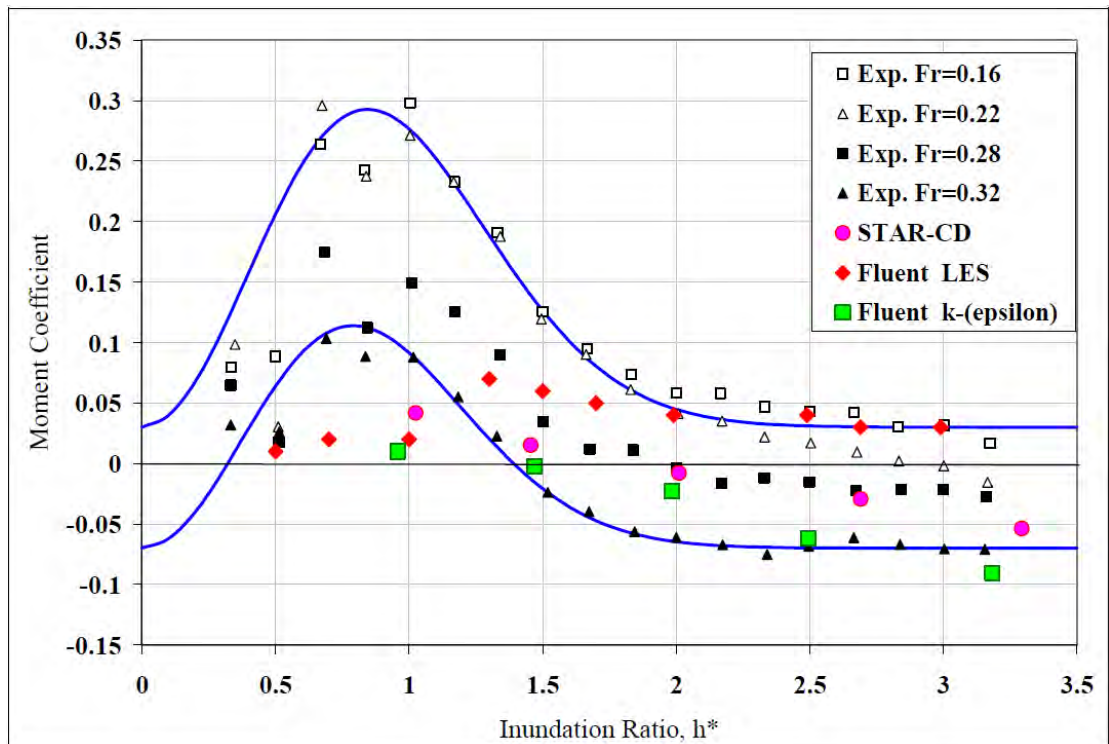


Figure 1.7 Moment coefficient vs. inundation ratio for the six-girder bridge (Kerenyi et al. 2009)

In the calculation of the integrated vertical force, F_L , its component associated with buoyancy force is excluded. The general equation for buoyancy force can be written as follows

$$F_B = Vol_{dis} \rho g \quad (1.1.4)$$

where Vol_{dis} is the volume of water displaced by the bridge, ρ is the density of water with a value of 1.92 slugs/ft³ and g is gravity with a value of 32.2 ft/s². Force balances were calibrated for zero lift under no-flow conditions. The hydrostatic buoyancy force F_{BH} is used to determine the appropriate displaced volume calculation for the correct buoyancy force acting on the bridge (Jenson, 2000). F_{BH} is calculated using a level free surface and is the force on the bridge in the hydrostatic state. Three methods were proposed by Jenson (2000) to calculate the displaced volume. The method adopted in this research involves using the water level at the upstream face, i.e. h^* , to calculate Vol_{dis} (Jenson 2000). When calculating the design lift force, first the value from equation 1.1.1 would be obtained for a specific h^* value, then the corresponding buoyancy force would be calculated via equation 1.1.4 and the values would be summed. Inundation ratio is readily available in the force calculations due to the analysis method used in this research. The main error in the Vol_{dis} value would come from flows at high Froude numbers when the water level at the upstream face is fluctuating.

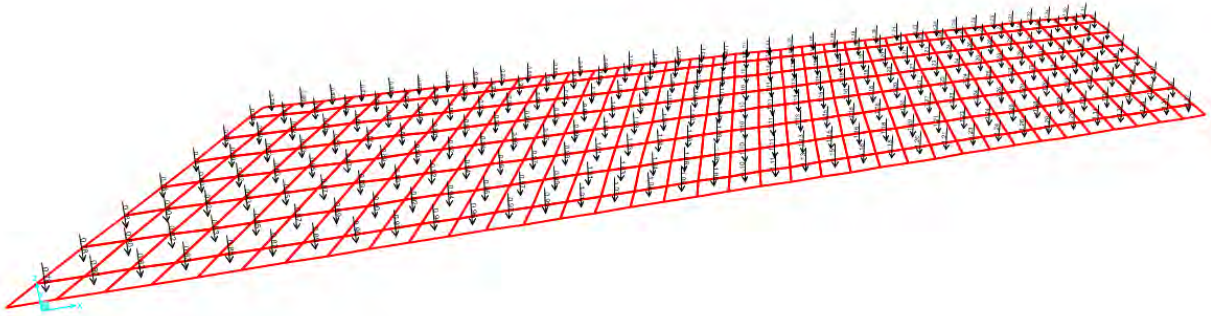


Figure 1.8 An example of the applied net lift force on the bridge superstructures

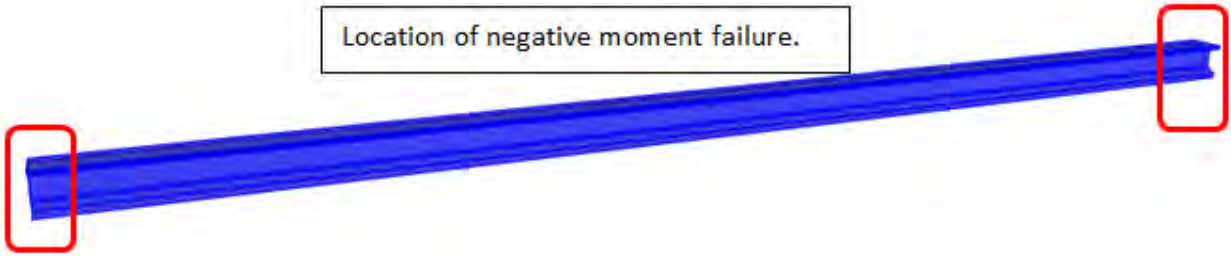


Figure 1.9 Failure locations for the girders in this study

Development of probability-based design began with the American National Standards Institute (ANSI) Standard A58 (Ellingwood et al. 1980). This was the first use of reliability theory to determine load and resistance factors for design of civil engineering structures and was widely accepted. However, Load and Resistance Factor Design (LRFD) wasn't introduced into bridge construction until the 1994 when The American Association of State Highway Transportation Officials (AASHTO) published the first edition of AASHTO LRFD Bridge Design Specification (AASHTO 1994). In LRFD, the safety performance requirement is expressed by the following equation (AASHTO LRFD-BDS 1994) where:

$$\phi R_n > \sum \gamma_i Q_i \quad (1.1.5)$$

R_n = nominal capacity of a member, connection, or a component; ϕ = resistance factor that takes into account the uncertainties in the material strength; Q_i = load effect such as moment, shear, or axial load; γ_i = load factor that takes into account the uncertainties in the load.

Reliability analysis starts with the formulation of a limit state function, $g(x)$, such that failure corresponds to $g(x) < 0$, where x =vector of basic variables (e.g. material properties, geometric properties, etc.). The form of the limit state function is often expressed as

$$g(x) = R - S \quad (1.1.6)$$

where R = structural resistance and S = load effect. Both can either be a random variable or a function of multiple random variables. The failure probability, p_f , can be calculated using any one of several numerical techniques (e.g. MCS, FORM, etc.). Lastly, the reliability index, β , can be determined by

$$\beta = \Phi^{-1} (1 - p_f) \quad (1.1.7)$$

where Φ^{-1} = the inverse of the standard normal distribution function. A target reliability index is selected in this study such that all structures have a uniform reliability index. For example, the target reliability for girder bridges in the AASHTO LRFD Bridge Design Specification is 3.5 (Nowak 1995). This research applies the same target reliability value of 3.5 when assessing the p_f of inundated bridge decks, which ensures that only two out of 10,000 design components will have the sum of the factored loads greater than the factored resistance during the design life of the bridge. An example of beta values and their corresponding p_f can be seen below in Table 1.2.

Table 1.2 Reliability index and probability of failure values

Reliability index	Probability of failure
0	0.5
1	0.159
2	0.0228
3	0.00135
4	0.00003167
5	0.0000002867

2. FRAGILITY MODELING

2.1 Fragility Analysis

Fragility modeling provides a structured outline for evaluating performance, including uncertainty, and reliability of a structural system subjected to a loading condition. The first step is to identify the conditions or limit states in which the structural system fails a certain performance objective, which can be either strength- or deformation-related (and a number of other states not discussed herein). The probability of a limit state or a function subjected to loading can be expressed as

$$P (LS) = \sum P (LS|D = x) P (D = x) \quad (2.1.1)$$

where D is a random demand on the system, e.g., inundation ratio, wind speed, or spectral acceleration, and $P(LS/D = x)$ is the conditional probability of demand equaling the limit state. The hazard is defined by the probability $P (D = x)$ and the fragility is defined as the conditional probability $P(LS/D = x)$. If the hazard is expressed as a continuous function of x , then the summation in Eq. (2.1.1) is replaced by the convolution integral of structural reliability theory (Rosowsky and Ellingwood, 2002).

Eq. (2.1.1) underscores the need to have structural fragilities for a fully coupled analysis. Rosowsky and Ellingwood (2002) state that the fragility provides a less informative measure of safety than a fully coupled risk analysis; however, there are numerous benefits from solely a fragility analysis. A fragility analysis is less complex than a fully coupled risk analysis and the hazard probability is not required. In addition, it is independent of location since only the structure and loading intensity are used in its development.

The fragility of a structural component or system is often modeled by a lognormal cumulative distribution function, CDF,

$$FR(x) = \Phi \left[\ln \left(\frac{x}{\lambda_R} \right) / \xi_R \right] \quad (2.1.2)$$

in which λ_R is the logarithmic mean of capacity, R , and ξ_R is the logarithmic standard deviation (Rosowsky and Ellingwood 2002).

When performing a risk analysis, hazard curves can be obtained from a number of sources or from a statistical analysis. For example, flood discharge values can be obtained from the insurance agency in the area of interest, or data regarding wind can be obtained from the National Weather Service (NWS). Figure 2.1 displays a set of fragilities based on a certain demand. In this study, the demand would be a range of inundation ratios from 0 to 1 with tick marks every 0.1 increment.

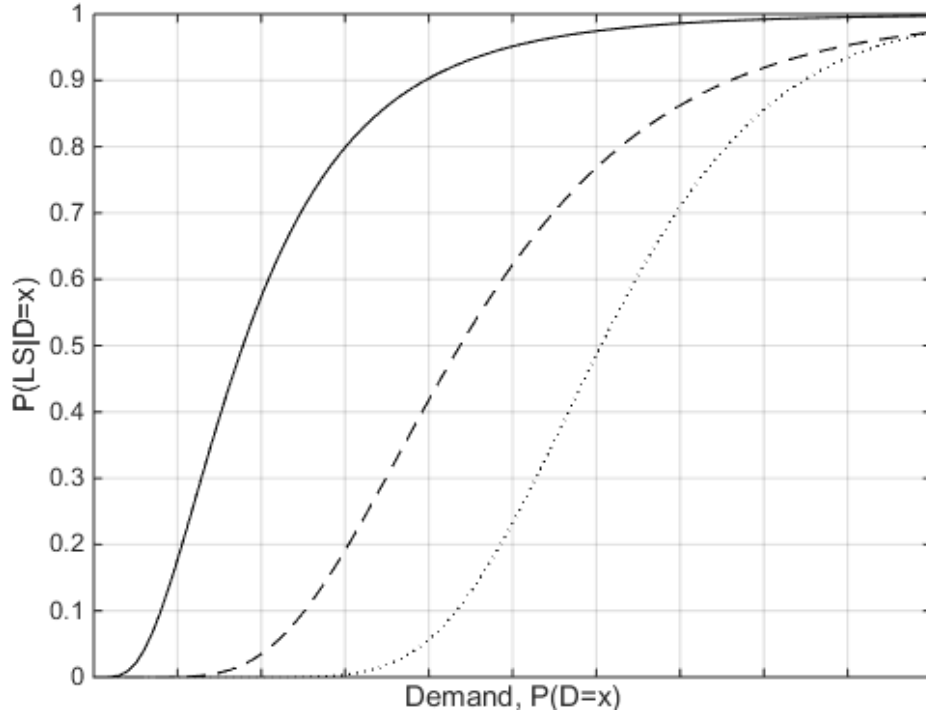


Figure 2.1 Example fragilities for illustration

2.2 Limit States

For this research, only the bridge superstructure was considered (i.e. the girders and bridge deck). The three flood-induced forces were applied to the SAP2000 bridge models to determine what mode of failure would govern. It was determined that the drag and moment forces were negligible and the lift force governed. Under this condition, the negative moment capacity of the girders was used for the strength limit state and the deflection was used for serviceability. The basic limit state function Eq. 1.1.6 is used for both cases. For negative moment, the resistance is replaced by the nominal moment capacity, M_n , of the girder and the load effect is replaced by the maximum negative moment from the SAP model. The equation used for the negative moment capacity for prestressed concrete girders was taken from AASHTO LRFD Bridge Design Specification 4th edition Eq. (5.7.3.2.2-1).

$$M_n = A_s f_s \left(d_s - \frac{a}{2} \right) + 0.85 f'_c (b - b_w) h_f \left(\frac{a}{2} - \frac{h_f}{2} \right) + A_{ps} f_{ps} \left(d_p - \frac{a}{2} \right) - A'_s f'_s \left(d'_s - \frac{a}{2} \right) \quad (2.2.1)$$

Where A_{ps} =area of prestressing steel, f_{ps} =average stress in prestressing steel, d_p =distance from extreme compression fiber to the centroid of prestressing tendons, A_s =area of mild tension steel, A'_s =area of mild compression steel, b =width of compression face member, b_w =width of web, a =depth of equivalent rectangular stress block, and h_f =compression flange depth. The presented equation in AASHTO was for positive moment capacity and was adjusted for negative moment.

The serviceability limit state was set as a displacement equal to the span length/100. Ghosn and Moses (1998) defined several limit states in the formulation of a methodology for bridge redundancy factors. Among them, a functionality limit state was set as span length/100. This is defined as the maximum perceptible displacement the public will accept. It is proposed on the basis of engineering judgement and is consistent with displacement levels used by engineers and researchers. The demand in Eq. 1.1.6 was set equal to a constant value of span length/100 and the load effect is equal to the respective displacement values pulled from the SAP model under varying lift forces.

2.3 Resistance Statistics

Moment capacity of prestressed girders and steel W sections are influenced by several variables. The steel component areas and yield strength were the most influential, i.e., the mild and prestressing steel. Compressive strength of the concrete was also an important factor. Table 2.1 shows the parameters used in the Monte Carlo simulation for generating a Weibull distribution of the nominal moment capacity, i.e., the resistance in the equation 1.6. In Monte Carlo simulation, a system is simulated a large number of times (e.g., 10,000) where each simulation is equally likely to occur, which is often denoted as a realization of the system. Several random numbers are generated between 0 and 1 which then pull values from the uncertain variables CDF function. This results in a large number of separate and independent values, each representing a probable outcome for the system. The final results are fitted to probability density function, PDF, which represents all the possible values the system can take. In this research, the system is equal to Eq. (2.2.1) and the resulting PDF is the nominal moment capacity of the girder. An example of a PDF generated via Monte Carlo simulation can be seen in Figure 2.2. The variables were either a normal or a lognormal distribution, which requires the input of two parameters: the mean and standard deviation. The mean used in the simulation was equal to the nominal area calculated via the construction drawings multiplied by a factor. For the standard deviation, the calculated mean would be multiplied by the coefficient of variation.

Table 2.1 Statistical information for the variables used in the monte carlo simulation

Variable	Distribution	Mean	Coefficient of variation	Reference
A_s	Normal	$0.9A_s$	0.015	Siriaksorn and Naaman (1980)
f_y	Lognormal	$1.13f_{yn}$	0.03	Nowak et al. (2008)
f'_c	Lognormal	$1.2f'_{cn}$	0.525625	Biondini et al. (2006)
A_{ps}	Normal	A_{ps}	0.0125	Naaman and Siriakson (1982)
f_{ps}	Normal	f_{ps}	0.025	Mirza et al. (1980)

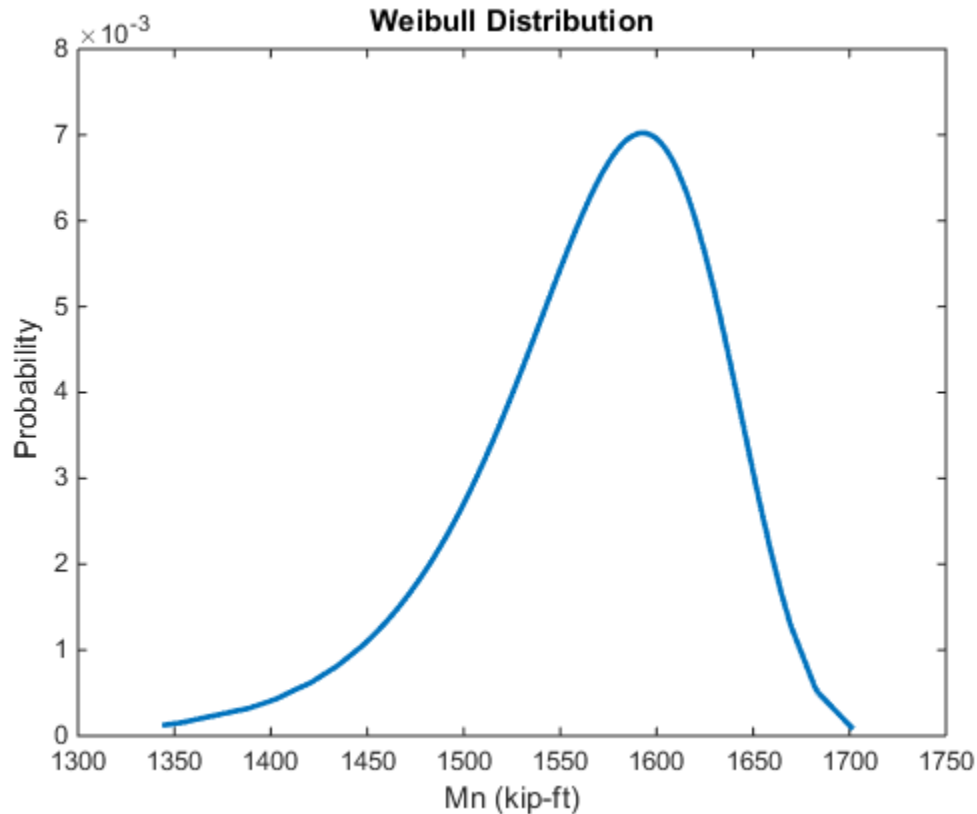


Figure 2.2 Nominal moment capacity for an external girder for bridge C-15-Y

2.4 Hydraulic Modeling

The U.S. Army Corps of Engineers River Analysis System (HEC-RAS) developed by the Hydrologic Engineering Center was used to generate a discharge-water height rating curves for the eight bridges along US 34. HEC-RAS is designed to perform one-dimensional hydraulic calculations for a full network of constructed and natural channels (Brunner (a), 2010). The steady flow water surface profile component was used to create the rating curves. The steady flow module is capable of modeling subcritical, supercritical, and mixed flow water regimes. For the computational procedure, the solution to the one-dimensional energy equation is used. Energy losses are calculated by friction (Manning's equation) and the contraction/expansion coefficient multiplied by the change in velocity head (Brunner (a), 2010). Losses through a bridge are calculated based on the standard step method, i.e. the energy equation.

When developing a bridge rating curve, there are four unique cross sections needed to compute the energy losses due to the structure. Figure 2.3 displays a plan view of said cross sections. Cross section 1 is located a distance downstream from the structure where the flow has fully expanded. The HEC-RAS User's Manual provides a table which provides an estimate of the expansion reach length based upon the degree of constriction, level of the flow, shape of the constriction, and the velocity of the flow. In the case of this research, changing the downstream parameters such as the location of cross section one and the expansion ratio had little to no effect on the rating curve at cross section four. Cross section 4 is located upstream where the flow lines are roughly parallel and the full cross section is effective and is also known as the approach section (Brunner (b), 2010). In general, flow contractions occur over shorter distances than flow expansions. There are regression equations and contraction ratio limits, which require an iterative process to correctly model the location of cross section 4. Due to backwater effects, the bridge discharge-water height rating curve should be generated at cross section 4. Cross section 2 should be

placed such that it represents the natural channel and floodplain of the modeled reach. The cross section is on the order of 10–30 feet downstream of the bridge opening for this research. It is placed enough distance downstream to allow for some flow expansion due to piers, or pressurized flow, coming out of the bridge (Brunner (b), 2010). Cross section 3 is similar to cross section two, except on the upstream face of the bridge. It is placed at the toe of the upstream embankment allowing for abrupt acceleration and contraction of the flow (Brunner (b), 2010).

Both cross sections 2 and 3 should include ineffective flow areas such that lengths AB and CD in Figure 2.3 are not included in the active flow area. The ineffective flow area option is used to keep the active flow in the area of the bridge opening until the elevations associated with the ineffective flow areas are exceeded by the computed water elevation (Brunner (b), 2010). The station locations should be placed to allow for the expansion and contraction of the flow that occurs at the bridge. A rule of thumb is to assume a 1:1 contraction and expansion rate in the immediate vicinity of the bridge (Brunner (b), 2010). For example, if cross section 2 is 15 feet downstream from the bridge face, the ineffective flow areas should be placed 15 feet wider than the location of B and C on Figure 2.3. The same is true for cross section 3. The elevation used for the ineffective flow area at cross section 3 should be equal to the top of the road or curb (Brunner (b), 2010). For the downstream side, the elevation used should be equal to the average elevation between the low chord and the top of the road or curb (Brunner (b), 2010). Using the ineffective area option allows the overbank areas to become effective once the ineffective area elevations are overtopped. Figure 2.4 shows an example of the geometric data view in HEC-RAS with the four cross sections specified in Figure 2.5. It is important to note that bridge wing walls were not included in the HEC-RAS models. Bob Jarrett, an expert in paleoflood and flood hydrology, stated that this modeling assumption was reasonable because debris and erosion around bridges can introduce errors and uncertainty. The modeling results also confirmed this by being similar in magnitude to the published rating curve on the construction drawings.

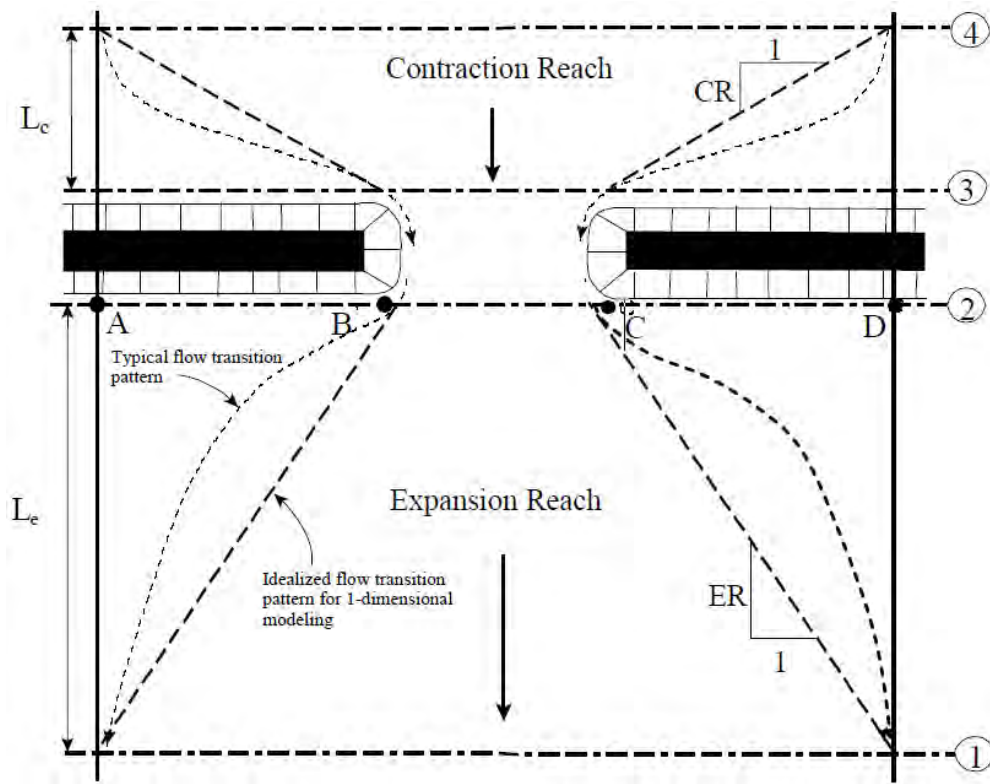


Figure 2.3 Cross section locations at a bridge (excerpted from Brunner, 2010)

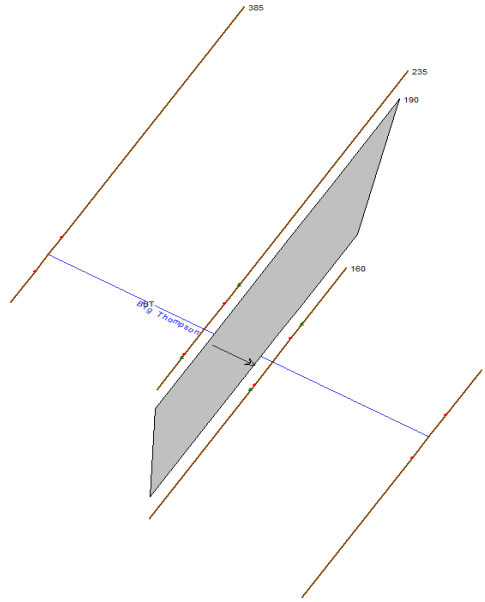


Figure 2.4 Geometric data plan view of HEC-RAS model for bridge C-15-AM

When developing the rating curves for the eight bridges along US 34, six of them had rating curves available from the construction drawings. In most cases, the plan curves didn't include an overtopping discharge value that was needed in determining the flow rates associated with an inundation ratio between 0 and 1. The plan curves simply gave a good measure of the accuracy of the generated rating curves via HEC-RAS. Some difference is expected due to the September 2013 flood altering the channel and the large sediment transportation. Nonetheless, the generated curves were similar in magnitude to the plan's curves which validated the models.

For generating the cross sectional elevations, post-flood LiDAR data was used. LiDAR, which stands for Light Detection and Ranging, is a remote sensing method that uses light in the form of a pulsed laser to measure variable distances to the Earth. A pulse of near-infrared laser light is fired at the ground via an aircraft-borne laser (Bradbury et al. 2005). The laser pulse spreads as it descends forming a circular footprint at the ground level. The reflection and the timing of the return pulse is used to derive a measure of the elevation. These measurements are combined with data on the position and altitude of the aircraft by a global positioning system (GPS) and an inertial navigation unit, which measures the roll, pitch, and yaw enabling the position and elevation of each point to be identified (Bradbury et al. 2005). When scanning an area with high levels of vegetation, the ground elevation values are usually interpolated through the known ground points. LiDAR radiation doesn't transmit through a structure such as a leaf, but it will transmit through holes in the structure (Bradbury et al. 2005). The footprint size of each pulse is usually on the order of < 1 meter with a pulse rate of a 100 kHz (Bradbury et al. 2005). This high sampling rate allows sampling densities of up to 10–20 footprints per square meter (Bradbury et al. 2005). For this research, there were only two bridge locations with copious vegetation. To counter this, field observations were supplemented with the LiDAR data to generate the HEC-RAS cross sections.

Figure 2.5 displays an example of the procedure followed to generate the cross sections necessary to input into HEC-RAS. The locations needed for cross sections 1 and 4 required an iterative process to make sure the expansion and contraction reach lengths were correct as specified in the HEC-RAS User's Manual. Figure 2.6 displays the raw data elevation graph that can be exported into excel for conversion into feet and elevation adjustments if warranted by the field investigation.

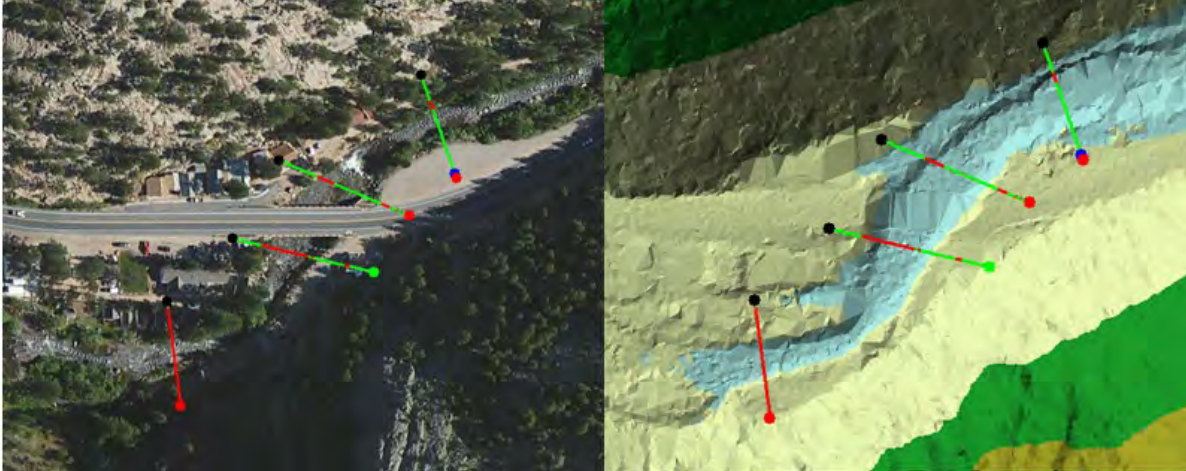


Figure 2.5 An example of the cross sections pulled from ArcMap with LiDAR data obtained from Colorado GeoData at bridge C-15-AM

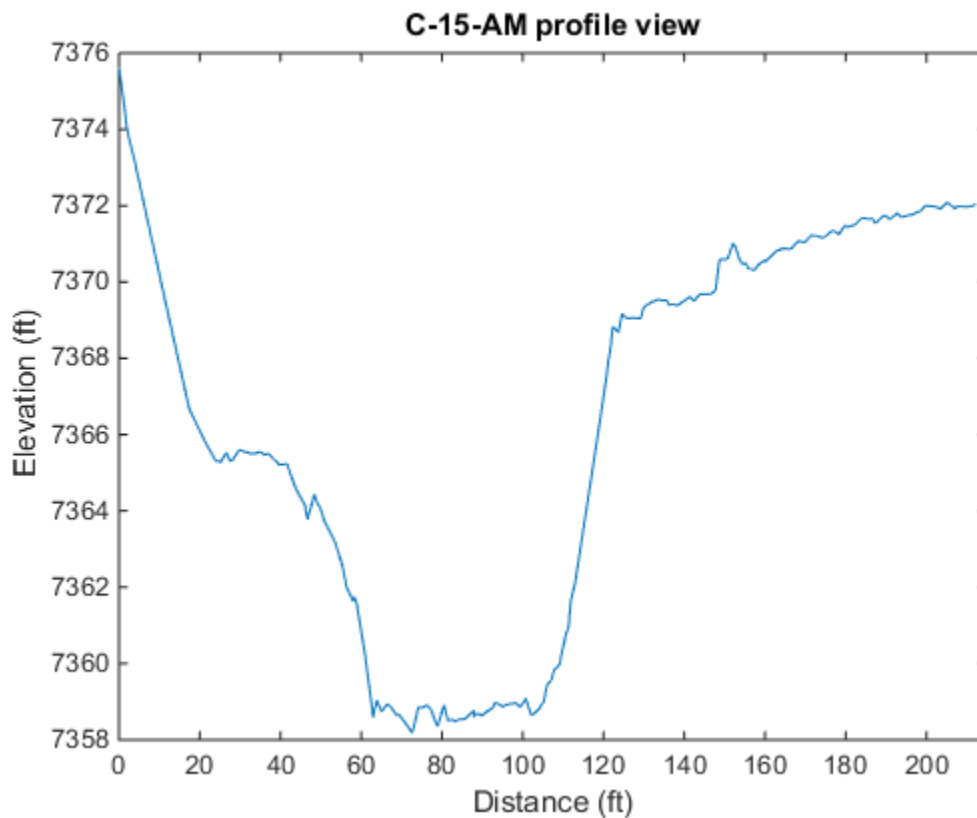


Figure 2.6 The profile graph of the elevation data pulled from cross section 1 (the furthest right line on Figure 2.5)

Field measurements were needed to supplement the LiDAR data. Steven Griffin from CDOT supplied the construction plans and hydraulic information for the eight US 34 bridges. His consulting defined the criteria for the field measurements. The criteria for elevation adjustments were as follows: if there was significant aggradation in the streambed, CDOT would excavate the channel to adhere to the elevations listed in the construction drawings; if there was degradation greater than 1–2 feet, CDOT would fill the streambed to the construction drawings elevation to meet bridge scour concerns. The data was collected by measuring

the height difference between the low chord of the bridge and the channel bottom every four feet on the upstream and downstream side. These measurements were compared to data on the construction drawings to determine if any aggradation/degradation had occurred. Comparing the numbers to the construction drawings converted the field measurements into elevation data, which could be directly compared to the LiDAR data shown in Figure 2.5. If any adjustments were warranted to the channel bottom, then the LiDAR data would be altered accordingly. It was assumed that the channel would have similar aggradation/degradation along the strip from cross section 1 to 4. For example, if two feet of aggradation was measured, then all four cross sections would uniformly be adjusted by -2 feet.

2.5 Flood Frequency Analysis

The flood frequency analysis was necessary in determining the hazard associated with the developed rating curves' discharge values. In August 2014, CDOT and the Colorado Water Conservation Board (CWCB) funded a report titled "*Hydrologic Evaluation of the Big Thompson Watershed*," which was compiled by Jacobs Engineering Group, Muller Engineering Company, Parsons Brinckerhoff, and Ayres Associates. The most recent flood frequency analysis prior to this report was published in 1981. These flow rates were put into question after the devastating September 2013 flood.

The final predictive model that gave the discharge estimates for the Big Thompson River, North Fork Big Thompson River, and Buckhorn Creek involved several steps. Peak discharge estimates for the September flood were made, an updated flood frequency analysis was performed, a rainfall/runoff model was developed for the September 2013 event, and the National Oceanic and Atmospheric Administration (NOAA) rainfall for a number of return periods was used to develop the final values (Jacobs, 2014).

Estimates of peak discharges based on field observations were undertaken by Bob Jarrett of Applied Weather Associates (AWA). Over a long career with USGS, Bob has developed techniques for making peak discharge estimates based on paleoflood evidence and high water mark observations. The discharge estimates provided by Bob Jarrett and other available estimates were compared to current regulatory discharges gage the severity of the September flood (Jacobs, 2014). This information is documented in a memo titled *CDOT/CWCB Hydrology Investigation Phase One-2013 Flood Peak Flow Determinations*, dated January 21, 2014 (Jacobs, 2014).

Flood frequency analyses (FFA) were conducted to supplement the hydrologic evaluation of the Big Thompson River (Jacobs, 2014). The analyses followed methods described in the document "*Guidelines for Determining Flood Flow Frequency*" published by the USGS on September 1981 (Jacobs, 2014). This document is referred to as *Bulletin 17B*. FFA by Bulletin 17B involves inputting the highest peak flow discharge at gage stations for every year and a regional skew coefficient. CDOT and CWCB analyzed 24 gage stations along the northern front range with gage records ranging from 9 to 89 years (Jacobs, 2014). These records were then analyzed using a log-Pearson Type III distribution as recommended in Bulletin 17B. Values for the 2, 5, 10, 50, 100, and 500-year floods were then produced at a location for each reach. Based on the results, the 2013 flood was slightly larger than a 100-year event at the mouth of the Big Thompson Canyon and on the North Fork Big Thompson at Drake (Jacobs, 2014).

A hydrologic analysis was performed on the Big Thompson watershed to evaluate and try to replicate the September flood event. The September 2013 flood event was modeled using the U.S. Army Corps of Engineers Hydrologic Engineering Center's Hydrologic Modeling System (HEC-HMS) to calculate the peak runoff experienced during the flood within the three reaches (Jacobs, 2014). Topographic data used was 10 meter Digital Elevation Data (DEM) shaded relief and Digital Raster Graphic (DRG) dataset, which is essentially LiDAR data (Jacobs, 2014). The topographic data imported via HEC-GeoHMS is used to develop watershed boundaries and flow paths (Jacobs, 2014). In total, the watershed is approximately 460 square miles. The first step in the model calibration process was to calibrate the

rainfall data from 2013 to ground measurements (Jacobs, 2014). The second step involved calibrating the model to the estimated 2013 peak discharges with the help of information on the stage storage-discharge relationship for Lake Estes (Jacobs, 2014).

Once the rainfall-runoff model was calibrated to represent the September 2013 flood, the model was used to predict peak discharges based on NOAA rainfall (Jacobs, 2014). The NOAA Atlas 14, Volume 8 was used to determine point precipitation frequency estimates for the basin (Jacobs, 2014). Isopluvials, or lines of equal precipitation, for 24-hour precipitation depths from NOAA were used to divide The Big Thompson watershed into four rainage zones to account for the variability of precipitation (Jacobs, 2014). The rainage depths were then applied to the standard 24-hour SCS Type II rainfall distribution and incorporated into the HEC-HMS model to evaluate peak discharges for the predictive storms (Jacobs, 2014). The revised predictive model results were compared to the FFA at the mouth of the canyon and the expected unit discharges to check accuracy (Jacobs, 2014). Figure 2.5 shows the final output from the predictive model. The dashed lines represent the previous 1981 regulatory discharge values and the solid lines represent the updated values. The 100 and 500-year values are significantly larger in most locations along the stream, most noticeably at the confluence with North Fork Big Thompson, which is at bridge C-15-Y.

The eight bridges of interest start from slightly downstream of Lake Estes to the mouth of the canyon. The log Pearson type III distribution was used as recommended by Bulletin 17B for the FFA. To fit the three parameters to the distribution, the statistical program R was utilized. From the figure, values would be pulled from the solid lines for the 10, 50, 100, 500-year return intervals at the location of each bridge. Nonlinear least squares was used in R to minimize the square distance between the log Pearson type III survival function and the known four return intervals. Table 2.2 shows the resulting fitted parameters used in the generation of the hazard probabilities. The bridges are listed in location order starting from near Lake Estes (C-15-AM) to just before the mouth of the canyon (C-16-DI).

Table 2.2 Log Pearson type III distribution fitted parameters used for the hazard probabilities

Bridge	C-15-AM	C-15-AL	C-15-O	C-15-U	C-15-Y	C-15-C	C-15-AN	C-16-DI
Iterations	26	26	24	25	30	24	28	31
Shape	5.864	5.855	5.852	5.876	7.457	7.014	7.721	7.766
Location	2.169	2.164	2.158	2.169	2.956	2.272	2.551	2.550
Threshold	2.732	2.726	2.726	2.743	3.595	3.115	3.458	3.456

When running a Monte Carlo simulation, there must be a distribution for the resistance and the load or demand. The resistance statistics discussed in chapter 2.3 explain how variability in the resistance was modled. Variability in the demand was handled a little differently. The published report for the updated FFA gave discharge estimates for different return intervals. However, there is uncertainty associated with the provided discharges due to high and low-outliers, mixed-population sources of flooding, effects of long-term variability on flood estimates, and several other factors (Jacobs, 2014). The rule of thumb is that hydrologic uncertainty associated with estimates is within the range of 15 to 25 percent (Jacobs, 2014). The report estimates that uncertainty can be as high as +/- 20% (Jacobs, 2014). After consulting with Bob Jarrettt, a good way to account for the variability in the demand is to use a normal distribution for the discharge value expected and a standard deviation of $0.20 \times$ the expected discharge. For example, say a discharge value of 10,000 cfs resulted in an $h^*=0.5$. When running the Monte Carlo simulation, 100,000 values between 0 and 1 would be generated and different possible discharge values associated with that 10,000 cfs would be pulled from the PDF function for the discharge. Those discharge values would then be converted into an h^* value and any number less than 0 or greater than 1 would be thrown

out. This results in many possible h^* values arising from the initial 10,000 cfs assumption. There would then be several different h^* values that would be plugged into the Mu graph on Figure 2.5.1, which is a fitted polynomial line to the resulting negative moment values from the SAP2000 model. Next, the numerous Mu values would be fit to a Weibull distribution. Finally, using the resistance and the demand distribution would allow a Monte Carlo simulation to generate several possible values for each and determine how many times the member would fail. The fail counter would be divided by the total number of simulations, which results in a probability of failure value at a specific inundation ratio.

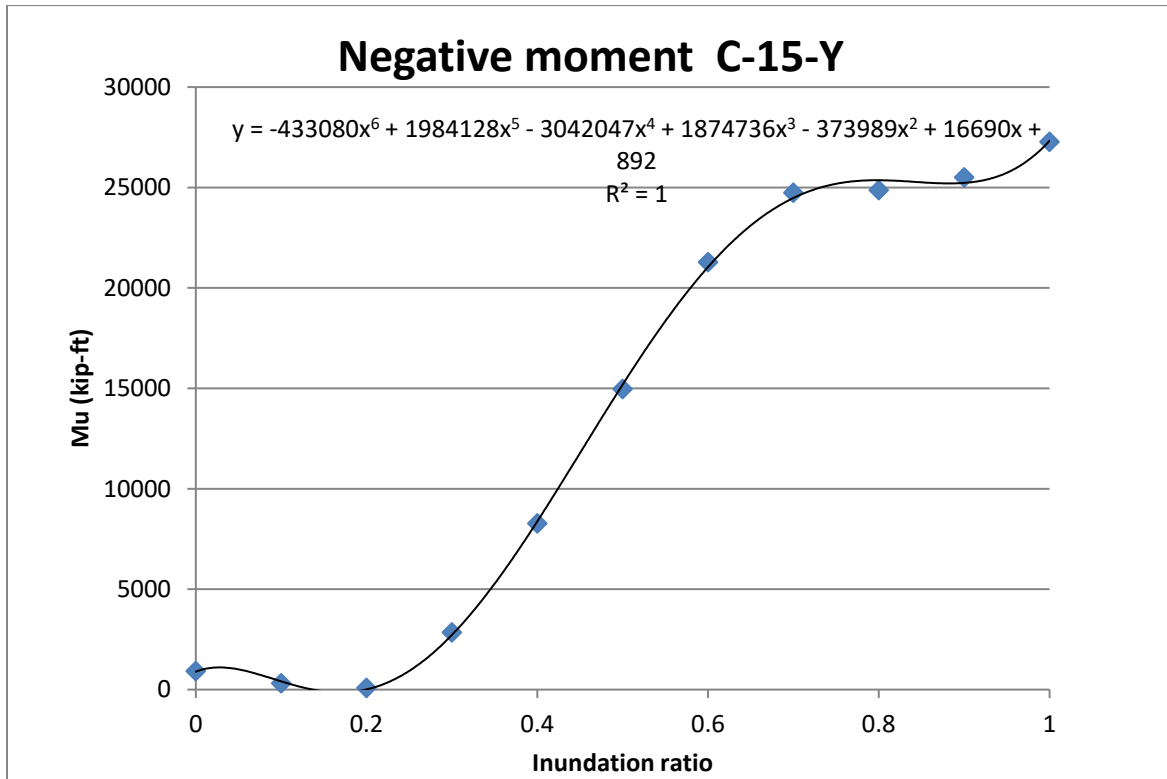


Figure 2.7 Applied negative moment for an external girder on bridge C-15-Y

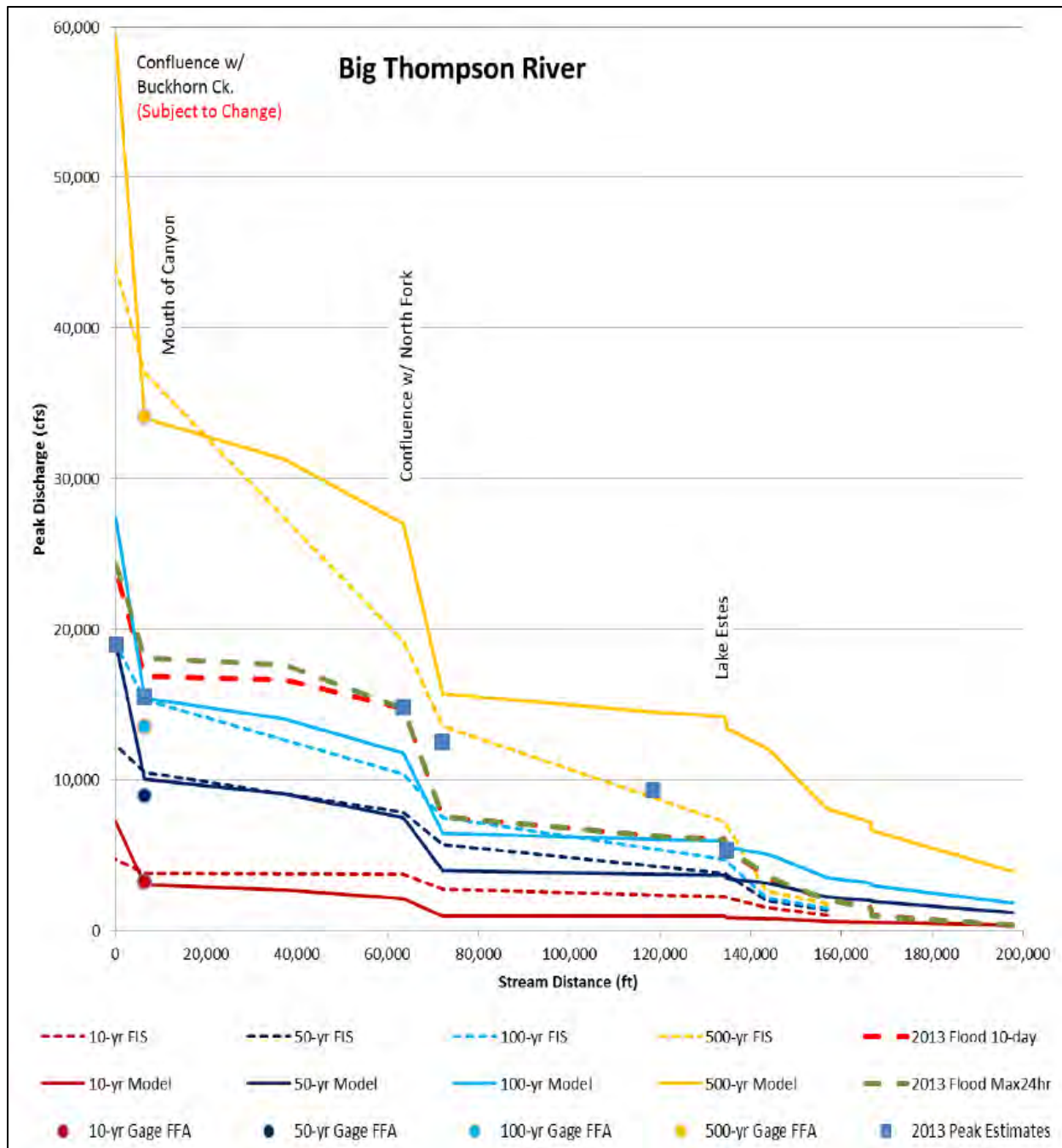


Figure 2.8 Peak discharge profile for the Big Thompson River (Excerpted from Jacobs, 2014)

2.6 Finite Element Modeling

SAP2000 was the finite element program used for modeling of the bridge superstructures. The deck was modeled using quadrilateral shell elements with 6 degrees of freedom (DOF) at each node, and the girders and diaphragms were modeled as frame elements with 6 DOF at each node. To properly model the composite action, the shell and frame elements were each modeled at their respective center of gravity and connected via rigid links. All bridges in this study were integral abutment bridges, which equates to fixed supports at the abutments. The barriers' stiffness was not included in the analysis.

To verify the approach for modeling a composite beam, a test section was modeled as a fixed-fixed condition with a 10' beam and a 6'x10'x0.5' slab. A shell load was applied equating to a distributed load of 22 kips per foot (k/ft). The maximum positive moment was calculated by the equation $\frac{w*L^2}{24}$ where w is the distributed load. Next, the max midspan moment from the beam was subtracted off to determine the moment carried by the slab. This resulted in the slab picking up 354 k-in of the total 1100 k-in. Last, the shell stress was calculated by the flexure stress formula $\sigma = \frac{M*y}{I}$, where y is the distance to the neutral axis, I is the second moment of area about the neutral axis x, and M is the moment about the neutral axis. With the values of y=3.594", I=221 in⁴, and M=354 k-in for the top of the slab, the resulting stress calculated equals 5.76 kips per square inch (ksi). Figure 2.9 displays the SAP2000 results for the slab stresses. The model gave a stress value of 5.96 ksi, which is a 3.4% error, and was thought to be an acceptable result. Therefore, the same procedure for composite beam modeling was followed for the eight bridges in this study.

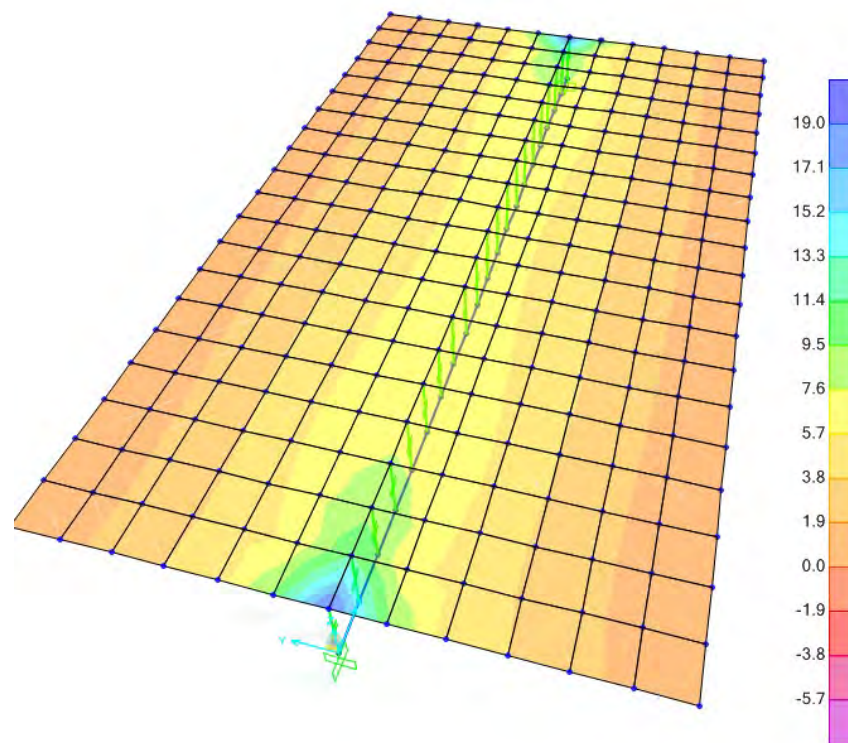


Figure 2.9 Shell stresses for the modeling procedure check

Variation in elevation between the abutments and piers was accounted for as was the bridge skew. For cases where the upstream and downstream elevations were different, the upstream elevation was applied to the downstream side. Some bridges had partial-depth precast concrete deck panels between girders, which varied from 3" to 4". The panels act as a form to support the wet concrete of the cast in place deck. This expedites the construction process due to avoiding any formwork. Installation of the formwork takes the most time for constructing a reinforced concrete deck (Culmo, 2009). Instead of modeling two separate shell elements, the area of the panels were converted into an area for the lower strength cast in place deck using the modular ratio. This resulted in an additional 0.31" of deck thickness in the model, which took into account the added stiffness the panels had on the overall system.

The rigid links acted as shear studs in the model transferring the load and moment from the slab to the girders. Due to this behavior, the placement and number of links were directly related to the shear stud spacing in the construction plans, which resulted in a 3' or 4' spacing in the model. The link location also dictated the location of the shell elements nodal location. The X and Y grid location for the nodes on the girders and the slab had to line up to ensure that the load was transferred without an additional moment from eccentric loading.

Once the grid and the material properties were input for a bridge, the modeling followed these steps: the frame elements were drawn and special joints were added at the locations of rigid links; the diaphragms were drawn with a pin-pin connection; the joint restraints were assigned (fixed for abutments, roller for bearing plates, and pin for bolted connection); the prestressing tendon was added as a tendon element with the force equaling the jacking force after all losses as stated in the construction plans; the shell elements were drawn and divided based on grid marks at link locations; and rigid links were drawn connecting the shell with the frame elements. Next, the meshing of the shell elements was selected such that the shell length/width aspect ratio was less than 5 as per AASHTO-LRFD recommendations. Finally, the loading was applied as a uniform shell load based on the total lift force for each respective inundation ratio.

Figure 2.10 displays the elements utilized in SAP2000. The shell elements will be meshed once the analysis is run. Also, note that the frame, tendon, and shell elements are drawn at their respective elevation. Figure 2.11 is an extruded view of the same bridge as Figure 2.10 post analysis. C-15-Y is a rectangular composite prestressed box girder bridge.

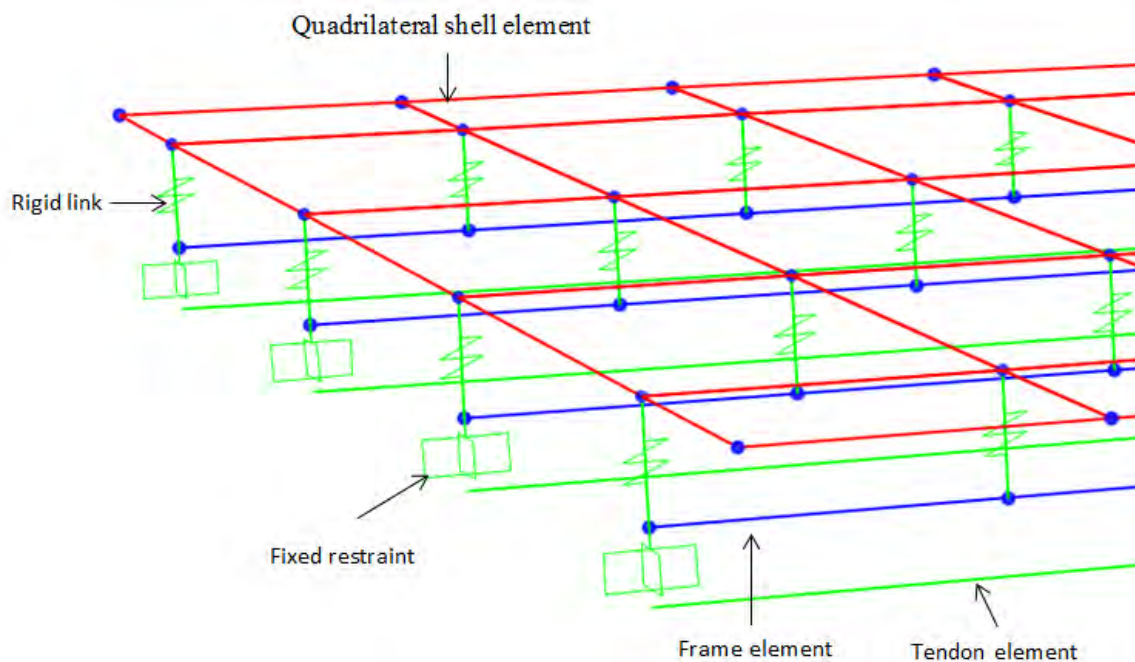


Figure 2.10 Labeled example of SAP2000 elements used

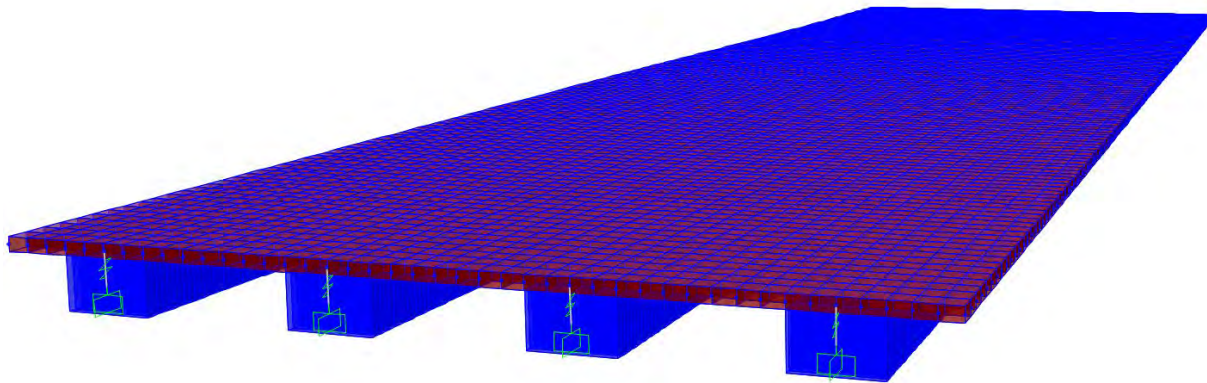


Figure 2.11 Extruded view of bridge C-15-Y under the loading for $h^*=0.3$

All models were analyzed as static linear-elastic. Ghosn and Moses (1998) stated for the definition of the member failure limit state, an elastic analysis of the structural system should be performed to be consistent with evaluation techniques at the time. A linear-elastic analysis results in more conservative force results, however the deflections tend to be underestimated, but were deemed appropriate for this research. For example, the steel girder bridge C-15-C under a loading corresponding to $h^*=0.3$ resulted in a negative moment of 2,515 k-ft with a stress of 59 ksi. The member is still in the linear-elastic range, but the applied negative moment is much greater than the plastic moment capacity of 1,580 k-ft as shown in Figure 2.12. When generating the probabilities of failure, an applied moment of 1,600 k-ft or 20,000 k-ft would both be treated as failed. Therefore, a less robust approach, linear-elastic was adopted for this research.

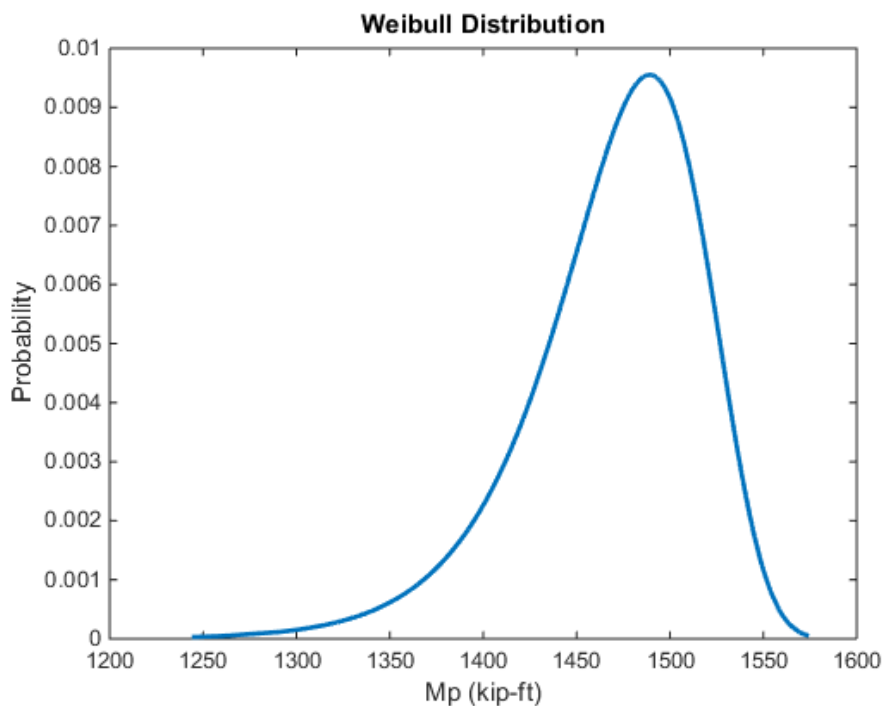


Figure 2.12 Negative plastic moment capacity for an internal girder on bridge C-15-C

Also, out of all of the bridges analyzed, only four had deflection beta values less than 3.5. Of those four, the beta values corresponding to negative moment was 0.14-0.42 less than the deflection values. For this reason, the negative moment criterion was deemed the most critical. Once the bridges are adjusted for the more critical ultimate strength capacity, then the deflection criterion will be met.

2.7 Procedure

Figure 2.13 presents a flow chart displaying the steps followed for the analysis of the bridges. The flowchart is organized such that the log Pearson type III parameters and construction drawings were already obtained. The analysis and results chapter will summarize the values obtained for each respective bridge following the procedure in Figure 2.13.

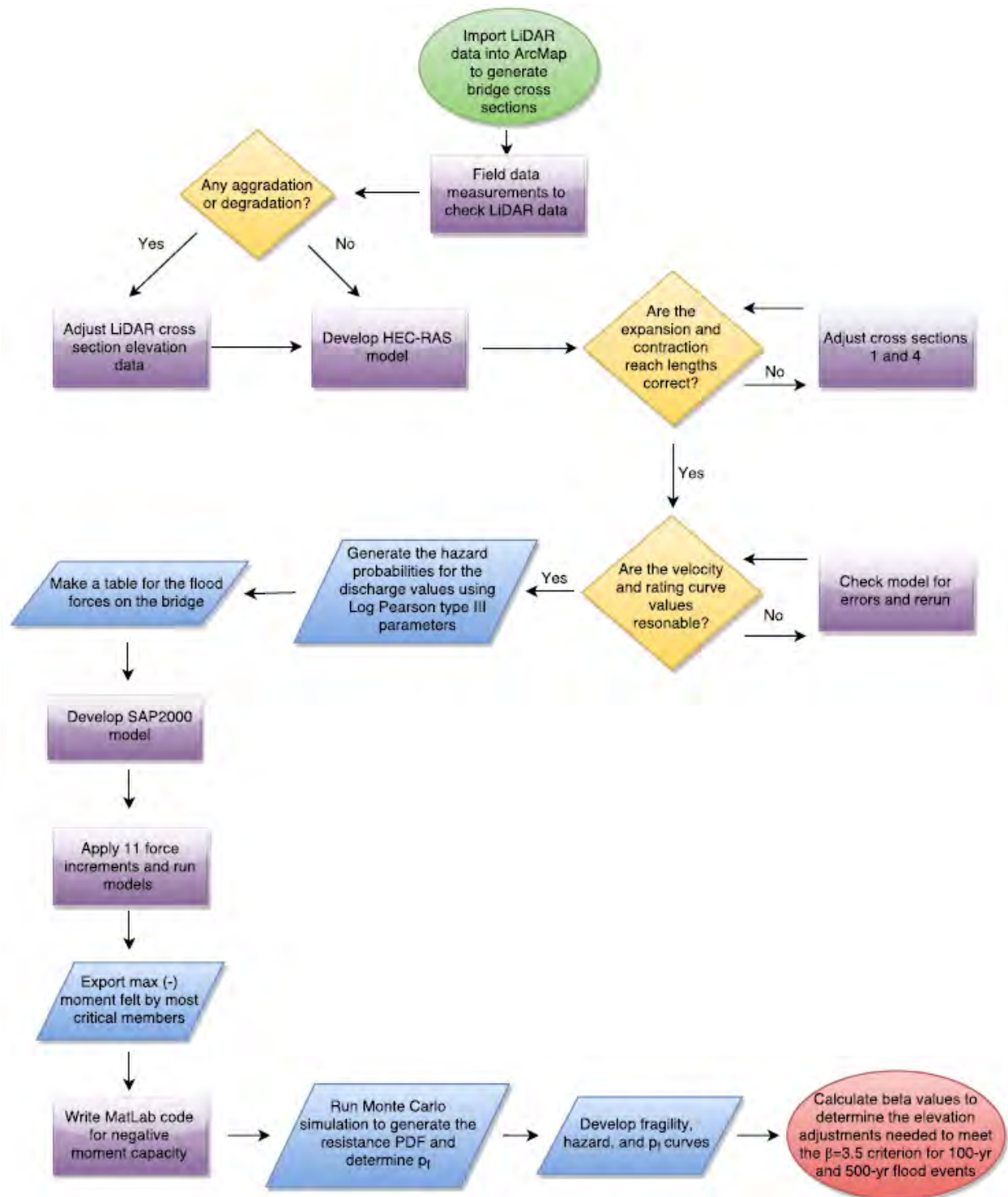


Figure 2.13 Flow chart of the procedure followed for calculating the beta values

3. RESULTS AND DISCUSSION

The methodology for developing fragilities for the bridge superstructure under flood-induced loads was thoroughly explained in the previous chapter. This chapter will go through the full procedure for each bridge and a discussion of the results. The discussion will start with the furthest upstream bridge C-15-AM and work downstream following the list in Table 2.1.1.

3.1 Bridge C-15-AM results

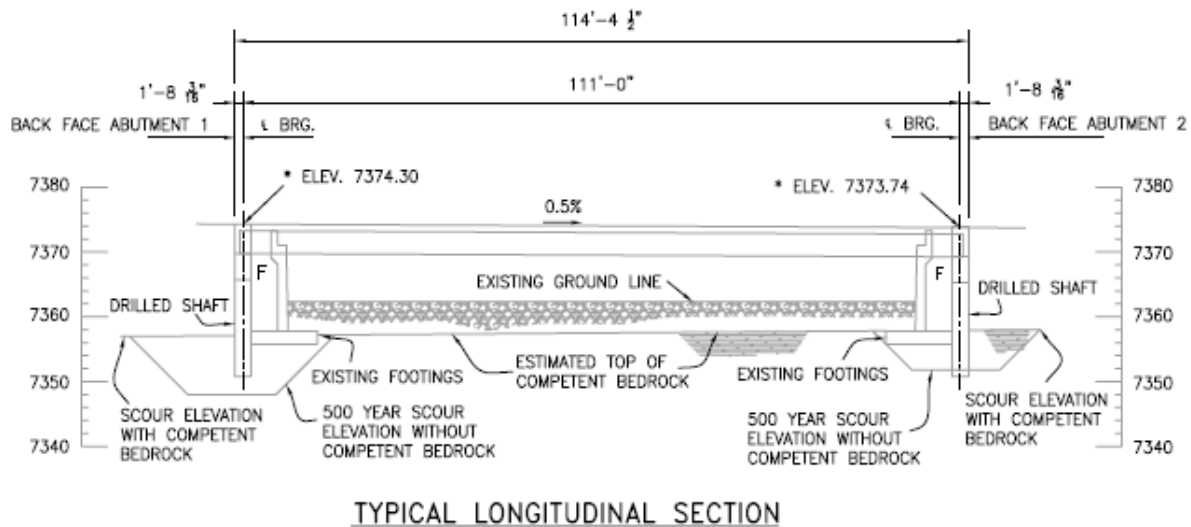


Figure 3.1 Longitudinal view of C-15-AM (CDOT see Appendix A)

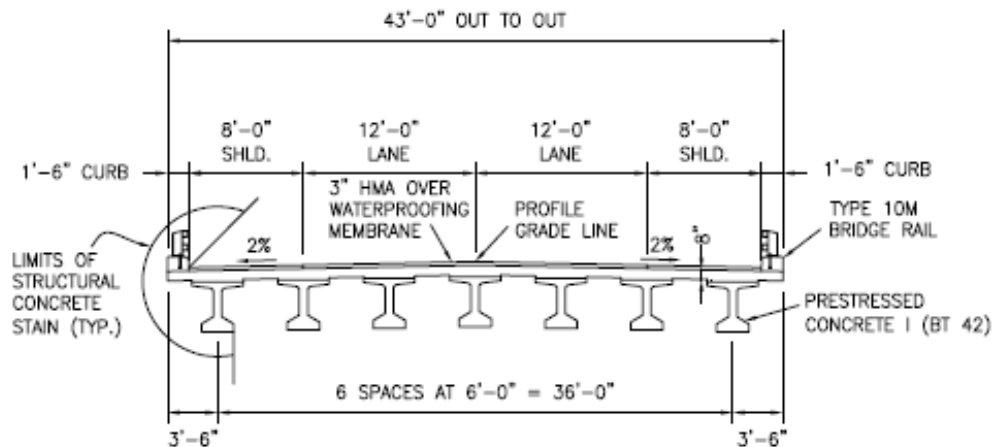


Figure 3.2 Cross sectional view of C-15-AM (CDOT see Appendix A)

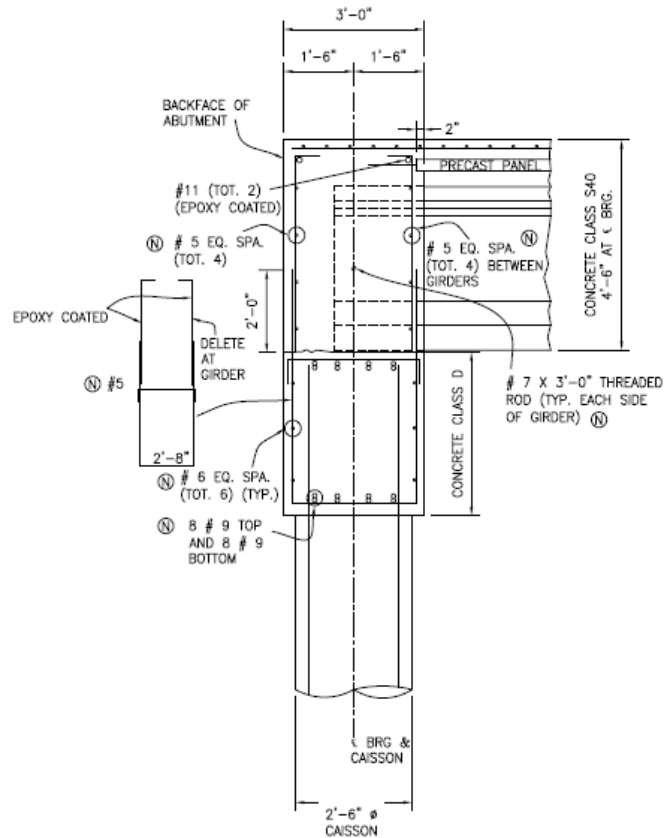


Figure 3.3 Typical integral abutment layout (CDOT see Appendix A)

Figures 3.1 and 3.2 are typical construction drawings for the bridges analyzed in this study. The bridges include prestressed bulb tee (most common), prestressed box girder, and steel I beams. A full list of the construction drawings are provided in Appendix A. Figure 3.3 shows the structural configuration of an integral abutment bridge. The girders are embedded two feet into the cast in place concrete, which leads to a fixed condition.

C-15-AM had 1-2 ft of aggradation in the channel. The LiDAR raw data was adjusted such that the channel elevations were the same as the construction plans. Damage due to the September flood was minimal at this location. There was minor erosion behind the wingwall at abutment 2, abrasion and scaling on abutment 2 and a crack in the asphalt at abutment 1.



Figure 3.4 Cross sections generated in ArcMap for C-15-AM

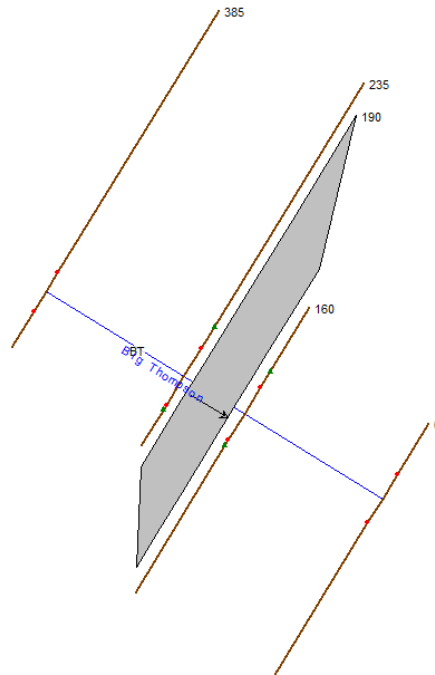


Figure 3.5 HEC-RAS geometric plan view for C-15-AM

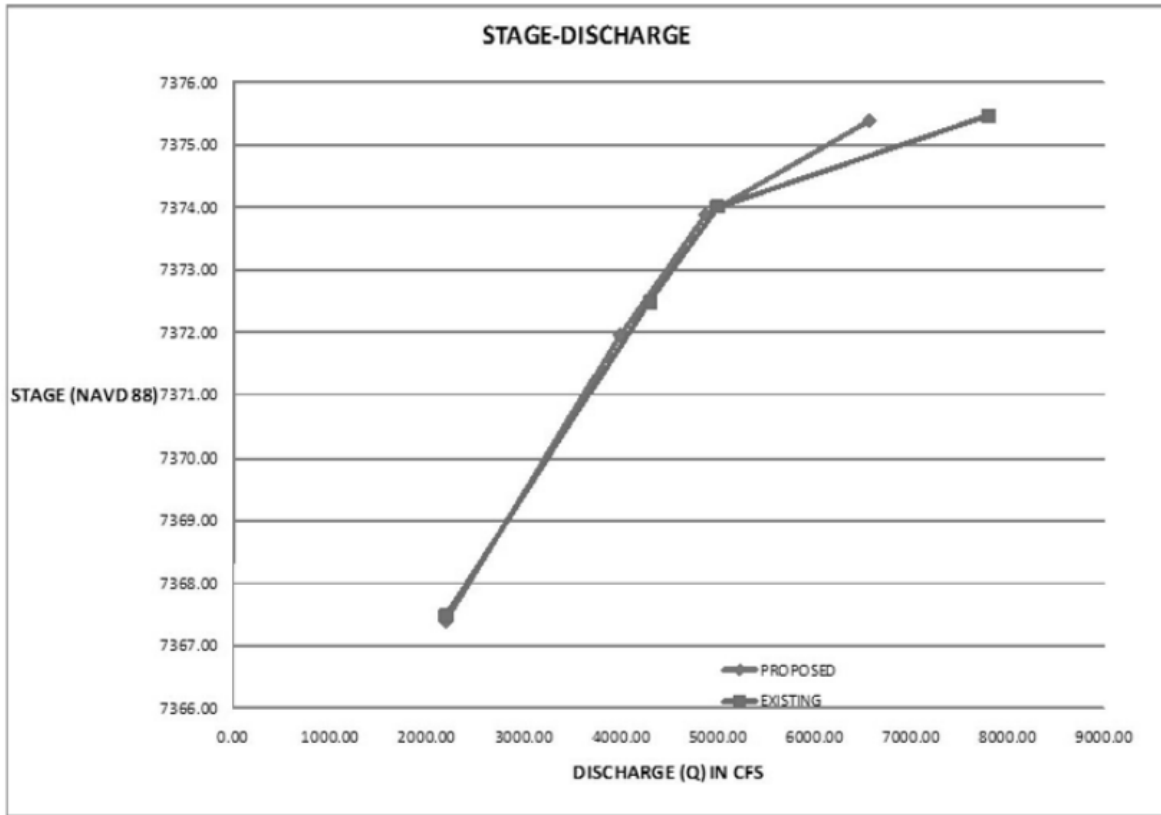


Figure 1.6 Plan rating curve for C-15-AM (CDOT see Appendix A)

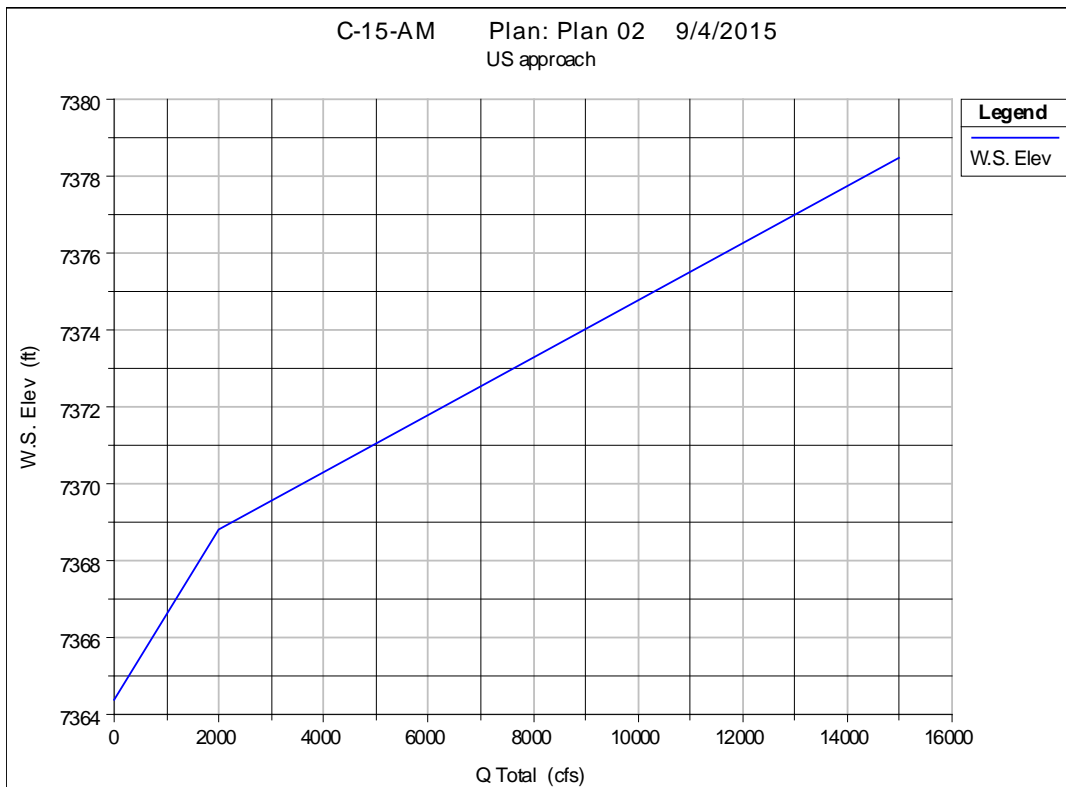


Figure 3.7 HEC-RAS generated rating curve for C-15-AM

A comparison of the actual configuration and the HEC-RAS model can be seen in Figures 3.7 and 3.8. Using the required four cross sections for generating a rating curve at a bridge was sufficient enough to capture the interaction between the natural stream and the bridge. Figure 3.1.6 and 3.1.7 are the rating curves from the construction plans and the HEC-RAS model. The contact and overtopping discharge for the plans is 2,500 and 5,200 cfs respectfully. In comparison, the HEC-RAS curves' values are 1,900 and 9,200 cfs. The velocity values for the model are 2 ft/s higher in magnitude. The model shows close agreement with the construction plans and slight differences are expected.

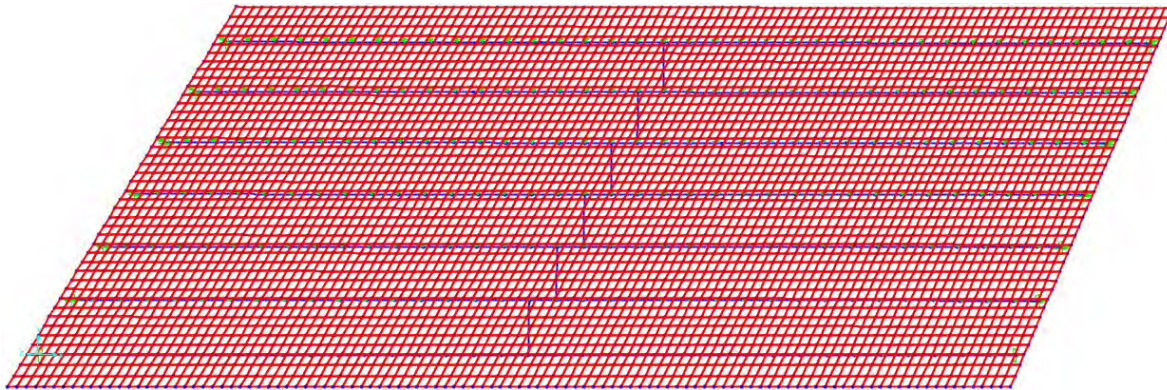


Figure 3.8 SAP2000 model for C-15-AM

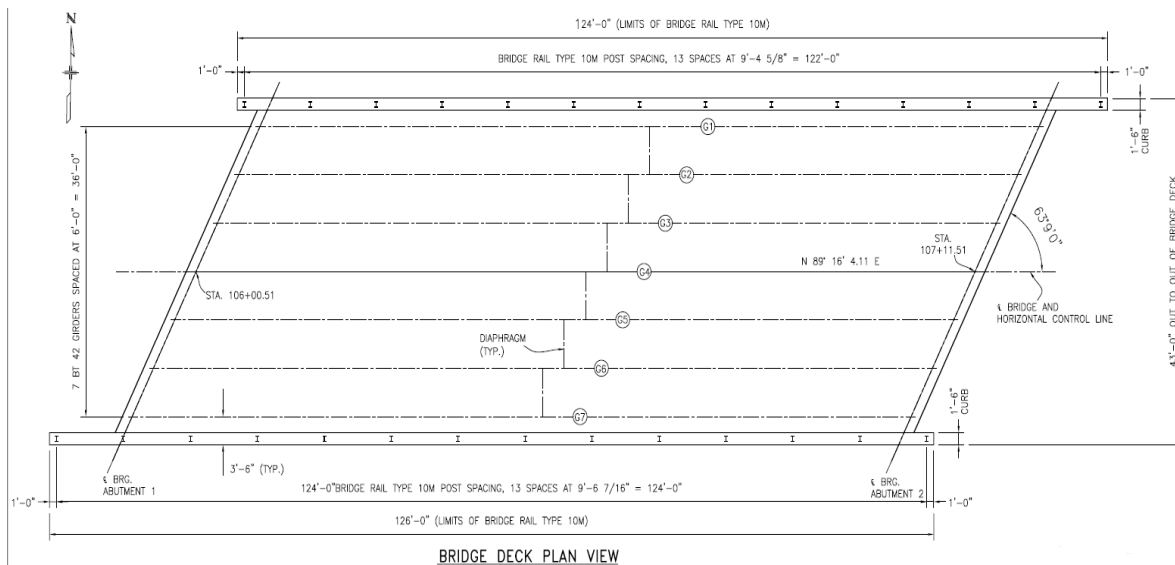


Figure 3.9 Plan view of C-15-AM (CDOT see Appendix A)

Figure 3.8 is a plan view of the SAP2000 prestressed bulb tee bridge C-15-AM. The girders are labeled starting with the northern-most girder, G1, down to the southern-most girder, G7. For the fragility analysis, the most critical external and internal girder was selected. In the case of this bridge, G7 and G2 were the most critical. It should be noted that beta values for the internal girder were always equal to or slightly greater than the external girders for every bridge in this study. Therefore, once the external criterion is met, the internal criterion is also satisfied.

Figure 3.9 is a plan view taken from the construction drawings for bridge C-15-AM. The SAP model compares well with the construction plans. The skew angle is 63.15° on the plans versus 63.17° on the model. Also, the length of the bridge, girder spacing, and the diaphragm locations are identical to the actual bridge. These similarities allow the model to transfer the loads and behave in the same manner as the constructed bridge.

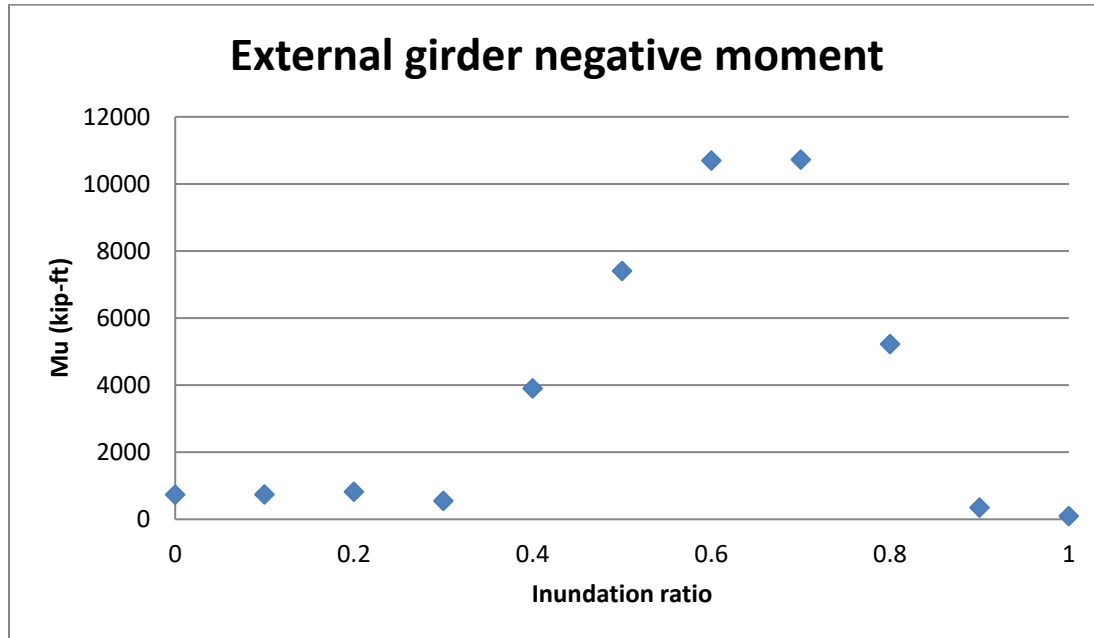


Figure 3.10 Applied negative moment felt by girder G7 for C-15-AM

Figure 3.10 displays the SAP2000 results for bridge C-15-AM. The reason for the decrease in magnitude after $h^*=0.7$ is attributed to the sharp increase in positive buoyancy force at $h^*=0.8$. At that value, the bridge deck is inundated, and the displaced volume increases from 5,660 to 8,700 ft^3/ft . Another reason for the decline is due to the shape of the lift coefficient. It peaks at $h^*=0.8$ and slightly decreases at $h^*=0.9$ and $h^*=1.0$, which can be seen on Figure 1.2. For this bridge, a polynomial best fit line did not result in a good fit to the Mu values. To counter this, a for loop was used to determine where each unique h^* value fell. For example, if the simulated h^* value was 0.235, then the resulting Mu value would be linearly interpolated from the data points on Figure 3.10.

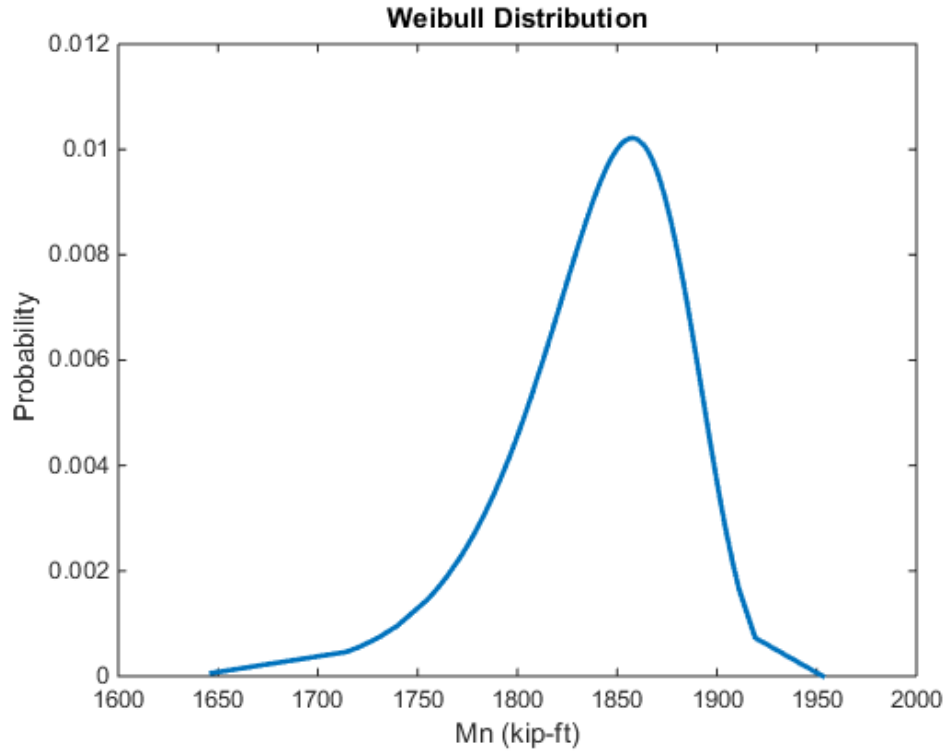


Figure 3.11 Negative nominal moment capacity for an external girder for C-15-AM

Figure 3.11 is a Weibull-fitted PDF function to the Monte Carlo simulation for the negative moment capacity. A goodness of fit test was performed to determine how well the fitted distribution matched the Monte Carlo simulation values. The normalized root mean square error was used where a value of negative infinity is a bad fit and a value of 1 is a perfect fit. The fitted parameters resulted in a value of 0.9146 — a very good fit for the data.

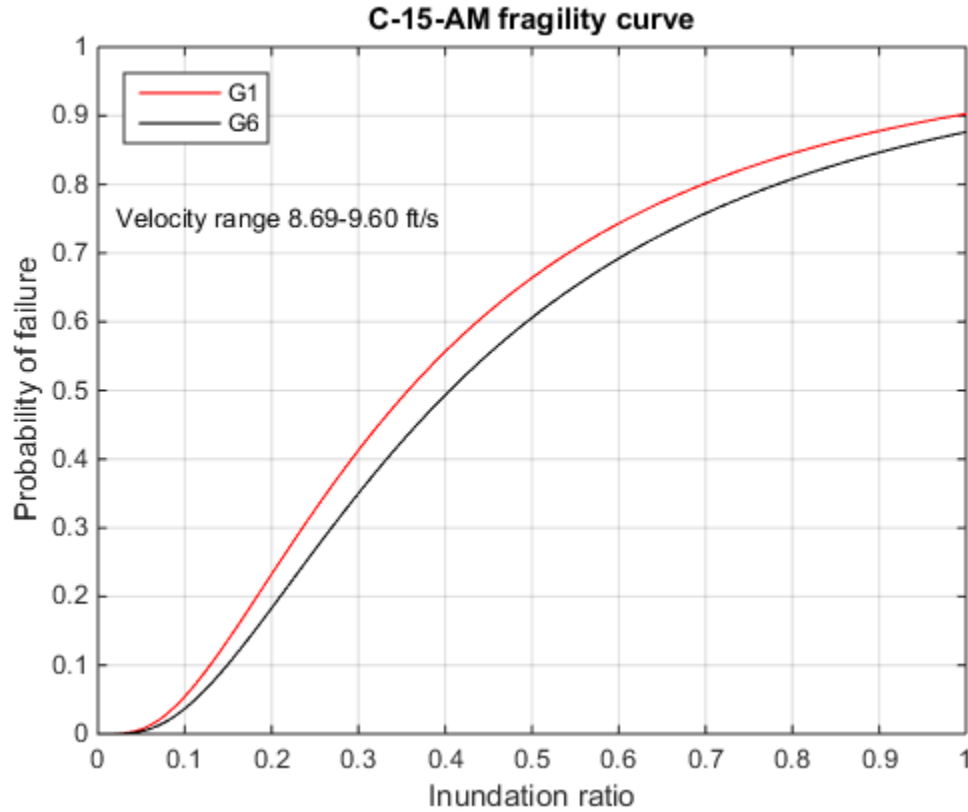


Figure 3.12 Fitted lognormal CDF function to the fragility values for C-15-AM

Utilizing the resistance and the demand distributions, a Monte Carlo simulation was then run to determine the fragility values for this specific bridge configuration. Fragilities do not incorporate hazard probabilities, which are very convenient for designers and stakeholders since they are, in theory, independent of location. If this bridge was built in any other location with the hazard probabilities and stage-discharge relationship known, then the bridge could be built to satisfy any target beta value. However, in the case for all bridges in this study, the fragility curves are a function of the velocity in the channel. Equations 1.1, 1.2, and 1.3 have a velocity squared term, which significantly affects the magnitude of the flood forces on bridge superstructures. If this bridge was built in the plains with shallow channel slopes, then the velocity values would obviously be less. This phenomenon limits the fragility curves in this study to steep fast-moving mountain streams or rivers. The fragility curve could be applied to a slower stream, but it would be overly conservative. Notice the velocity range on Figure 3.12. The range corresponds to the velocity at $h^*=0$ to $h^*=1$. Also, note that the two curves are for the most critical external and internal girder. The shape is the same, but the external girder is a scaled-up version of the internal girder due to the lower capacity of the external composite girder.

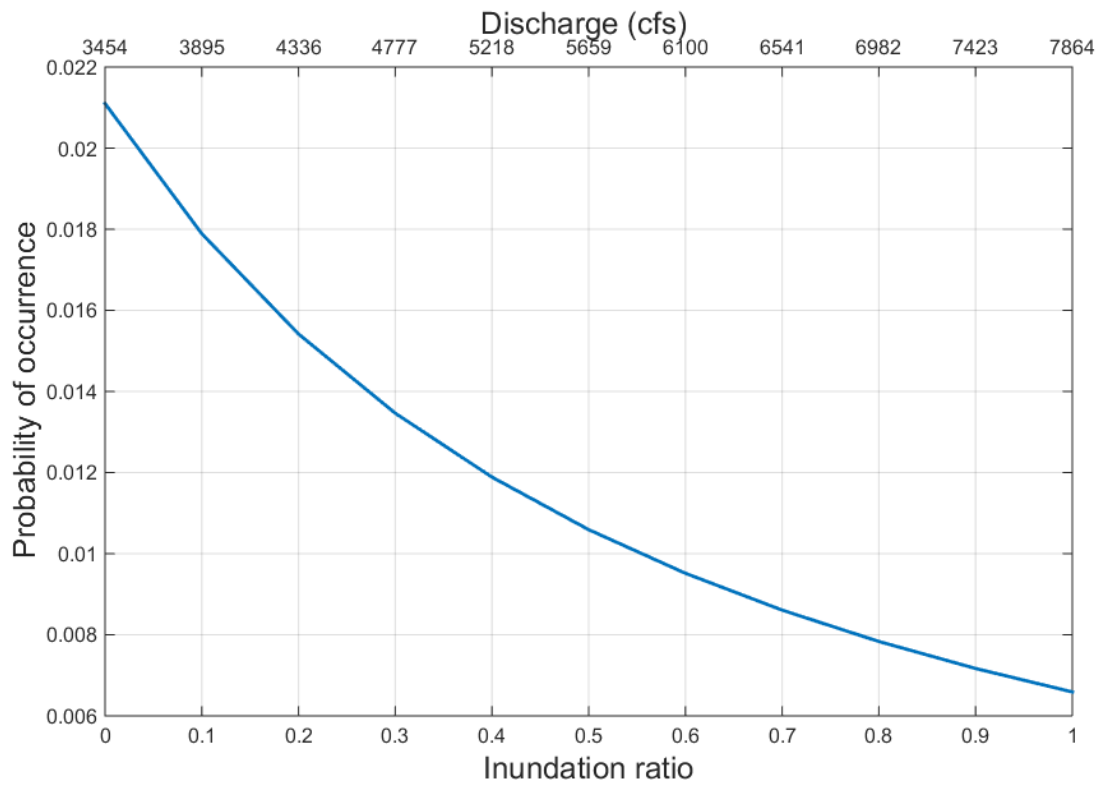


Figure 3.13 Hazard probabilities used to generate the probability of failure curve for C-15-AM

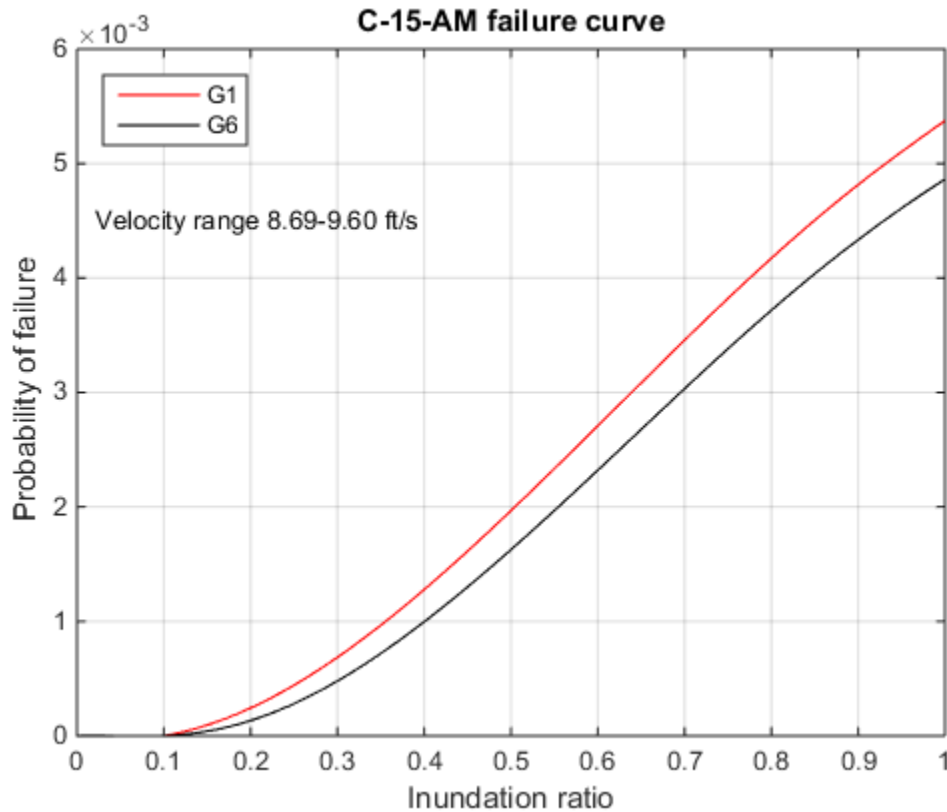


Figure 3.14 Probability of failure curve for C-15-AM

Due to the hazard being a continuous function of x , defined herein as the inundation ratio, the convolution integral was used to generate the probability of failure curve listed in Figure 3.14. The fragility values from Figure 3.12 were convolved with the hazard probabilities from Figure 3.13 to get the failure values. The value at $h^*=1$ was then used in equation 1.7 to calculate the reliability index. For this bridge, the reliability indices are 2.55 and 2.59 for the external and internal girders. To reach the target beta value of 3.5 for the 100-year flood, the bridge would have to be raised two feet. For the 500-year flood, the bridge would have to be raised 12.5 feet, which is likely infeasible. These values are calculated assuming the same stage-discharge relationship as the original bridge elevation.

3.2 Bridge C-15-AL results

The adjacent bridge downstream from C-15-AM is bridge C-15-AL. The length, number of girders, and structural configuration is the same as bridge C-15-AM minus a few differences, including are the skew angle and slope of the bridge. Figure 3.15 displays the difference in slope and Figure 3.16 shows the opposite skew relative to C-15-AM.

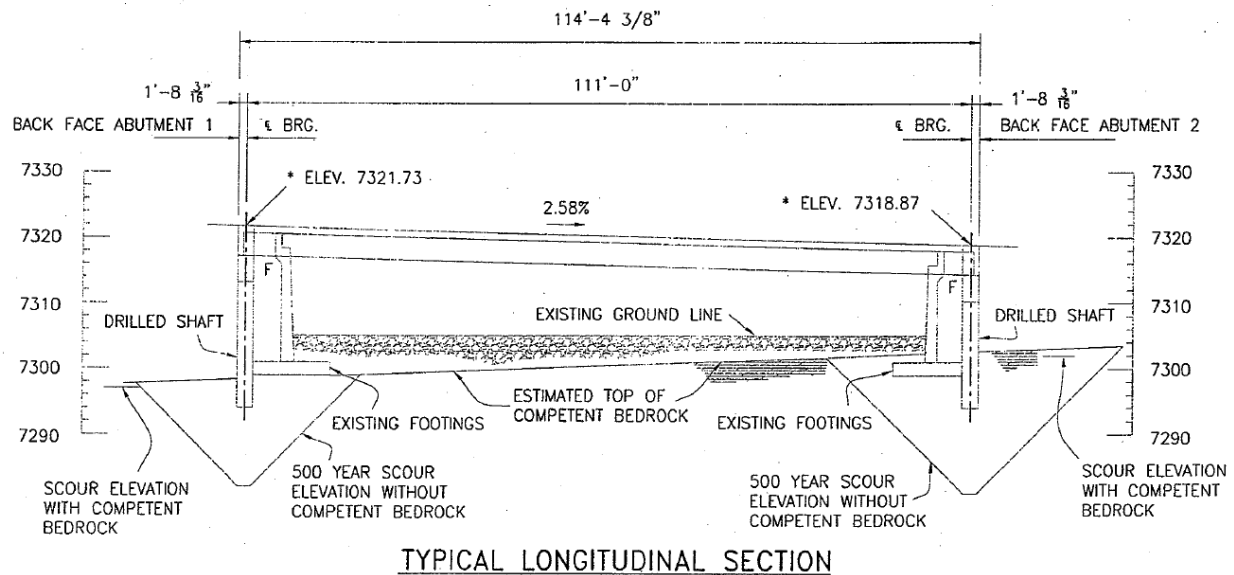


Figure 3.15 Longitudinal section of C-15-AL (CDOT see Appendix A)

The LiDAR data showed two feet of aggradation, but the field measurements showed two feet of degradation at abutment 1 and no change at abutment 2. Due to scour concerns, it was assumed that CDOT would adjust the channel bottom such that it would match the construction drawings. The LiDAR data was adjusted to reflect that assumption. No rating curve was provided for this bridge, so the bridge hydraulic information from C-15-AM was used to help gauge the accuracy of the developed HEC-RAS model for C-15-AL. The bridge geometry and distance between the low chord and the channel bottom were similar enough to deem this acceptable. The generated rating curve was not altered to match the plan curve due to the differences in the channel geometry where bridge C-15-AL had a higher level of meandering. The damage suffered at this bridge was limited to a crack in the asphalt.



Figure 3.16 Cross sections generated in ArcMap for C-15-AL

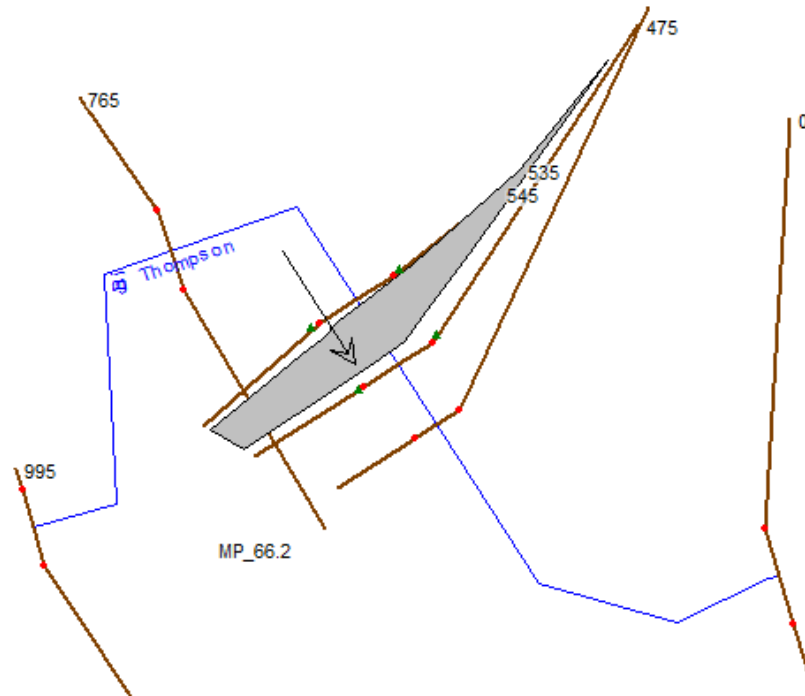


Figure 3.17 HEC-RAS geometric plan view for C-15-AL

Figure 3.16 is an aerial view of the cross sections exported from ArcMap for the HEC-RAS model. The LiDAR data layer is turned off to give a good view of the vegetation and shape of the channel. An extra cross section up and downstream was used for this reach to account for the meandering of the reach. In most cases, deleting the furthest upstream and downstream cross sections had minimal effects on the produced rating curve. For this bridge the extra cross sections resulted in a more reasonable rating curve when compared to the curve for bridge C-15-AM. Figure 3.17 is the geometric data view for the cross sections inputted into HEC-RAS. It should be noted that the blue reach lines have no factor in the model output. If the reach was drawn as a straight line, the rating curve yielded would be identical to the one in Figure 3.18.

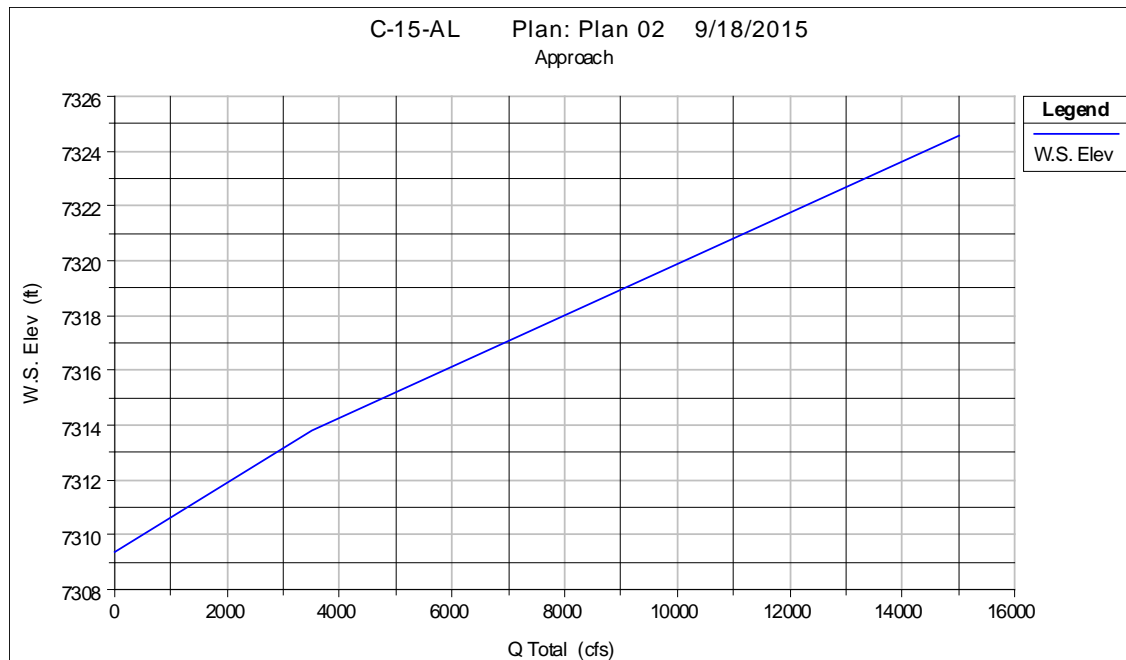


Figure 3.18 HEC-RAS rating curve for C-15-AL

The rating curve in Figure 3.18 gave reasonable values when compared to the contact and overtopping discharge values for bridge C-15-AM. The low chord and top of curve elevations are 7314.05' and 7319.30', which yields discharge values of 3789 and 9400 cfs. This compares well to the values for C-15-AM of 3454 and 7866 cfs. The velocity values range from 11.27 to 10.03 ft/s. The decrease in velocity can be attributed to the high friction losses from the furthest upstream cross section to the approach section in Figure 3.19. There is a shallow transition from the top of the right bank to the road. This gradual slope engages more of the floodplain for the increased discharge values associated with overtopping of the bridge.

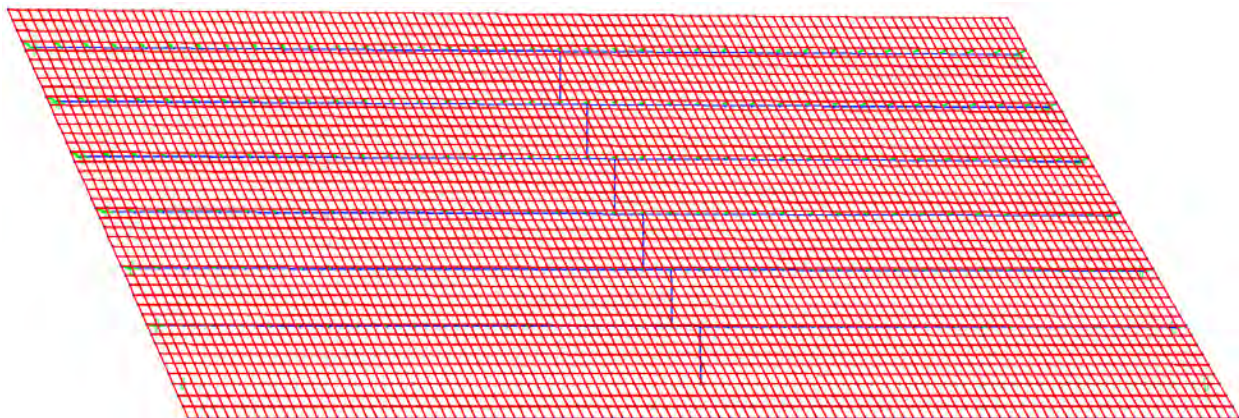


Figure 3.19 SAP2000 model for C-15-AL

Figure 3.22 presents the negative moment felt at each inundation ratio due to the lift force for the critical external member G1. The reason for the slight drop in moment from $h^*=0$ to $h^*=0.3$ is because the net lift force is positive due to the small lift coefficient relative to the positive buoyancy force. The slight dip occurring after $h^*=0.8$ is attributed to the volume of the slab being included in the buoyancy force which lowers the applied load.

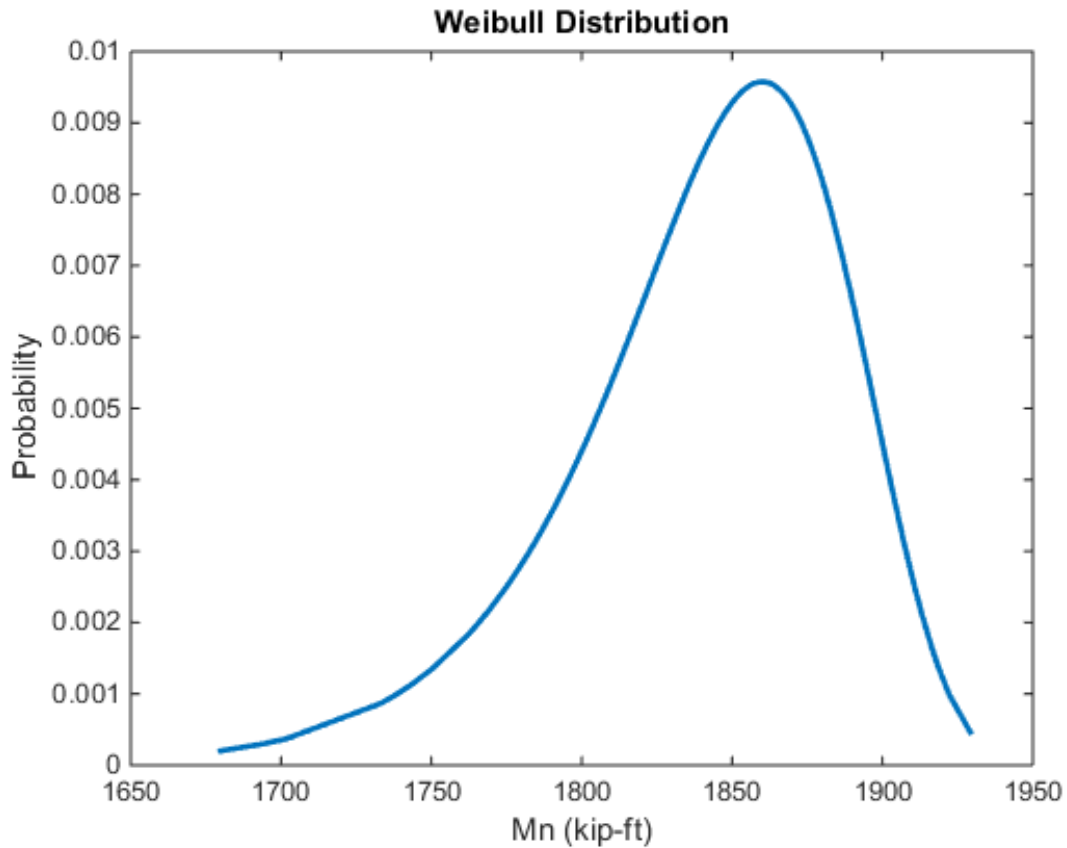


Figure 3.22 Negative nominal moment capacity for an external girder for C-15-AL

Figure 3.23 displays the resulting fitted Weibull PDF to the Monte Carlo simulation for the negative moment capacity. The normalized mean square error test resulted in a value of 0.8927, which is a good fit.

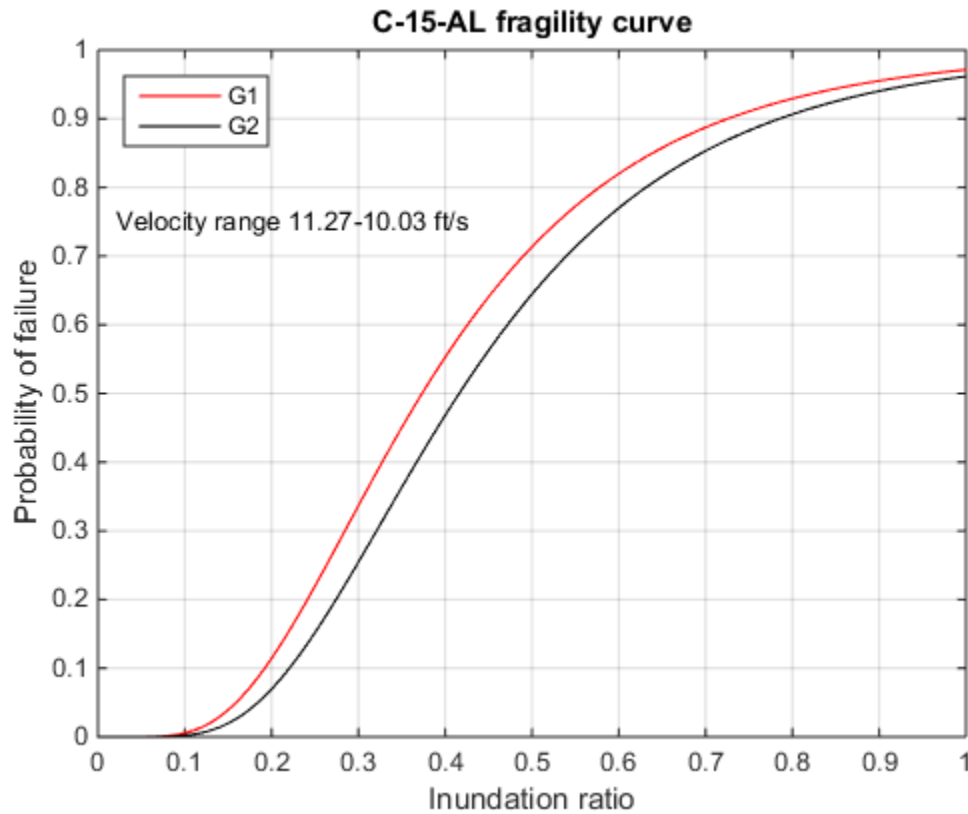


Figure 3.23 Fitted lognormal CDF function to the fragility values for C-15-AL

Figure 3.24 displays the fragility curve for C-15-AL under the velocity range of 11.27 to 10.03 ft/s. The shape and magnitudes are similar to C-15-AM, which is expected due to the similarities in structural configuration and location along the Big Thompson River.

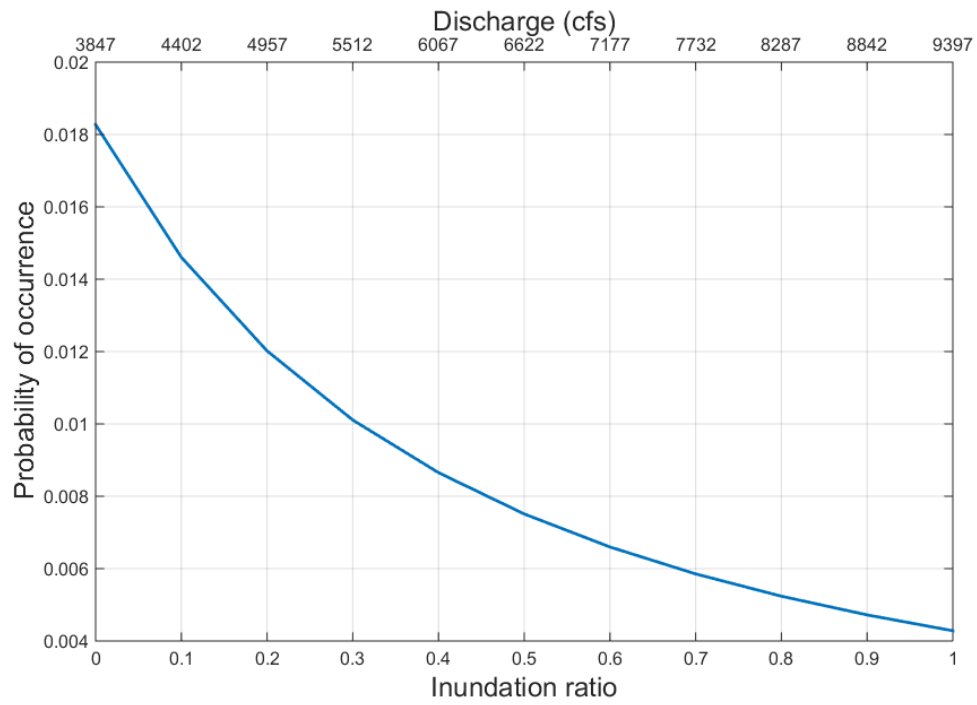


Figure 3.24 Hazard probabilities used to generate the probability of failure curve for C-15-AL

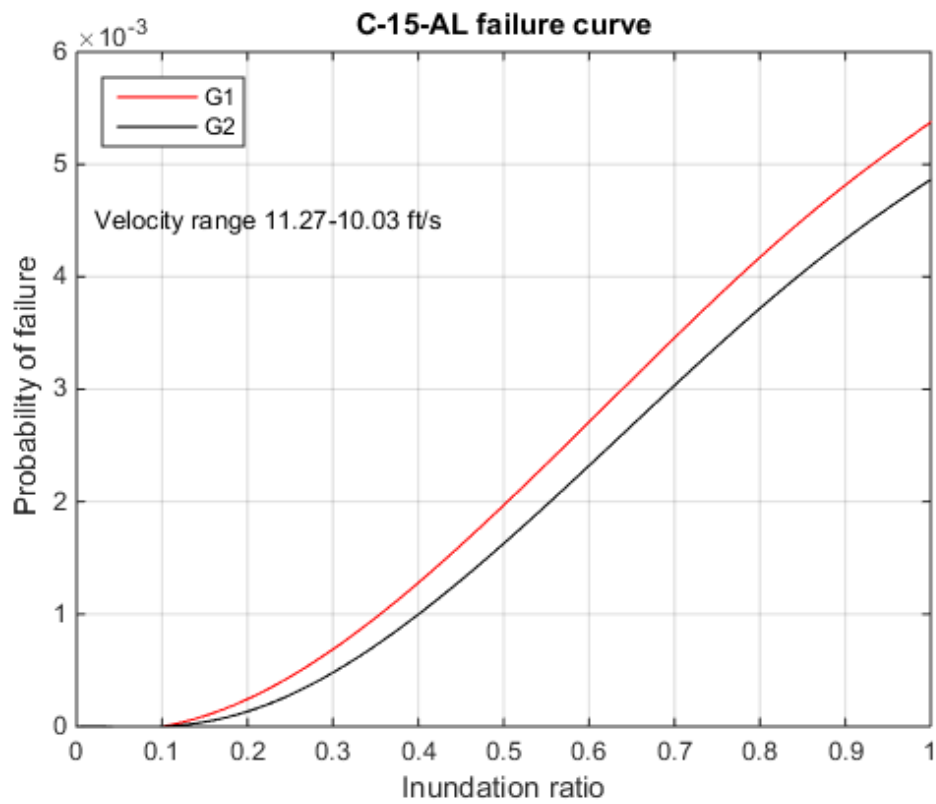


Figure 3.25 Probability of failure values for C-15-AL

The beta values are 2.67 and 2.70 for the external and internal girders. To satisfy the target beta value criterion for the 100 and 500 year flood event, the bridge would need to be raised by 1' and 9' respectively. These values are very similar to C-15-AM, which is to be expected.

3.3 Bridge C-15-O results

C-15-O is a 2 span prestressed box girder bridge located 2.65 miles downstream from C-15-AL. The floodplain has limited vegetation and the river approaches with little meandering. This leads to higher velocity values when compared to the previous bridges. Field measurements determined that there was 1.5' of degradation at the bridge exit, which led to altering the LiDAR data to reflect the post flood repairs by CDOT.



Figure 3.2 Cross sections generated in ArcMap for C-15-O

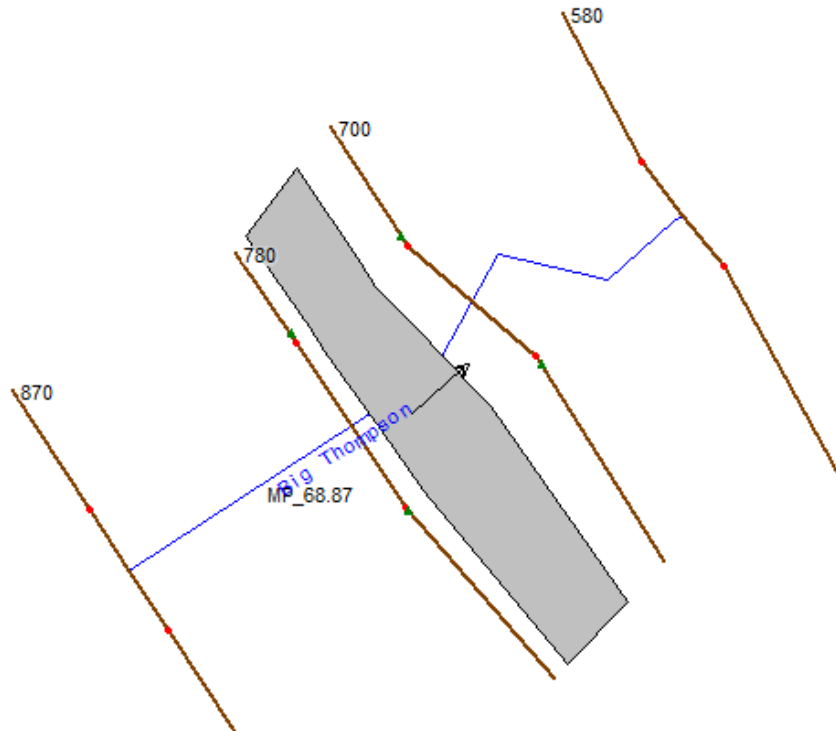


Figure 3.3 HEC-RAS geometric plan view for C-15-O

The cross sections used for the HEC-RAS model only required the four necessary cross sections for generating a rating curve at a bridge. When adding an additional cross section further up or downstream, the produced curve values stayed the same. This makes sense for the downstream cross section due to the flow having already fully expanded and there are little obstructions to affect the flow at the approach section. The additional upstream cross section had no affect for this bridge due to the channel slope and floodplain topography being identical to the already present cross sections. Damage suffered at C-15-O as a result of the September flood was 2.5' of erosion at abutment 1's retaining wall, 4–12" of exposed caisson top for two of the pier columns, crack in asphalt overlay at abutment 1 and multiple minor cracks throughout the wingwalls and retaining walls.

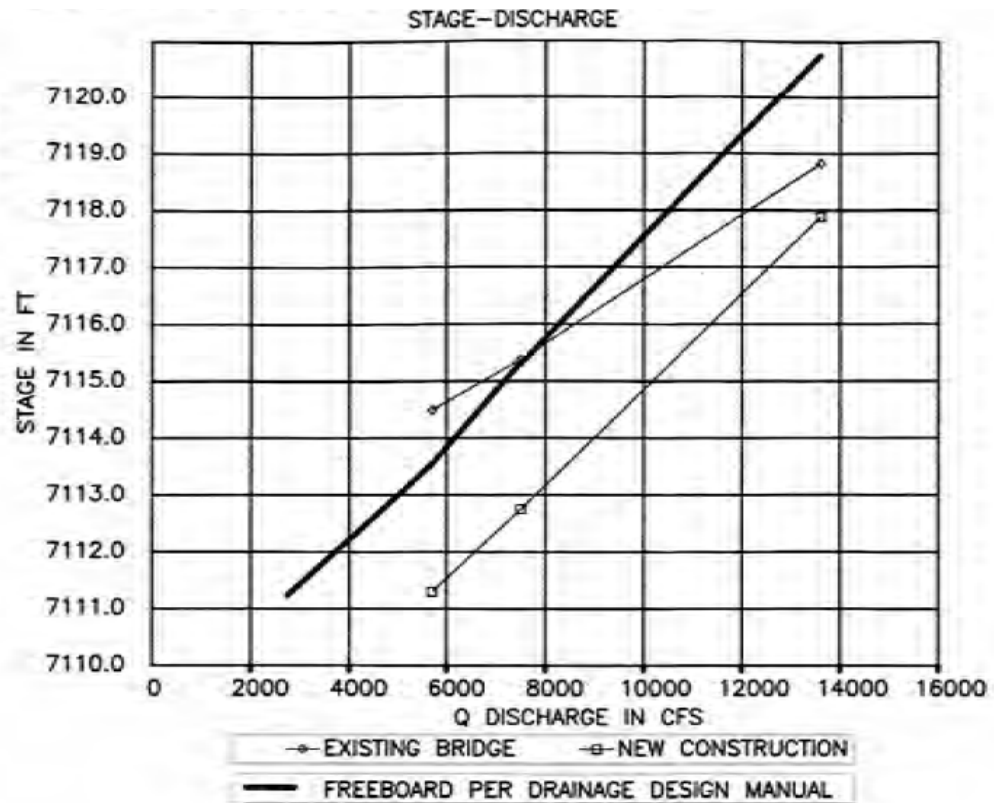


Figure 3.4 Plan rating curve for C-15-O (CDOT see Appendix A)

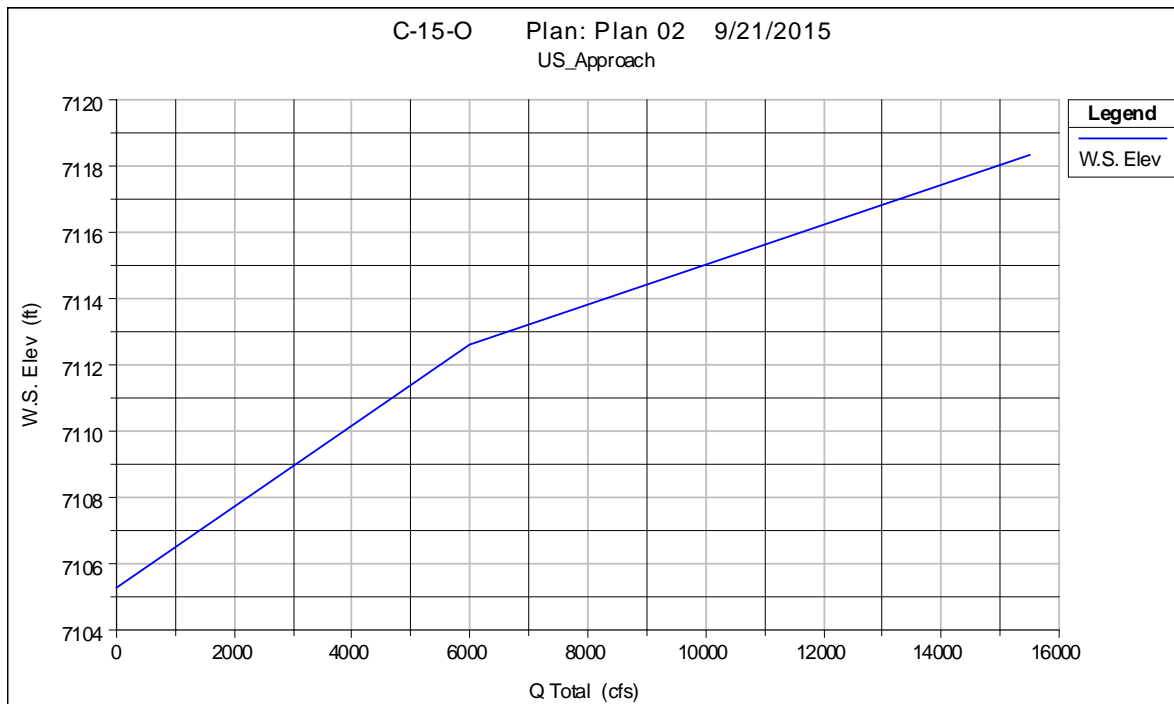


Figure 3.5 HEC-RAS rating curve for C-15-O

Figure 3.30 and 3.31 display the rating curve from the bridge hydraulic information sheet and the generated curve from HEC-RAS. The contact and overtopping discharge values for the plans' curve are 7800 and 11900 cfs respectively, whereas the HEC-RAS curve values are 6400 and 12300 cfs. This compares very well, and the main difference lies with the velocity values. The bridge information gives a single value for velocity of 10.6 ft/s, which is considerably lower than the HEC-RAS values of 14.32-16.19 ft/s. Channel and floodplain alterations since the time of the construction can lead to this discrepancy.

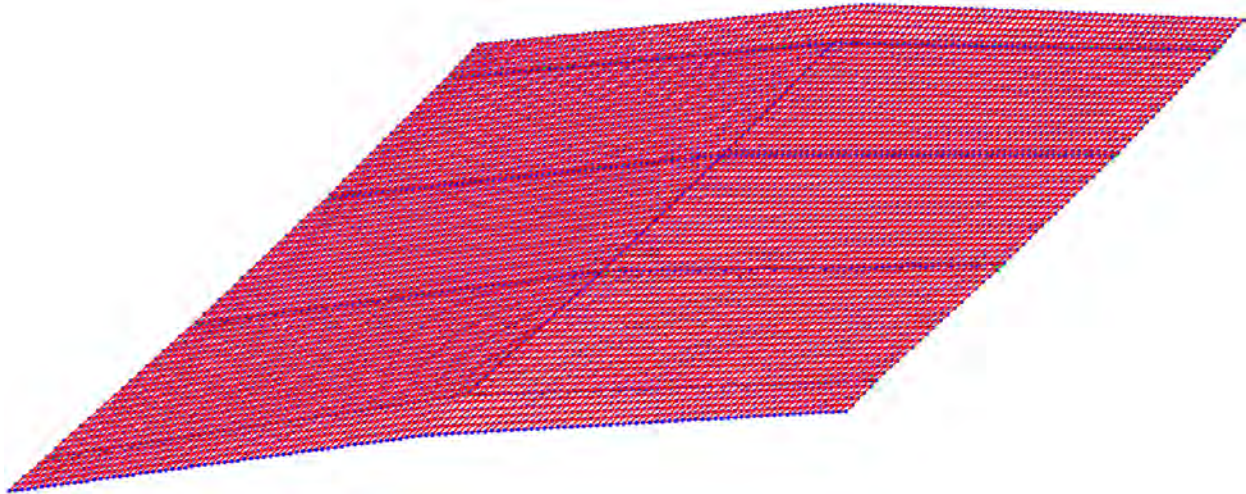


Figure 3.30 SAP2000 model for C-15-O

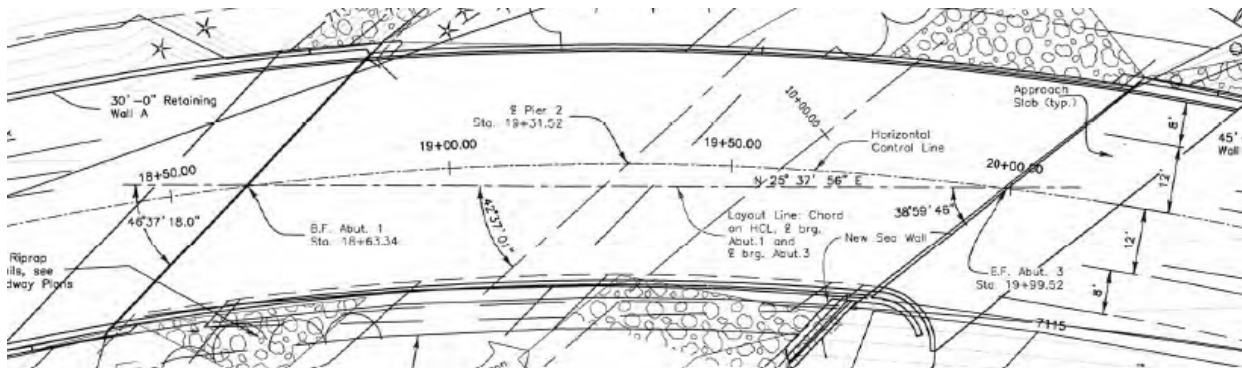


Figure 3.31 Plan view of the bridge deck of C-15-O (CDOT see Appendix A)

This bridge had several different skew angles at each bent that made it difficult to mesh uniformly and not have any misaligned rigid links. When comparing the skew at abutment one, the models skew is 40.76° as opposed to the plans value of 46.62° . At the pier, the angle stayed the same and resulted in a difference of 1.86° . At abutment 3, the model skew was 38.84° versus 39.99° from the plans. Overall, there is good agreement with the FE model and the actual bridge.

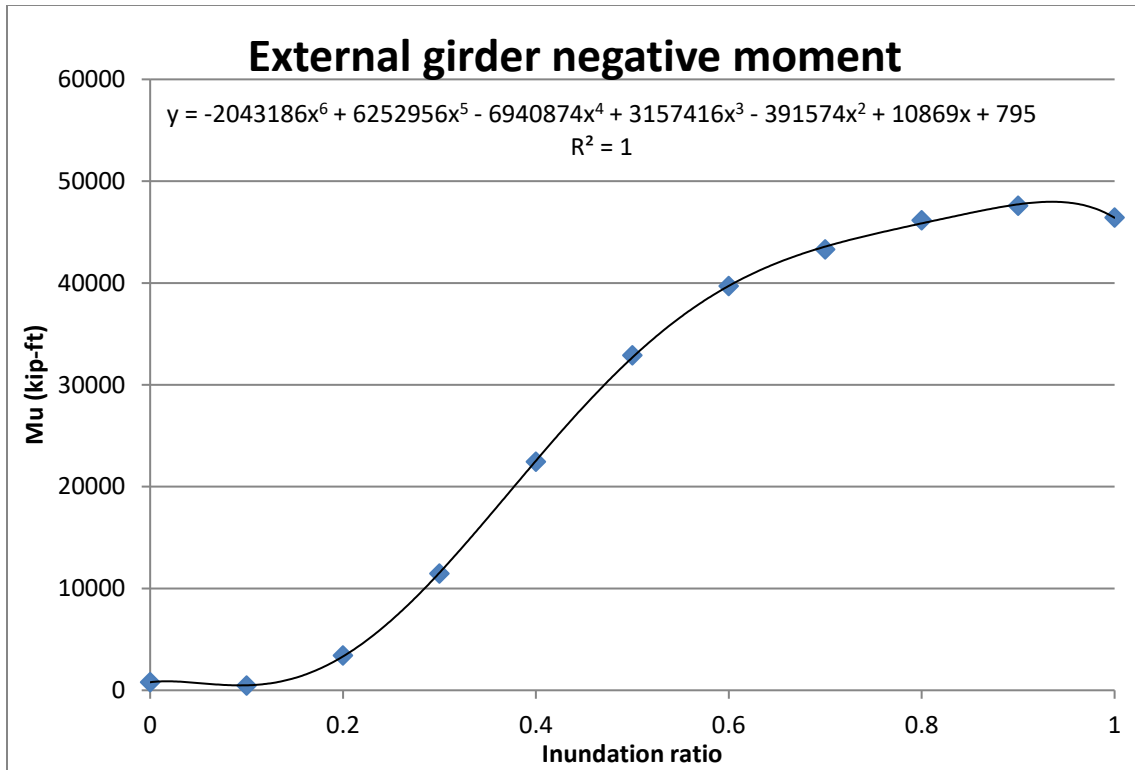


Figure 3.32 Applied negative moment felt by G1 span 2 for C-15-O

Figure 3.32 is a polynomial best fit line for the resulting negative moment on G1 due to the applied negative lift force. The overall trend is expected and follows the lift coefficient shape. The initial dip at $h^*=0.2$ is due to the buoyancy force controlling and exerting an uplift force on the bridge.

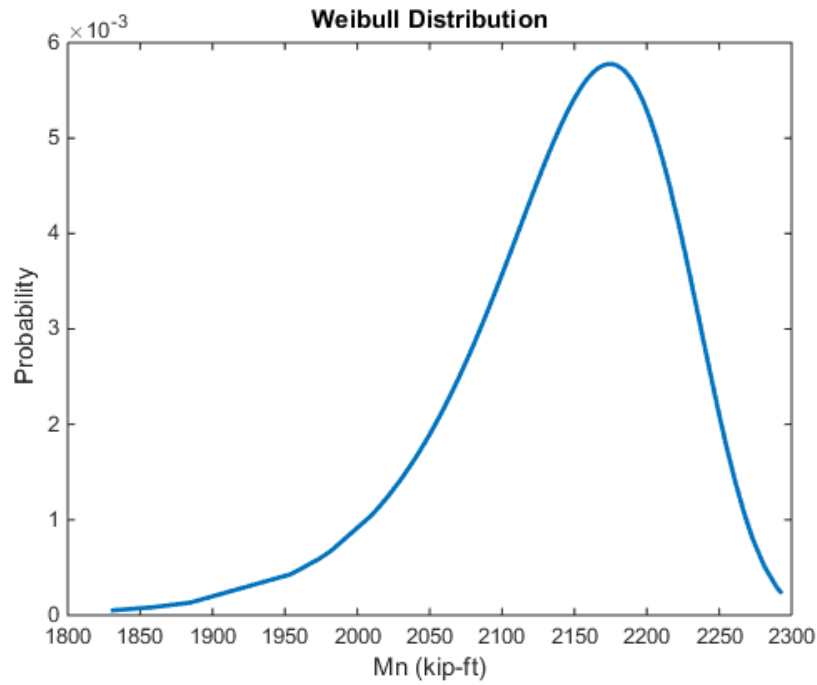


Figure 3.33 Negative nominal moment capacity for an external girder for C-15-AL

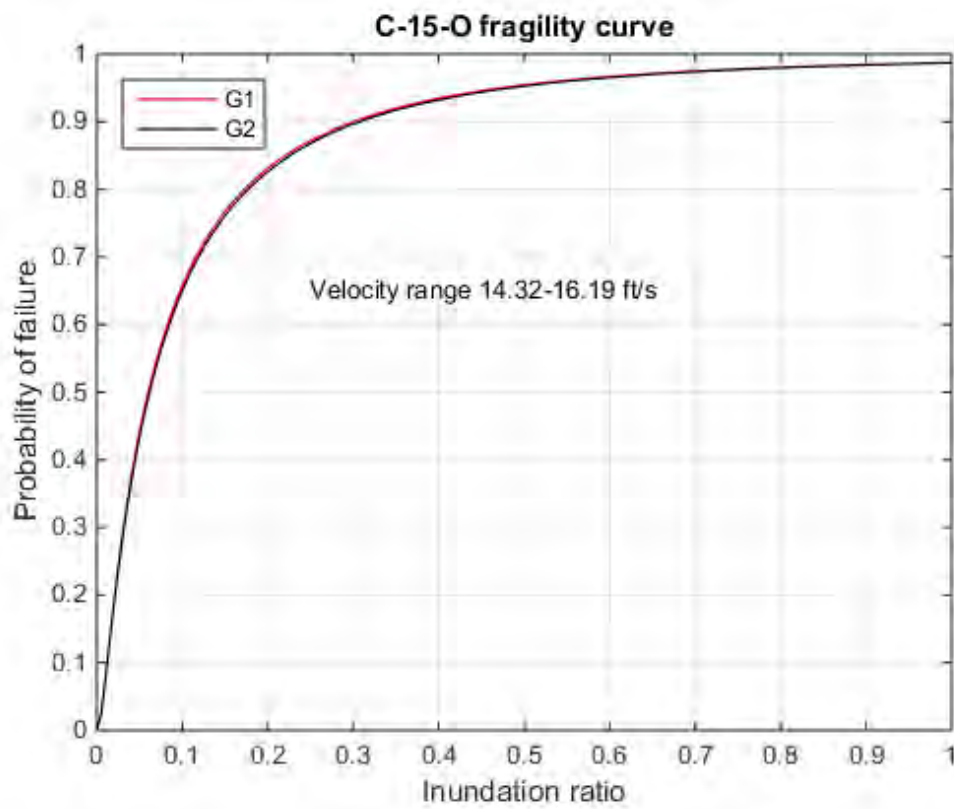


Figure 3.6 Fitted lognormal CDF function to the fragility values for C-15-AM

Figure 3.33 displays the resulting fitted Weibull PDF to the Monte Carlo simulation for the negative moment capacity. The normalized mean square error test resulted in a value of 0.9512, which is a good fit.

Figure 3.35 displays the fragility curve for C-15-O under the velocity range of 14.32 to 16.19 ft/s. The curve is very steep due to the high velocity and force values. The negative moment capacity was reached between $h^*=0.1$ and $h^*=0.2$.

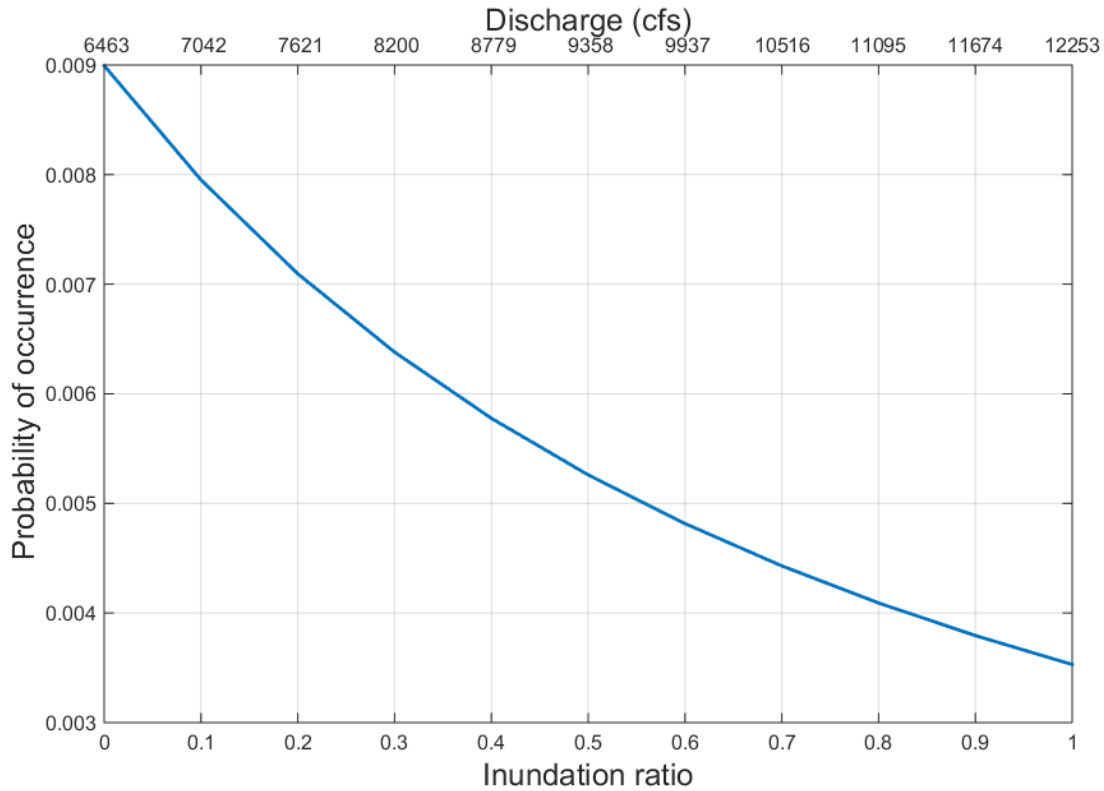


Figure 3.7 Hazard probabilities used to generate the probability of failure curve for C-15-O

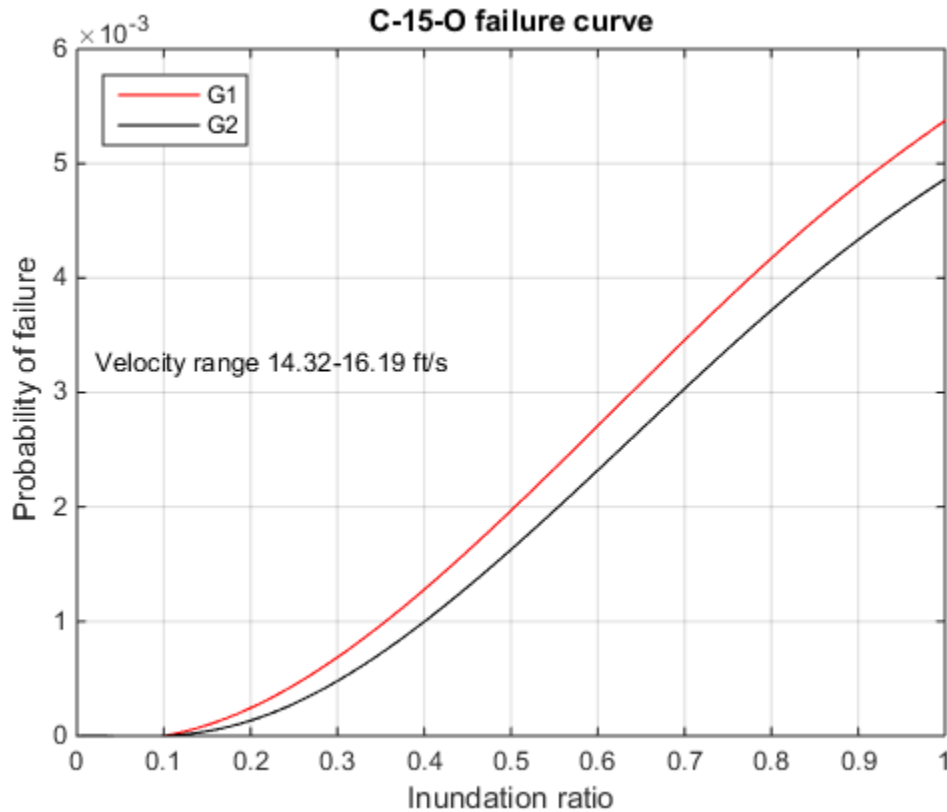


Figure 3.8 Probability of failure values for C-15-O

After incorporating hazard probabilities, the probability of failure values for the Big Thompson River location can be obtained. For this bridge, the beta values for the critical external and internal girder were 2.59. To meet the beta value criterion for the 100-year flood no adjustments are needed due to the flood not making contact with the low chord of the bridge. However, to meet the criterion for the 500-year flood, the bridge would need to be raised five feet.

3.4 Bridge C-15-U results

C-15-U suffered minor damage as a result of the September 2013 flood. There were cracks with efflorescence on the wingwall at abutment 1, cracks in the asphalt with small settlements at both abutments, exposed rebar at the downstream side of the wingwall at abutment 1 and spalling throughout the length of one of the four girders. The LiDAR data showed good agreement with the plan sheet elevations, so no revisions were necessary.

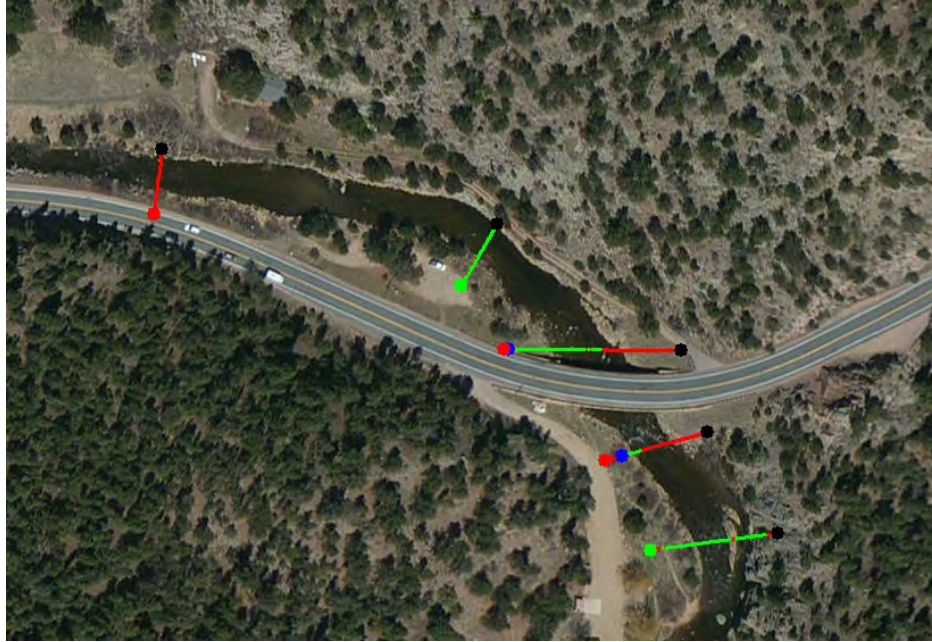


Figure 3.9 Cross sections generated in ArcMap for C-15-U

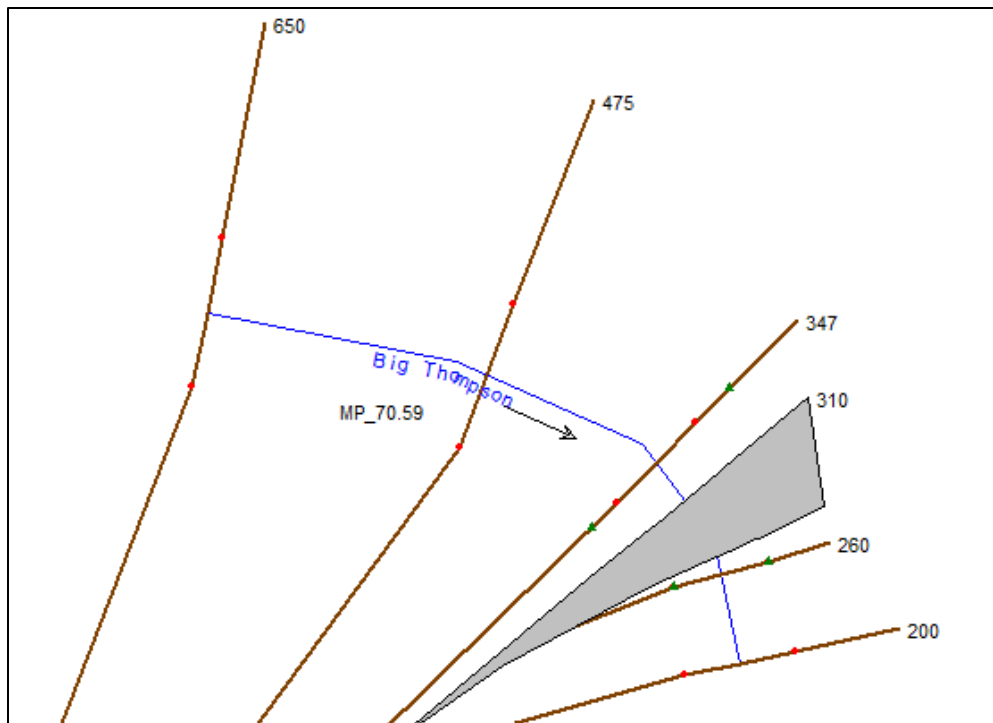


Figure 3.10 HEC-RAS geometric plan view for C-15-U

Figure 3.37 and 3.38 show a plan view of the actual bridge and the HEC-RAS model. For this bridge, the extra upstream cross section was deemed necessary due to the change in floodplain and constricted channel overbank areas.

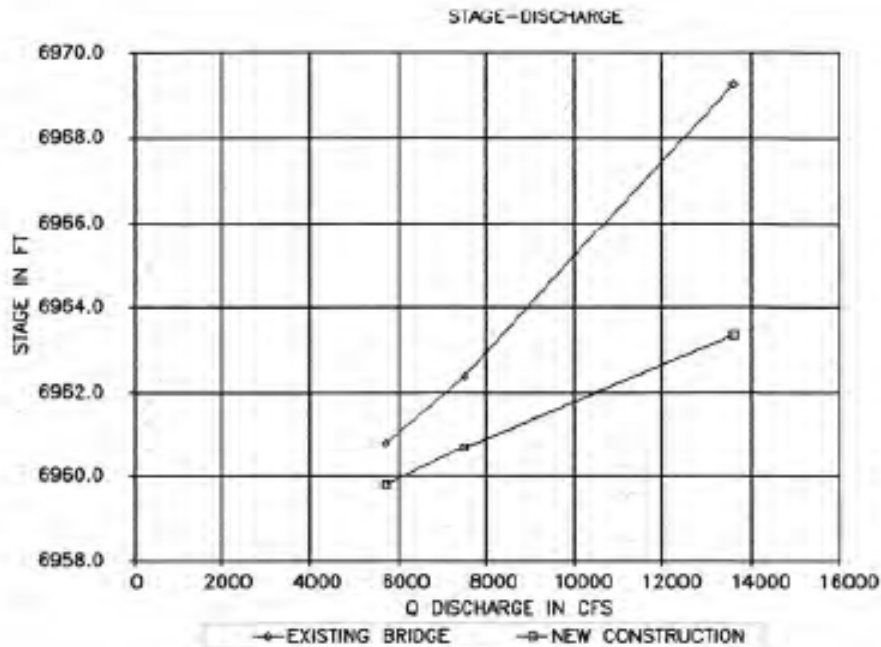


Figure 3.11 Plan rating curve for C-15-U (CDOT see Appendix A)

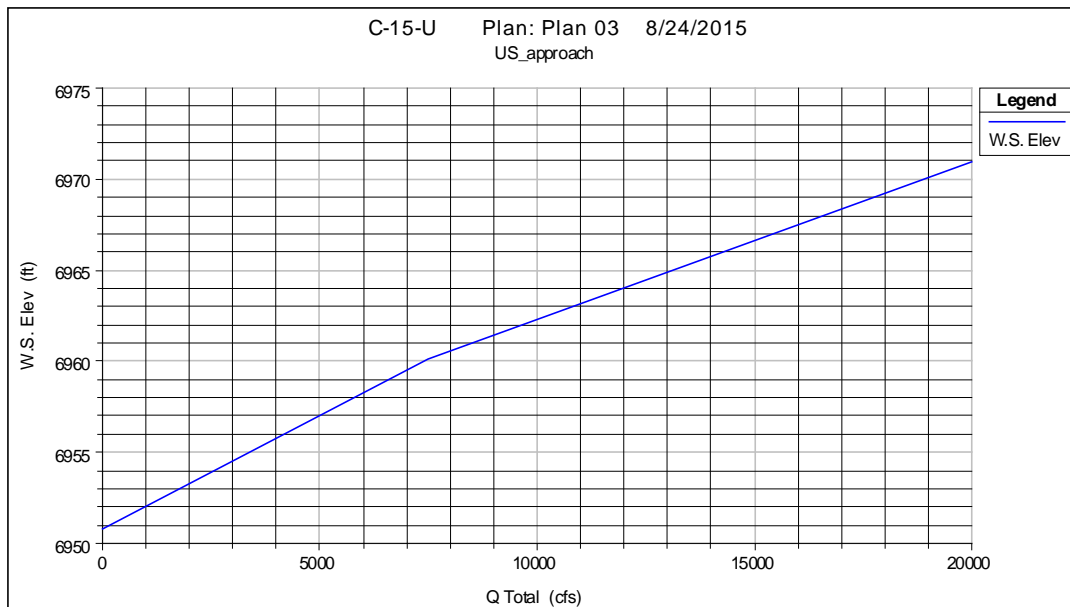


Figure 3.40 HEC-RAS rating curve for C-15-U

Due to the overtopping discharge not being listed on the plan rating curve, the only gauge of accuracy was on the contact discharge. The plans had a contact discharge value of 11000 cfs compared to 10400 cfs from the HEC-RAS curve. The velocity values generated on the HEC-RAS model are in close agreement with the ultimate velocity on the plans. The models velocity ranges from 7.22 to 5.13 ft/s compared to the ultimate velocity of 7.60 ft/s.

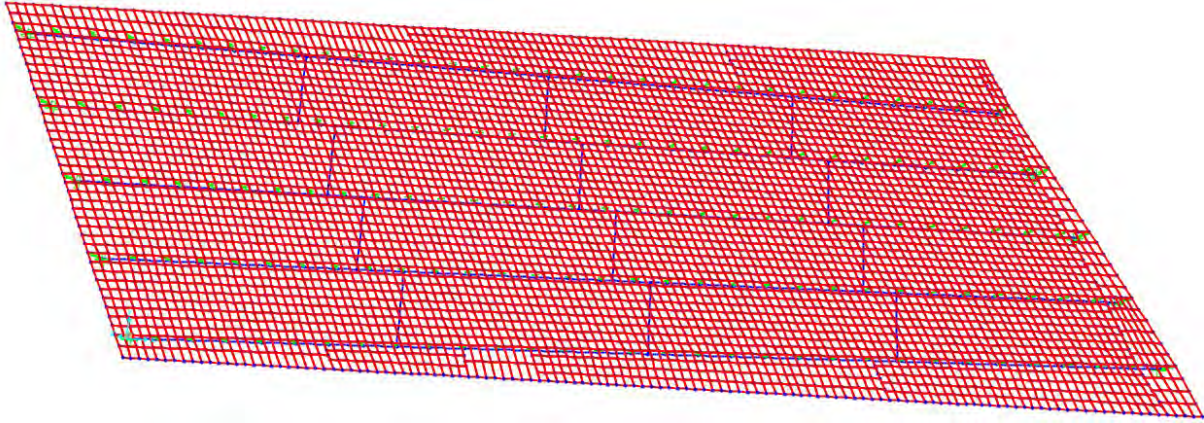


Figure 3.41 SAP2000 model for C-15-U

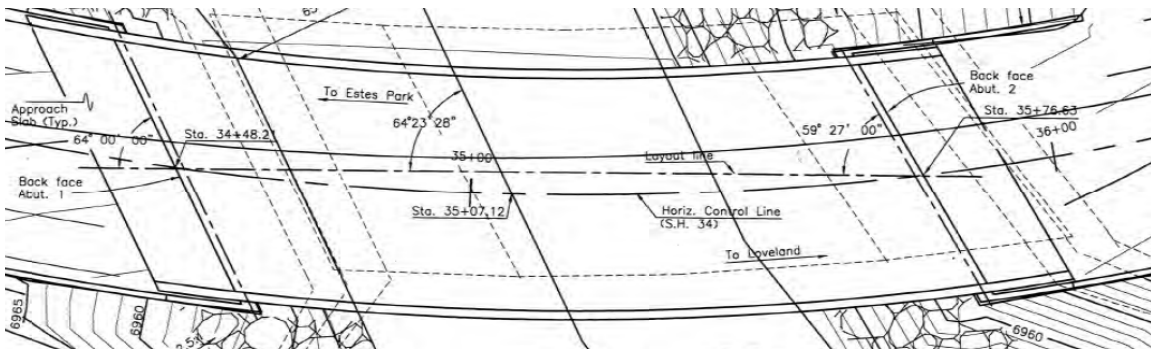


Figure 3.42 Plan view of the bridge deck of C-15-U (CDOT see Appendix A)

The difference in the skew angles at abutment 1 and 2 are 0.01° and 0.15° respectively. This is a prestressed bulb tee 5 girder single span bridge. There are some meshes on the shell elements whose nodes do not line up due to the varying overhang distances throughout the bridge length. Instead of modeling the curved nature of the slab, it was modeled as a trapezoidal shape taking into account the overhang values at each abutment. The few nodes whose meshes do not line up are not an issue as long as it does not occur at the rigid link locations, which it does not.

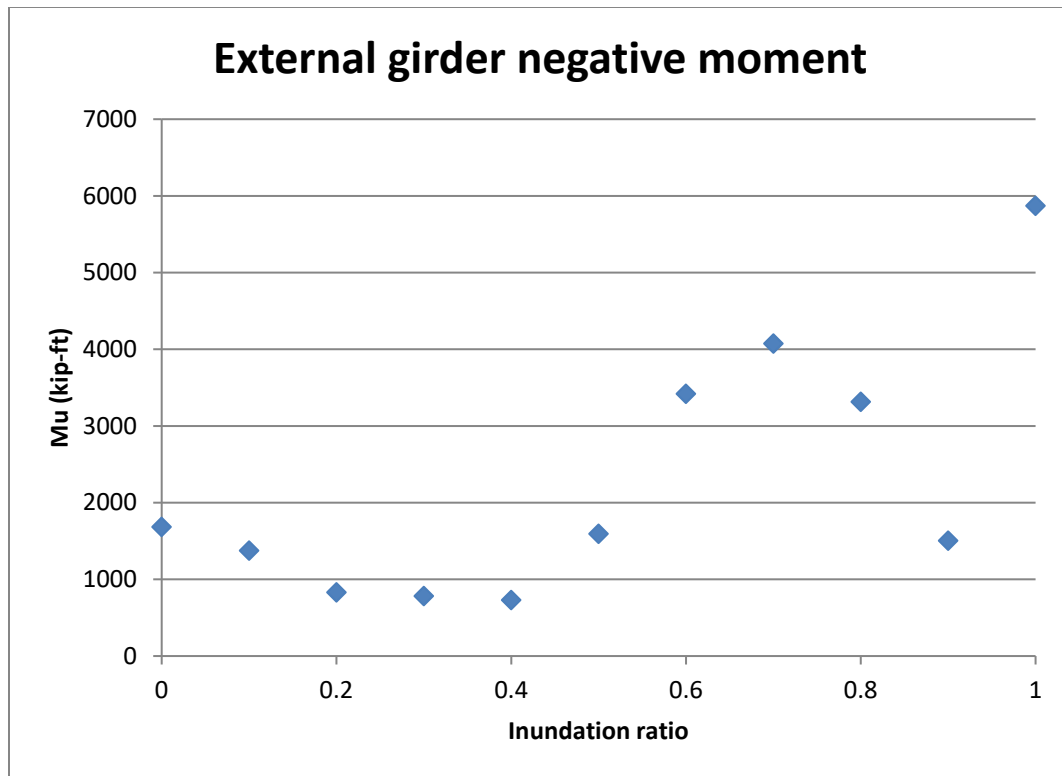


Figure 3.43 Applied negative moment felt by G1 for C-15-U

Figure 3.43 displays the negative moment felt by G5 under the negative lift force. The relatively low velocity values, large variation in abutment heights and buoyancy forces leads to the roller-coaster values for the girder. For example, if abutment 2 is under the condition of $h^*=1.0$, then abutment 1 feels $h^*=0.595$.

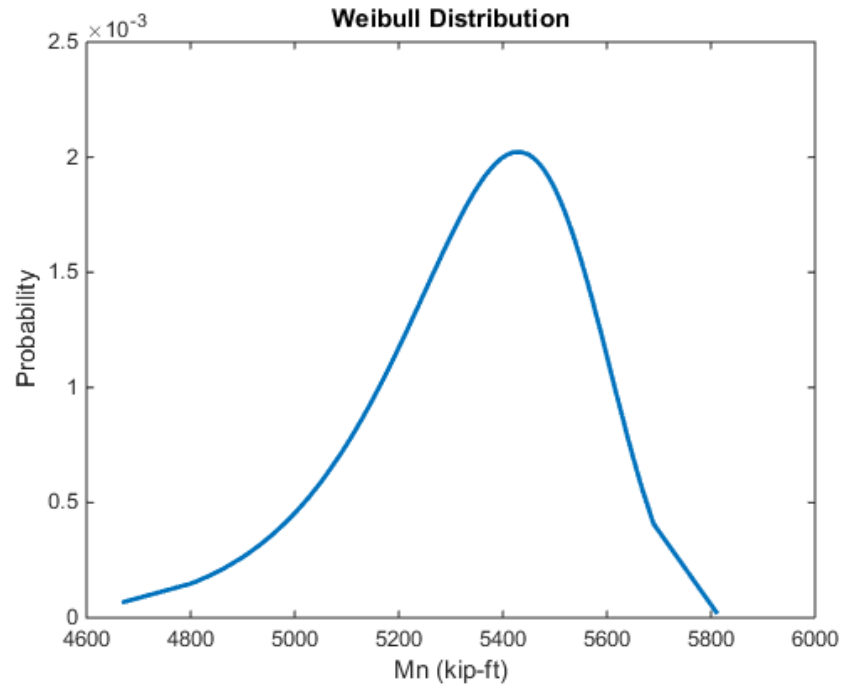


Figure 3.12 Negative nominal moment capacity for an external girder for C-15-U

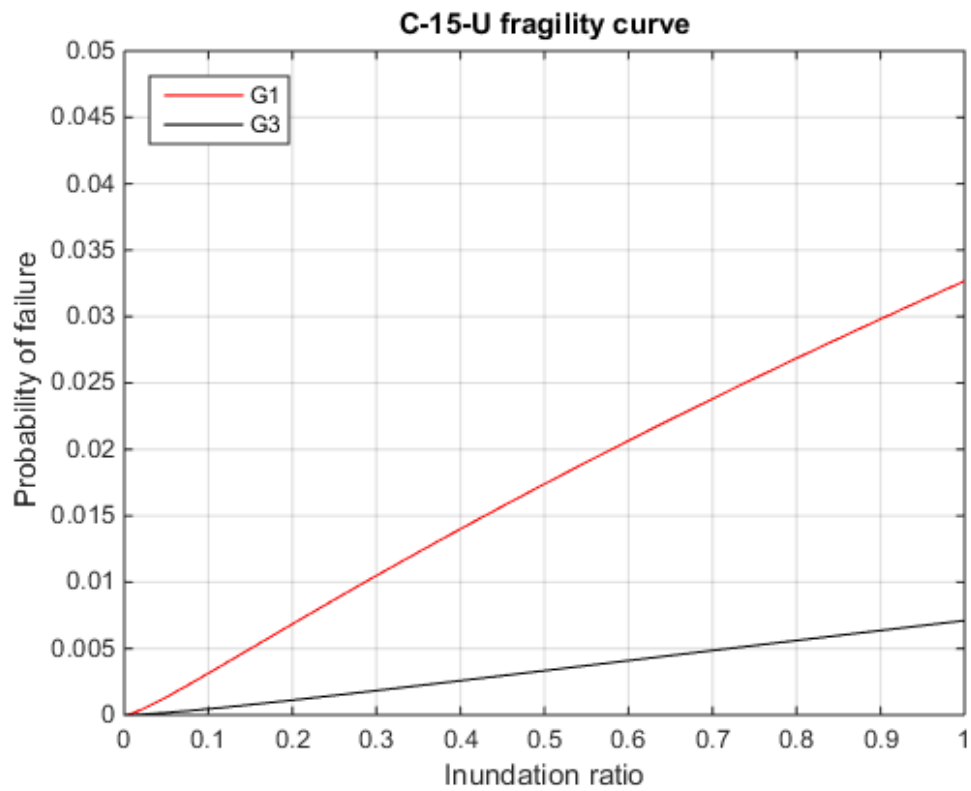


Figure 3.13 Fitted lognormal CDF function to the fragility values for C-15-U

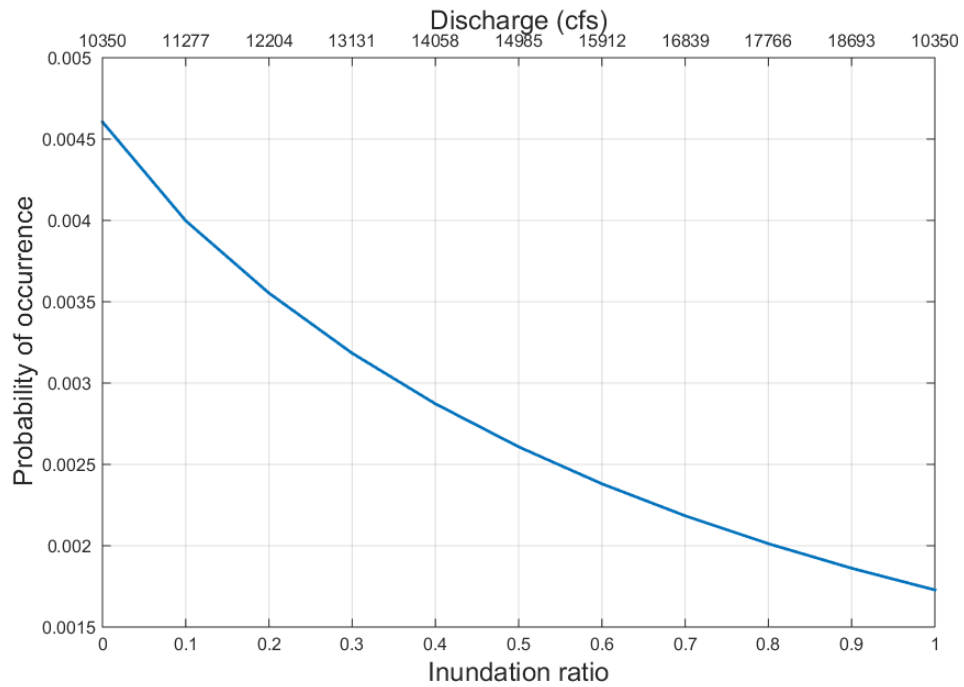


Figure 3.14 Hazard probabilities used to generate the probability of failure curve for C-15-U

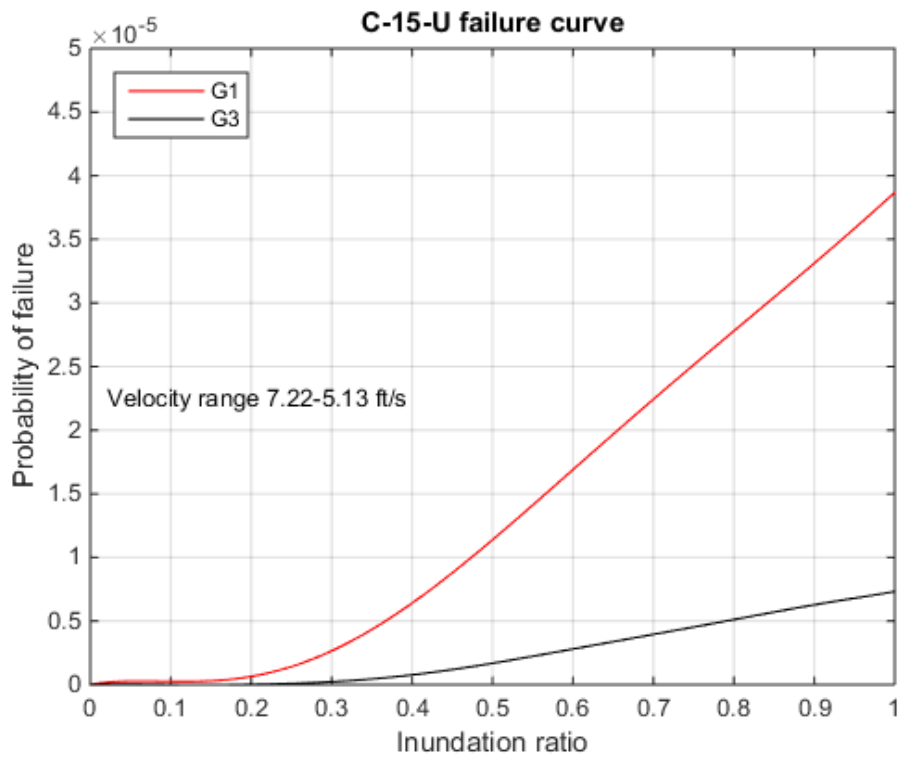


Figure 3.15 Probability of failure values for C-15-U

For this bridge, the fragility and probability of failure curve values are very small due to the high member capacity coupled with a low applied moment. The minimum nominal negative moment capacity value of 4600 kip-ft as shown in Figure 3.44 is exceeded by the applied moment felt at $h^*=1.0$. This leads to the very low failure probabilities, which can be seen on Figure 3.46 and 3.47. Not surprisingly, the beta value criterion is already met at the current bridge elevation. The beta values are 3.95 and 4.33 for the external and internal girders respectfully.

3.5 Bridge C-15-Y results

C-15-Y is located at the confluence with the North Fork Big Thompson River. This bridge suffered the most damage in this study as a result of the 2013 flood. All the fill and riprap was washed out at both wing walls, the channel bottom aggraded over five feet, a portion of the approach roadway was destroyed due to structural fill being washed out and there were transverse and vertical cracks on the underside of the bridge deck. Due to the severe channel damage, the LiDAR data was adjusted to the elevations on the construction plans.

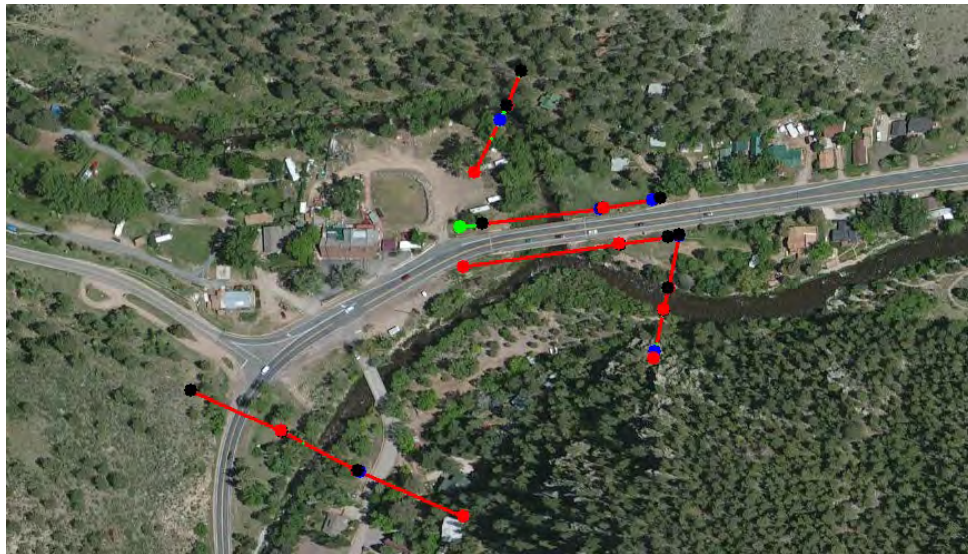


Figure 3.16 Cross sections generated in ArcMap for C-15-Y

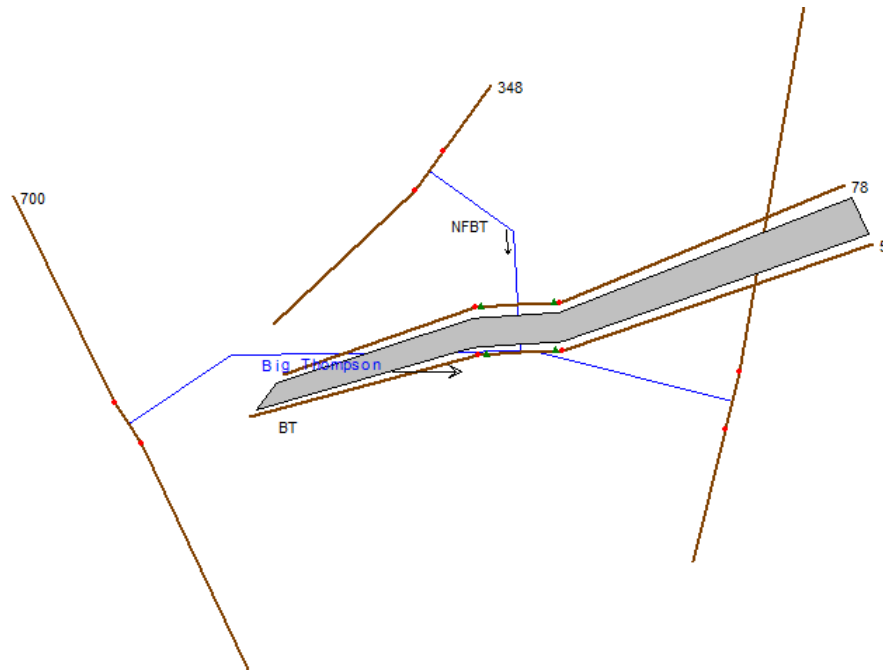


Figure 3.17 HES-RAS geometric plan view for C-15-Y

Figure 3.48 and 3.49 display the ArcMap and HEC-RAS cross sections used for C-15-Y at the mouth of the North Fork Big Thompson River. As a result of the confluence of the two rivers, an extra upstream cross section was needed for the Big Thompson River. Bridge C-15-Y is located at the center of Drake, CO. It should be noted that although the bridge section seems to overlap the Big Thompson River, the model does not treat it as such. Due to the flat and wide floodplain for this area, the bridge was extended to account for the road elevation.

The contact and overtopping discharge values for the model match well with the bridge hydraulic information sheet. For contact and overtopping discharge, the plan sheet has values of 2500 and 7500 cfs which compare well with the values of 2007 and 8736 cfs from the HEC-RAS model. For velocity, the plan has an ultimate value of 6.63 ft/s as opposed to 8.95-14.10 ft/sec on the model. However, considering the extent of damage to the bridge under the flood forces, the bridge sheet could easily have underestimated the velocity values.

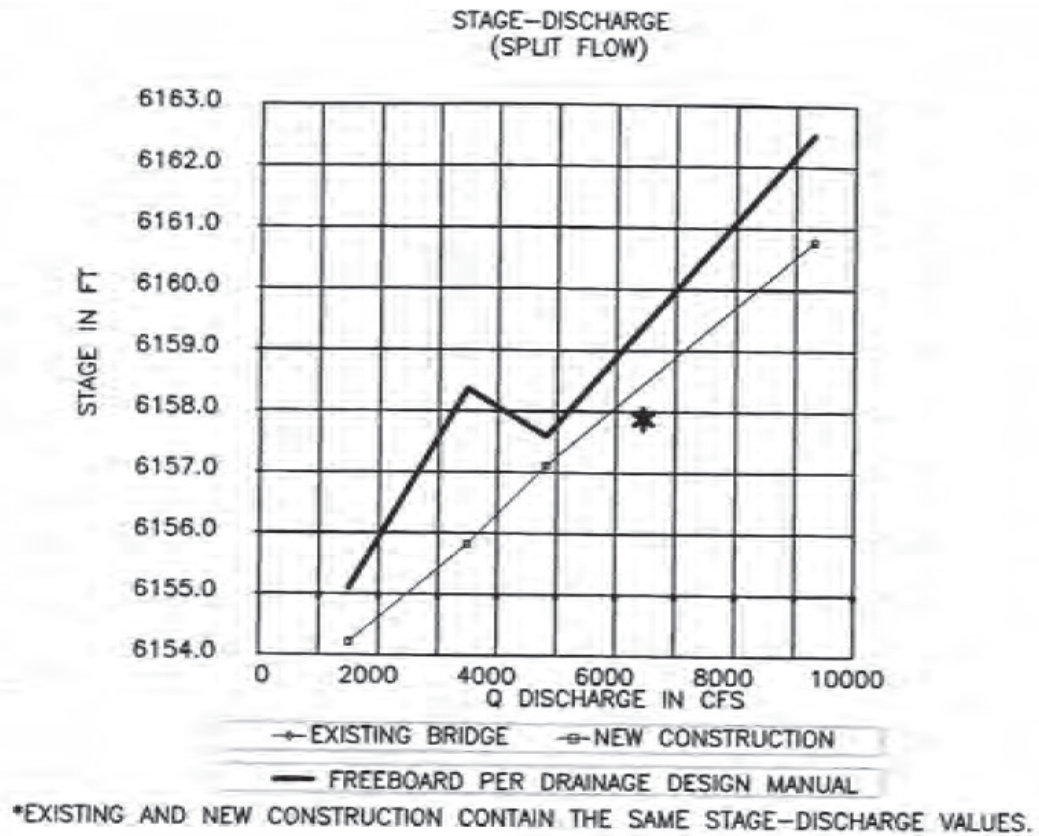


Figure 3.50 Plan rating curve for C-15-Y (CDOT see Appendix A)

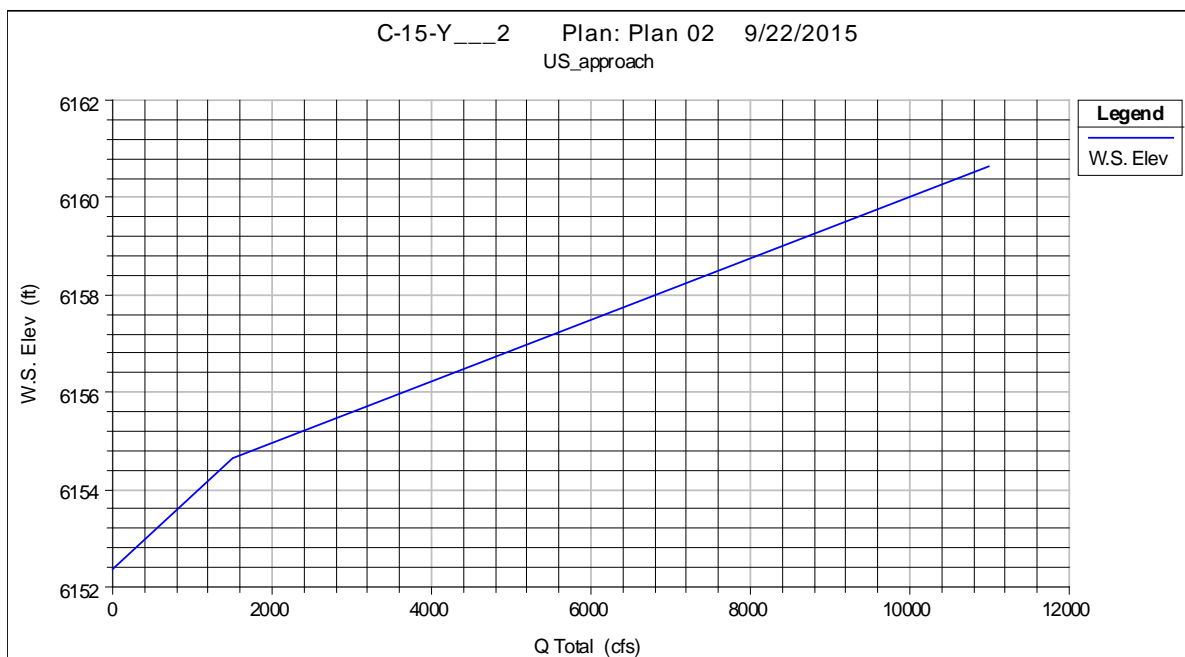
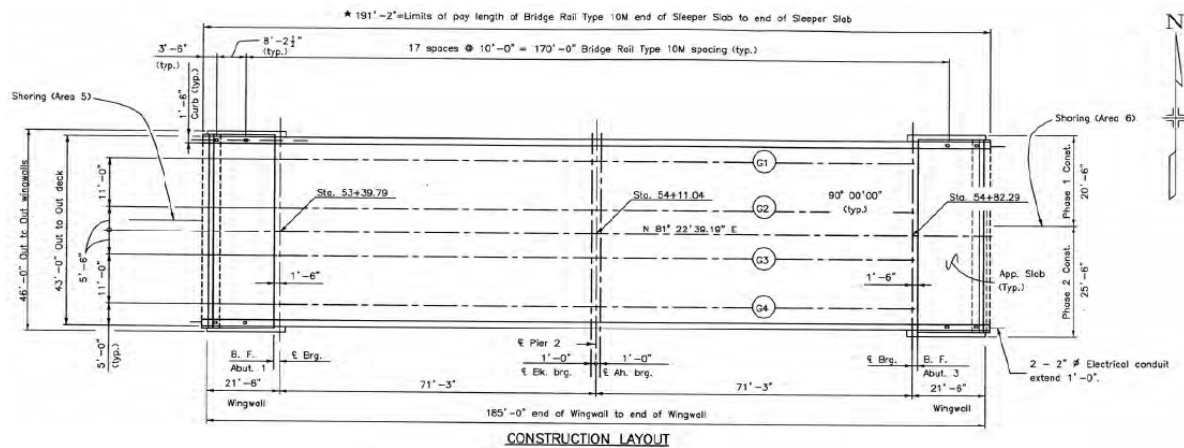
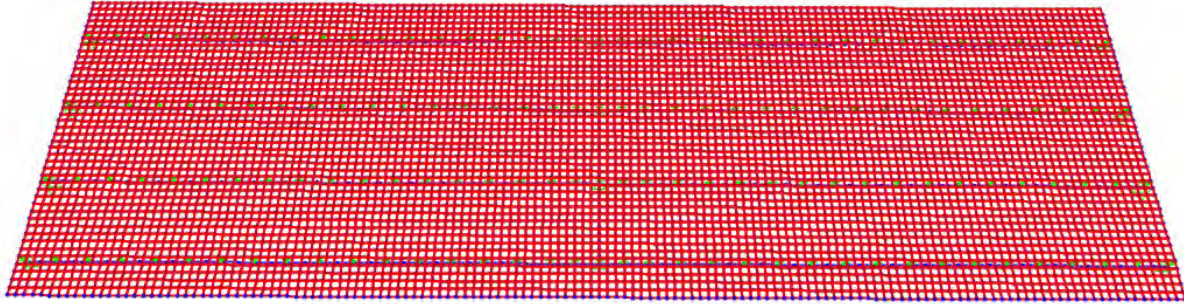
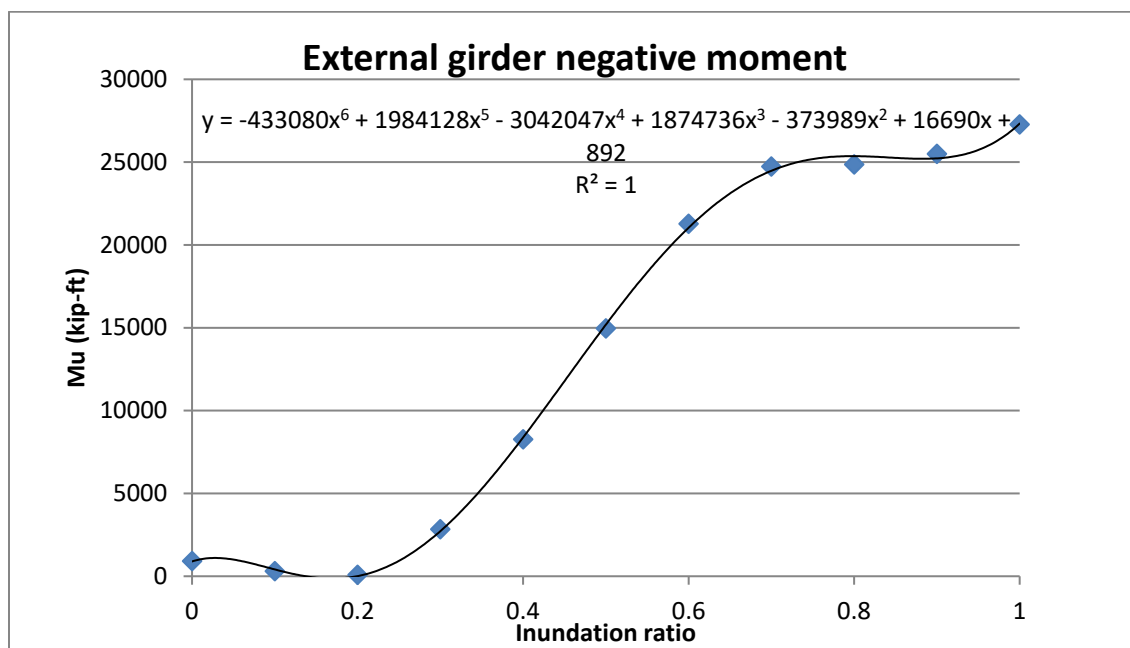


Figure 3.51 HEC-RAS rating curve for C-15-Y



C-15-Y is a rectangular four girder prestressed box girder bridge with a fixed condition at the abutments and a pin condition at the pier. Given the symmetry and lack of a skew, meshing and aligning the nodes was a straightforward task.



The slight dip after $h^*=0$ is due to the net lift force being positive at the lower h^* values. The overall trend is expected and follows the lift coefficient shape.

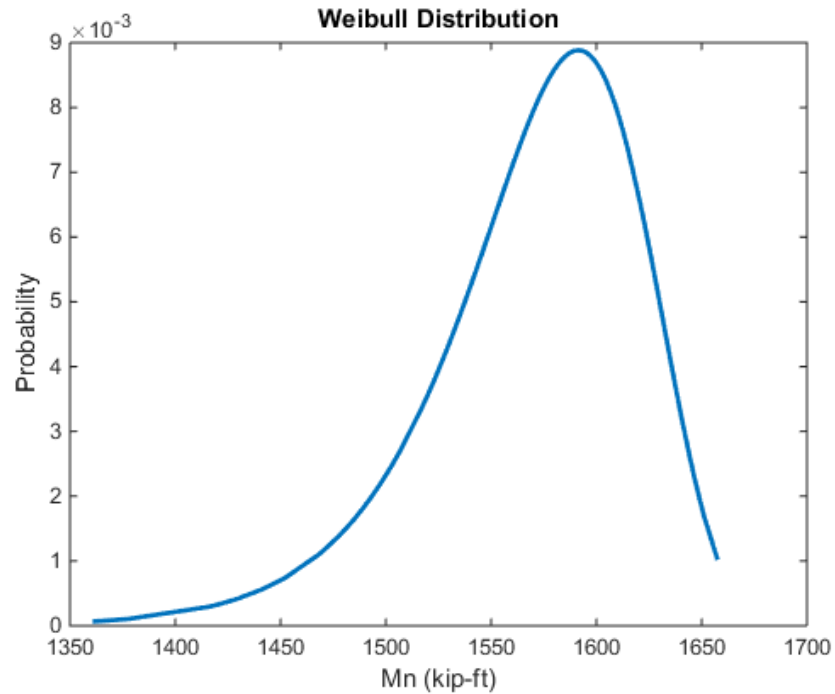


Figure 3.19 Negative nominal moment capacity for an external girder for C-15-Y

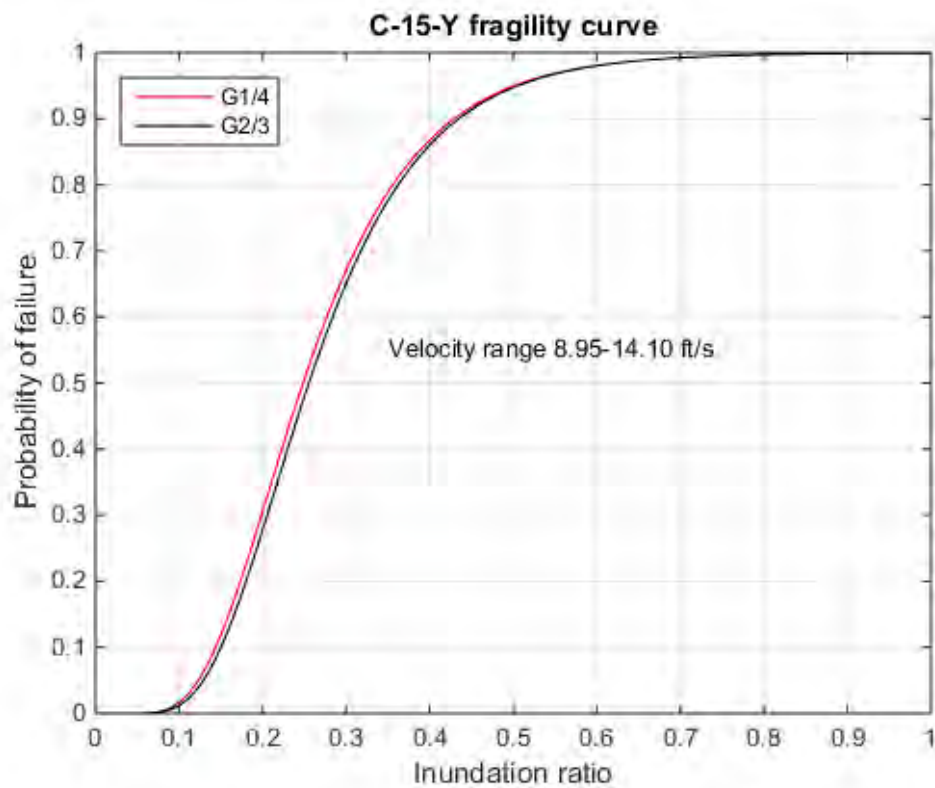


Figure 3.20 Fitted lognormal CDF function to the fragility values for C-15-Y

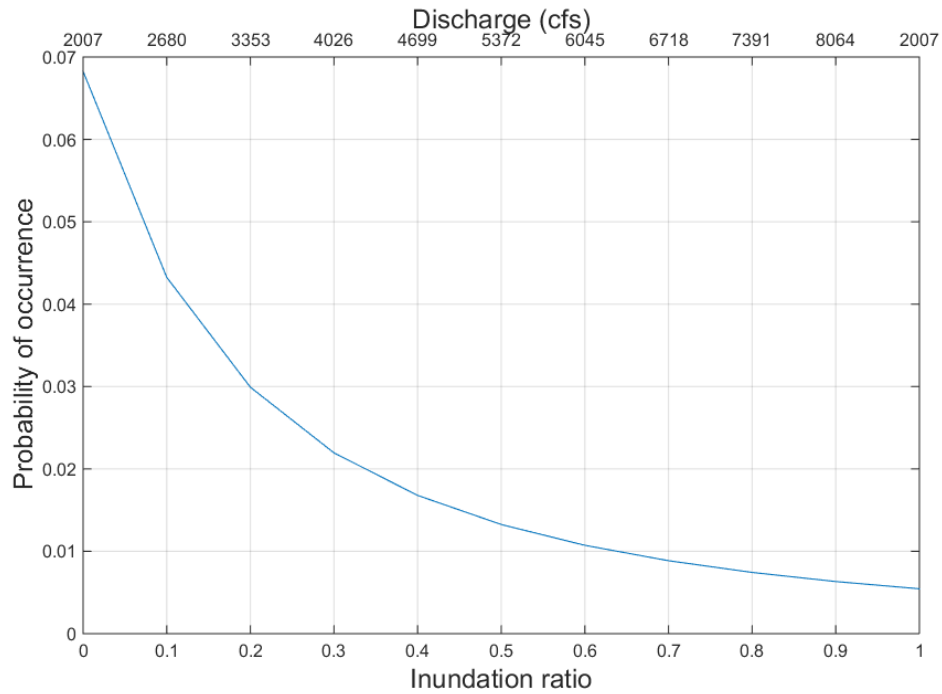


Figure 3.21 Hazard probabilities used to generate the probability of failure curve for C-15-Y

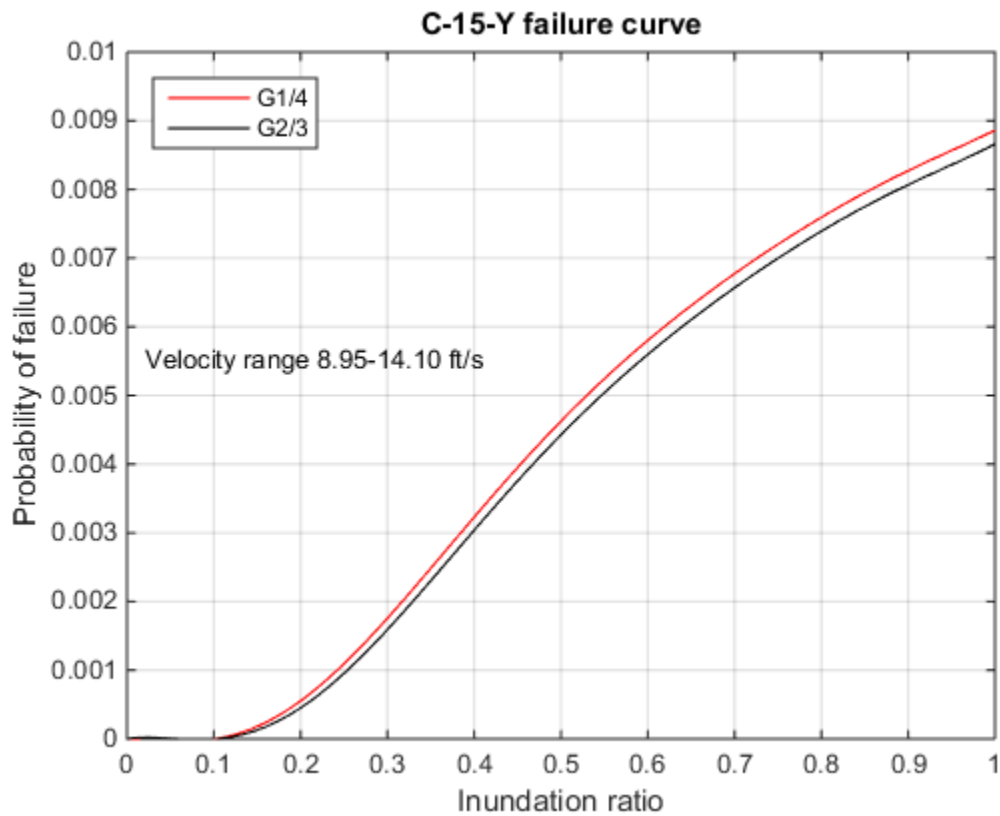


Figure 3.22 Probability of failure values for C-15-Y

The beta values for the external and internal girders are 2.37 and 2.38 respectfully. To meet the target beta value for the 100 and 500-year floods, the bridge would need to be raised 2' and 6'. Another flood resiliency effort for this bridge would be to redesign the riprap to increase the protection from erosion. Erosion due to fast moving flood waters as well as debris impacts caused the majority of the damage from the September 2013 flood.

3.6 Bridge C-15-C results

C-15-C is the only steel I beam bridge in this study and was originally constructed in 1936. Major rehab was performed in 1997 to reconstruct the whole bridge. No rating curve or channel elevation was provided for this site. Also, no damage was reported due to the September 2013 flood. Based on field data, there was a 16–18' clear distance from the low chord of the girder to the channel bottom. When comparing this to the LiDAR data, no adjustments were needed and data was taken as is with some minor adjustments made to the overbank areas.



Figure 3.23 Cross sections generated in ArcMap for C-15- C

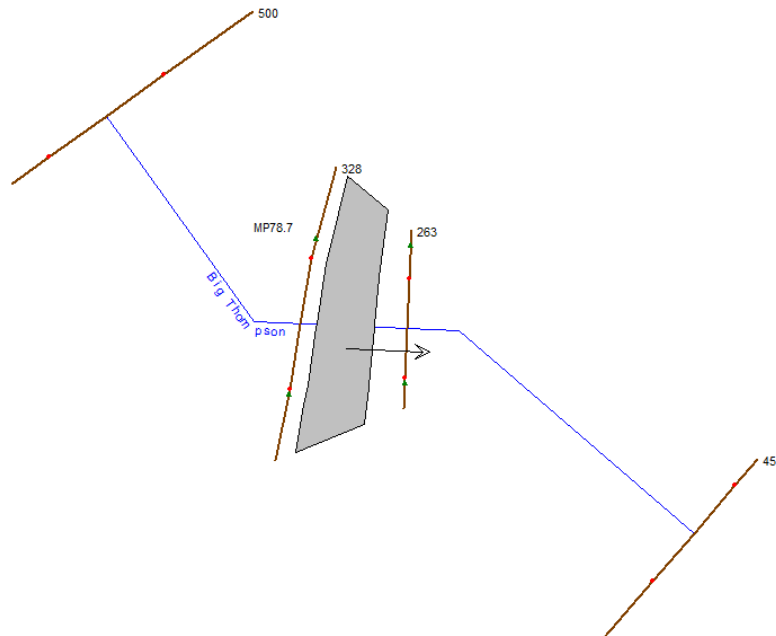


Figure 3.240 HEC-RAS geometric plan view for C-15- C

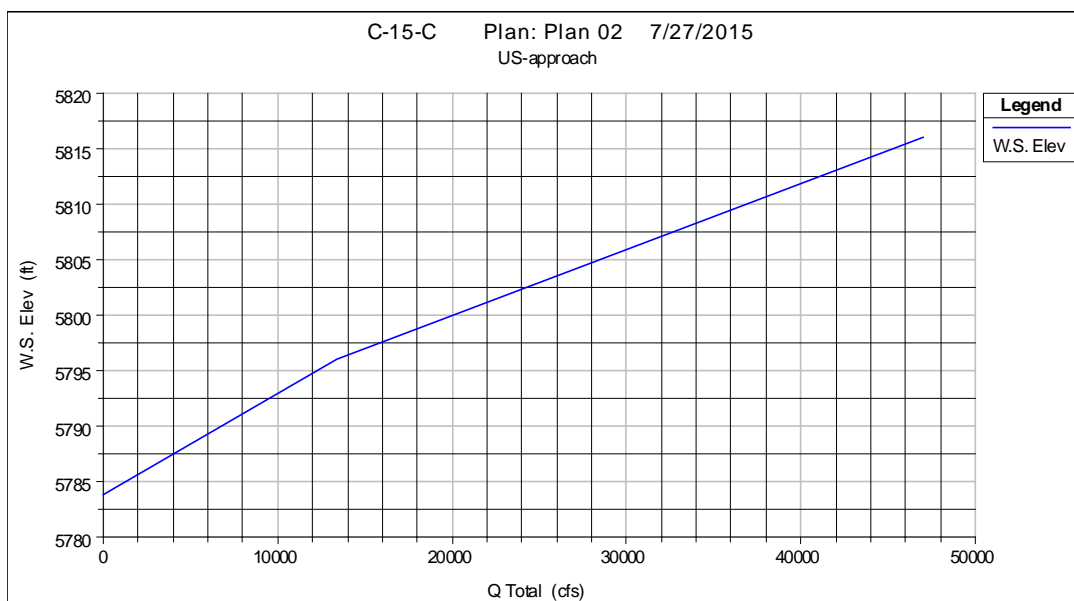


Figure 3.61 HEC-RAS rating curve for C-15- C

The best gauge of accuracy for the generated rating curve for C-15-C was to compare the contact and overtopping discharge values to the next downstream bridge C-15-AN. The contact and overtopping discharge values were 16754 and 24557 cfs, which differed by 1300 cfs for each value. A difference was expected, but the closeness of the magnitudes confirms that the values are not unreasonable. The velocity values for this bridge have a range of 14.80-15.62 ft/s.

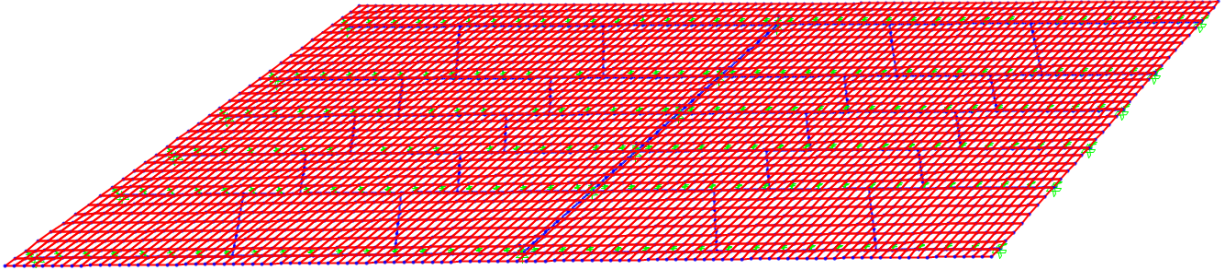


Figure 3.25 SAP2000 model for C-15- C

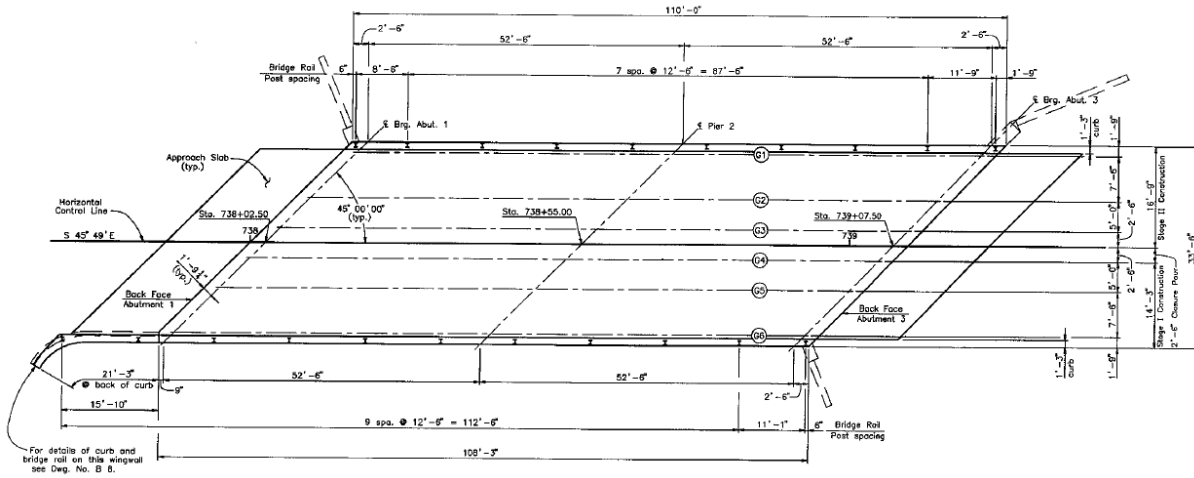


Figure 3.26 Plan view of the bridge deck of C-15- C (CDOT see Appendix A)

There is a uniform skew angle of 45° , which the SAP2000 model replicates exactly. C-15-C is a 6 girder 2 span bridge with a difference in elevation of 1.55' between abutments.

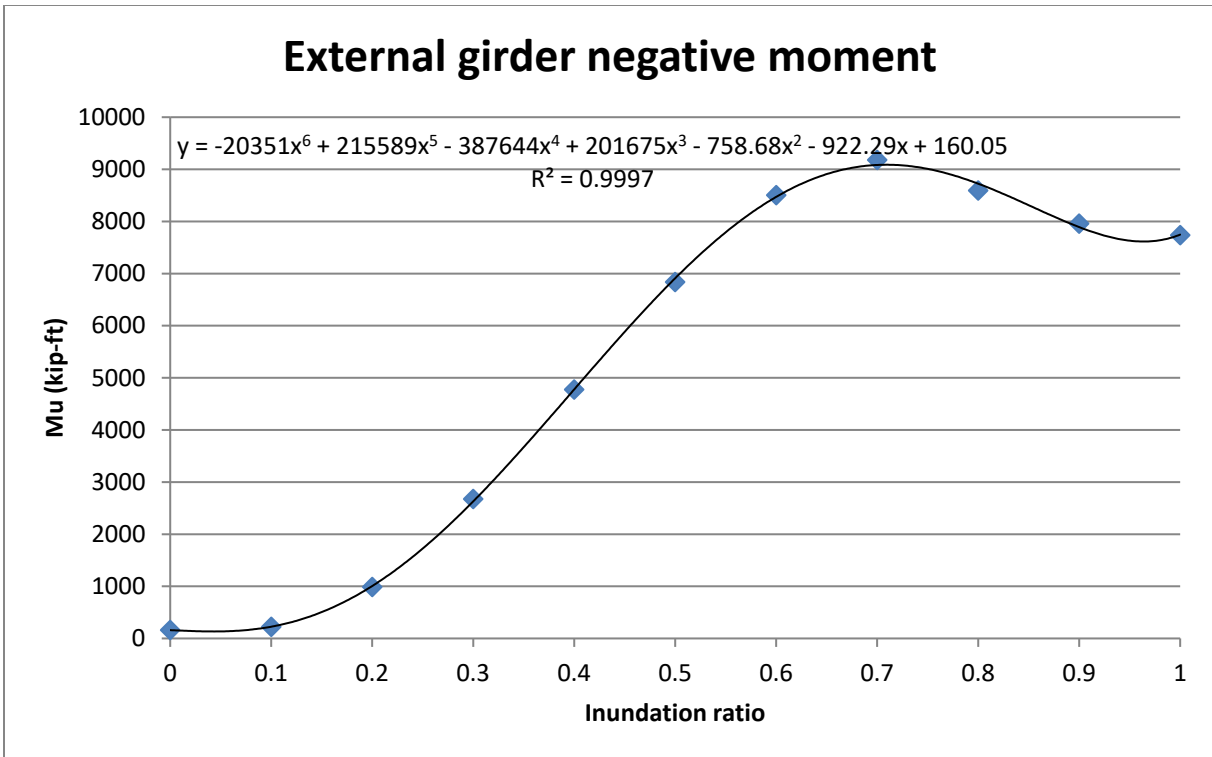


Figure 3.27 Applied negative moment felt by G6 for C-15- C

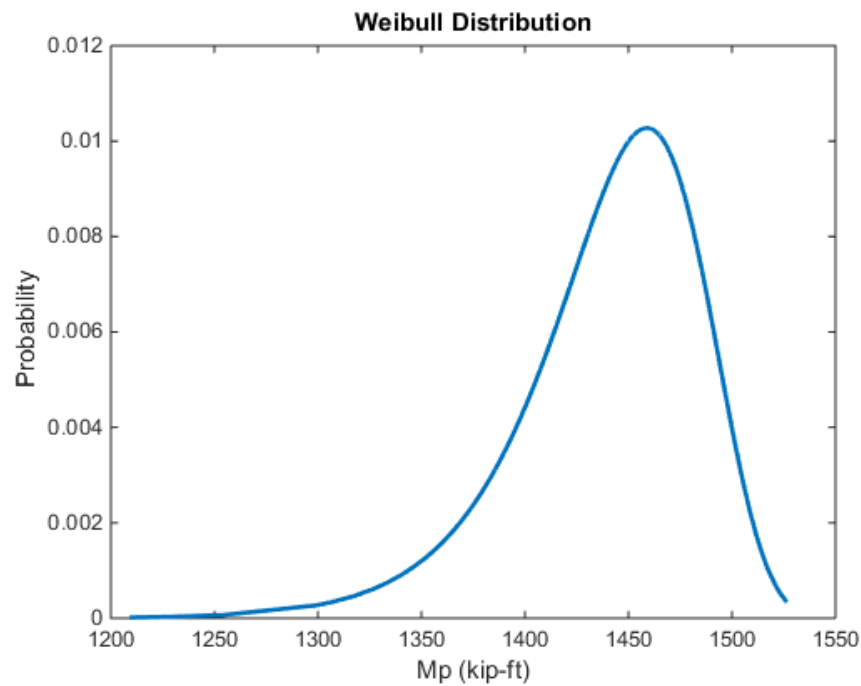


Figure 3.28 Negative nominal moment capacity for an external girder for C-15- C

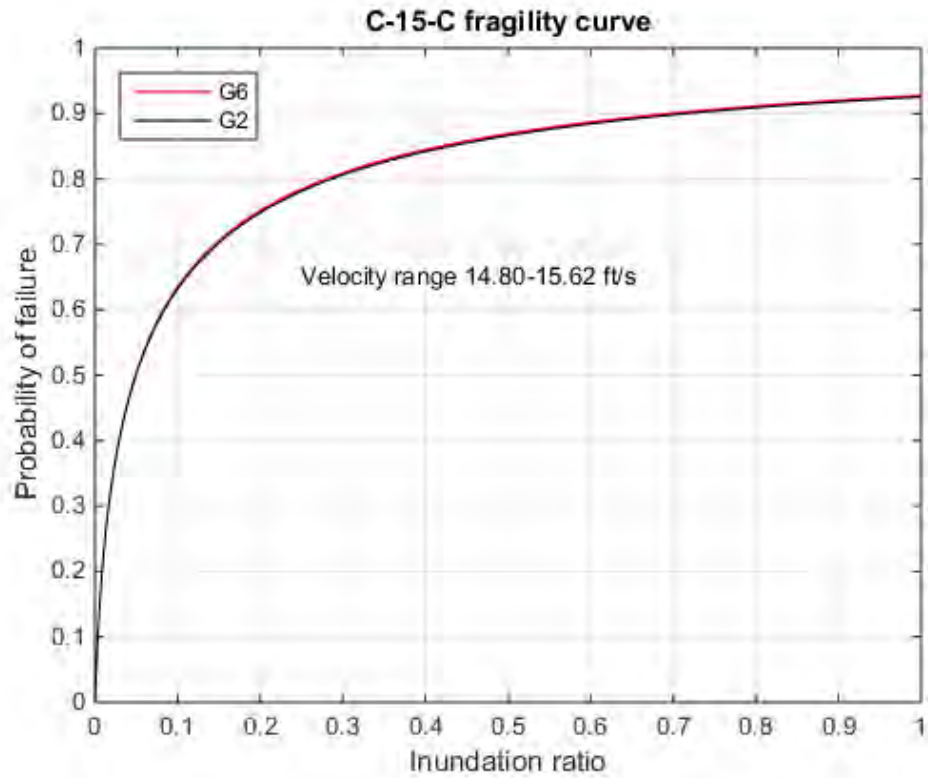


Figure 3.29 Fitted lognormal CDF function to the fragility values for C-15- C

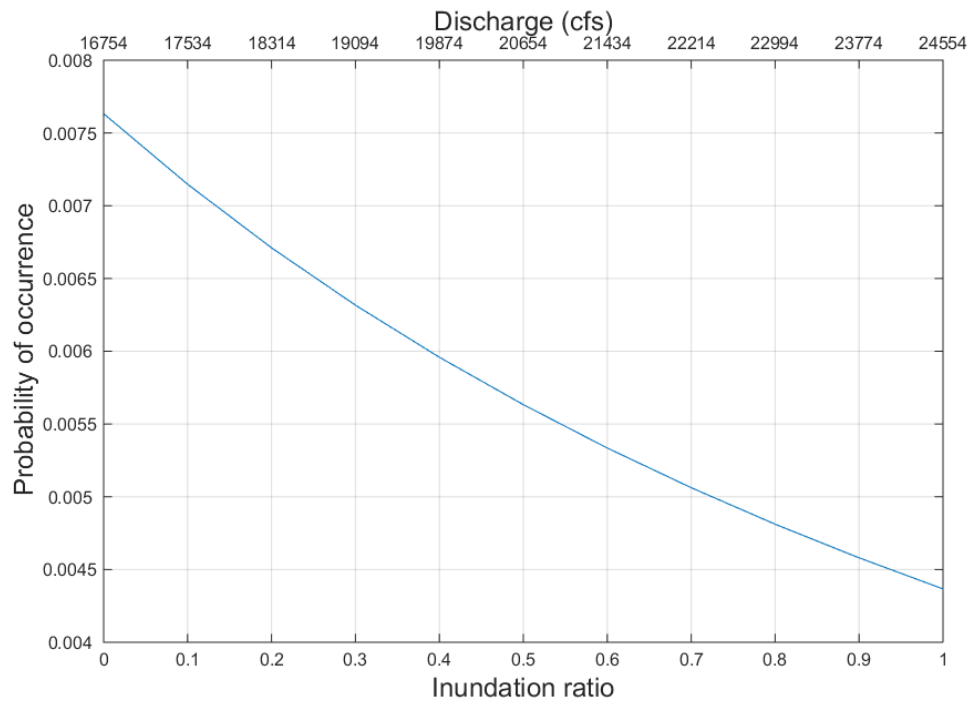


Figure 3.30 Hazard probabilities used to generate the probability of failure curve for C-15- C

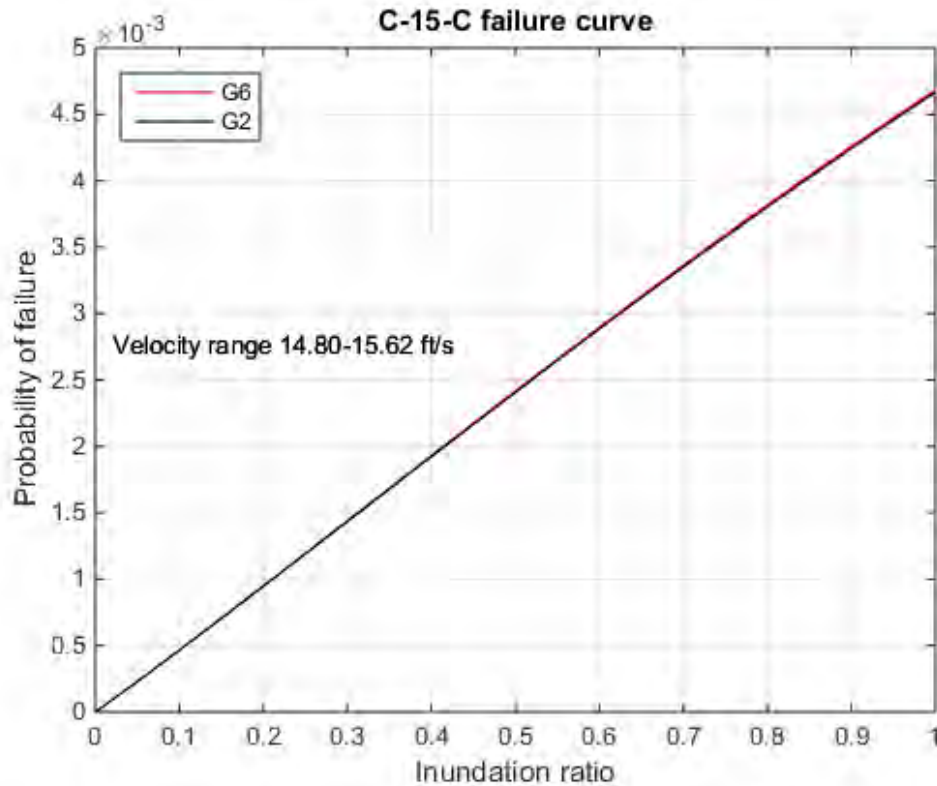


Figure 3.31 Probability of failure values for C-15- C

The beta values for the exterior and interior girder are 2.60. To reach the target beta value for the 100 and 500-year flood, the bridge would need to be raised 0' and 7.5'. The 100-year storm doesn't come in contact with the superstructure hence the lack of adjustments needed. For the 500-year flood, the bridge needs to be raised such that no contact is made with the superstructure due to the low capacity of the girders and the high demand as a result of the lift force.

3.7 Bridge C-15-AN results

C-15-AN is a prestressed box girder 3 span bridge located 2.42 miles downstream of C-15-C. No damage was suffered due to the September flood at this site. Comparing the field measurements to the plan elevations resulted in about one foot of degradation in the center of the channel. The LiDAR data was adjusted to match the plan elevations because of post flood repairs by CDOT. The channel overbank areas consist of a steep hill on the left bank and a large open area on the right bank with a gradual slope.



Figure 3.32 Cross sections generated in ArcMap for C-15- AN

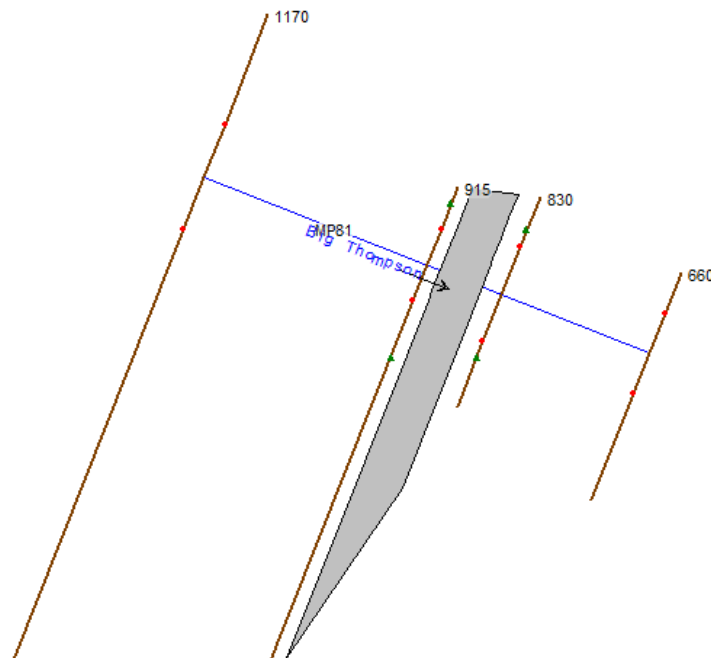


Figure 3.70 HEC-RAS geometric plan view for C-15- AN

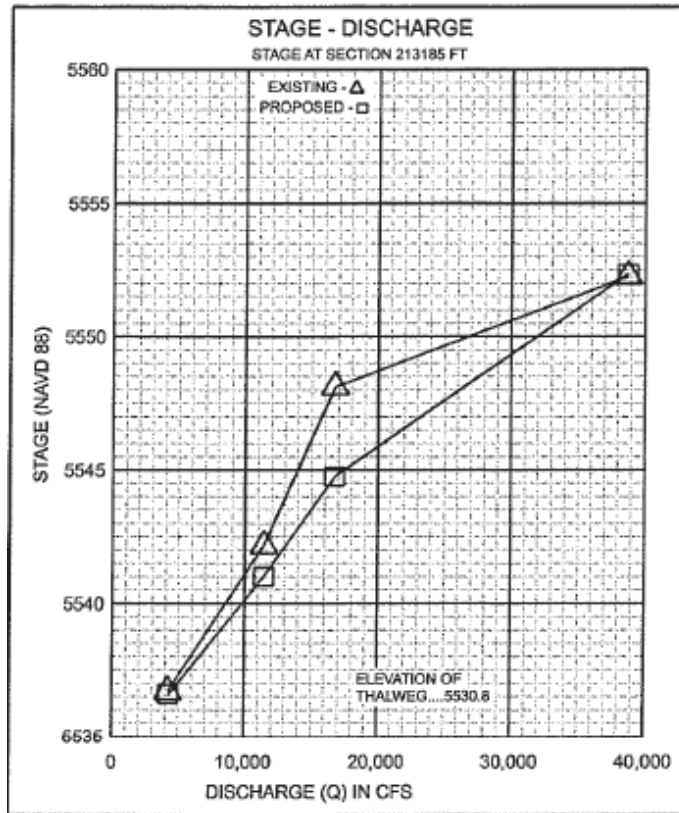


Figure 3.331 Plan rating curve for C-15- AN (CDOT see Appendix A)

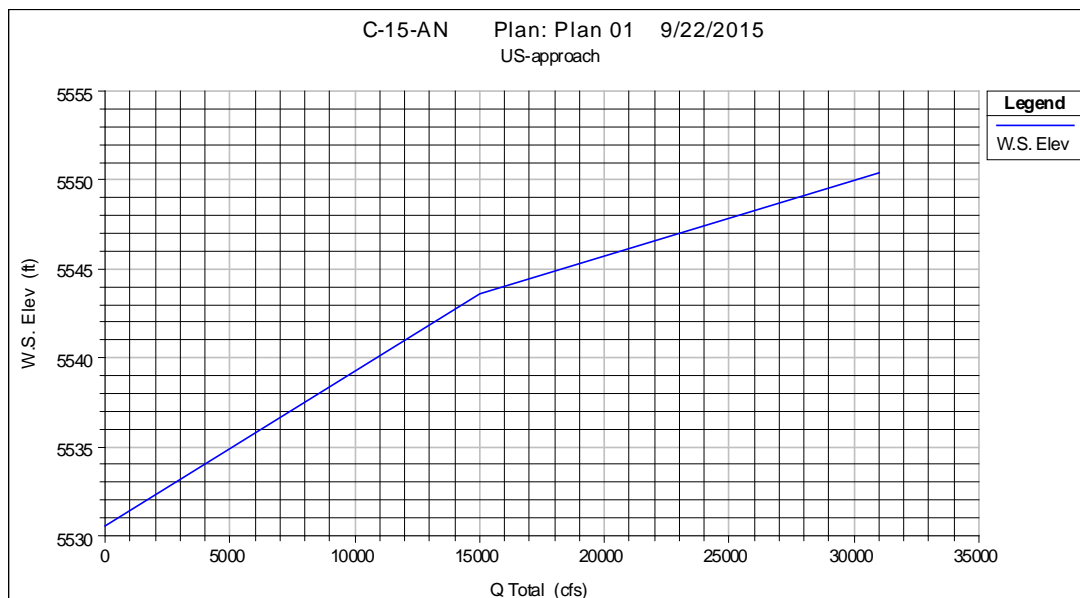


Figure 3.72 HEC-RAS rating curve for C-15- AN

The contact and overtopping discharge values from the plans' curve are 15500 and 23000 cfs, which compare well with the models' values of 15446 and 23258 cfs. The main difference lies with the velocity values. For this bridge, the HEC-RAS models' values are much lower than the plans. The ultimate velocity is 14.26 ft/s as opposed to the range of 7.26-6.83 ft/s from the model. The velocity and discharge values generated in HEC-RAS were used to be consistent.

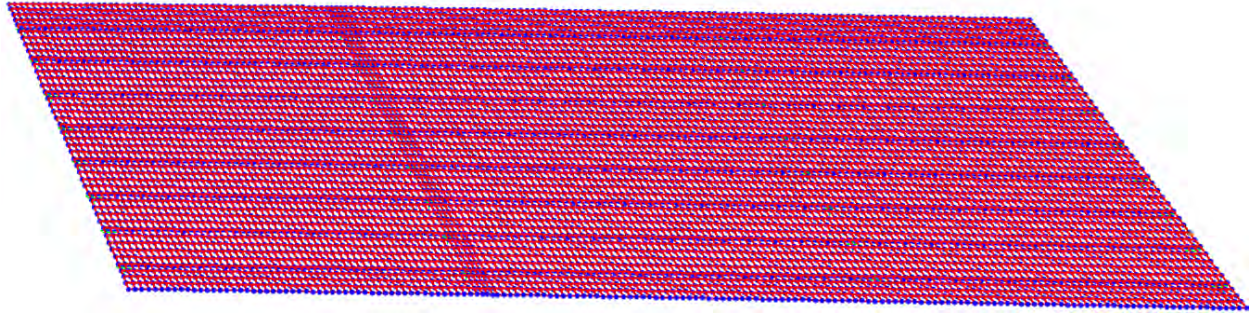


Figure 3.73 SAP2000 model for C-15- AN

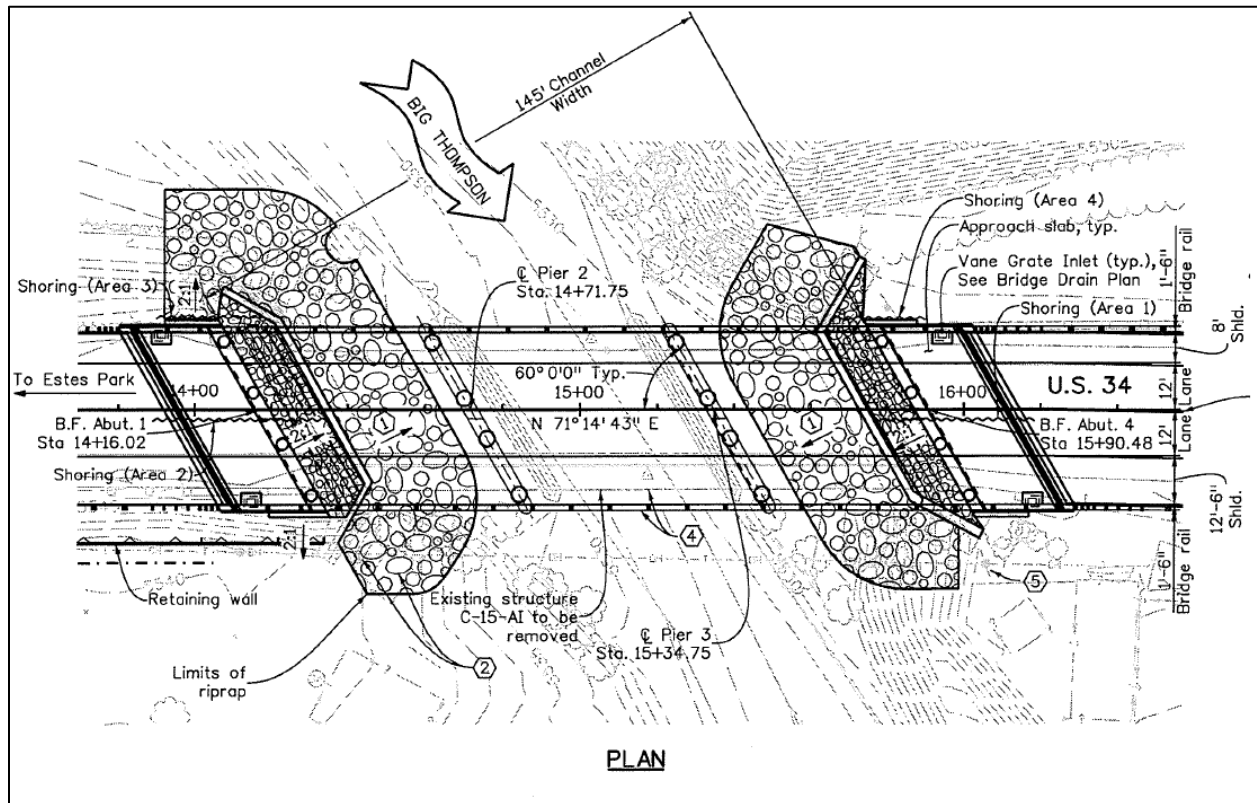


Figure 3.34 Plan view of the bridge deck of C-15- AN (CDOT see Appendix A)

The model skew is 60.02° and the real bridge has a skew angle of 60° . Also, the differential elevation occurs at the piers, which are 0.44' greater than the abutments.

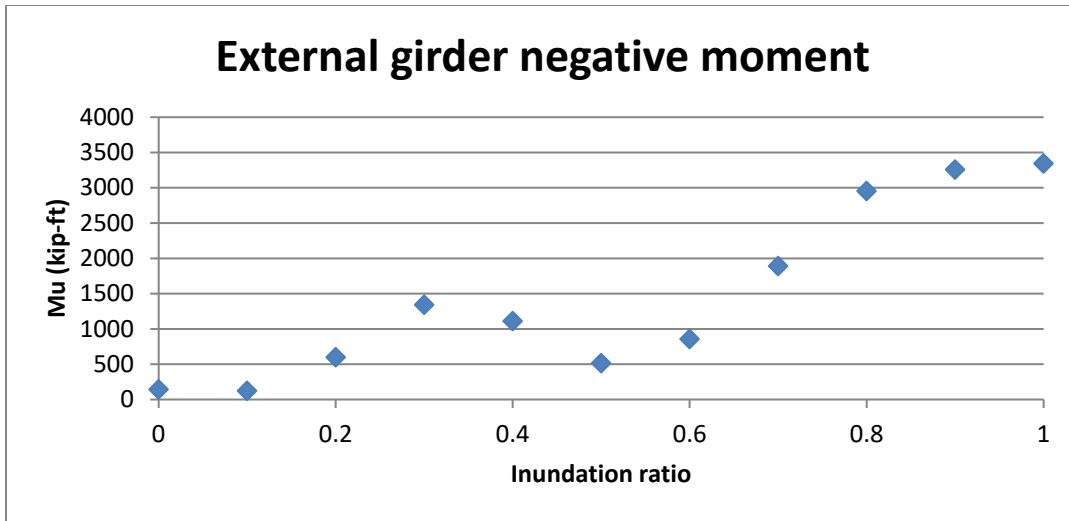


Figure 3.35 Applied negative moment felt by G1 for C-15- AN

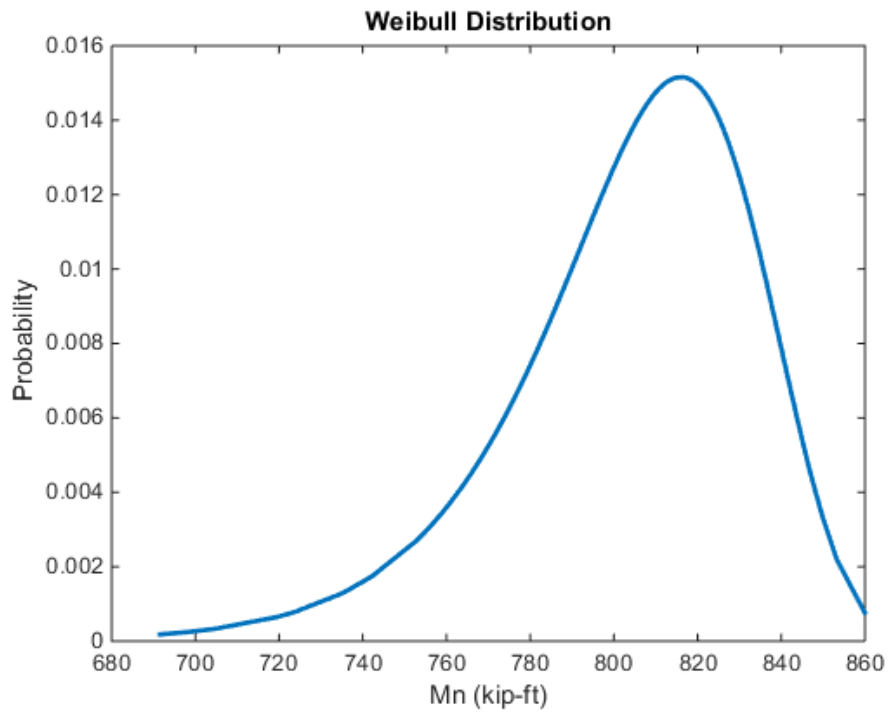


Figure 3.36 Negative nominal moment capacity for an external girder for C-15- AN

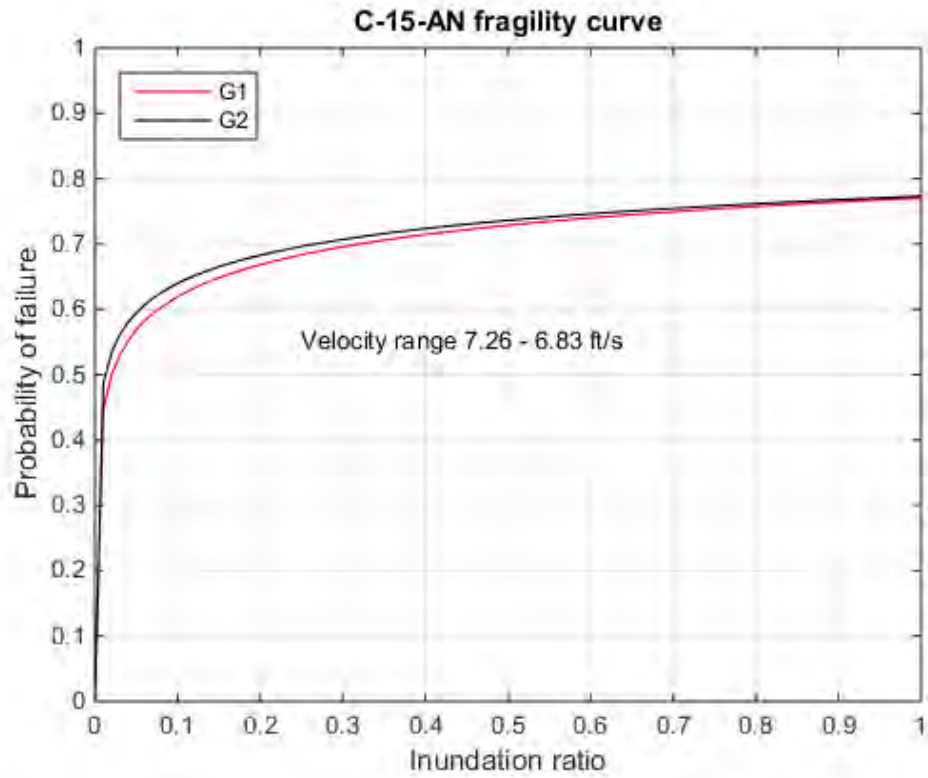


Figure 3.37 Fitted lognormal CDF function to the fragility values for C-15- AN

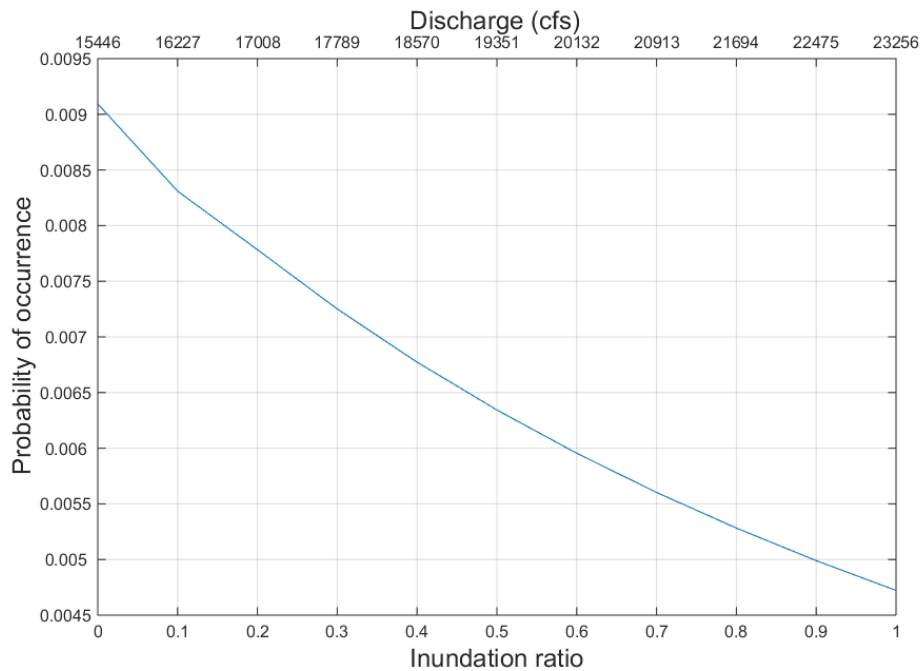


Figure 3.38 Hazard probabilities used to generate the probability of failure curve for C-15- AN

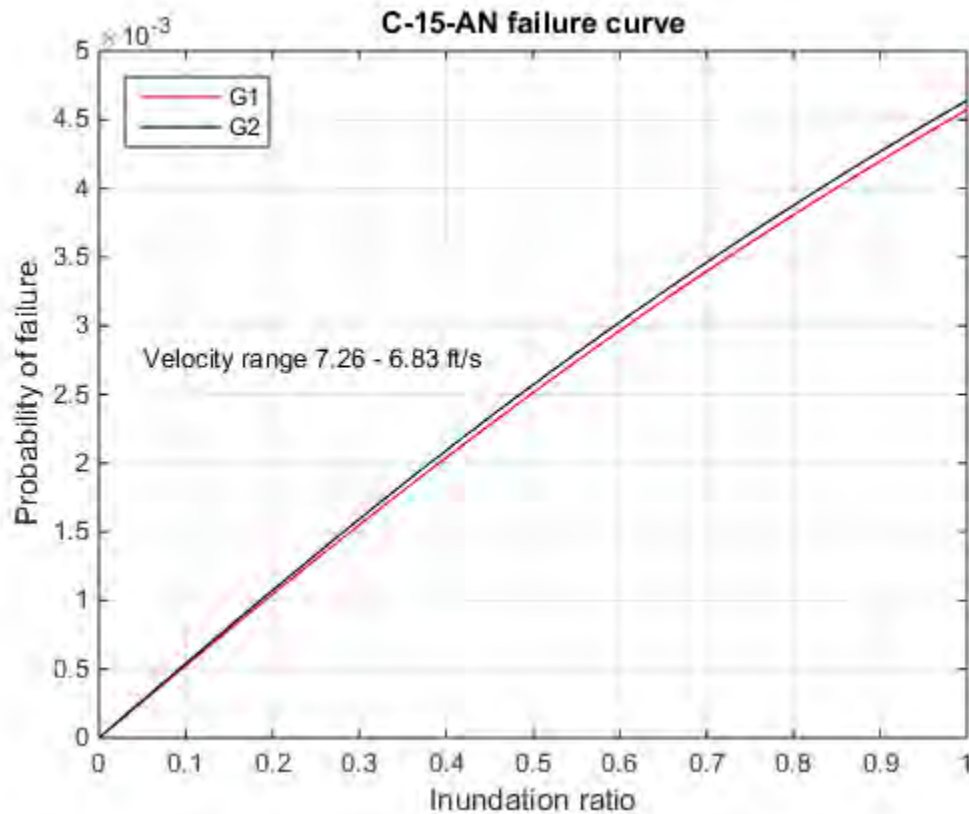


Figure 3.39 Probability of failure values for C-15- AN

The low capacity and variability in the inundation ratio results in a jump of the fragility curve at $h^*=0$ to $h^*=0.1$. The beta values are 2.61 and 2.60 for the external and internal girders. To reach the target beta value for the 100 and 500-year flood, the bridge would need to be raised 0' and 7'. The 100-year storm doesn't come in contact with the superstructure hence the lack of adjustments needed.

3.8 Bridge C-16-DI Results

C-16-DI is located a mile upstream from the mouth of the canyon and is the only bridge in the study to be modeled as supercritical flow. This is due to the nature of the overbank areas, which are vertical rock cliffs and corrugated metal retaining walls. Velocity values are the greatest at this location which leads to very high forces. Due to the large clearance distance of 18-22', the probability of being inundated is small. Field measurements determined that there was 3-5' of degradation to the channel bottom so the LiDAR data was adjusted to match the plan elevations. Damage done was limited to asphalt cracking and slight settlement at the roadway-bridge interface. Also, there was a mild erosion hole at the back right wingwall.



Figure 3.80 Cross sections generated in ArcMap for C-16-DI

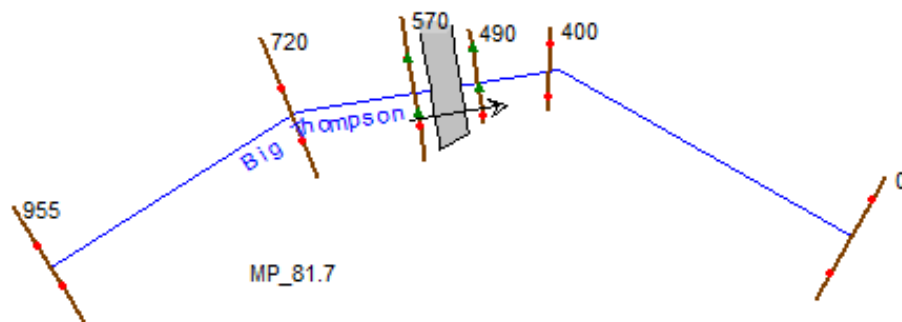


Figure 3.81 HEC-RAS rating curve for C-16-DI

The degree of meandering plus the fast moving flow required two additional cross sections for the HEC-RAS model.

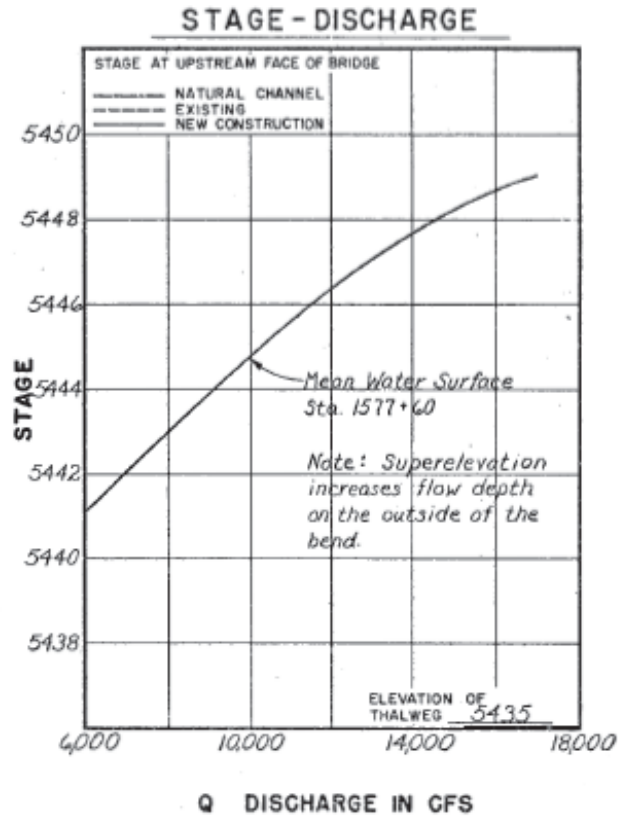


Figure 3.402 Plan rating curve for C-16-DI (CDOT see Appendix A)

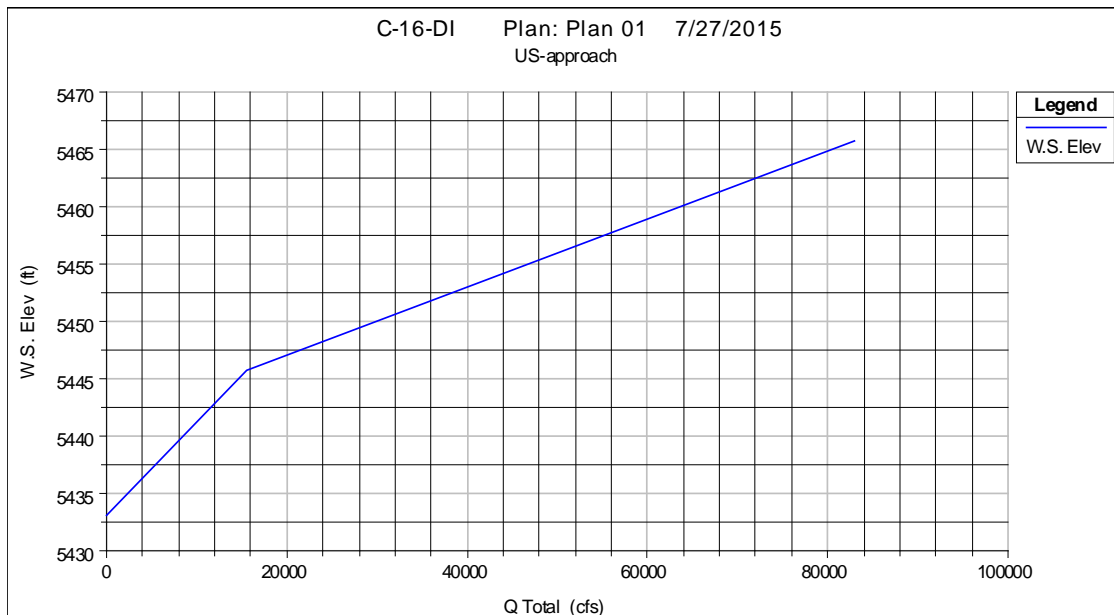


Figure 3.83 HEC-RAS rating curve for C-16-DI

The plan rating curve does not include a contact or overtopping discharge value, but there is a velocity value provided. Due to the supercritical nature of the channel, the velocity values are the highest at this location when compared to the previous bridges in this study. The plan sheet gives a velocity value of 25

ft/s, which corresponds to much lower discharge values. Velocity values range from 30.92-36.31 ft/s at discharge values of 46539 to 63639 cfs for the HEC-RAS model.

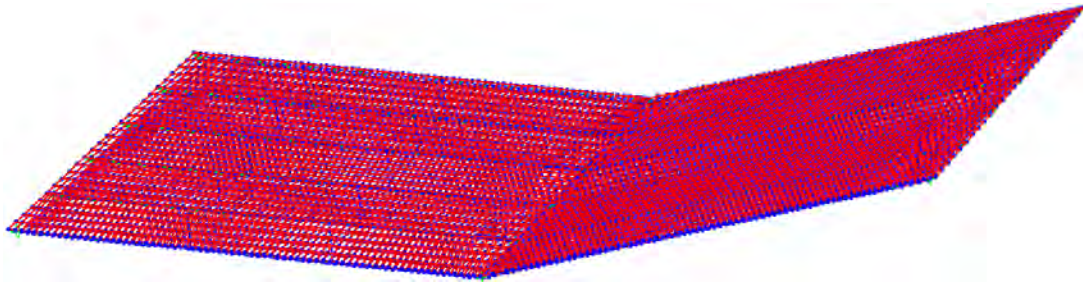


Figure 3.41 SAP2000 model for C-16-DI

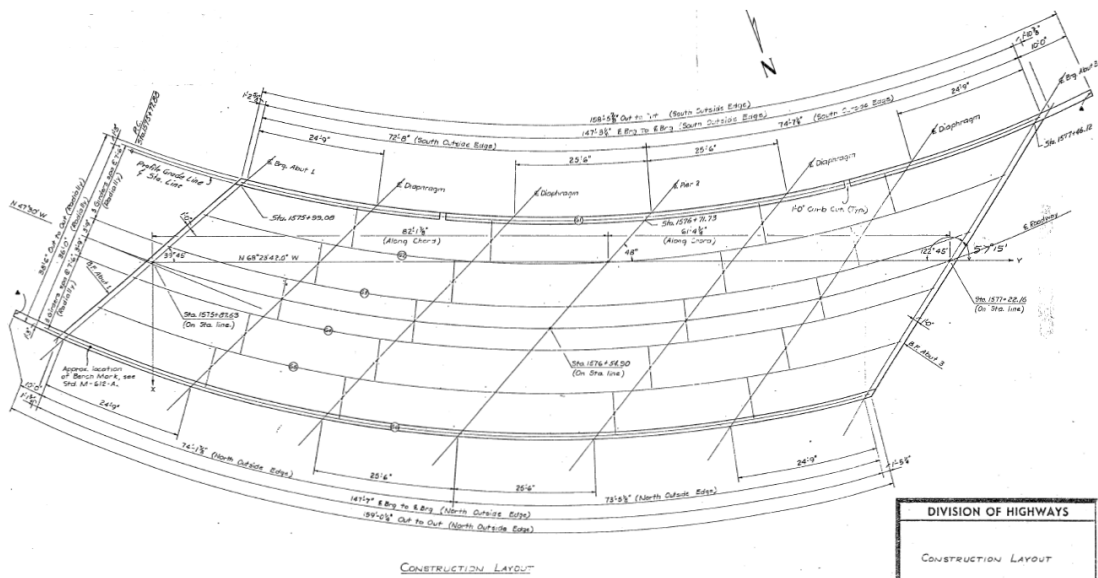


Figure 3.42 Plan view of the bridge deck of C-16-DI (CDOT see Appendix A)

The structural configuration of this bridge was unique and handled slightly differently than previous bridges. Instead of a single element for the box girders, it was modeled as shell elements for the top and bottom slab plus rectangular frame elements for the columns. This is felt to align better with the staged construction for this project. The bottom slab and girder web columns were poured first and then the top slab was poured. This differs from other box girder bridges because the deck is part of the box girder as opposed to the box girder top flange being compositely connected via shear studs to the bridge deck slab. The concrete web girders were modeled as straight frames and the curvature was not taken into account. For this bridge, the concrete strength was very low, 1600 psi, which led to a low capacity. Coupling the low capacity with the high demand led to the less robust approach, straight elements, for this bridge.

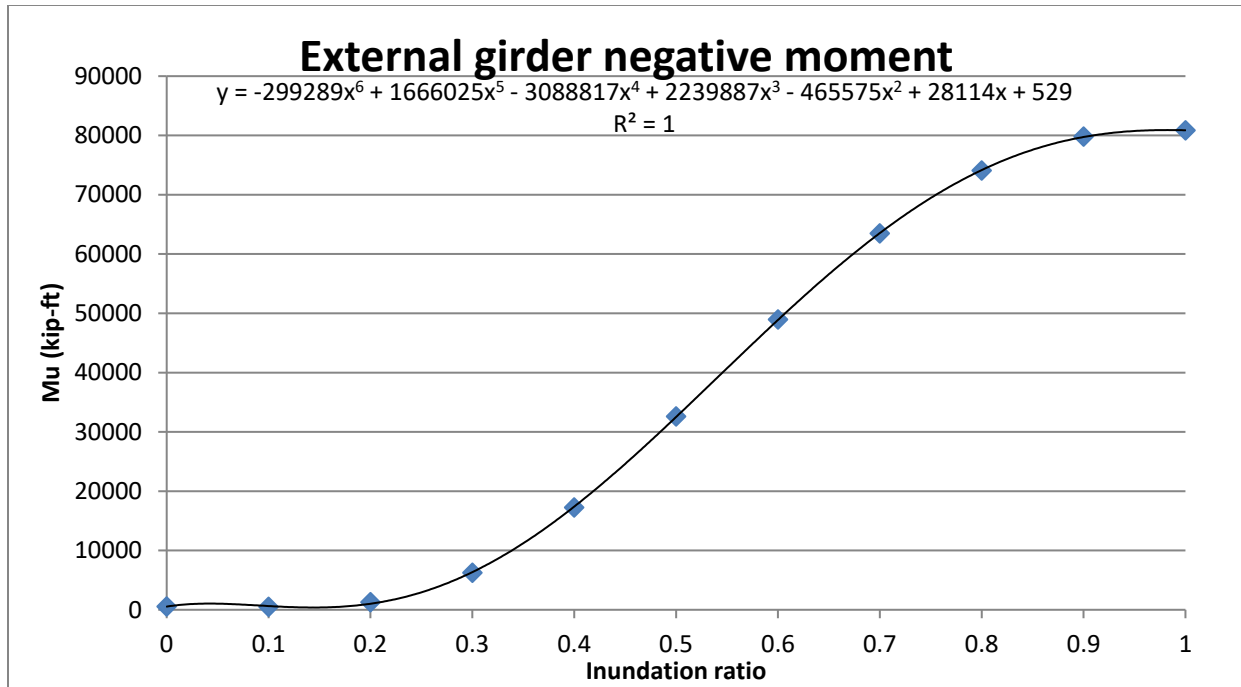


Figure 3.43 Applied negative moment felt by G6 span 2 for C-16-DI

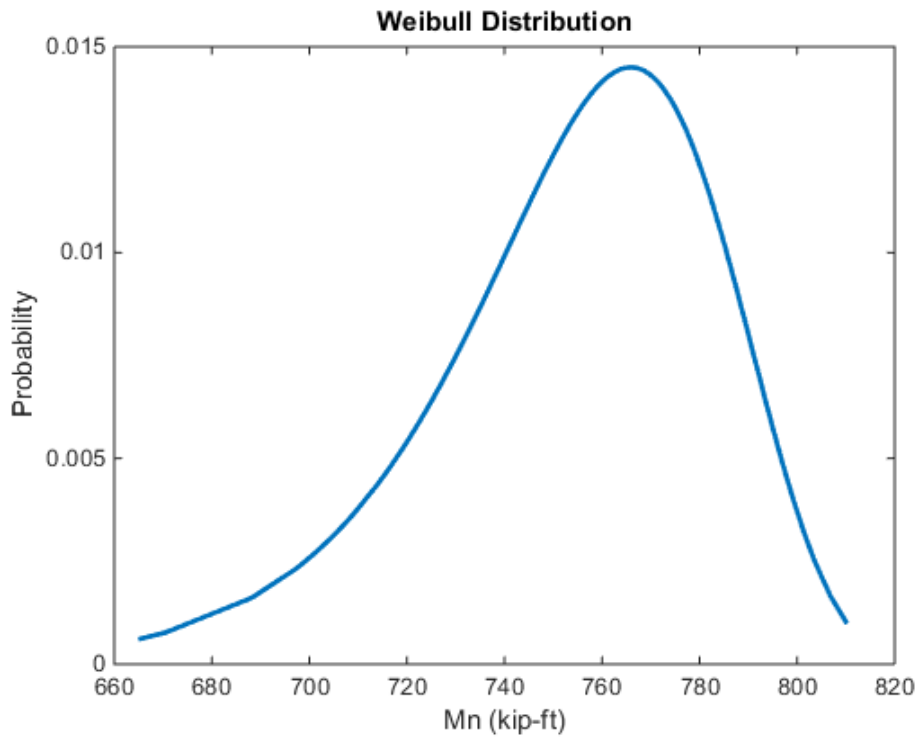


Figure 3.44 Negative nominal moment capacity for an external girder for C-16-DI

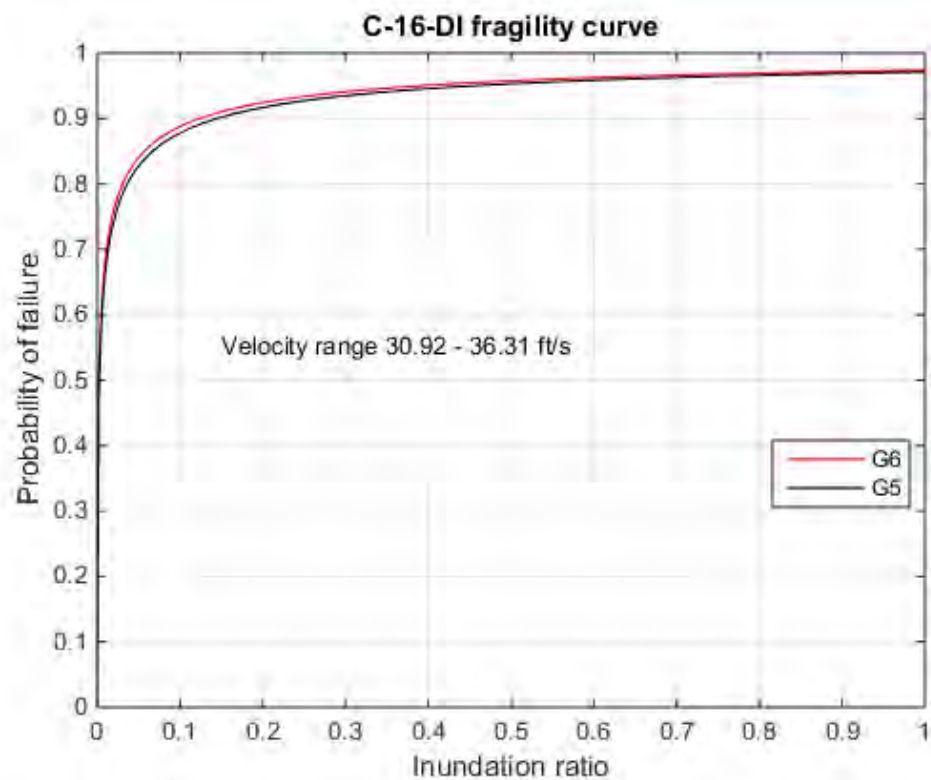


Figure 3.45 Fitted lognormal CDF function to the fragility values for C-16-DI

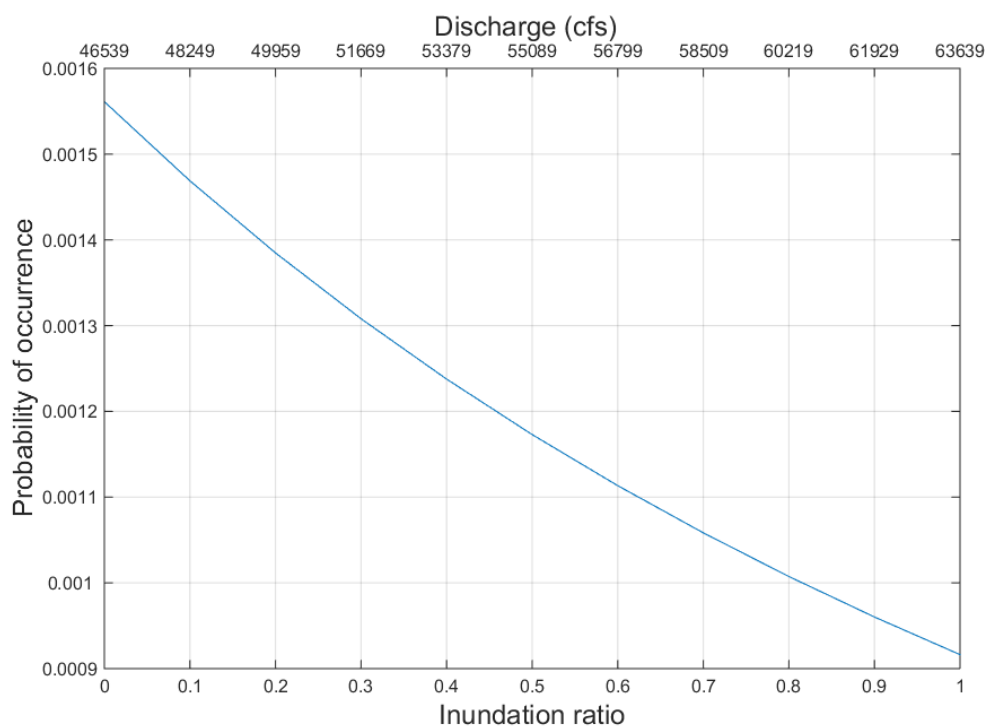


Figure 3.46 Hazard probabilities used to generate the probability of failure curve for C-16-DI

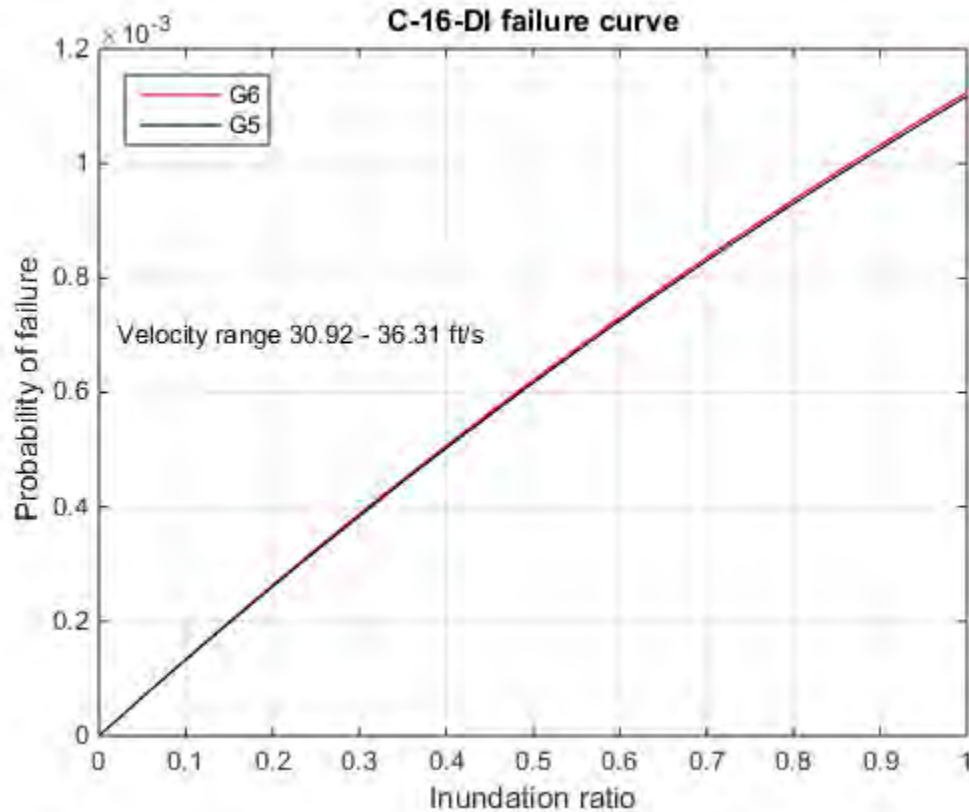


Figure 3.90 Probability of failure values for C-16-DI

For variation in the demand, 20% of the predicted discharge value was used, as discussed in the previous chapter, and the standard deviation ranges from 9300 to 12700 cfs. Such a large range in the discharge, or the demand, leads to several high inundation ratios at every point. When a distribution is fit to the resulting Mu values, it leads to very high fragility probabilities at even low inundation ratios as seen in Figure 3.90. The current beta values are 3.06 for the external and internal girders. However, due to the large clearance distance, no adjustments are needed to reach the target beta value for the 100 and 500 year storm due to no contact being made with the superstructure.

4. CONCLUSIONS, CONTRIBUTIONS AND RECOMMENDATIONS

The community of Drake, CO, was the focal point of this research. Eight bridges were selected and analyzed under flood loading as per the design equations proposed by Kerenyi et al. (2009). Fragilities were developed for the most critical internal and external composite girders. The results obtained from fragility analysis were then used to determine the elevation adjustments needed to reach a target beta value of 3.5. These adjustments would reduce post-flood repair cost, increase bridge safety during a low probability storm event, and increase the flood resiliency of the Big Thompson Canyon.

Currently, bridge superstructures are designed based on the 100-year flood, which in the case of the bridges in this study, would not have resulted in any inundation of the bridge deck at the time of construction based on the knowledge at that time. In fact, there is a required amount of freeboard, or clearance distance between the water surface and the low chord of the girder, for bridges to allow for wave surges and debris to pass under the bridge. This methodology results in bridge superstructures not properly being analyzed for flood forces due to inundation, more specifically the lift force that has proven to be significant in this study. The negative lift force is especially significant for fast moving rivers such as the Big Thompson River.

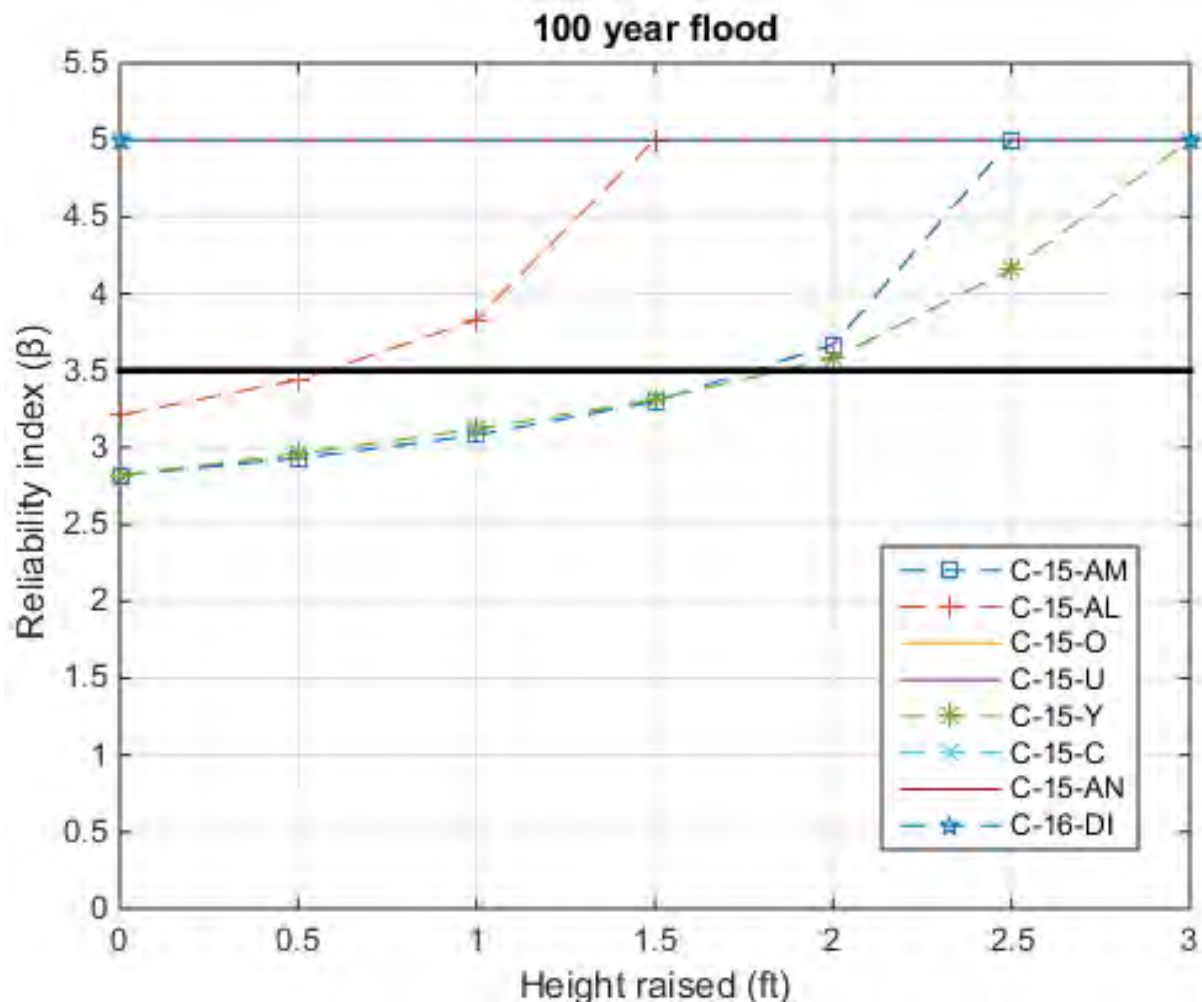


Figure 4.1 100 year flood beta values for all bridges

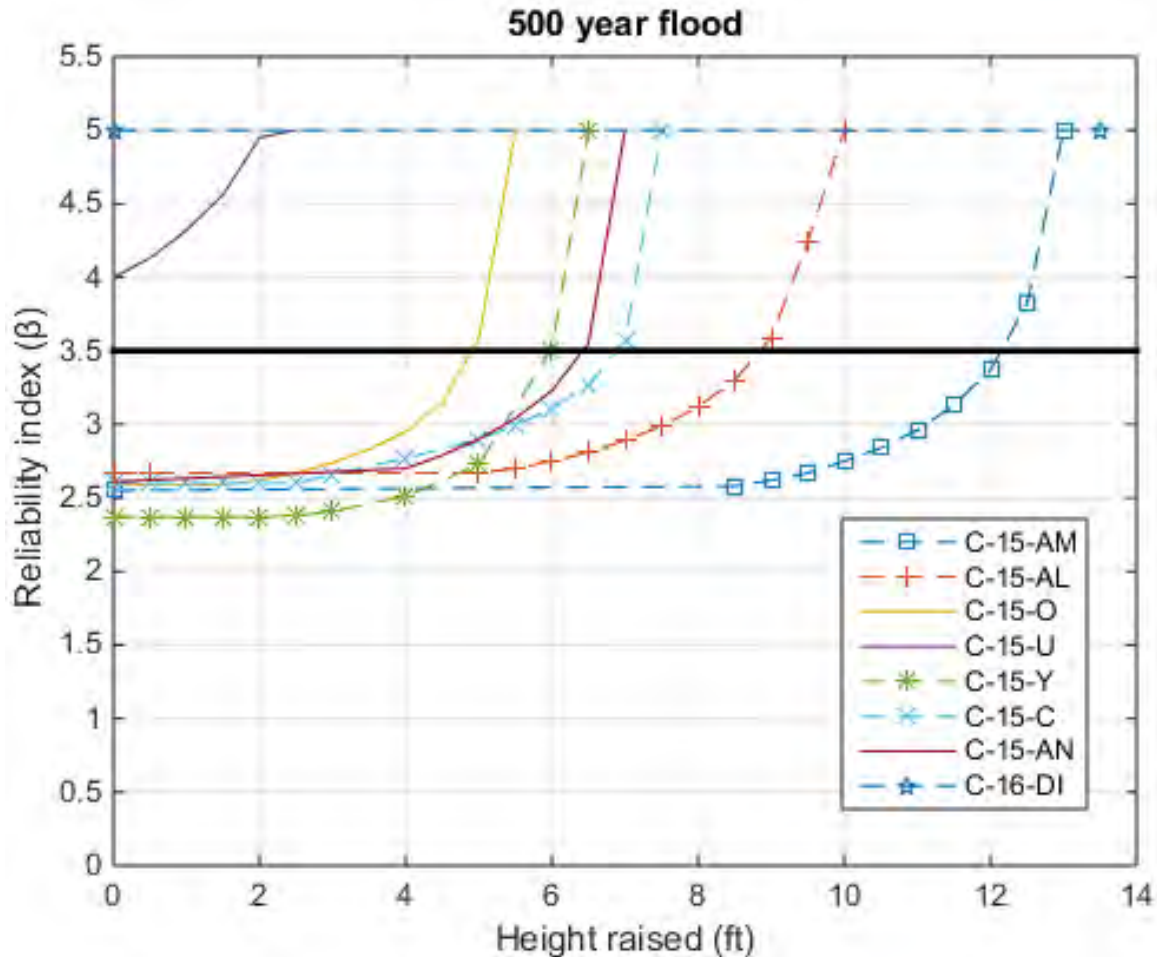


Figure 4.2 500 year flood beta values for all bridges

Figures 4.1 and 4.2 display the elevation adjustments needed for each bridge to satisfy the target beta value for the 100 and 500-year floods. If a bridge had zero probability of failure, then the beta value was set to 5. Also, the bridges were assumed to be raised in 0.5' increments. The height adjustments needed for the 100 year flood range from 1' to 2' and only three bridges require alterations. C-15-Y is the most critical of the three. This makes sense, considering it suffered the most damage due to the September 2013 flood. The height adjustments needed for the 500-year flood range from 5' to 12.5' for six of the eight bridges in this study. The reason why such high adjustments are warranted for the 500-year flood is due to the high probability of failure at low inundation ratios for this type of flow. So even though the 500-year flood results in $h^*=0.25$ for certain bridges, the high demand coupled with low capacity would require adjustments such that the 500-year flood doesn't result in inundation.

As a result of bridge scour concerns, lowering the channel elevation would not be a feasible mitigation strategy to reduce the failure probability of the superstructure. Bridge scour is currently designed based on the 500-year flood due to it being a catastrophic failure mechanism and decreasing the riprap and depth of soil around bridge foundations would be ill advised. Raising the height of the bridge deck would be the most practical solution.

Bridge substructure components take into account the numerous forces associated with flood flows. This study solely analyzed the superstructure as to quantify the risk associated with inundation. With the trend of a higher frequency of low probability flood events, the risk will only rise. Also, the uncertainty in discharge estimates increases the probability of failure. Future research should be based on the analysis of several different bridge configurations under varying velocity flows as to produce a wide array of fragilities applicable all kinds of flow conditions. Another consideration should be made to assess the fragilities of embankments and approach roadway failure due to erosion.

REFERENCES

- American Association of State Highway and Transportation Officials (AASHTO). (1994). AASHTO LRFD bridge design specifications, 1st Ed., Washington, D.C.
- Aguilar, J. (2014). Colorado re-emerging from \$2.9 billion flood disaster a year later. Retrieved September, 2015.
- Biondini, F., Bontempi, F., Frangopol, D. M., & Malerba, P. G. (2006). Probabilistic service life assessment and maintenance planning of concrete structures. *Journal of structural engineering*, 132(5), 810-825.
- Bolinger, B. (2013). Colorado Flood 2013. Retrieved September, 2015.
- Botts et al. (2013). Natural Hazard Risk Summary and Analysis. Retrieved August, 2015.
- Bradbury, R. B., Hill, R. A., Mason, D. C., Hinsley, S. A., Wilson, J. D., Balzter, H., ... & Bellamy, P. E. (2005). Modelling relationships between birds and vegetation structure using airborne LiDAR data: a review with case studies from agricultural and woodland environments. *Ibis*, 147(3), 443-452.
- (a) Brunner, G. W. (2010). HEC-RAS River Analysis System Hydraulic Reference Manual Version 4.1 (Report CPD-69).
- (b) Brunner, G. W. (2010). HEC-RAS River Analysis System User's Manual Version 4.1 (Report CPD-68).
- Computer and Structures, Inc. (2013). SAP2000, Analysis Reference Manual, Berkeley, Calif.
- Culmo, M. P. (2009). Connection Details for Prefabricated Bridge Elements and Systems. (Report No. FHWA-IF-09-010).
- Denson, K. H. (1982). *Steady-state drag, lift and rolling-moment coefficients for inundated inland bridges* (No. FHWA-MSHD-RD-82-077 Final Rpt.).
- Disaster Recovery. (n.d.). Retrieved September, 2015 from: <https://www.colorado.gov/pacific/dola/node/101531>.
- Ellingwood, B. R., Galambos, T. V., MacGregor, J. G., & Cornell, C. A. (1980). Development of a Probability Based Load Criterion for American National Standard A58. Washington (DC).
- Erdman, J. (2013). Colorado Flash Flooding: How It Happened, How Unusual? Retrieved September, 2015.
- Ghosn, M., & Moses, F. (1998). NCHRP Report 406. *Redundancy in Highway Bridge Superstructures*.
- Hydrologic Information Center - Flood Loss Data. (2015). Retrieved August, 2015
- Jacobs. (2014). Hydrologic Evaluation of the Big Thompson Watershed. Retrieved from Big Thompson River Restoration Coalition: http://bigthompson.co/wp-content/uploads/2015/05/CDOT-2014_Hydrologic-evaluation-of-the-Big-T.pdf
- Jempson, M. (2000). Flood and debris loads on bridges.
- Kerenyi, K., Sofu, T., & Guo, J. (2009). Hydrodynamic forces on inundated bridge decks.
- Malavasi, S., & Guadagnini, A. (2003). Hydrodynamic loading on river bridges. *Journal of Hydraulic Engineering*, 129(11), 854-861.
- Matsuda, K., Cooper, K. R., Tanaka, H., Tokushige, M., & Iwasaki, T. (2001). An investigation of Reynolds number effects on the steady and unsteady aerodynamic forces on a 1: 10 scale bridge deck section model. *Journal of Wind Engineering and Industrial Aerodynamics*, 89(7), 619-632.

- McCain, J. F., Shroba, R. R., & Soule, J. M. (1979). *Storm and flood of July 31-August 1, 1976, in the Big Thompson River and Cache la Poudre River basins, Larimer and Weld Counties, Colorado* (Vol. 1115). US Govt. Print. Off.: for sale by the Supt. of Docs., GPO.
- Mirza, S. A., Kikuchi, D. K., and MacGregor, J. G. (1980). "Flexural strength reduction factor for bonded prestressed concrete beams." *J. ACI*, 77(4), 237-246.
- Naaman, A. E., & Siriakorn, A. (1982). Reliability of partially prestressed beams at serviceability limit states. *PRECAST/PRESTRESSED CONCRETE INSTITUTE. JOURNAL*, 27(6).
- Naudascher, E., & Medlarz, H. J. (1983). Hydrodynamic loading and backwater effect of partially submerged bridges. *Journal of Hydraulic Research*, 21(3), 213-232.
- Nowak, A. S. (1995). Calibration of LRFD bridge code. *Journal of Structural Engineering*.
- Nowak, A., E. Szeliga, and M. Szerszen. 2008. Reliability-Based Calibration for Structural Concrete, Phase 3. Portland Cement Association Research and Development Serial No. 2849, pp. 1–110
- Okajima, A., Yi, D., Sakuda, A., & Nakano, T. (1997). Numerical study of blockage effects on aerodynamic characteristics of an oscillating rectangular cylinder. *Journal of wind engineering and industrial aerodynamics*, 67, 91-102.
- Parry ML, Canziani O, Palutikof JP, Hanson C, van der Linden P (eds) (2007) Climate change 2007: Impacts, adaptation and vulnerability. Contribution of Working Group II to the Fourth Assessment Report of the Intergovernmental Panel on Climate Change. Cambridge University Press, New York
- Rosowsky, D. V., & Ellingwood, B. R. (2002). Performance-based engineering of wood frame housing: Fragility analysis methodology. *Journal of Structural Engineering*, 128(1), 32-38.
- Siriakorn, A., & Naaman, A. E. (1980). Reliability of Partially Prestressed Beams at Serviceability Limit States. *Department of Civil Engineering, Report*, (80-1).
- Solomon S, Qin D, Manning M, Chen Z, Marquis M, Averyt KB, Tignor M, Miller HL (eds) (2007) Climate change 2007: The physical science basis. Contribution of Working Group I to the Fourth Assessment Report of the Intergovernmental Panel on Climate Change. Cambridge University Press, New York
- Ulcellini L.W. (2014). The Record Front Range and Eastern Colorado Floods of September 11-17, 2013. Retrieved September, 2015.
- Wright, L., Chinowsky, P., Strzepek, K., Jones, R., Streeter, R., Smith, J. B., . . . Perkins, W. (2012). Estimated effects of climate change on flood vulnerability of U.S. bridges. *Mitigation and Adaptation Strategies for Global Change*, 17(8), 939-955. doi:<http://dx.doi.org/10.1007/s11027-011-9354-2>

APPENDIX A. CONSTRUCTION DRAWINGS

C-15-AM Construction Drawings

GENERAL NOTES

EXCEPT AS SHOWN IN THE PLANS, STRUCTURE EXCAVATION AND BACKFILL SHALL BE IN ACCORDANCE WITH M-208-2.

EXPANSION JOINT MATERIAL SHALL CONFORM TO ASHTO SPECIFICATION M213.

THE EXPOSED SURFACES OF THE MINORALS AND THE EXTERIOR SURFACES (SEE THE PLANS) SHALL BE STAINED. THE COLOR SHALL BE BEIGE, EQUIVALENT TO FEDERAL COLOR STANDARD 3925, COLOR NO. 33446, AND SHALL EXTEND AT LEAST 1 FOOT BELOW FINAL GRADE ON THE MINORALS.

LEVELING PADS ARE UNMAINTAINED BEARINGS. THEY SHALL BE CUT OR MOULDED FROM A MOISTURE ELASTOMER GRADE 3, 4, OR 5 AS DESCRIBED IN TABLES 702-1 AND 702-2 WITH A HARDNESS OF 60.

GRADE 60 REINFORCING STEEL IS REQUIRED.

ALL REINFORCING STEEL SHALL BE EPOXY COATED UNLESS OTHERWISE NOTED.

⑤ DENOTES NON COATED REINFORCING STEEL.

THE FOLLOWING TABLE GIVES THE MINIMUM LAP SPlice LENGTH FOR EPOXY COATED REINFORCING BARS PLACED IN ACCORDANCE WITH SUBSECTION B02.06. THESE SPlice LENGTHS SHALL BE INCREASED BY 25% FOR BARS SPACED AT LESS THAN 8" ON CENTER.

BAR SIZE	#4	#5	#6	#7	#8	#9	#10	#11
SPlice LENGTH FOR CLASS 30 CONCRETE AND CLASS 30	1'-3"	1'-7"	2'-5"	2'-10"	3'-8"	4'-8"	5'-11"	7'-3"

THE FOLLOWING TABLE GIVES THE MINIMUM LAP SPlice LENGTH FOR BLACK REINFORCING BARS PLACED IN ACCORDANCE WITH SUBSECTION B02.06. THESE SPlice LENGTHS SHALL BE INCREASED BY 25% FOR BARS SPACED AT LESS THAN 8" ON CENTER.

BAR SIZE	#4	#5	#6	#7	#8	#9	#10	#11
SPlice LENGTH FOR CLASS 30 CONCRETE AND CLASS 30	1'-1"	1'-4"	1'-7"	1'-11"	2'-5"	3'-1"	3'-11"	4'-10"

FOR STRUCTURE NUMBER INSTALLATION, SEE STANDARD S-61A-12.

DESIGN DATA

ASHTO, FOURTH EDITION, LRFD WITH CURRENT INTERIMS

DESIGN METHOD: LOAD AND RESISTANCE FACTOR DESIGN

LIVE LOAD: HL-93 (DESIGN TRUCK OR TANDUM AND DESIGN LANE LOAD) ASSUMES 30 KIPS PER SQ. FT. FOR BRIDGE DECK OVERLAY

DEAD LOAD: UNIFORM 100 LBS./SQ. FT.

REINFORCED CONCRETE: $f'_c = 4,500$ psi

REINFORCING STEEL: $f_y = 60,000$ psi

THE BRIDGE DECK HAS BEEN DESIGNED FOR AN f'_c OF 4,500 psi. THE BRIDGE DECK CAN BE OPENED TO TRAFFIC WHEN THE CONCRETE HAS ATTAINED A MINIMUM FIELD COMPRESSIVE STRENGTH OF 4,000 psi AND IT HAS CURED A MINIMUM OF 5 DAYS. THE CONCRETE SHALL BE CURED BY COVERING WITH A MINIMUM OF 1 INCH OF MOISTURE CURING COMPOUND. THE STRUCTURE SITE IN ACCORDANCE WITH ASHTO 2.3.1 AND TESTED IN ACCORDANCE WITH ASHTO 7.22 OR A MATURITY RELATIONSHIP ESTABLISHED IN ACCORDANCE WITH THE SPECIFICATIONS.

CAISSON CONCRETE:

CLASS 30 CONCRETE: $f'_c = 4,000$ psi

REINFORCING STEEL: $f_y = 60,000$ psi

PRESTRESSED PRECAST CONCRETE: $f'_c = 5,000$ psi

PRESTRESSING STEEL: $f'_c = 270,000$ psi

Print Date: 04/15/15

Drawing File Name: PLES

Rele. Scale: 1/4"=1'-0"

Unit: Feet

Sheet Revisions

Date:

Comments:

Init.

Comments:

Init.

Colorado Department of Transportation

2207 EAST HIGHWAY 402

LOVELAND, COLORADO 80537

Phone 970-657-4670 FAX 970-689-0288

REGION 4

As Constructed

No. Revisions:

Revised:

Valid:

GENERAL INFORMATION AND SUMMARY OF QUANTITIES

Project No./Code

BR 0341-068

15546

Sheet Number 62

As Constructed

No. Revisions:

Revised:

Valid:

GENERAL INFORMATION AND SUMMARY OF QUANTITIES

Project No./Code

BR 0341-068

15546

Sheet Number 62

As Constructed

No. Revisions:

Revised:

Valid:

SUMMARY OF QUANTITIES

ITEM NO.	ITEM DESCRIPTION	UNIT	SUPPLY QUANTITY	ADJUSTMENT 1	ADJUSTMENT 2	TOTAL
200	REMOVAL OF STRUCTURE	EACH	1			1
201	STRUCTURE EXCAVATION	CY	300	300		600
202	STRUCTURE BACKFILL (CLASS 2)	CY	36	36		74
203	STRUCTURE BACKFILL (FLOWALL)	CY	36	36		74
403	HOT MIX ASPHALT (SPACING 3X) (PG 64-25)	TON	30.5			30.5
503	PAVEMENT OVERLAY (3X)	LF	14.4	14.4		110.9
504	PAVEMENT (3X)	CY				66.9
601	WATER-PROOFING (MEMBRANE)	SY	365.9			177
602	CONCRETE CLASS 0 (BRIDGE)	CY	139	139		2803
603	STRUCTURAL CONCRETE 2'-4IN	SY	2000			12 410
604	REINFORCING STEEL	LB	21,200	21,200		75,066
605	REINFORCING STEEL (FLOWALL)	LB	1,170	1,170		231
606	BRIDGE RAIL TYPE 10A	LF	225	225		229
607	2 INCH RAIL CONCRETE (BRIDGE)	LF	163.8	163.8		712.8

INDEX OF DRAWINGS

- B 1 GENERAL INFORMATION AND SUMMARY OF QUANTITIES
- B 2 GENERAL LAYOUT
- B 3 ENGINEERING GEOLOGY
- B 4 BRIDGE HYDRAULIC INFORMATION - C-15-AM
- B 5 CONSTRUCTION LAYOUT
- B 6 CAISSON LAYOUT
- B 7 ADJUNCT 1 DETAILS
- B 8 ADJUNCT 2 DETAILS
- B 9 MINOR DETAILS
- B 10 BRIDGE DECK DETAILS
- B 11 PRESTRESSED CONCRETE I
- B 12 PRESTRESSED CONCRETE I (MSC)
- B 13 PRECAST PANEL DECK FORM (SHEET 1 OF 2)
- B 14 PRECAST PANEL DECK FORM (SHEET 2 OF 2)
- B 15 STRUCTURE BACKFILL (FLOWALL)
- B 16 BRIDGE RAIL TYPE 10A
- B 17 BRIDGE RAIL TYPE 10A (MSC)
- B 18 BRIDGE DECK ELEVATIONS (SHEET 1 OF 4)
- B 19 BRIDGE DECK ELEVATIONS (SHEET 2 OF 4)
- B 20 BRIDGE DECK ELEVATIONS (SHEET 3 OF 4)
- B 21 BRIDGE DECK ELEVATIONS (SHEET 4 OF 4)



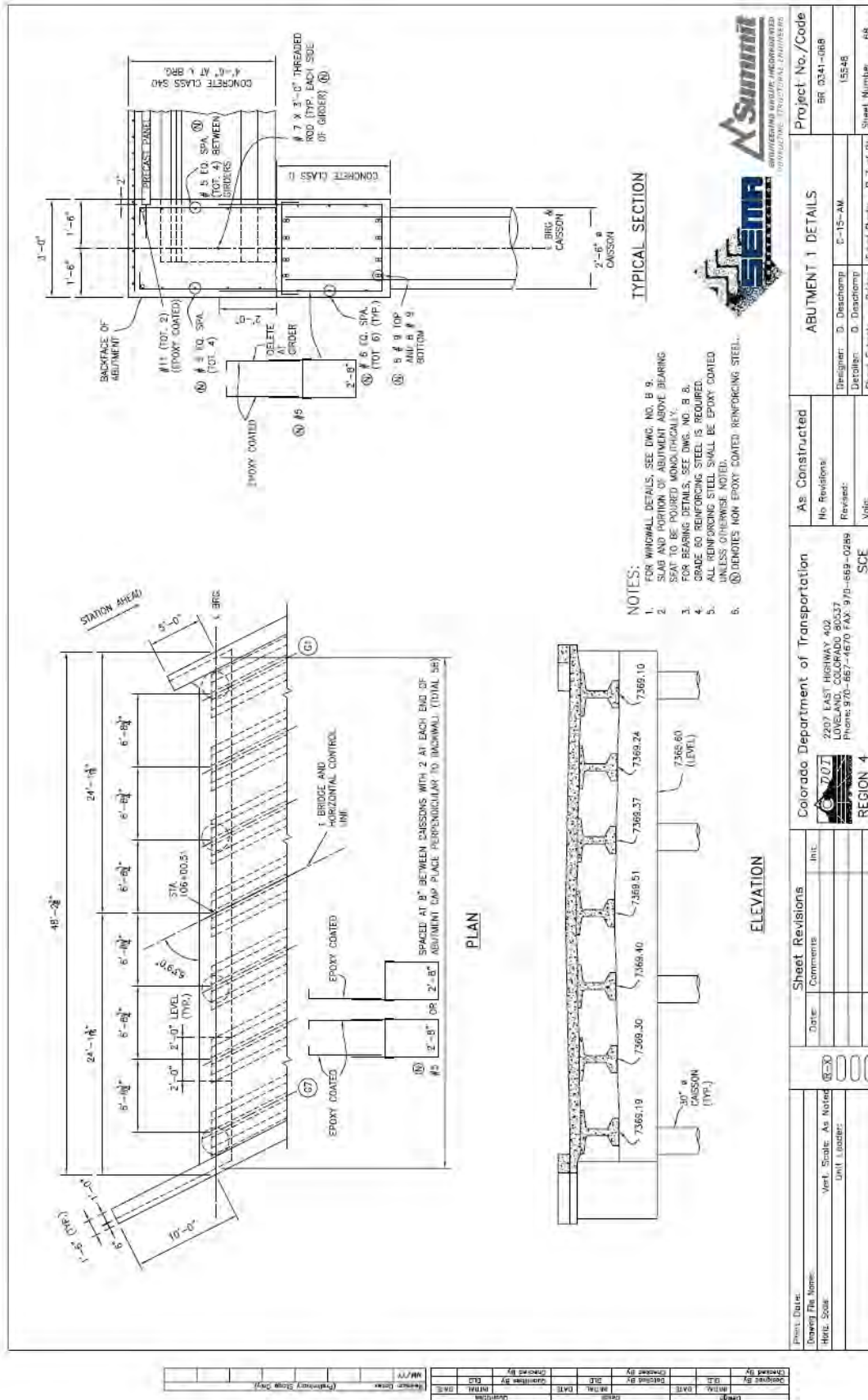
BRIDGE DESCRIPTION

A ONE SPAN (111'-0") BRIDGE WITH PRESTRESSED PRECAST CONCRETE ORDERS (BT 42'S) OVER THE RIO THOMPSON RIVER WITH A 43'-0" WIDE BRIDGE DECK, 4.5' ON 0.0' SKIN AND BRIDGE RAIL TYPE 10A.

CROSS-REFERENCE DRAWING NUMBER

XX (IF BLANK, REFERENCE IS TO SAME SHEET)

XX SECTION OR DETAIL IDENTIFICATION



[illegible]

C-15-AL Construction Drawings

GENERAL NOTES

EXCEPT AS SHOWN IN THE PLANS, STRUCTURE EXCAVATION AND BACKFILL SHALL BE IN ACCORDANCE WITH M-206-2.

EXPANSION JOINT MATERIAL SHALL CONFORM TO ASHTO SPECIFICATION M213.

THE EXPOSED CONCRETE SURFACES OF THE WINGWALLS AND THE EXTERIOR GIRDERS (SEE THE PLANS) SHALL BE STAINED. THE COLOR SHALL BE BEIGE, EQUIVALENT TO FEDERAL COLOR STANDARD 555B, COLOR NO. 33446, AND SHALL EXTEND AT LEAST 1 FOOT BELOW FINAL GRADE ON THE WINGWALLS.

LEVELING PADS ARE UNLIMITED BEARINGS. THEY SHALL BE CUT OR MOLED FROM ASHTO (SHORE "A") JOINTS OF 10" OR AS DESCRIBED IN TABLES 705-1 AND 705-2 WITH A DOROMETER

GRADE 60 REINFORCING STEEL IS REQUIRED.

ALL REINFORCING STEEL SHALL BE EPOXY COATED UNLESS OTHERWISE NOTED.

(X) DENOTES NON COATED REINFORCING STEEL

THE FOLLOWING TABLE GIVES THE MINIMUM LAP SPICE LENGTH FOR EPOXY COATED REINFORCING BARS PLACED IN ACCORDANCE WITH SUBSECTION 602.06. THESE SPICE LENGTHS SHALL BE INCREASED BY 25% FOR BARS SPACED AT LESS THAN 6" ON CENTER.

BAR SIZE	#4	#5	#6	#7	#8	#9	#10	#11
SPICE LENGTH FOR CLASS 80 CONCRETE AND CLASS 540	1'-3"	1'-7"	2'-5"	2'-10"	3'-8"	4'-8"	5'-11"	7'-3"

THE FOLLOWING TABLE GIVES THE MINIMUM LAP SPICE LENGTH FOR BLACK REINFORCING BARS PLACED IN ACCORDANCE WITH SUBSECTION 602.06. THESE SPICE LENGTHS SHALL BE INCREASED BY 25% FOR BARS SPACED AT LESS THAN 6" ON CENTER.

BAR SIZE	#4	#5	#6	#7	#8	#9	#10	#11
SPICE LENGTH FOR CLASS 80 CONCRETE	1'-1"	1'-5"	1'-9"	1'-12"	2'-4"	3'-5"	3'-11"	4'-10"

EXISTING AND BAR SPACING IS 12" OR GREATER ON CENTER.

FOR STRUCTURE NUMBER INSTALLATION, SEE STANDARD S-614-12.

DESIGN DATA

ASHTO, FOURTH EDITION LRD WITH CURRENT INTERMS

DESIGN METHOD: LOAD AND RESISTANCE FACTOR DESIGN

LIVE LOAD: H-20 (DESIGN TRUCK OR TANKER AND DESIGN LANE LOAD)

DEAD LOAD: ASSUMES 36 LBS./PER SQ. FT. FOR BRIDGE DECK OVERLAY UTILITIES: 100 LBS./LIN. FT.

REINFORCED CONCRETE: $f'_c = 4,500$ psi $f_y = 60,000$ psi

CLASS 80 CONCRETE: $f'_c = 4,500$ psi $f_y = 60,000$ psi

CLASS 540 CONCRETE: $f'_c = 4,500$ psi $f_y = 60,000$ psi

PRESTRESSED PRECAST CONCRETE: $f'_c = 4,000$ psi $f_y = 60,000$ psi

CLASS PS CONCRETE: $f'_c = 4,000$ psi $f_y = 60,000$ psi

PRESTRESSING STEEL: $f'_c = 270,000$ psi

THE BRIDGE DECK HAS BEEN DESIGNED FOR AN f'_c OF 4,500 PSI. THE BRIDGE DECK CAN BE OPENED TO TRAFFIC WHEN THE CONCRETE HAS ATTAINED A MINIMUM FIELD COMPRESSIVE STRENGTH OF 4,500 PSI AND IT HAS CURED A MINIMUM OF 5 DAYS. THE BRIDGE DECK SHALL BE CURED WITH A MINIMUM OF 5 DAYS. THE BRIDGE DECK SHALL BE CURED AT THE STRUCTURE SITE IN ACCORDANCE WITH ASHTO T-23 AND TESTED IN ACCORDANCE WITH ASHTO T-22 OR A MATURITY RELATIONSHIP ESTABLISHED IN ACCORDANCE WITH THE SPECIFICATIONS.

CAISSON CONCRETE:

CLASS 87 CONCRETE: $f'_c = 4,000$ psi $f_y = 60,000$ psi

REINFORCING STEEL: $f'_c = 60,000$ psi

PRESTRESSED PRECAST CONCRETE: $f'_c = 4,000$ psi $f_y = 60,000$ psi

CLASS PS CONCRETE: $f'_c = 4,000$ psi $f_y = 60,000$ psi

PRESTRESSING STEEL: $f'_c = 270,000$ psi

SUMMARY OF QUANTITIES (STRUCTURE NO. C-15-AL)

ITEM NO.	ITEM DESCRIPTION	UNITS	SUPERSTRUCTURE	ABUTMENT 1	ABUTMENT 2	TOTAL
202-00400	REMOVAL OF STRUCTURE	EACH	1			1
206-00000	STRUCTURE EXCAVATION	CY		305	320	625
208-00000	STRUCTURE BACKFILL (CLASS 2)	CY		44	59	103
208-00065	STRUCTURE BACKFILL (FLOWELL)	CY		95	137	232
403-34751	HOT MK ASPHALT (GRADEING SX) (75) (FG 64-28)	TON	82.5			82.5
503-00030	DRILLED CAISSON (20 INCH)	LF		79.4	47.9	127.3
506-00009	REPAIR (97)	CY		6	6	12
515-00120	WATERPROOFING (MEMBRANE)	SY	505.9			505.9
601-03040	CONCRETE CLASS D (BRIDGE)	CY		22	22	44
601-05045	CONCRETE CLASS S40	CY	139			139
601-40401	STRUCTURAL CONCRETE STAIN	SF	2800			2800
602-00000	REINFORCING STEEL	LB	27771	5335	5334	38440
602-00020	REINFORCING STEEL (EPOXY COATED)	LB	23285	840	840	25005
608-11030	BRIDGE RAIL TYPE 10M	LF	267	1359	1459	2685
613-00000	2 INCH ELECTRICAL CONDUIT	LF	267			267
618-00142	PRESTRESSED CONCRETE I (BT42)	LF	782.8			782.8

INDEX OF DRAWINGS

BA 1	GENERAL INFORMATION AND SUMMARY OF QUANTITIES
BA 2 <td>GENERAL LAYOUT</td>	GENERAL LAYOUT
BA 3 <td>ENGINEERING GEOLOGY</td>	ENGINEERING GEOLOGY
BA 4 <td>BRIDGE HYDRAULIC INFORMATION</td>	BRIDGE HYDRAULIC INFORMATION
BA 5 <td>CONSTRUCTION LAYOUT</td>	CONSTRUCTION LAYOUT
BA 6 <td>CAISSON LAYOUT</td>	CAISSON LAYOUT
BA 7 <td>ABUTMENT 1 DETAILS</td>	ABUTMENT 1 DETAILS
BA 8 <td>ABUTMENT 2 DETAILS</td>	ABUTMENT 2 DETAILS
BA 9 <td>WINGWALL DETAILS</td>	WINGWALL DETAILS
BA 10 <td>BRIDGE DECK DETAILS</td>	BRIDGE DECK DETAILS
BA 11 <td>PRESTRESSED CONCRETE I (MISC.)</td>	PRESTRESSED CONCRETE I (MISC.)
BA 12 <td>PRESTRESSED CONCRETE I (MISC.)</td>	PRESTRESSED CONCRETE I (MISC.)
BA 13 <td>PRECAST PANEL DECK FORM (SHEET 1 OF 2)</td>	PRECAST PANEL DECK FORM (SHEET 1 OF 2)
BA 14 <td>PRECAST PANEL DECK FORM (SHEET 2 OF 2)</td>	PRECAST PANEL DECK FORM (SHEET 2 OF 2)
BA 15 <td>STRUCTURE BACKFILL (FLOWELL)</td>	STRUCTURE BACKFILL (FLOWELL)
BA 16 <td>BRIDGE RAIL TYPE 10M</td>	BRIDGE RAIL TYPE 10M
BA 17 <td>BRIDGE RAIL TYPE 10M</td>	BRIDGE RAIL TYPE 10M
BA 18 <td>BRIDGE DECK ELEVATIONS (SHEET 1 OF 4)</td>	BRIDGE DECK ELEVATIONS (SHEET 1 OF 4)
BA 19 <td>BRIDGE DECK ELEVATIONS (SHEET 2 OF 4)</td>	BRIDGE DECK ELEVATIONS (SHEET 2 OF 4)
BA 20 <td>BRIDGE DECK ELEVATIONS (SHEET 3 OF 4)</td>	BRIDGE DECK ELEVATIONS (SHEET 3 OF 4)
BA 21 <td>BRIDGE DECK ELEVATIONS (SHEET 4 OF 4)</td>	BRIDGE DECK ELEVATIONS (SHEET 4 OF 4)

BRIDGE DESCRIPTION

A ONE SPAN (111'-0") BRIDGE WITH PRESTRESSED PRECAST CONCRETE GIRDERS (BT 42'S) OVER THE BIG THOMPSON RIVER WITH A 43'-0" WIDE BRIDGE DECK, 6.3' 0" 0" SKEW AND BRIDGE RAIL TYPE 10M.

CROSS REFERENCE DRAWING NUMBER: 2207 EAST HIGHWAY 402, LOVELAND, COLORADO 80037, Phone: 970-687-4670 FAX: 970-689-0289

SECTION OR DETAIL IDENTIFICATION: REGION 4

SHEET REVISIONS

No.	Date	Comments
1	8-23	As Noted
2		Unit Leader

As Constructed

No Revisions: 6-30-2010

Revised: 6-30-2010

Void: 6-30-2010

GENERAL INFORMATION AND SUMMARY OF QUANTITIES

Project No./Code: BR 0341-068

Design: D. Deschamps

Detail: D. Deschamps

Sheet Number: 83

STATE OF OHIO
REGISTERED PROFESSIONAL ENGINEER
No. 24552
John P. Kelly
6-30-70
PROFESSIONAL ENGINEER

A = girder depth = 3" - 3'-3"

[illegible]

Pri

NOTES

All diaphragm materials, including bolts, nuts, and washers, shall be galvanized. Contractor after fabrication.

★ If the construction layout does not call for internally diaphragms, there shall be at least one diaphragm at mid span.

Bolts, nuts and washers may be zinc plated in lieu of being galvanized.

► Diaphragms A, B and C shall be shown on the shop drawings.

The diaphragms may be placed on a skew such that they are between 30° and 100° to the girders. Additionally, all diaphragms shall be installed level.

The Contractor is responsible for determining necessary bracing requirements and for providing adequate bracing for the diaphragms. The Contractor shall be responsible for any bracing encountered for each specific project.

When bracing or diaphragms are required no girders shall be erected and left unbraced. The intermediate diaphragms (when used) shall be connected to the adjacent girders simultaneously.

Use and installation of the internal diaphragms shall not be the Contractor's sole responsibility to construct the Work in a manner which provides unnecessary rigidity.

► The Contractor shall be responsible for providing the proper structure, the lines and grades indicated on the plans.

★ If the construction layout does not specify diaphragms, there shall be at least one diaphragm at midspan.

Bolts, nuts and lock washers may be zinc plated in lieu of being galvanized.

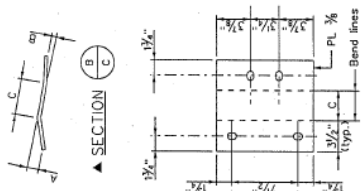
▲ Dimensions A, B and C shall be shown on the shop drawings.

The diaphragms may be placed on a skew such that they are between 80° and 100° to the girders. Additionally, all diaphragms shall be installed level.

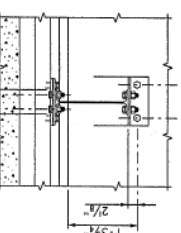
The Contractor is responsible for determining necessary bracing requirements and for providing adequate bracing for the specific wind and weather conditions to be encountered for each specific project.

When bracing or diaphragms are required, no girders shall be erected and left unbraced. The intermediate diaphragms (when used) shall be connected to the adjacent girders simultaneously with the erection of the girders.

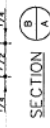
Use and installation of the intermediate diaphragms shall not relieve the Contractor of full responsibility to construct the Work in a manner which provides oil necessary rigidly, supports oil loads imposed, and provides in the finished structure the lines and grades indicated on the plans.



SECTION

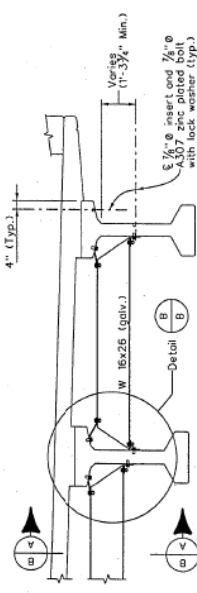


1



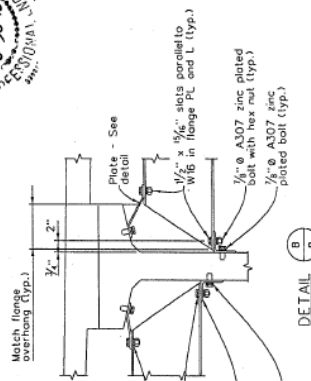
PLAN

(Before bending)
PLATE DETAIL




INTERMEDIATE DIAPHRAGM DETAILS

★ For location of diaphragms, see Construction Layout.



DETAILS



CONSULTING STRUCTURAL ENGINEERS		Colorado Department of Transportation		As Constructed		PRESTRESSED CONCRETE I (MISC.)		Project No./Code	
		2207 EAST HIGHWAY 402		No Revisions: 6-30-2010				BR 0341-068	
						Designer: D DESCHAMP		Structure	
		REGION 4				Detailer: D DESCHAMP		Numbers	
						Sheet Subset: Bridge		C-15-AL	
						Sheet Subset: BA 12 of 21		94	
								Sheet Number	

C-15-O Construction Drawings

Computer File Information		Sheet Revisions		Colorado Department of Transportation		As Constructed		GENERAL INFORMATION		Project No./Code	
Creation Date:	11/25/89	Initials:	A.A.H.	7-3-01	Revised note	4001 East Arapahoe Avenue, Room 300 Denver, Colorado 80202 Phone: 303-757-2352 FAX: 303-757-8197	No Revisions:	0	Designer:	A. Ruppel/Structure	BR 0341-053
Last Modification Date:	07/02/01	Initials:	T.O.E.	000000					Checker:	T. Gierke/Structure	13488
Full Path:	C:\N13488-PROJ\SAVC-15-ON								Sheet Number:	28	
Drawing File Name:	07Zerc.dwg								Sheet Sublot:	Bridge Sublot Sheets: B1 of 46	
Acad Ver:	15.0	Scale:	Scale varies	Unit:	Feet						

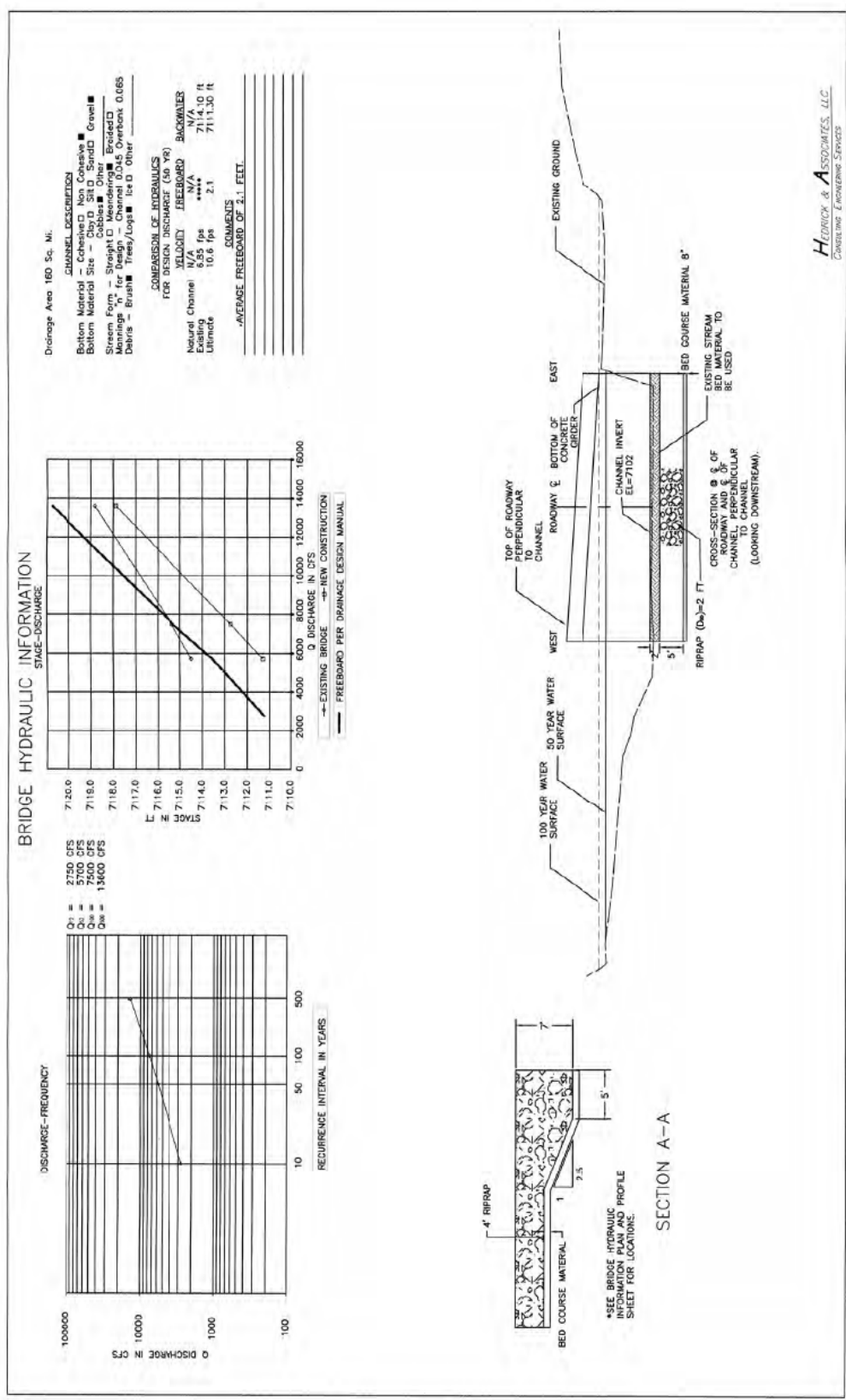
INDEX OF DRAWINGS	
B 01	General Information
B 02	Summary of Quantities
B 03	General Layout
B 04	Engineering Geology Sit 34 Crossing Big Thompson River
B 05	Bridge Hydraulic Information
B 06	Bridge Hydraulic Information Details
B 07	Construction Layout
B 08	Construction Details
B 09	Foundation Details
B 10	Foundation Details
B 11	Abutment 1 Details
B 12	Abutment 2 Details
B 13	Wingwall Details
B 14	Retaining Wall A, B, and C
B 15	Retaining Wall Details (1 of 2)
B 16	Retaining Wall Details (2 of 2)
B 17	See Wall Details
B 18	See Pier 2 Details (1 of 3)
B 19	Pier 2 Details (2 of 3)
B 20	Pier 2 Details (3 of 3)
B 21	Superstructure Details (1 of 3)
B 22	Superstructure Details (2 of 3)
B 23	Superstructure Details (3 of 3)
B 24	Precast Box Girder Details
B 25	Precast Pier Deck Forms (Optional)
B 26	Precast Pier Deck Forms (Optional)
B 27	Approach Box Details (1 of 2)
B 28	Approach Box Details (2 of 2)
B 29	Bridge Expansion Details (G-4 feet)
B 30	Bridge Expansion Details (G-4 feet)
B 31	Bridge Rail Type 10M (1 of 4)
B 32	Bridge Rail Type 10M (2 of 4)
B 33	Bridge Rail Type 10M (3 of 4)
B 34	Bridge Rail Type 10M (4 of 4)
B 35	Excavation and Backfill for Bridges in Fill
B 36	Excavation and Backfill for Bridges in Cut
B 37	Mechanically Stabilized Earthfill
B 38	Decking Mechanical And Electrical Vault
B 39	Bridge Deck Details (1 of 8)
B 40	Bridge Deck Details (2 of 8)
B 41	Bridge Deck Details (3 of 8)
B 42	Bridge Deck Details (4 of 8)
B 43	Bridge Deck Details (5 of 8)
B 44	Bridge Deck Details (6 of 8)
B 45	Bridge Deck Details (7 of 8)
B 46	Bridge Deck Details (8 of 8)

BRIDGE DESIGN DATA	
ASHTO, SECOND EDITION LRFD WITH 2003 INTERIMS	
DESIGN METHOD: LOAD AND RESISTANCE FACTOR DESIGN	
SIDE LOAD: 14-03 DESIGN TRUCK OR TANDON, AND DESIGN LANE LOAD	
DEAD LOAD: ASSUMES 38 LBS PER SQ. FT. FOR BRIDGE DECK OVERLAY	
DEAD LOAD: ASSUMES 5 LBS PER SQ. FT. FOR PERMANENT STEEL DECK FORMS	
REINFORCED CONCRETE (BRIDGE):	
CLASS D CONCRETE:	$f'_c = 4,500$ psi
REINFORCING STEEL:	$f_y = 60,000$ psi
CAST-IN-PLACE CONCRETE:	
CLASS B2 CONCRETE:	$f'_c = 4,000$ psi
REINFORCING STEEL:	$f_y = 60,000$ psi
PRESTRESSED CONCRETE:	
CLASS 3 CONCRETE:	$f'_c =$ SEE DETAILS
REINFORCED CONCRETE (RETAINING WALLS):	$f'_c = 270,000$ psi
CLASS D CONCRETE:	$f'_c = 4,500$ psi
REINFORCING STEEL:	$f_y = 60,000$ psi
SEA WALL DESIGN DATA	
DESIGN METHOD: LOAD AND RESISTANCE FACTOR DESIGN	
EQUIVALENT FLUID PRESSURE = 80.0 LB/FT.	
CLASS 3 CONCRETE:	$f'_c = 4,500$ psi
LIVE LOAD SURCHARGE = 2 FT.	

GENERAL NOTES	
NOTES AS SHOWN IN THE PLANS, STRUCTURE, ELEVATION AND BAKETILL SHALL BE IN ACCORDANCE WITH M-206-1 FOR CAST-IN-PLACE RETAINING WALLS.	
EXPANSION JOINT MATERIAL SHALL MEET ASHTO SPECIFICATION M-311.	
A COLORED STRUCTURAL CONCRETE FINISH WILL BE REQUIRED AS SHOWN ON THE PLANS.	
5658 COLOR NO. 33446, AND IS TO BE SELECTED FROM TEST PANELS PROVIDED BY THE CONTRACTOR.	
GRADE 60 REINFORCING STEEL IS REQUIRED.	
ALL REINFORCING STEEL SHALL BE EPOXY COATED UNLESS OTHERWISE NOTED.	
THE FOLLOWING TABLE GIVES THE MINIMUM LAP SPICE LENGTH FOR EPOXY COATED REINFORCING BARS PLACED IN ACCORDANCE WITH SUBSECTION 802.06. THESE SPICE LENGTHS SHALL BE INCREASED BY 25% FOR BARS SPACED AT LESS THAN 6" ON CENTER.	
BAR SIZE	#4 #5 #6 #7 #8 #9 #10 #11
SPICE LENGTH FOR	1'-3" 1'-5" 1'-10" 2'-2" 3'-8" 4'-8" 5'-11" 7'-3"
WHEN THE CONTRACTOR ELECTS TO SUBSTITUTE EPOXY COATED REINFORCEMENT FOR BLACK REINFORCING BARS, THE MINIMUM LAP SPICE SHALL BE AS DESCRIBED ABOVE.	
THE FOLLOWING TABLE GIVES THE MINIMUM LAP SPICE LENGTH FOR BLACK REINFORCING BARS PLACED IN ACCORDANCE WITH SUBSECTION 802.06. THESE SPICE LENGTHS SHALL BE INCREASED BY 25% FOR BARS SPACED AT LESS THAN 6" ON CENTER.	
BAR SIZE	#4 #5 #6 #7 #8 #9 #10 #11
SPICE LENGTH FOR	1'-0" 1'-4" 1'-7" 1'-10" 2'-5" 3'-1" 3'-11" 4'-10"
THE ABOVE SPICE LENGTHS SHALL BE INCREASED BY 20 PERCENT FOR 3 BAR BUNDLES AND 33 PERCENT FOR 4 BAR BUNDLES.	
THE CONTRACTOR SHALL BE RESPONSIBLE FOR THE STABILITY OF THE STRUCTURE DURING CONSTRUCTION.	
B.F. = BACK FACE	
F.F. = FACE	
P.F. = FACE	
N.E. = NON-EPXY COATED REINFORCING	
PERMANENT DECK FORMS NON-REMOVABLE	
FOR STRUCTURE NUMBER INSTALLATION, SEE STANDARD S-614-12	
STATIONS, ELEVATIONS, AND DIMENSIONS CONTAINED IN THESE PLANS ARE CALCULATED FROM A MEAN SEA LEVEL DATUM. THE CONTRACTOR SHALL VERIFY ALL DIMENSIONS IN THE FIELD BEFORE ORDERING OR FABRICATING ANY MATERIAL.	
THE INFORMATION SHOWN ON THESE PLANS CONCERNING THE TYPE AND LOCATION OF UNDERGROUND UTILITIES IS NOT GUARANTEED TO BE ACCURATE OR ALL INCLUSIVE. THE CONTRACTOR IS RESPONSIBLE FOR MAKING HIS OWN DETERMINATION AS TO THE LOCATION AND DEPTH OF ALL UTILITIES. THE CONTRACTOR SHALL BE RESPONSIBLE FOR OBTAINING ALL NECESSARY PERMITS AND NOTIFICATIONS FROM THE APPROPRIATE AGENCIES AS REQUIRED BY THE COLORADO CONSTRUCTION ACT AND THE COLORADO CONSTRUCTION ACT NOTIFICATION CENTER OF COLORADO A-1-800-942-1887 AT LEAST 2 DAYS (NOT INCLUDING THE DAY OF NOTIFICATION) PRIOR TO ANY EXCAVATION OR OTHER EARTHWORK.	

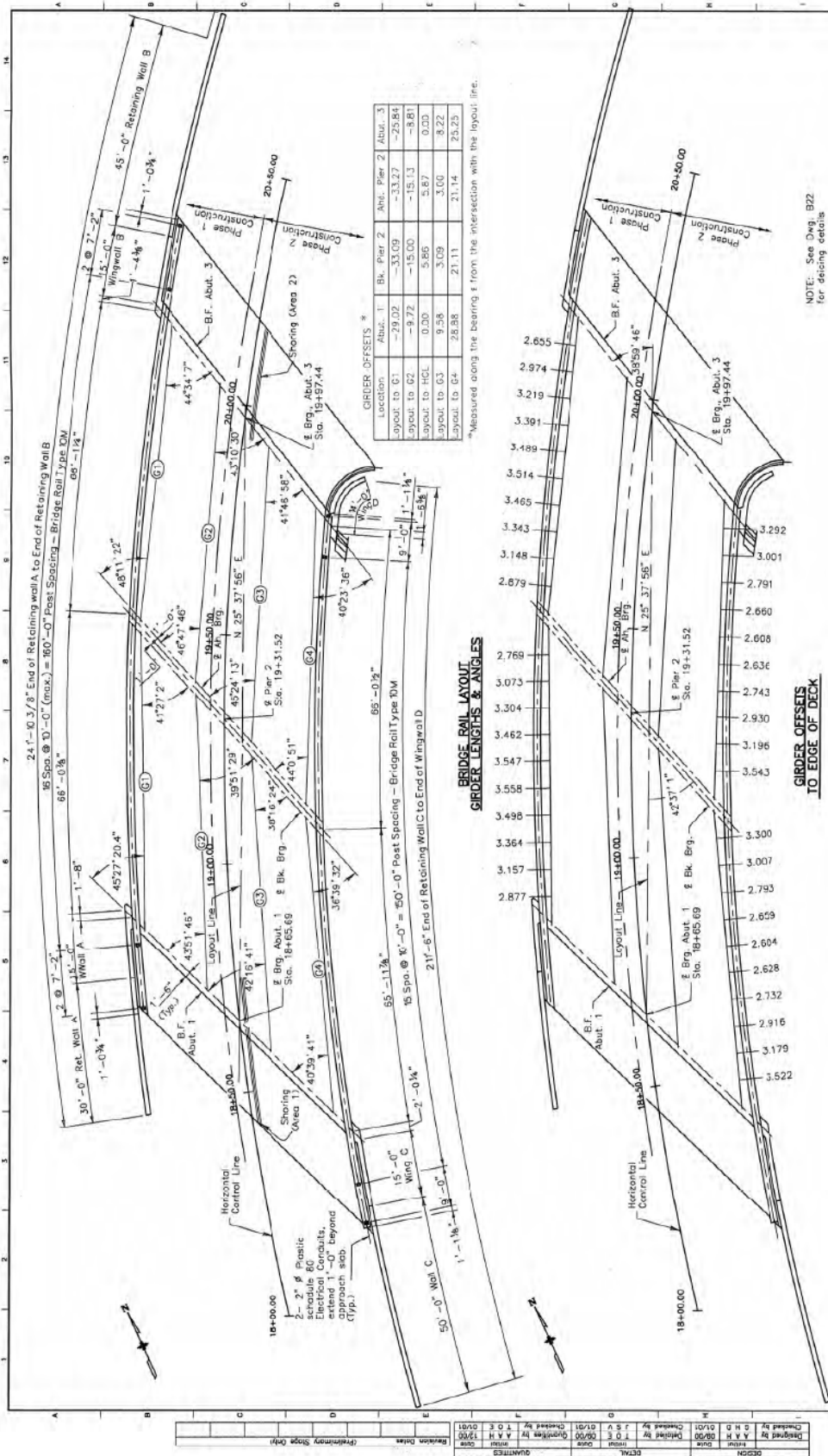
BRIDGE DESCRIPTION	
2-Span Bridge, 66'-11 1/2" x 64'-11 1/2" Concrete Deck and Prestressed Box Girder, Continuous.	
Over Big Thompson River, on U.S. Hwy 34, 40'-0" Curb to Curb, Right-of-Way 100'.	

CROSS REFERENCE DRAWING NUMBERS	
(IF BLANK, REFERENCE IS TO SAME SHEET)	
SECTION OR DETAIL IDENTIFICATION	

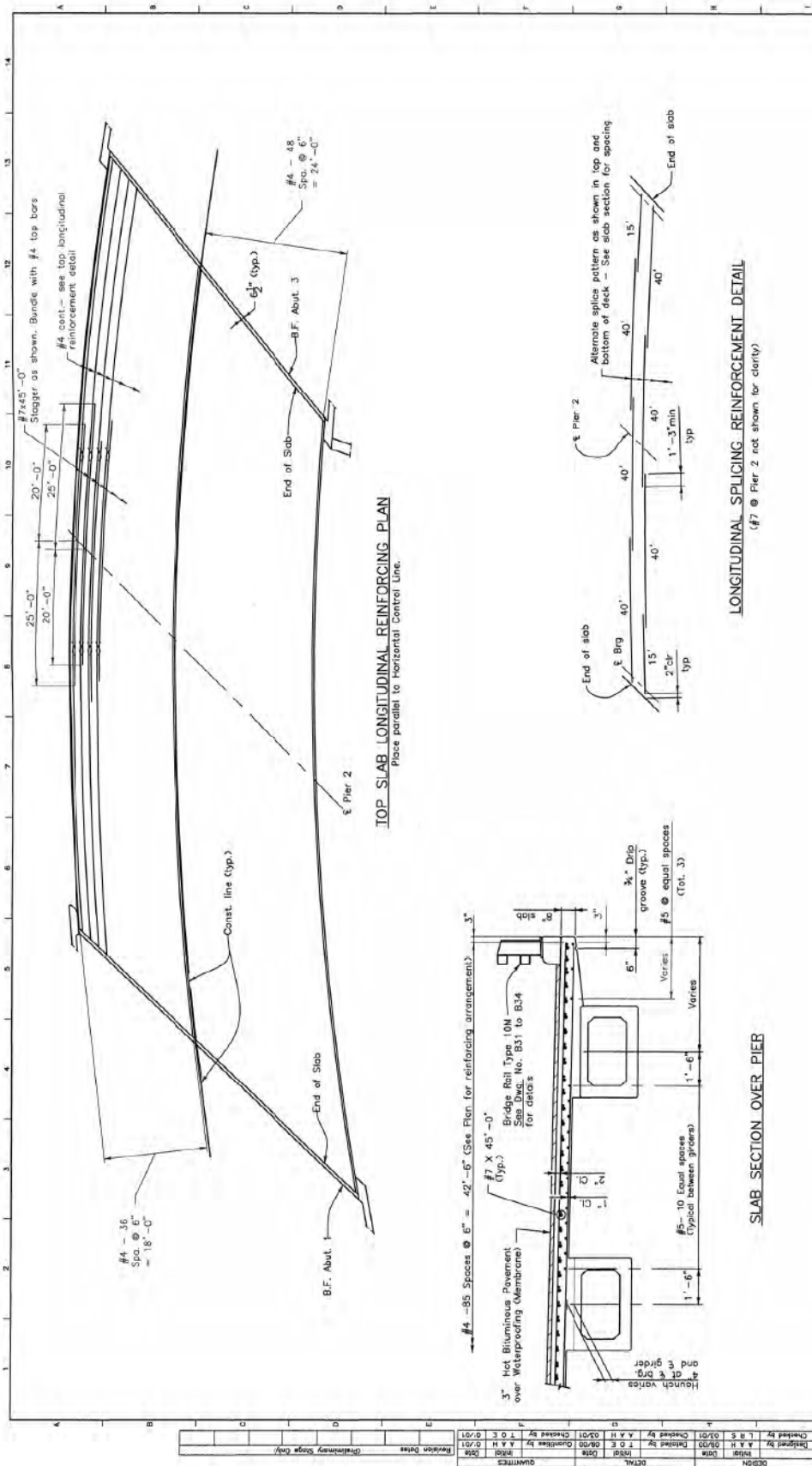


Computer File Information		Sheet Revisions		Colorado Department of Transportation		As Constructed		BRIDGE HYDRAULIC INFORMATION		Project No./Code	
Creation Date:	06/01/00	Mid:	EHS	CE3	mm/dd/yy	XXXX	XXX	Regar 4 - Loveland Residency	Details	BR 0341-053	
Last Modification Date:	1/13/2001	Mid:	EHS	CE3	mm/dd/yy	XXXX	XXX	2207 East Highway 402			
Full Path:	\\PSP4\SP44_Big Thompson\VC_15_H\cmg	Mid:	EHS	CE3	mm/dd/yy	XXXX	XXX	Phone: 970-407-4676 FAX: 970-409-3189	Designer: C. DRESEN	Structure Numbers: C-15-0	
Drawing File Name:	br_jh-hydr.dwg	Mid:	EHS	CE3	mm/dd/yy	XXXX	XXX	SEE	Checker: E. SAN	C-15-H (old)	13488
Asst Ver: R14	Side AS SHOWN	Units:	English	CE3	mm/dd/yy	XXXX	XXX		Steel Subst: BRIDGE	Sheet Sheet: 807 of 39	34

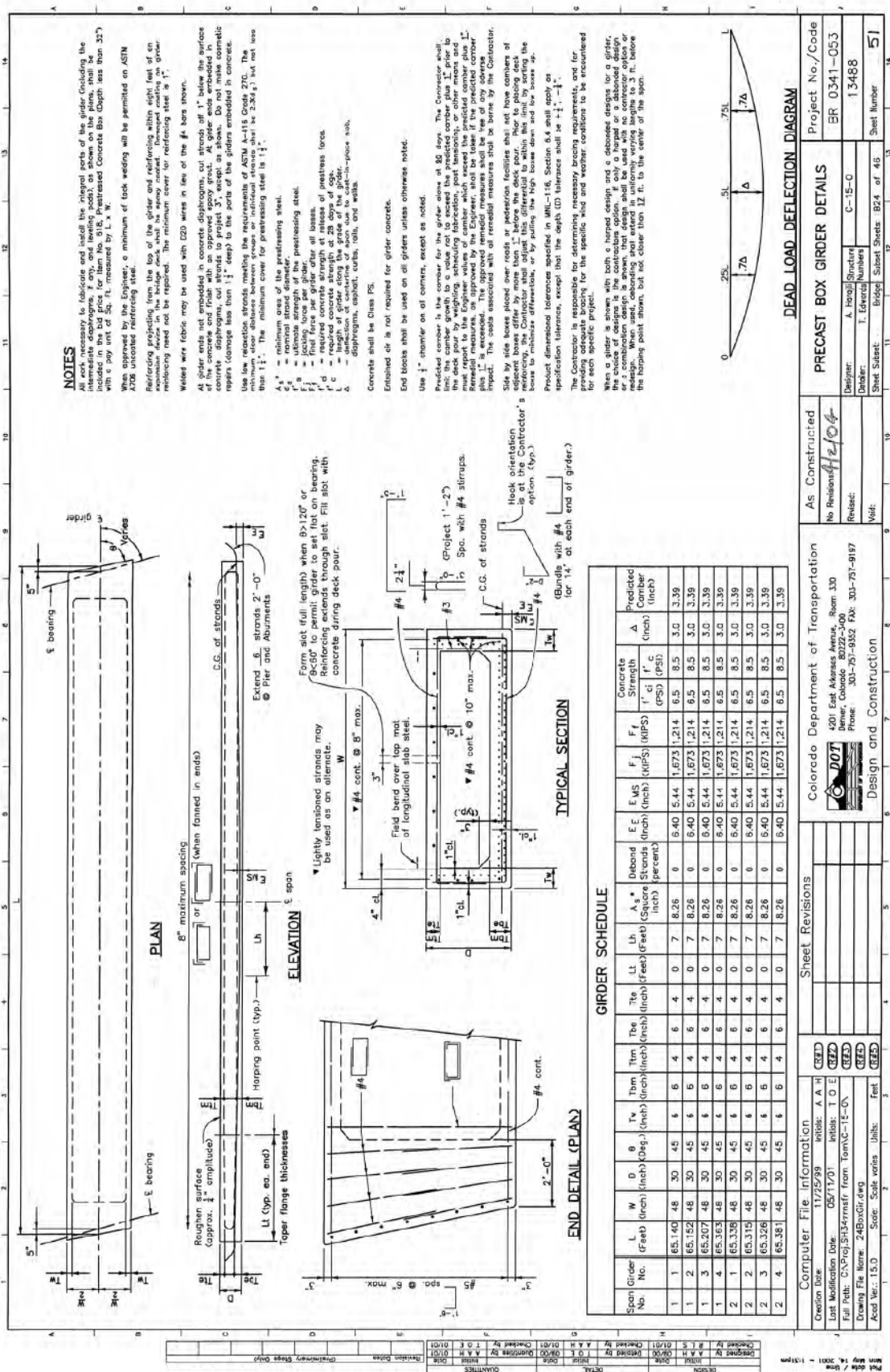
HEDRICK & ASSOCIATES, LLC
CONSULTING ENGINEERING SERVICES

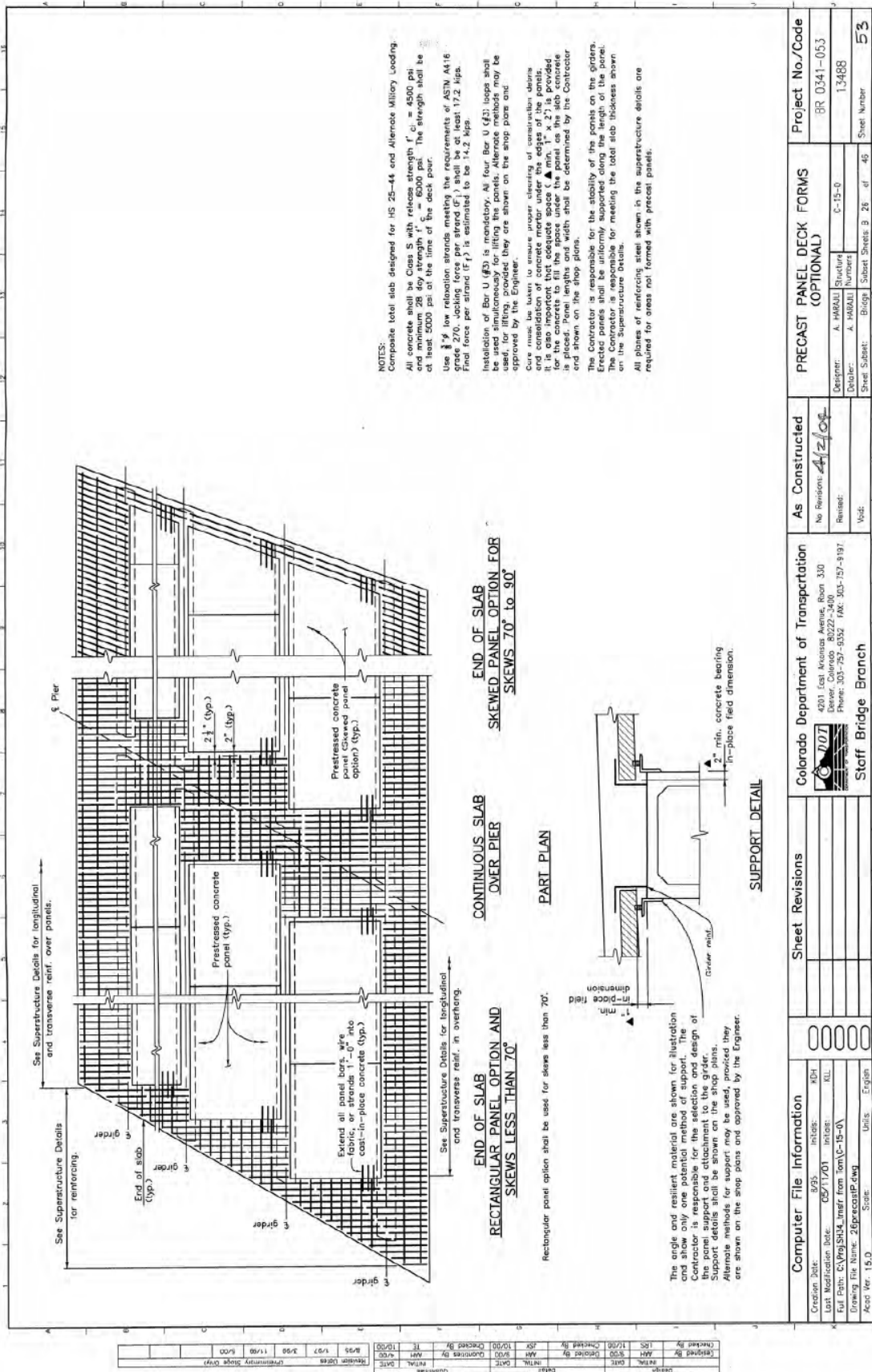


Computer File Information		Colorado Department of Transportation		As Constructed		CONSTRUCTION LAYOUT		Project No./Code	
Creation Date:	01/99	4201 East Arkansas Avenue, Room 330		No Revisions		DR		BR 0341-053	
Last Modification Date:	05/01/01	Denver, Colorado 80221-3400		Revised:		1		C-15-O	
Full Path:	C:\Pro\S434\mtrk from Tempe-19-a	Phone: 303-797-3552 Fax: 303-797-9197		Note:		1		13488	
Drawing File Name:	0341-053.dwg	Design and Construction		Sheet:		BRIDGE		Sheet Number	
Acad Ver.: 15.0	SOLE	UNITS		Sheet:		BRIDGE		35	









NOTES:

Composite total slab designed for HS 25-44 and Alternate Military Loading.

All concrete shall be Class S with release strength $f'_{ci} = 4500$ psi and minimum 28 day strength $f'_c = 6000$ psi. The strength shall be at least 5000 psi at the time of the deck pour.

Use $\frac{3}{8}$ " y low relaxation strands meeting the requirements of ASTM A416 grade 270. Jacking force per strand (P_j) shall be at least 17.2 kips. Final force per strand (P_f) is estimated to be 14.2 kips.

Installation of Bar U (#5) is mandatory. All four Bar U (#5) loops shall be used simultaneously for lifting the panels. Alternate methods may be used if approved by the Engineer.

Cure mass less water to ensure proper curing of vaporization during end consolidation of concrete mortar under the edges of the panels. It is also important that adequate space (Δ , min. 1" x 2") is provided for the concrete to be placed. Panel lengths and width shall be determined by the Contractor and shown on the shop plans.

The Contractor is responsible for the stability of the panels on the girders. Erected panels shall be uniformly supported along the length of the panel. The Contractor is responsible for meeting the total slab thickness shown on the Superstructure Details.

All phases of reinforcing steel shown in the superstructure details are required for areas not formed with precast panels.

CONTINUOUS SLAB OVER PIER PART PLAN

END OF SLAB RECTANGULAR PANEL OPTION AND SKEWS LESS THAN 70°

Rectangular panel option shall be used for skew angles less than 70°.

END OF SLAB SKEWED PANEL OPTION FOR SKEWS 70° TO 90°

SUPPORT DETAIL

The angle and resilient material are shown for illustration only. The Contractor is responsible for the selection and design of the panel support and attachment to the girder. Support details shall be shown on the shop plans. Alternate methods for support may be used, provided they are shown on the shop plans and approved by the Engineer.

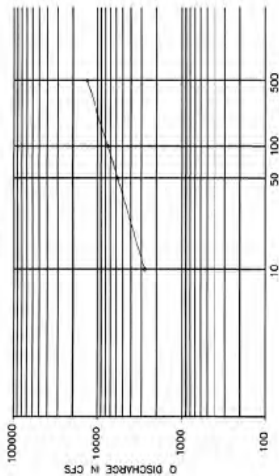
Computer File Information			Sheet Revisions		Colorado Department of Transportation		As Constructed		PRECAST PANEL DECK FORMS (OPTIONAL)		Project No./Code	
Creation Date: 5/95	Initials: ADH						No Revisions: 4/2/04		Optional		BR 0341-053	
Last Modification Date: 05/11/01	Initials: KLL						Revised:		Designer: A. MARALI	Quantity: C-15-0	13488	
Full Path: C:\proj\Std_mfr\form\03-15-01							Void:		Checker: A. MARALI	Number:	Sheet Number	
Drawing File Name: 26precaster.dwg									Sheet Subst: Bridge	Sheet Sheets: 26 of 45	53	
Acad Ver: 15.0	Scale:	Units: English										

C-15-U Construction Drawings



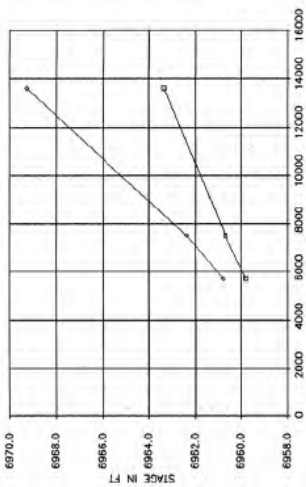
BRIDGE HYDRAULIC INFORMATION

DISCHARGE-FREQUENCY



Q₁₀ = 2750 CFS
Q₅₀ = 5700 CFS
Q₁₀₀ = 13600 CFS

STAGE-DISCHARGE



Drainage Area 5.3 Sq. Mi.
Channel Description
Bottom Material - Gravel, Sand, Cobble
Bottom Material Size - Clay, Silt, Sand, Gravel
Stream Form - Straight
Manning's "n" for Design - 0.045
Debris - Brush, Tree/Log, Ice, Other

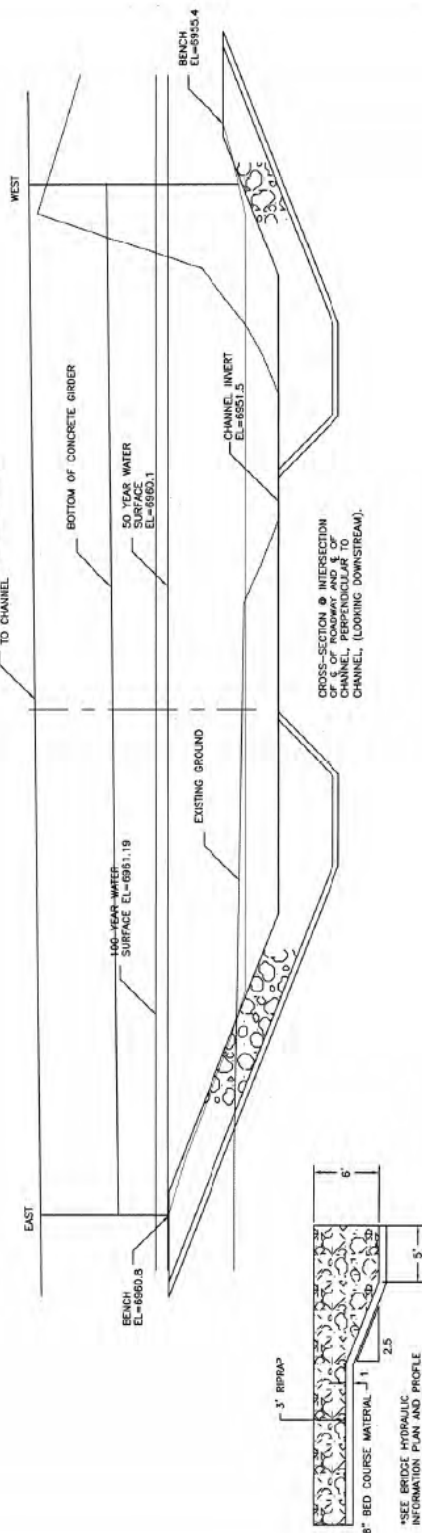
COMPARISON OF HYDRAULICS
FOR DESIGN DISCHARGE (50 YR)
Velocity 10.10 f/s
Natural Channel 10.10 f/s
Existing 7.60 f/s
Ultimate 7.60 f/s

Comments

FREQUENCY INTERVAL IN YEARS

DISCHARGE IN CFS

→ EXISTING BRIDGE → NEW CONSTRUCTION

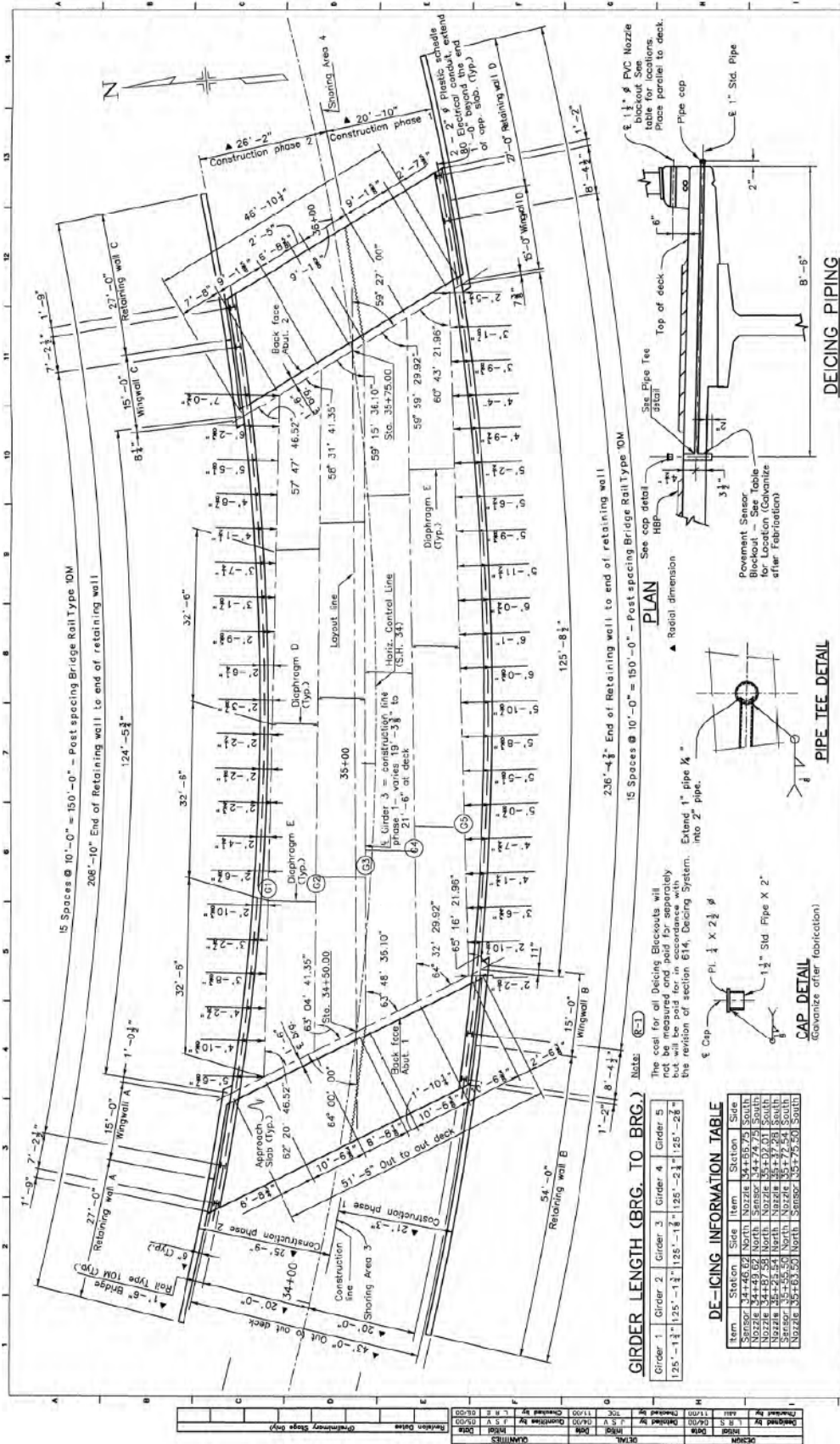


SECTION A-A

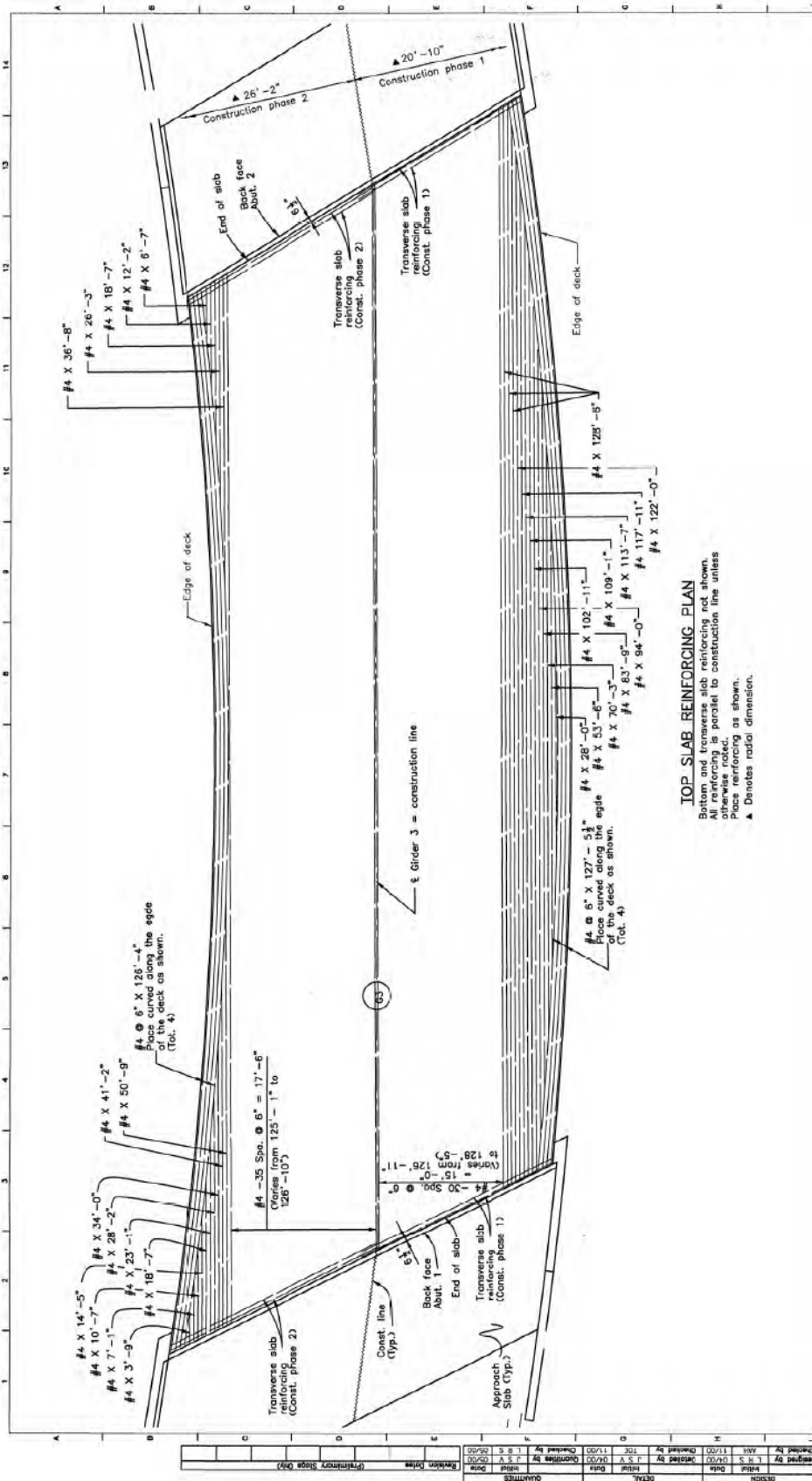
HEDRICK & ASSOCIATES, LLC
CONSULTING ENGINEERING SERVICES

Computer File Information		Sheet Revisions		As Constructed		BRIDGE HYDRAULIC INFORMATION		Project No./Code	
Revision	Date	Revised	By	No. Revisions	Revised	Designer	Checker	BR 0341-053	
1	08/01/00	1	EHS	4	mm/dd/yy	C. DRESEN	C-15-U	13488	
2	1/13/2001	2	EHS		mm/dd/yy	E. SAN	C-15-G (old)		
3	Full Path: \\NPSA\SH-34_Big Thompson\C-15-G.dwg	3			mm/dd/yy				
4	Drawing File Name: br-9-hy1.dwg	4			mm/dd/yy				
5	Acad Ver.: R14	5	Scale AS SHOWN	Unit: English	mm/dd/yy				
						Sheet Subst: BRIDGE		Sheet Number	
						Sheet Subst: B7 of 38		80	

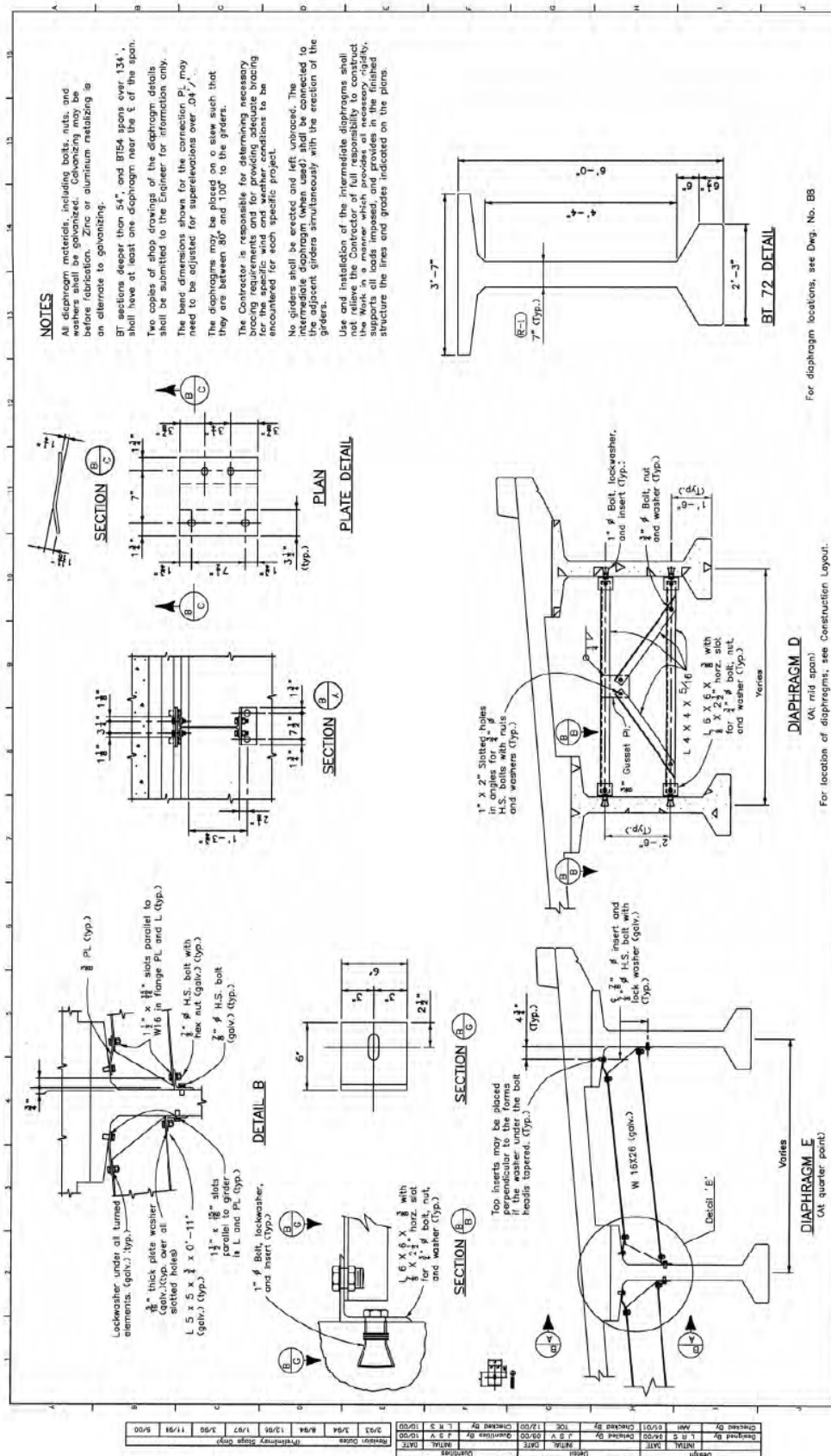
Colorado Department of Transportation
Region 4 - Loveland Residency
2207 East Highway 402
Loveland, Colorado 80537
Phone: 970-561-4673 FAX: 970-566-0188
SCE
Region 4



Computer File Information		Sheet Revisions		Colorado Department of Transportation		As Constructed		CONSTRUCTION LAYOUT		Project No./Code	
Creation Date:	04/05/00	Initials:	JSV	7-3-01	Changed note	RLO	No Revisions:	4/1/04			BR 0341-053
Last Modification Date:	04/19/01	Initials:	JSV				Revised:				13488
Full Path:	C:\VIRIDIAN\PROJ\34						Drawn:	L. Sackler	Structure		
Drawing File Name:	CONSTR150.DWG						Checker:	J. Ward	Number		
Acad Ver.:	ADAT8	Scale:	SCALE	Units:	UNITS		Sheet Subst:	Bridge	Sheet Sheet:	B8	of 39
							Sheet Number:				81




Computer File Information				Sheet Revisions				Colorado Department of Transportation				As Constructed		SUPERSTRUCTURE DETAILS				Project No./Code		
Credent Date:	04/06/00	initial:	US/							4201 East Arapahoe Avenue, Room 330 Denver, Colorado 80222-3400 Phone: 303-797-5352 FAX: 303-757-9197		No. Revisions: 42/04				Designer:	L. Sanchez	Structure:	C-15-U	BR 0341-053
Last Modification Date:	04/16/01	initial:	US/									Revised:				Checker:	J. Valenzuela			13488
Full Path: C:\VIRBIA\PROJ34												Revised:				Sheet Submitter:	Bridge Submitter	Sheet No.	91	
Drawing File Name: SUPERSTRG																				
Acad Ver: AADVER	Scale: SCALE	Units: UNITS																		



For diaphragm locations, see Dwg. No. B3

For location of diaphragms, see Construction Layout.

Computer File Information				Sheet Revisions		Colorado Department of Transportation		As Constructed		PRESTRESSED CONCRETE I		Project No./Code	
Creation Date:	12/88	initial:	qjh	7-3-01	Added dimension		4301 East Adams Avenue, Room 330 Denver, Colorado 80202-3400 Phone: 303-757-3352 FAX: 303-757-3197	No Revisions:	4/2/04			BR 0341-053	
Last Modification Date:	04/93	revised:	jvy					Revised:		13488			
Full Path:	C:\VIEWS\PROJ\2-16							Revised:					
Drawing File Name:	BR0341.DWG							Revised:					
Acad Ver:	R2000	Scale:	English			Staff Bridge Branch		Sheet Subject:	Bridge	Subst. Sheets:	B 23 of 39	Sheet Number	96

C-15-Y Construction Drawings

GENERAL NOTES

EXCEPT AS SHOWN IN THE PLANS, STRUCTURE ELEVATIONS AND BACKFILL SHALL BE IN ACCORDANCE WITH M-206-1 FOR CAST-IN-PLACE RETAINING WALLS.

EXPANSION JOINT MATERIAL SHALL MEET AASHTO SPECIFICATION M-213.

A COLORED STRUCTURAL CONCRETE COATING SHALL BE FURNISHED AS SHOWN ON THE PLANS ON EXPOSED CONCRETE SURFACES TO ONE FOOT BELOW THE GROUND LINE.

THE COLOR SHALL BE BEIGE, EQUIVALENT TO FEDERAL STANDARD 595B COLOR NO. 33446, AND IS TO BE SELECTED FROM TEST PANELS PROVIDED BY THE CONTRACTOR.

GRADE 40 REINFORCING STEEL IS REQUIRED.

ALL REINFORCING STEEL SHALL BE EPOXY COATED UNLESS OTHERWISE NOTED.

(S) DENOTES NON COATED REINFORCING STEEL.

THE FOLLOWING TABLE GIVES THE MINIMUM LAP SPACE LENGTH FOR EPOXY COATED REINFORCING BARS PLACED IN ACCORDANCE WITH SUBSECTION 602.09. THESE SPACE LENGTHS SHALL BE INCREASED BY 25% FOR BARS SPACED AT LESS THAN 6" ON CENTER.

BAR SIZE	#4	#5	#6	#7	#8	#9	#10	#11
SPACE LENGTH FOR CLASS 0 CONCRETE	1'-3"	1'-6"	1'-10"	2'-2"	3'-6"	4'-8"	5'-11"	7'-3"

WHEN THE CONTRACTOR ELECTS TO SUBSTITUTE EPOXY COATED REINFORCEMENT FOR BLACK REINFORCING BARS, THE MINIMUM LAP SPACE SHALL BE AS DESCRIBED ABOVE.

THE FOLLOWING TABLE GIVES THE MINIMUM LAP SPACE LENGTH FOR BLACK REINFORCING BARS PLACED IN ACCORDANCE WITH SUBSECTION 602.09. THESE SPACE LENGTHS SHALL BE INCREASED BY 25% FOR BARS SPACED AT LESS THAN 6" ON CENTER.

BAR SIZE	#4	#5	#6	#7	#8	#9	#10	#11
SPACE LENGTH FOR CLASS 0 CONCRETE	1'-3"	1'-6"	1'-10"	2'-2"	3'-6"	4'-8"	5'-11"	7'-3"

THE ABOVE SPACE LENGTHS SHALL BE INCREASED BY 20 PERCENT FOR 3 BAR BUNDLES AND 33 PERCENT FOR 4 BAR BUNDLES.

THE CONTRACTOR SHALL BE RESPONSIBLE FOR THE STABILITY OF THE STRUCTURE DURING CONSTRUCTION.

E.P. = EPOXY FACE
F.F. = FAR FACE
N.F. = NEAR FACE

PERMANENT DECK FORMS ARE OPTIONAL. (SEE 5)

DESIGN DATA

AASHTO, SECOND EDITION (1975) WITH 1989 INTERIMS

DESIGN METHOD: LOAD AND RESISTANCE FACTOR DESIGN

LIVE LOAD: HS-20 (DESIGN TRUCK OR TANDEN, AND DESIGN LANE LOAD)

ROAD LOAD: ASSUMES 5' TRUCK PER 50' FT. FOR PERMANENT RETAIL DECK FORMING

REINFORCED CONCRETE:

CLASS 0 CONCRETE: $f'_c = 4,500$ psi

REINFORCING STEEL: $f_y = 60,000$ psi

CAISSON CONCRETE:

CLASS 02 CONCRETE: $f'_c = 4,000$ psi

REINFORCING STEEL: $f_y = 60,000$ psi

PRESTRESSED CONCRETE:

CLASS 5 CONCRETE: $f'_c =$ (SEE DETAILS)

$f_p = 270,000$ psi

INDEX OF DRAWINGS

B 01	General Information -
B 02	General Layout
B 03	General Layout
B 04	Engineering Geology
B 05	Bridge Hydraulic Information
B 06	Construction Layout
B 07	Construction Detailing
B 08	Caisson Layout
B 09	Abutment 1 Details
B 10	Abutment 2 Details
B 11	Abutment 3 Details
B 12	Retaining Wall Details
B 13	Pier Miscellaneous Details
B 14	Shoring Details
B 15	Precast Box Girder Details
B 16	Precast Panel Deck Forms (optional)
B 17	Precast Panel Deck Forms (optional)
B 18	Bridge Rail Type 10 Details
B 19	Bridge Rail Type 10 Details
B 20	Bridge Extension Device (10-4 inch)
B 21	Bridge Extension Device (10-4 inch)
B 22	Approach Slab Details
B 23	Excavation and Backfill
B 24	Mechanically Stabilized Backfill
B 25	Bridge Deck Elevations
B 26	Bridge Deck Elevations
B 27	Bridge Deck Elevations
B 28	Bridge Deck Elevations
B 29	Bridge Deck Elevations
B 30	Bridge Deck Elevations
B 31	Bridge Deck Elevations
B 32	Bridge Deck Elevations

SUMMARY OF QUANTITIES

ITEM NUMBER	DESCRIPTION	UNITS EACH	SUPER-STRUCTURE	ABUT. 1	ABUT. 2	ABUT. 3	APPROACH SLAB (BOTH)	TOTALS
206	STRUCTURE EXCAVATION	CY		44.3		35.1		79.4
206	STRUCTURAL BACKFILL (CLASS 1)	CY		22.1		19.3		41.4
206	STRUCTURE BACKFILL (CLASS 2)	CY		30		4.2		34.2
206	MECHANICAL REINFORCEMENT OF SOIL	CY		22.1		19.3		41.4
206	SHORING (AREA 5)	LS		1				1
206	SHORING (AREA 6)	LS				1		1
403	3" BITUMINOUS PAVEMENT (S) (75) (PG 84-28)	LT	104				28	132
503	DRILLED CAISSON (30 INCH)	LF		58		82		140
503	DRILLED CAISSON (42 INCH)	LF			50			50
515	WATERPROOFING (MEMBRANE)	ST	647				199	846
518	BRIDGE EXPANSION DEVICE (6-4 INCH)	FT					80	80
601	CONCRETE CLASS 0 (BRIDGE)	CY	181	46	29	13	93	363
601	STRUCTURAL CONCRETE COATING	ST	399	46	120	48		613
602	REINFORCING STEEL	LB		4119				4119
605	BRIDGE RAIL TYPE 10M	FT	382					382
613	2 INCH ELECTRICAL CONDUIT	FT	775					775
614	CEILING SYSTEM	EA	1					1
618	PRESTRESSED CONCRETE BOX (DEPTH LESS THAN 32 INCHES)	SF	2275					2275

DESIGN DESCRIPTION

ASHTO, SECOND EDITION (1975) WITH 1989 INTERIMS

DESIGN METHOD: LOAD AND RESISTANCE FACTOR DESIGN

LIVE LOAD: HS-20 (DESIGN TRUCK OR TANDEN, AND DESIGN LANE LOAD)

ROAD LOAD: ASSUMES 5' TRUCK PER 50' FT. FOR PERMANENT RETAIL DECK FORMING

REINFORCED CONCRETE:

CLASS 0 CONCRETE: $f'_c = 4,500$ psi

REINFORCING STEEL: $f_y = 60,000$ psi

CAISSON CONCRETE:

CLASS 02 CONCRETE: $f'_c = 4,000$ psi

REINFORCING STEEL: $f_y = 60,000$ psi

PRESTRESSED CONCRETE:

CLASS 5 CONCRETE: $f'_c =$ (SEE DETAILS)

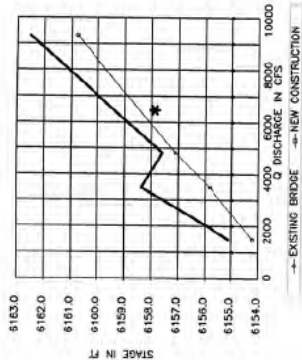
$f_p = 270,000$ psi

INDEX OF DRAWINGS

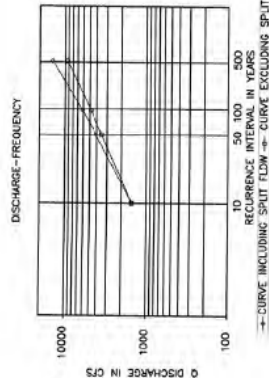
B 01	General Information -
B 02	General Layout
B 03	General Layout
B 04	Engineering Geology
B 05	Bridge Hydraulic Information
B 06	Construction Layout
B 07	Construction Detailing
B 08	Caisson Layout
B 09	Abutment 1 Details
B 10	Abutment 2 Details
B 11	

BRIDGE HYDRAULIC INFORMATION

STAGE-DISCHARGE
(SPILT FLOW)

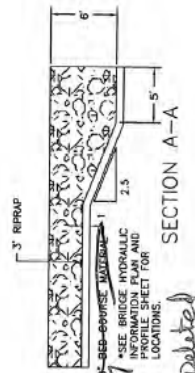
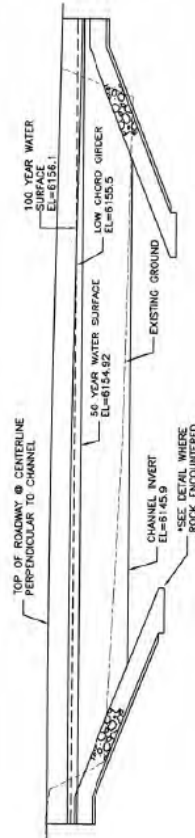


Q_s = 1500 CFS
Q_u = 4100 CFS
Q_u = 14100 CFS
TOTAL FLOW
Q_s = 1500 CFS
Q_u = 3480 CFS
Q_u = 9335 CFS
SPILT FLOW
(UNDER BRIDGE)



TO REFERENCE POINT IN YEAR 2000
+ CURVE INCLUDING SPILT FLOW + CURVE EXCLUDING SPILT FLOW

*EXISTING AND NEW CONSTRUCTION CONTAIN THE SAME STAGE-DISCHARGE VALUES.



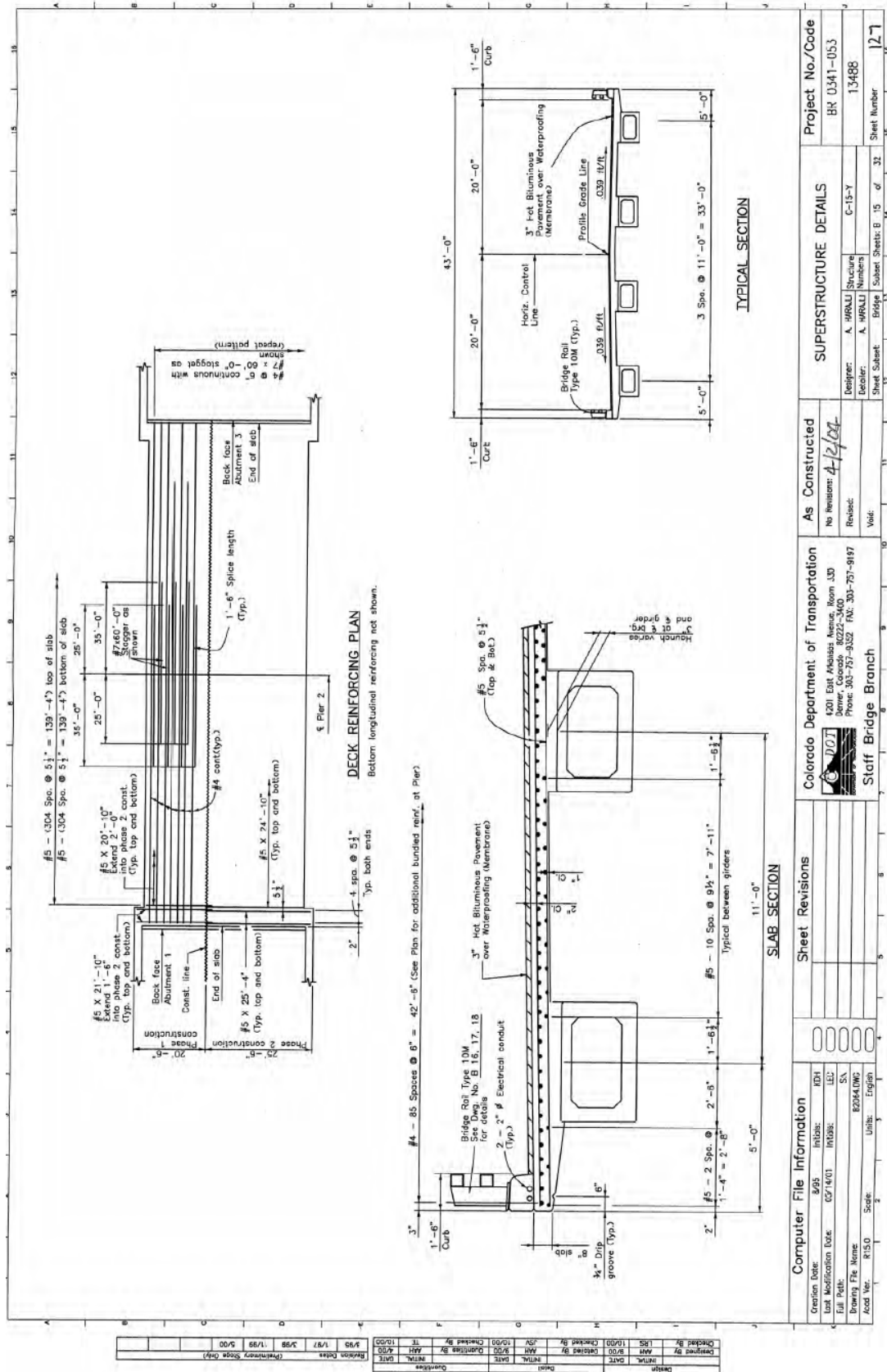
RIPRAP AT ROCK DETAIL

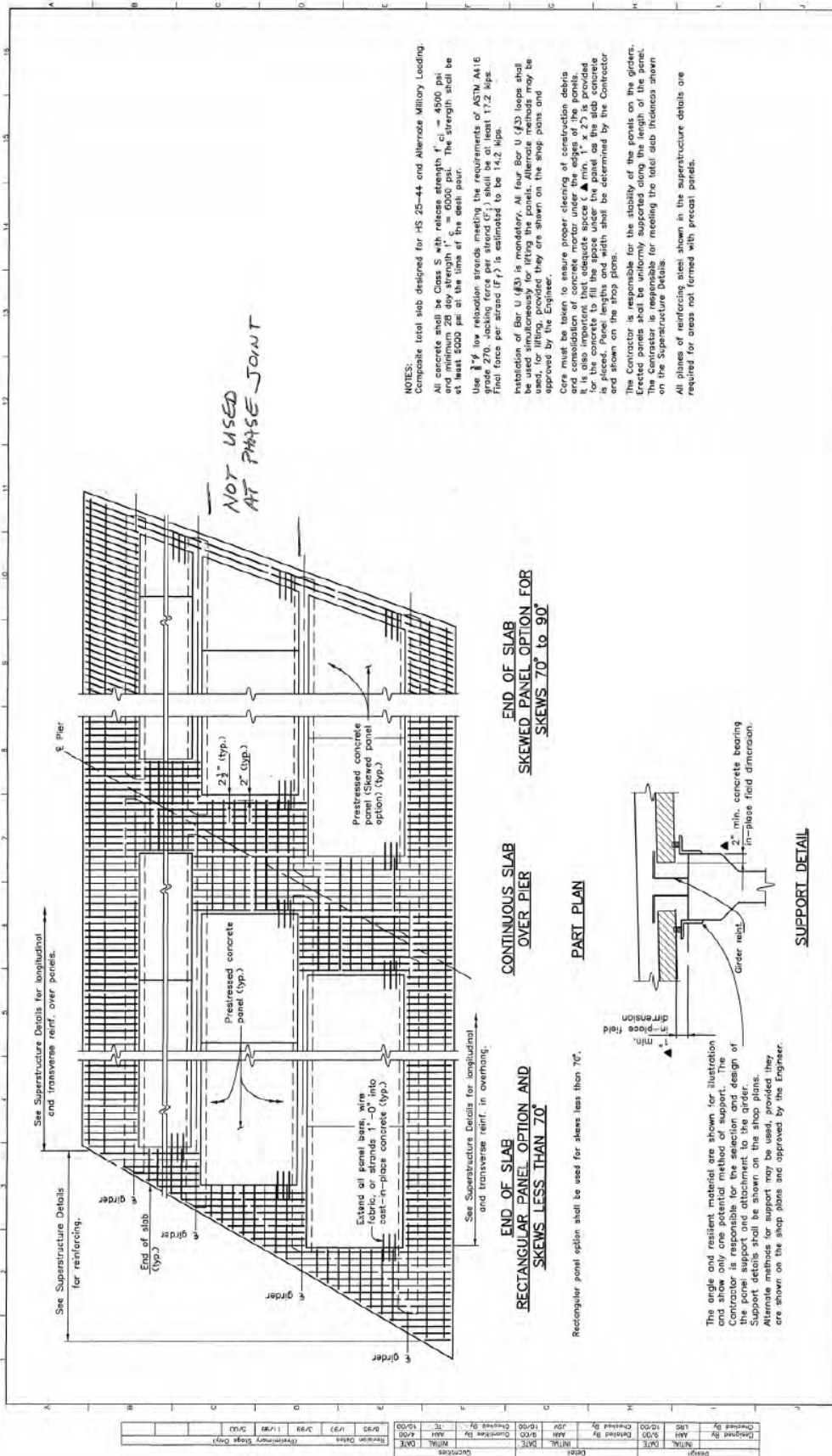
HEDRICK & ASSOCIATES, LLC
CONSULTING ENGINEERING SERVICES

Computer File Information		Sheet Revisions	
Revision Date:	08/01/00	Revised By:	EH
Last Modification Date:	1/18/2001	Revised By:	EH
File Path:	\\NPS4\SH34_Big Thompson\C-15-D.dwg	Revised By:	EH
Drawing File Name:	br_d_hyd.dwg	Revised By:	EH
Acad Ver.:	R14	Scale AS SHOWN	Units: English
Project No./Code		BR 0341-053	
BRIDGE HYDRAULIC INFORMATION		DETAILS	
As Constructed		mm/dd/yy	
No Revisions		mm/dd/yy	
Revised:		mm/dd/yy	
Voted:		mm/dd/yy	
Department of Transportation		Region 4	
Colorado		2007 East Highway 100	
2007 East Highway 100		Lewiston, Colorado 80037	
Phone: 970-967-6670		FAX: 970-669-0288	
SCE		SCE	
Project No./Code		BR 0341-053	
BRIDGE HYDRAULIC INFORMATION		DETAILS	
As Constructed		mm/dd/yy	
No Revisions		mm/dd/yy	
Revised:		mm/dd/yy	
Voted:		mm/dd/yy	
Department of Transportation		Region 4	
Colorado		2007 East Highway 100	
2007 East Highway 100		Lewiston, Colorado 80037	
Phone: 970-967-6670		FAX: 970-669-0288	
SCE		SCE	
Project No./Code		BR 0341-053	
BRIDGE HYDRAULIC INFORMATION		DETAILS	
As Constructed		mm/dd/yy	
No Revisions		mm/dd/yy	
Revised:		mm/dd/yy	
Voted:		mm/dd/yy	
Department of Transportation		Region 4	
Colorado		2007 East Highway 100	
2007 East Highway 100		Lewiston, Colorado 80037	
Phone: 970-967-6670		FAX: 970-669-0288	
SCE		SCE	

Sheet Number

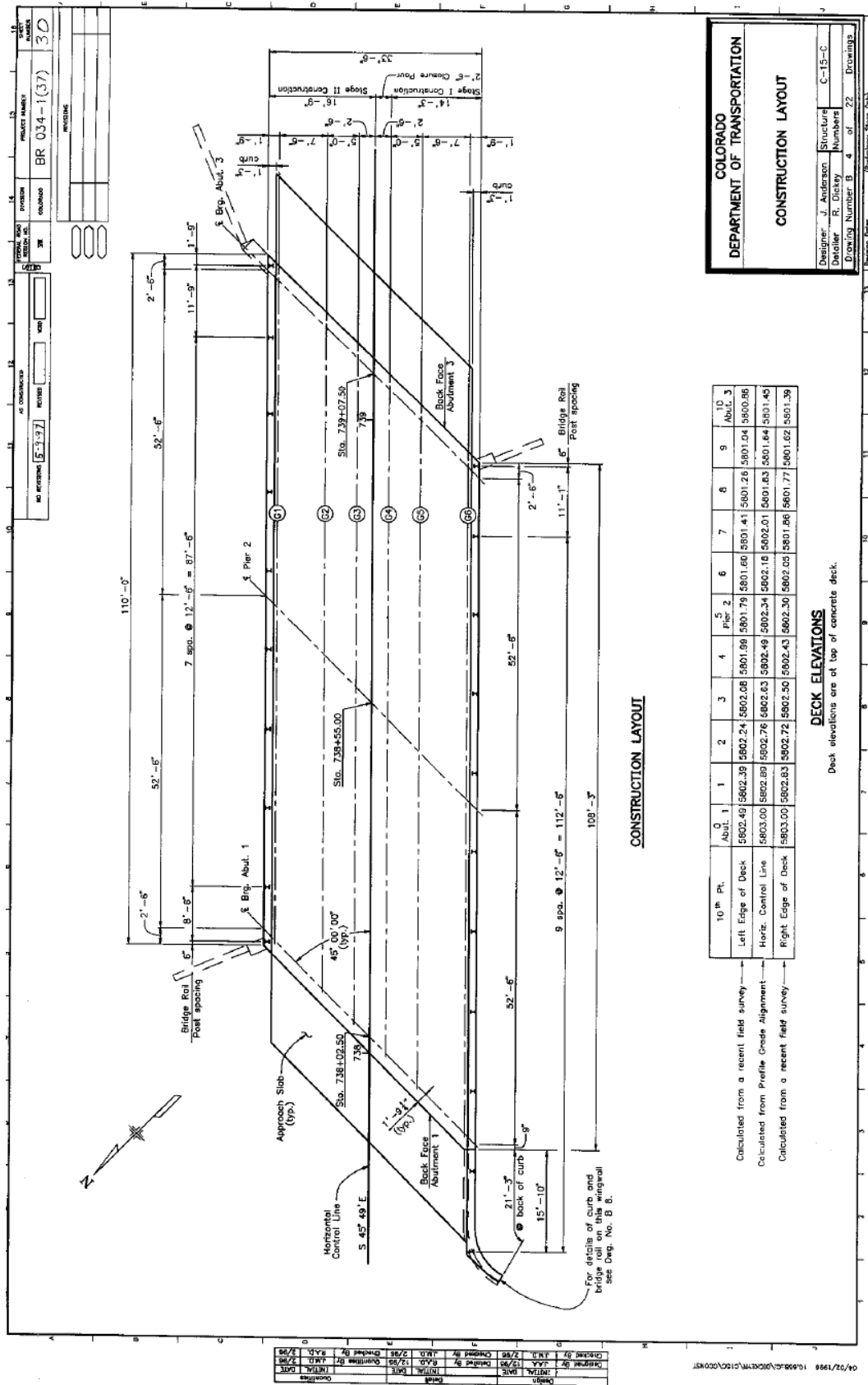
112

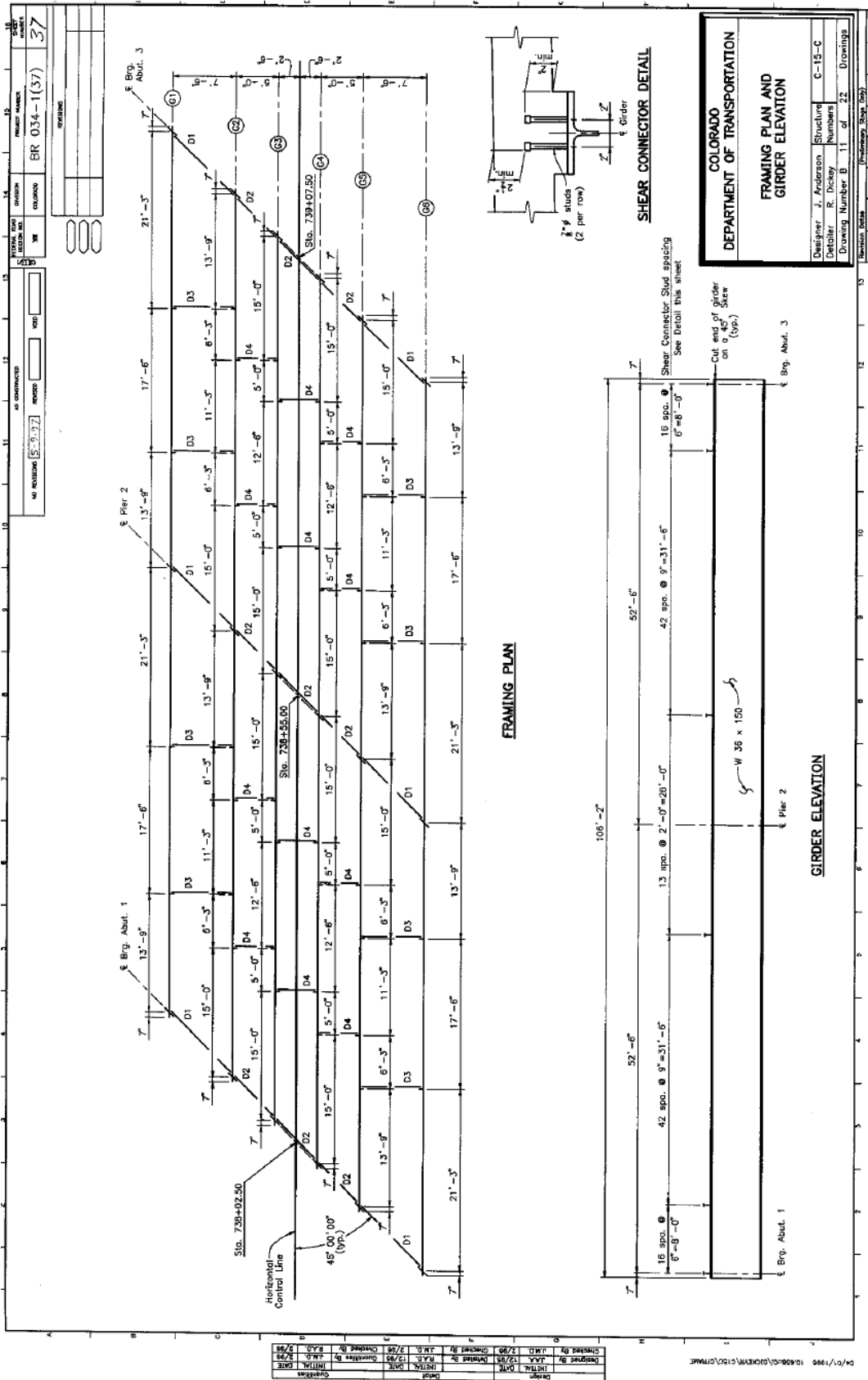


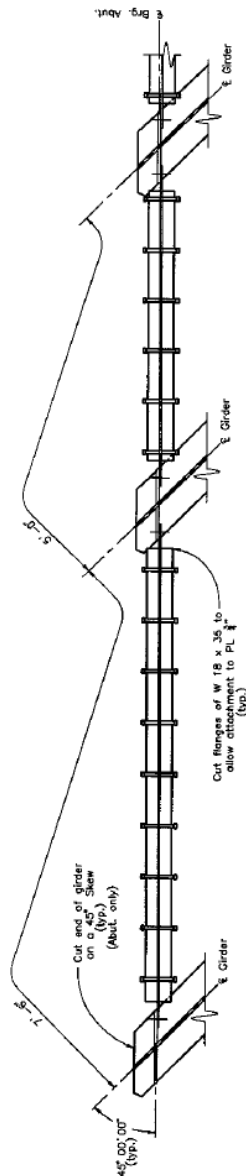


Computer File Information Revision: 0/00 Last Modification Date: 5/2/00 Full Project Name: 8204.Dwg Author: R14.01 State: Utah Units: English		Sheet Revisions 0000 0000 0000 0000		Colorado Department of Transportation 4201 East Avenue Avenue, Room 330 Denver, Colorado 80222-3400 Phone: 303-757-3352 FAX: 303-757-9197 Staff Bridge Branch		As Constructed No Revisions: 0/00 Revised: 4/2/04 Voted:		PRECAST PANEL DECK FORMS (OPTIONAL) Designer: A. HADJI Checker: A. HADJI Sheet Subst: Bridge Subst Sheet 9 of 32		Project No./Code BR 0341-053 13488 Sheet Number	
---	--	---	--	--	--	---	--	--	--	--	--

[illegible]

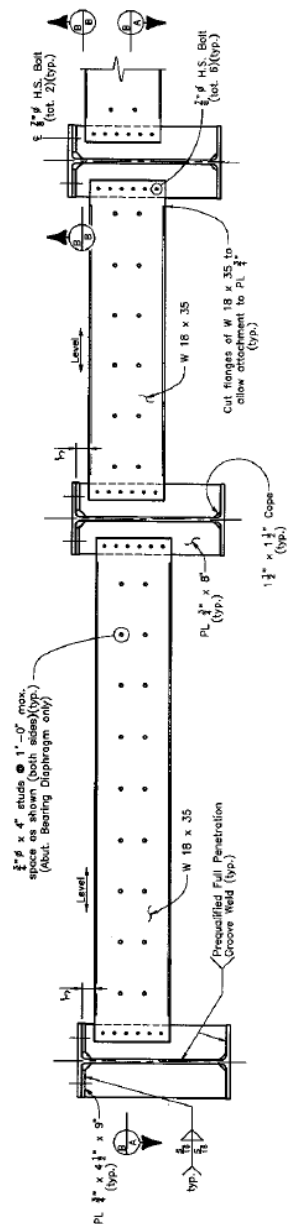
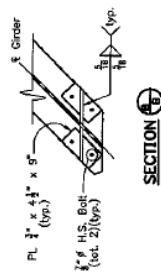




[illegible]

SECTION

Section at C Pier 2 is identical except for cutting the end of the girder and there are no shear studs on Pier Bearing Diaphragm.



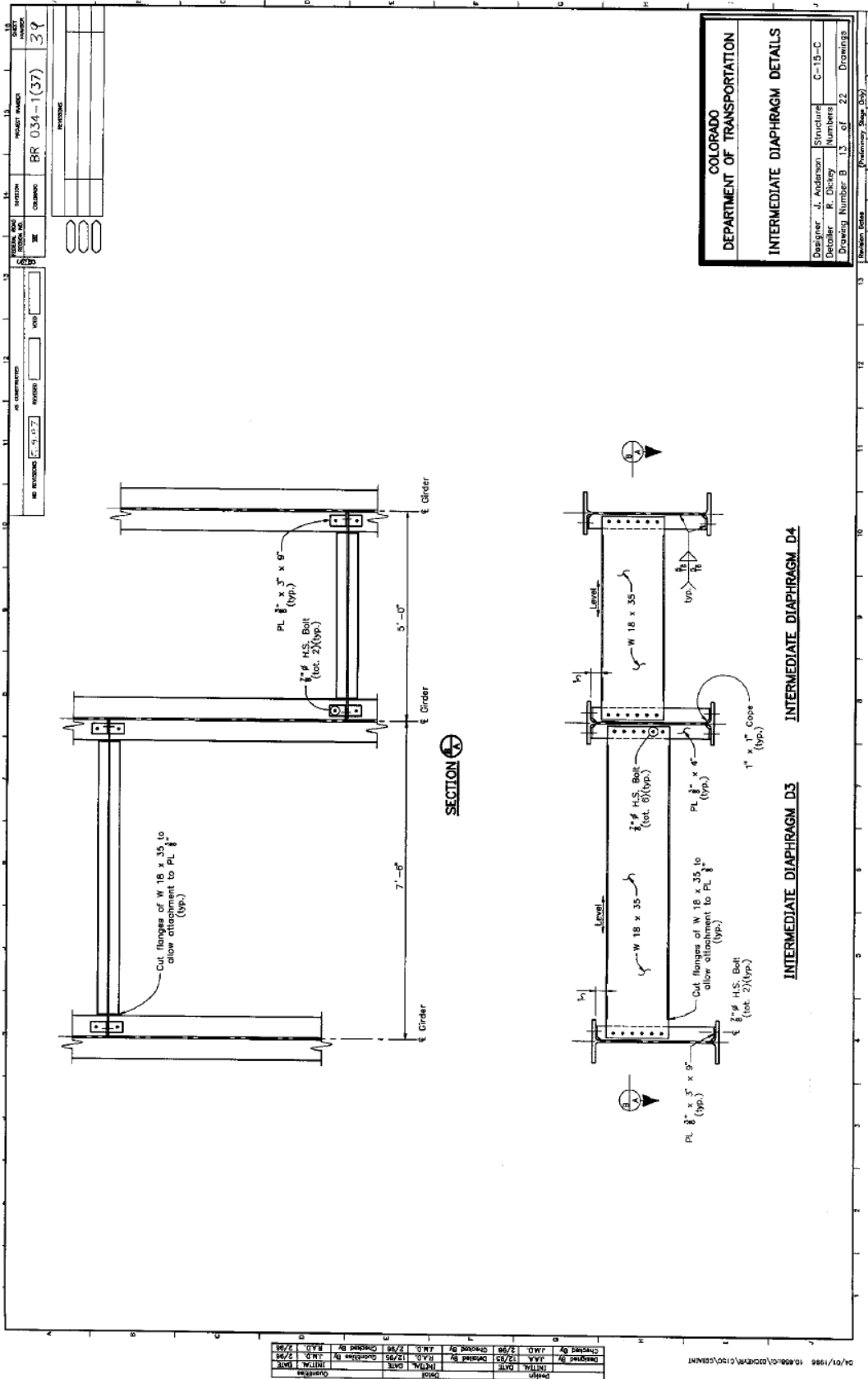
BEARING DIAPHRAGM D1

BEARING DIAPHRAGM D2

COLORADO
DEPARTMENT OF TRANSPORTATION

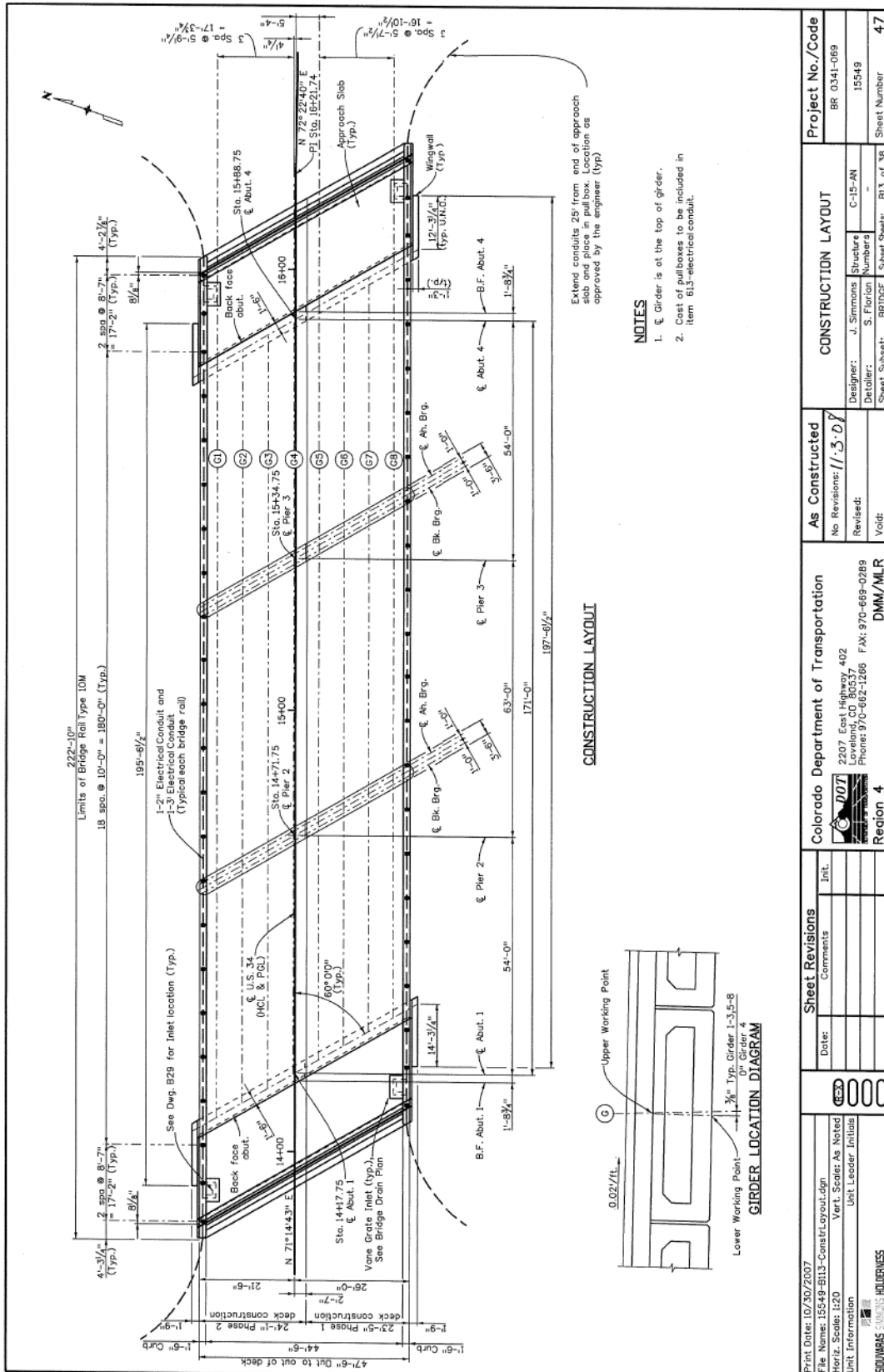
BEARING DIAPHRAGM DETAILS

Designer	J. Anderson	Structure	C-15-C
Detailer	R. Dickey	Numbers	
Drawing Number		9 12 of 22	Drawings



C-15-AN Construction Drawings

GENERAL NOTES		GENERAL NOTES (CONT.)		INDEX OF DRAWINGS																																		
<p>STRUCTURE EXCAVATION AND BACKFILL SHALL BE AS SHOWN ON THE PLANS, EXCEPT SHORING MAY BE REQUIRED FOR EXCAVATION ADJACENT TO THE EXISTING ROADWAY. TEMPORARY EXCAVATION SUPPORT SHALL BE PAID FOR BY ITEM 208 SHORING.</p> <p>EXPANSION JOINT MATERIAL SHALL MEET ASTM D1138 SPECIFICATION W/3.</p> <p>A COLORED STRUCTURAL CONCRETE STAIN FINISH WILL BE REQUIRED, AS SHOWN ON THE PLANS, ON EXPOSED CONCRETE SURFACES THE COLOR SHALL BE BEIGE EQUIVALENT TO FEDERAL SPECIFICATION 271. CONCRETE SHALL BE PLACED IN 12" MAXIMUM LIFT. THE CONTRACTOR SHALL EXTEND TO 1 FOOT BELOW RIPRAP ON ABUTMENTS AND WINGWALLS.</p> <p>LEVELING PADS ARE UNARMED BEARINGS THEY SHALL BE CUT OR MOVED FROM ANSUTLO EXISTING ROADWAY 3, 4, OR 5 AS DESCRIBED IN TABLES 705-H AND 705-2 WITH A DIRMETER (SHORE) W/0 HARDNESS OF 60.</p> <p>GRADE 60 REINFORCING STEEL IS REQUIRED.</p> <p>ALL REINFORCING STEEL SHALL BE EPOXY COATED UNLESS OTHERWISE NOTED.</p> <p>① DENOTES NON COATED REINFORCING STEEL.</p> <p>ALL THE PROVISIONS FOR BRIDGE DECK CONCRETE SHALL ALSO APPLY TO APPROACH SLAB CONCRETE.</p> <p>THE FOLLOWING TABLE GIVES THE MINIMUM LAP SPlice LENGTH FOR EPOXY COATED REINFORCING BARS PLACED IN ACCORDANCE WITH SUBSECTION 902.06. THESE SPlice LENGTHS SHALL BE INCREASED BY 25% FOR BARS SPACED AT LESS THAN 8" ON CENTER.</p> <table border="1" style="width: 100%; border-collapse: collapse; text-align: center;"> <tr> <th>BAR SIZE</th> <th>4 #</th> <th>5 #</th> <th>6 #</th> <th>7 #</th> <th>8 #</th> <th>9 #</th> <th>10 #</th> <th>11 #</th> </tr> <tr> <td>SPlice LENGTH FOR CLASS C CONCRETE</td> <td>1'-3"</td> <td>1'-7"</td> <td>2'-0"</td> <td>3'-0"</td> <td>4'-0"</td> <td>5'-11"</td> <td>7'-3"</td> <td></td> </tr> </table> <p>WHEN THE CONTRACTOR ELECTS TO SUBSTITUTE EPOXY COATED REINFORCEMENT FOR BLACK REINFORCING BARS, THE MINIMUM LAP SPlice LENGTH SHALL BE AS DESCRIBED ABOVE.</p> <p>THE FOLLOWING TABLE GIVES THE MINIMUM LAP SPlice LENGTH FOR BLACK REINFORCING BARS PLACED IN ACCORDANCE WITH SUBSECTION 902.06. THESE SPlice LENGTHS SHALL BE INCREASED BY 25% FOR BARS SPACED AT LESS THAN 8" ON CENTER.</p> <table border="1" style="width: 100%; border-collapse: collapse; text-align: center;"> <tr> <th>BAR SIZE</th> <th>4 #</th> <th>5 #</th> <th>6 #</th> <th>7 #</th> <th>8 #</th> <th>9 #</th> <th>10 #</th> <th>11 #</th> </tr> <tr> <td>SPlice LENGTH FOR CLASS D CONCRETE</td> <td>1'-4"</td> <td>1'-7"</td> <td>1'-10"</td> <td>2'-5"</td> <td>3'-4"</td> <td>3'-11"</td> <td>4'-10"</td> <td></td> </tr> </table> <p>THE ABOVE SPlice LENGTHS MAY BE REDUCED BY 20% WHEN 3" OF CLEAR COVER EXISTS AND BAR SPACING IS 8" OR GREATER ON CENTER.</p> <p>WHERE THE LAP LENGTH LISTED CANNOT BE ATTAINED ON AS NOTED ON THE PLANS, A DEVELOPED LAP LENGTH SHALL BE USED. THE DEVELOPED LAP LENGTH SHALL BE 125% OF THE YIELD STRENGTH OF THE REINFORCING BARS TO WHICH THEY ARE ATTACHED IN BOTH TENSION AND COMPRESSION. EPOXY COATING SHALL BE REMOVED PRIOR TO THE ATTACHMENT OF THE MECHANICAL COUPLER (SPliced) AS REQUESTED BY THE CONTRACTOR. THE CONTRACTOR SHALL BE RESPONSIBLE FOR THE COST OF THE WORK.</p> <p>THE CONTRACTOR SHALL BE RESPONSIBLE FOR THE STABILITY OF THE STRUCTURE DURING CONSTRUCTION.</p> <p>EQ. = EQUALITY F.F. = FAR FACE N.F. = NEAR FACE B.K. = BACK B.R. = BEARING C.R. = CLEAR C.N. = CONSTRUCTION C.S. = CONCRETE D.W. = DRAWING E.F. = EACH FACE E.V. = ELEVATION</p>	BAR SIZE	4 #	5 #	6 #	7 #	8 #	9 #	10 #	11 #	SPlice LENGTH FOR CLASS C CONCRETE	1'-3"	1'-7"	2'-0"	3'-0"	4'-0"	5'-11"	7'-3"		BAR SIZE	4 #	5 #	6 #	7 #	8 #	9 #	10 #	11 #	SPlice LENGTH FOR CLASS D CONCRETE	1'-4"	1'-7"	1'-10"	2'-5"	3'-4"	3'-11"	4'-10"		<p>ALL CONCRETE IN CONTACT WITH SOIL SHALL MEET CLASS C SULFATE EXPOSURE.</p> <p>STATIONS, ELEVATIONS, AND DIMENSIONS CONTAINED IN THESE PLANS ARE CALCULATED FROM A RECENT FIELD SURVEY. THE CONTRACTOR SHALL VERIFY ALL DIMENSIONED DIMENSIONS IN THE FIELD BEFORE ORDERING OR FABRICATING ANY MATERIAL.</p> <p>THE LOCATION OF THE FOUNDATIONS FOR THE EXISTING BRIDGE AS SHOWN IN THE PLANS WERE TAKEN FROM THE AS BUILT PLANS AND ARE APPROXIMATE.</p> <p>THE INFORMATION SHOWN ON THESE PLANS CONCERNING THE TYPE AND LOCATION OF UNDERGROUND UTILITIES IS NOT GUARANTEED TO BE COMPLETE OR ACCURATE. THE CONTRACTOR IS RESPONSIBLE FOR MAKING HIS OWN DETERMINATION AS TO THE TYPE AND LOCATION OF UNDERGROUND UTILITIES AS MAY BE NECESSARY TO AVOID DAMAGE THERETO. THE CONTRACTOR SHALL CONTACT THE UTILITY NOTIFICATION CENTER OF COLORADO AT (303) 733-7273 PRIOR TO ANY EXCAVATION OR OTHER EARTHWORK.</p> <p>CONSTRUCTION OPTION NOTES</p> <p>THE CONTRACTOR HAS THE OPTION TO CONSTRUCT THE BRIDGE BY EITHER ALTERNATE 1 OR ALTERNATE 2 AS SHOWN IN THE PLANS.</p> <p>ALTERNATE 1 - BRIDGE IS TO BE REMOVED AND RECONSTRUCTED IN TWO PHASES WHILE MAINTAINING TRAFFIC AS SHOWN IN THE PLANS.</p> <p>ALTERNATE 2 - BRIDGE IS TO BE REPLACED IN A SINGLE PHASE WHILE MAINTAINING TRAFFIC AS SHOWN IN THE PLANS.</p> <p>IF ALTERNATE 2 IS SELECTED, THE CONSTRUCTION JOINTS FOR PHASED BRIDGE CONSTRUCTION SHALL BE LOCATED AT THE ENDS OF THE ABUTMENTS, PIERS AND DECK AND THEIR ASSOCIATED MECHANICAL COUPLERS MAY BE OMITTED.</p> <p><i>Contractor elected to make pier 1 + pier 2 and sleeper slabs coated epoxy rather than black bars.</i></p>	<p>B1 GENERAL INFORMATION</p> <p>B2 SUMMARY OF QUANTITIES</p> <p>B3 GENERAL LAYOUT</p> <p>B4 CONSTRUCTION PHASING ALTERNATE 1 - SECTIONS</p> <p>B5 CONSTRUCTION PHASING ALTERNATE 1 - PLAN</p> <p>B6 CONSTRUCTION PHASING ALTERNATE 2 - SECTIONS</p> <p>B7 CONSTRUCTION PHASING ALTERNATE 2 - PLAN</p> <p>B8 CONSTRUCTION PHASING ALTERNATE 2 - TEMP. BRIDGE DETAILS</p> <p>B9 ENGINEERING GEOLOGY</p> <p>B10 BRIDGE HYDRAULIC INFORMATION (1 OF 2)</p> <p>B11 BRIDGE HYDRAULIC INFORMATION (2 OF 2)</p> <p>B12 BRIDGE HYDRAULIC INFORMATION (3 OF 2)</p> <p>B13 CANNON LAUNCH AND DETAILS</p> <p>B14 CANNON LAUNCH AND DETAILS</p> <p>B15 ABUTMENT 1 DETAILS</p> <p>B16 ABUTMENT 2 DETAILS</p> <p>B17 ABUTMENT 3 DETAILS</p> <p>B18 WHEEL DETAILS (1 OF 2)</p> <p>B19 PIER DETAILS (1 OF 2)</p> <p>B20 PIER DETAILS (2 OF 2)</p> <p>B21 BEARING DETAILS</p> <p>B22 CONCRETE BOX GIRDER</p> <p>B23 SUPERSTRUCTURE DETAILS</p> <p>B24 DECK REINFORCING PLAN</p> <p>B25 BRIDGE RAIL TYPE IOW</p> <p>B26 BRIDGE EXPANSION DETAILS (0-2 INCH)</p> <p>B27 APPROACH SLAB DETAILS</p> <p>B28 BRIDGE DRAINAGE PLAN (1 OF 2)</p> <p>B29 BRIDGE DRAIN DETAILS (2 OF 2)</p> <p>B30 BRIDGE DRAIN DETAILS (3 OF 2)</p> <p>B31 MECHANICALLY STABILIZED BACKFILL</p> <p>B32 BRIDGE DECK ELEVATIONS (1 OF 5)</p> <p>B33 BRIDGE DECK ELEVATIONS (2 OF 5)</p> <p>B34 BRIDGE DECK ELEVATIONS (3 OF 5)</p> <p>B35 BRIDGE DECK ELEVATIONS (4 OF 5)</p> <p>B36 BRIDGE DECK ELEVATIONS (5 OF 5)</p> <p>B37 BRIDGE DECK ELEVATIONS (6 OF 5)</p> <p>B38 BRIDGE DECK ELEVATIONS (7 OF 5)</p> <p>BRIDGE DESCRIPTION</p> <p>3-SPAN (54'-0", 63'-0", 54'-0") BRIDGE</p> <p>CONCRETE BOX GIRDER CONTINUOUS PRESTRESSED OVER BIG THOMPSON RIVER</p> <p>47'-0" ROADWAY OVERALL WIDTH 60'-0" SKEW, 1-0" TYPE IOW BRIDGE RAIL</p> <p>DESIGN DATA</p> <p>ASHTO, FOURTH EDITION LRFD.</p> <p>DESIGN METHOD: LRFD AND RESISTANCE FACTOR DESIGN</p> <p>LRFD LOADS: HL-93 (DESIGN TRUCK OR TANKER) AND DESIGN LANE LOAD</p> <p>BEAD LOADS: ASSUMES 36 LBS PER SQ. FT. FOR BRIDGE DECK OVERLAY</p> <p>REINFORCED CONCRETE:</p> <p>CONCRETE STRENGTH: $f_c = 4,500$ psi</p> <p>REINFORCING STEEL: $f_y = 60,000$ psi</p> <p>CANNON CONCRETE:</p> <p>MINIMUM CONCRETE STRENGTH: $f_c = 4,000$ psi</p> <p>REINFORCING STEEL: $f_y = 60,000$ psi</p> <p>PRECAST PRESTRESSED CONCRETE:</p> <p>MINIMUM CONCRETE STRENGTH: $f_c = 4,000$ psi</p> <p>REINFORCING STEEL: $f_y = 60,000$ psi</p> <p>CROSS REFERENCE DRAWING NUMBER</p> <p>(IF BLANK, REFERENCE IS TO SAME SHEET)</p> <p>SECTION OR DETAIL IDENTIFICATION</p> <p>SECTION OR DETAIL IDENTIFICATION</p>
BAR SIZE	4 #	5 #	6 #	7 #	8 #	9 #	10 #	11 #																														
SPlice LENGTH FOR CLASS C CONCRETE	1'-3"	1'-7"	2'-0"	3'-0"	4'-0"	5'-11"	7'-3"																															
BAR SIZE	4 #	5 #	6 #	7 #	8 #	9 #	10 #	11 #																														
SPlice LENGTH FOR CLASS D CONCRETE	1'-4"	1'-7"	1'-10"	2'-5"	3'-4"	3'-11"	4'-10"																															

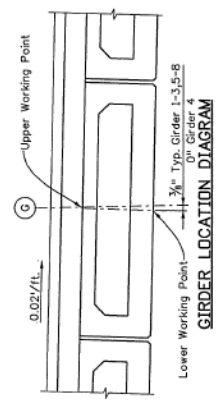


Extend conduits 25' from end of approach slab and place in pulbox. Location as approved by the engineer (typ)


NOTES

1. G Girder is at the top of girder.
2. Cost of pulboxes to be included in item 615 electrical conduit.

CONSTRUCTION LAYOUT



Print Date: 10/30/2007		Project No./Code	
File Name: 15549-B13-Const'd Layout.dgn		BR 0341-089	
North: Scale: As Noted		Structure: C-15-AN	
Unit Information		Detailer: S. Florian	
Unit Leader Initials		Sheet Submitt: BRIDGE	
SOURCING HOLDINESS		Subst Sheets: B13 of 36	
Sheet Revisions		As Constructed	
Date:	Comments:	No Revisions: 11/3/07	CONSTRUCTION LAYOUT
		Revised:	
		Void:	
Colorado Department of Transportation		Region 4	
2207 East Highway 402 Loveland, CO 80537 Phone: 970-602-1266 FAX: 970-669-0289		DMM/MLR	
Region 4		Sheet Number	
		47	

Print Date: 10/30/2007		Sheet Revisions		Colorado Department of Transportation		As Constructed		Project No./Code	
File Name: 15549-BI23-SuperDetails.dgn		Date:		Init.		No Revisions: 11-3-08		BR 0341-059	
Vert. Scale: As Noted		Comments		2207 East Highway 402 Loveland, CO 80537 Phone: 970-662-1266 FAX: 970-669-0289		Revised:		C-15-AN	
Unit Information						Designer:		Structure	
				Region 4		Detailer: P. Hernandez		Numbers	
						Void:			
								Sheet Number 57	

GENERAL NOTES

ALL WORK SHALL BE DONE ACCORDING TO THE LATEST SPECIFICATIONS OF THE DIVISION OF HIGHWAYS, STATE OF CALIFORNIA, APPLICABLE TO THE PROJECT.

THE CONTRACTOR SHALL BE RESPONSIBLE FOR OBTAINING ALL NECESSARY PERMITS AND APPROVALS FROM THE DIVISION OF HIGHWAYS, STATE OF CALIFORNIA, AND ALL OTHER AGENCIES CONCERNED.

THE CONTRACTOR SHALL BE RESPONSIBLE FOR OBTAINING ALL NECESSARY PERMITS AND APPROVALS FROM THE DIVISION OF HIGHWAYS, STATE OF CALIFORNIA, AND ALL OTHER AGENCIES CONCERNED.

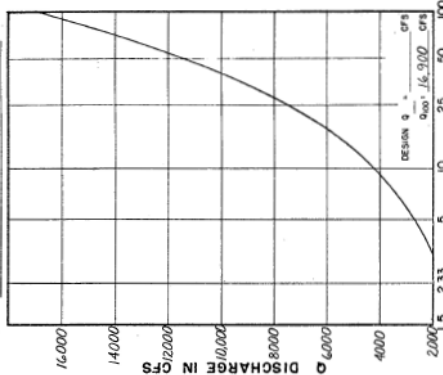
THE CONTRACTOR SHALL BE RESPONSIBLE FOR OBTAINING ALL NECESSARY PERMITS AND APPROVALS FROM THE DIVISION OF HIGHWAYS, STATE OF CALIFORNIA, AND ALL OTHER AGENCIES CONCERNED.

INDEX OF DRAWINGS

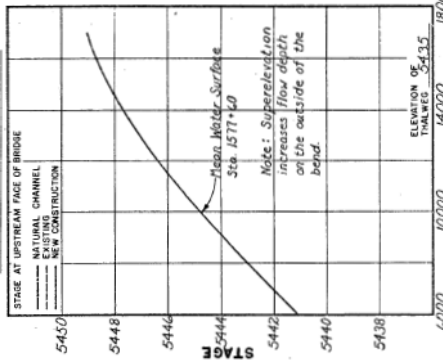
NO.	DESCRIPTION	DATE	BY	CHKD.	APP'D.
1	GENERAL INFORMATION - SUMMARY OF QUANTITIES				
2	GENERAL LAYOUT				
3	MAJOR MATERIAL INFORMATION				
4	STRUCTURAL SECTION				
5	MAJOR SECTION ELEVATIONS				
6	MAJOR SECTION ELEVATIONS				
7	MAJOR SECTION ELEVATIONS				
8	MAJOR SECTION ELEVATIONS				
9	MAJOR SECTION ELEVATIONS				
10	MAJOR SECTION ELEVATIONS				
11	MAJOR SECTION ELEVATIONS				
12	MAJOR SECTION ELEVATIONS				
13	MAJOR SECTION ELEVATIONS				
14	MAJOR SECTION ELEVATIONS				
15	MAJOR SECTION ELEVATIONS				
16	MAJOR SECTION ELEVATIONS				
17	MAJOR SECTION ELEVATIONS				
18	MAJOR SECTION ELEVATIONS				
19	MAJOR SECTION ELEVATIONS				
20	MAJOR SECTION ELEVATIONS				
21	MAJOR SECTION ELEVATIONS				
22	MAJOR SECTION ELEVATIONS				
23	MAJOR SECTION ELEVATIONS				
24	MAJOR SECTION ELEVATIONS				
25	MAJOR SECTION ELEVATIONS				
26	MAJOR SECTION ELEVATIONS				
27	MAJOR SECTION ELEVATIONS				
28	MAJOR SECTION ELEVATIONS				
29	MAJOR SECTION ELEVATIONS				
30	MAJOR SECTION ELEVATIONS				
31	MAJOR SECTION ELEVATIONS				
32	MAJOR SECTION ELEVATIONS				
33	MAJOR SECTION ELEVATIONS				
34	MAJOR SECTION ELEVATIONS				
35	MAJOR SECTION ELEVATIONS				
36	MAJOR SECTION ELEVATIONS				
37	MAJOR SECTION ELEVATIONS				
38	MAJOR SECTION ELEVATIONS				
39	MAJOR SECTION ELEVATIONS				
40	MAJOR SECTION ELEVATIONS				
41	MAJOR SECTION ELEVATIONS				
42	MAJOR SECTION ELEVATIONS				
43	MAJOR SECTION ELEVATIONS				
44	MAJOR SECTION ELEVATIONS				
45	MAJOR SECTION ELEVATIONS				
46	MAJOR SECTION ELEVATIONS				
47	MAJOR SECTION ELEVATIONS				
48	MAJOR SECTION ELEVATIONS				
49	MAJOR SECTION ELEVATIONS				
50	MAJOR SECTION ELEVATIONS				
51	MAJOR SECTION ELEVATIONS				
52	MAJOR SECTION ELEVATIONS				
53	MAJOR SECTION ELEVATIONS				
54	MAJOR SECTION ELEVATIONS				
55	MAJOR SECTION ELEVATIONS				
56	MAJOR SECTION ELEVATIONS				
57	MAJOR SECTION ELEVATIONS				
58	MAJOR SECTION ELEVATIONS				
59	MAJOR SECTION ELEVATIONS				
60	MAJOR SECTION ELEVATIONS				
61	MAJOR SECTION ELEVATIONS				
62	MAJOR SECTION ELEVATIONS				
63	MAJOR SECTION ELEVATIONS				
64	MAJOR SECTION ELEVATIONS				
65	MAJOR SECTION ELEVATIONS				
66	MAJOR SECTION ELEVATIONS				
67	MAJOR SECTION ELEVATIONS				
68	MAJOR SECTION ELEVATIONS				
69	MAJOR SECTION ELEVATIONS				
70	MAJOR SECTION ELEVATIONS				
71	MAJOR SECTION ELEVATIONS				
72	MAJOR SECTION ELEVATIONS				
73	MAJOR SECTION ELEVATIONS				
74	MAJOR SECTION ELEVATIONS				
75	MAJOR SECTION ELEVATIONS				
76	MAJOR SECTION ELEVATIONS				
77	MAJOR SECTION ELEVATIONS				
78	MAJOR SECTION ELEVATIONS				
79	MAJOR SECTION ELEVATIONS				
80	MAJOR SECTION E				

BRIDGE HYDRAULIC INFORMATION

DISCHARGE - FREQUENCY



STAGE - DISCHARGE



RECURRENT INTERVAL IN YEARS

Drainage Area 30.3 Sq. Mi.

CHANNEL DESCRIPTION
 Bottom Material — Cohesive ☐ Non Cohesive ☒
 Bottom Material Size — Clay ☐ Silt ☐ Sand ☐ Gravel ☒
 Cobbles ☒ Other — Boulderz
 Stream Form — Straight ☒ Meandering ☐ Braided ☐
 Mannings "n" for Design — Channel — .033 Overbank —
 Debris — Brush ☒ Trees/Logs ☐ Ice ☐ Other —

COMPARISON OF HYDRAULICS

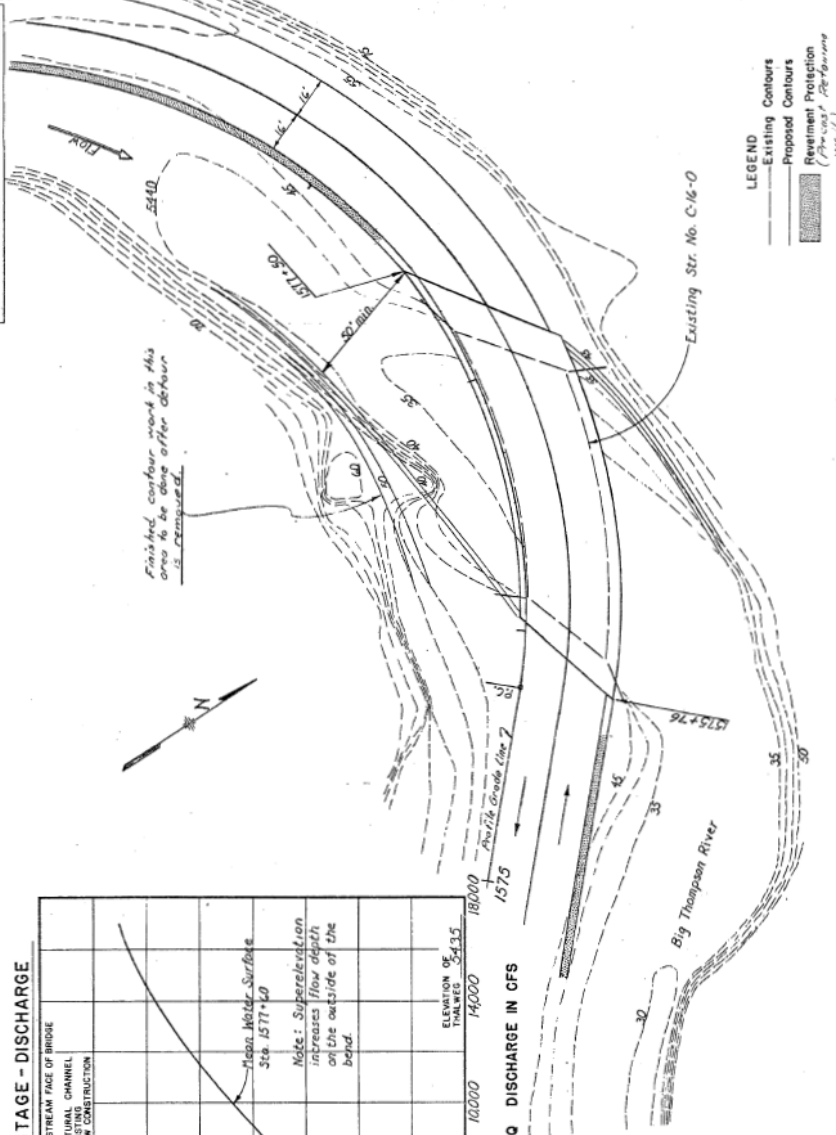
	Velocity - f/s	Froude No.	Max. Backwater
Natural Channel			
Existing			
Proposed	2.5	1.2	0"

*AT PROPOSED BRIDGE LOCATION DURING DESIGN DISCHARGE

COMMENTS

Since a retaining wall is proposed along the shoulder, a comparison of natural and existing channel hydraulics is of no value. Flow is supercritical.

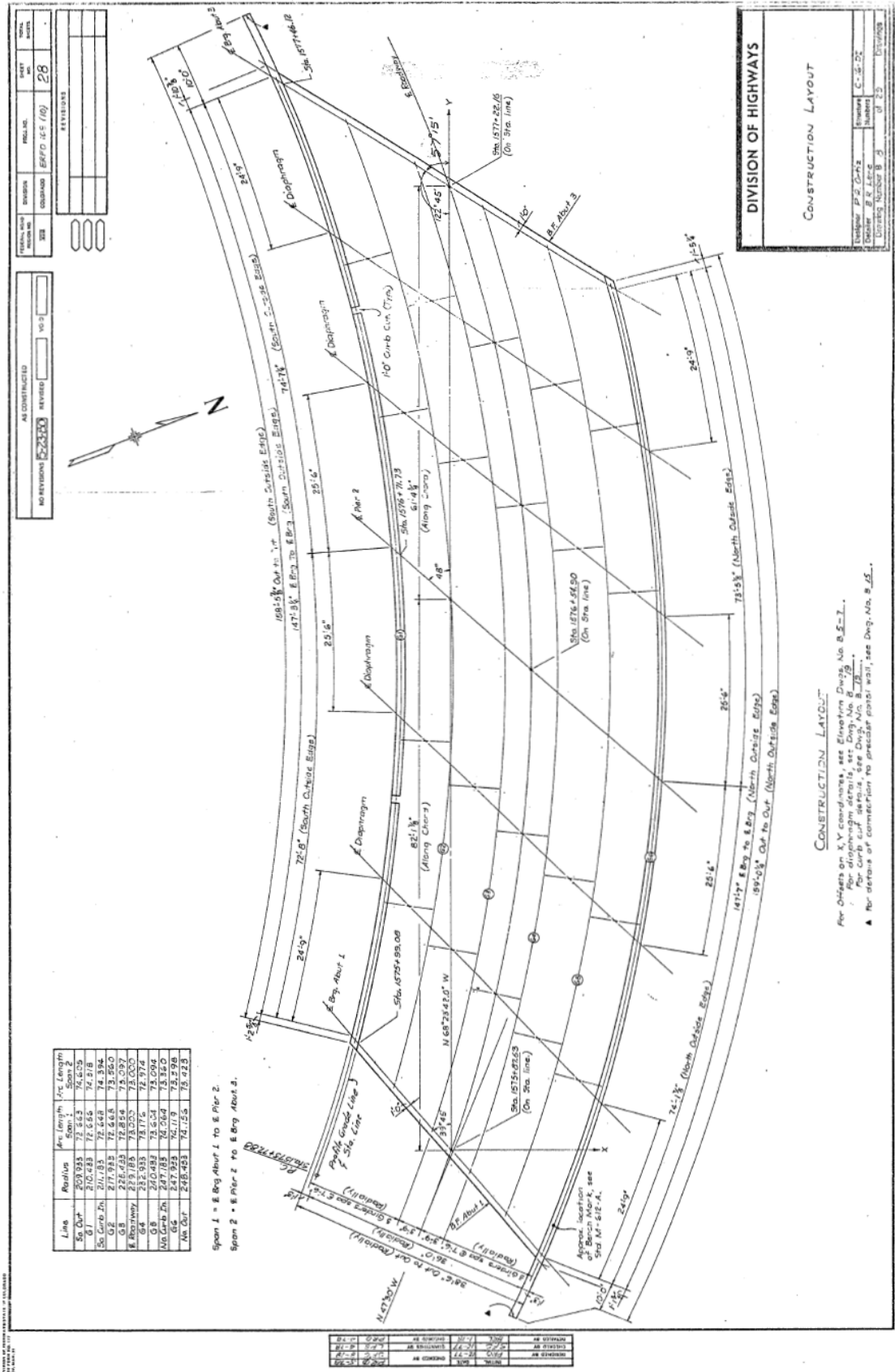
PROJECT NO.	1001	DATE	2.3
DESIGNER	COO	AS CONSTRUCTED	
NO. OF SHEETS	VII	NO. OF SHEETS	1001
NO REVISIONS TO BE MADE			



LEGEND
 Existing Contours
 Proposed Contours
 Retaining Protection
 (Previous Performance)

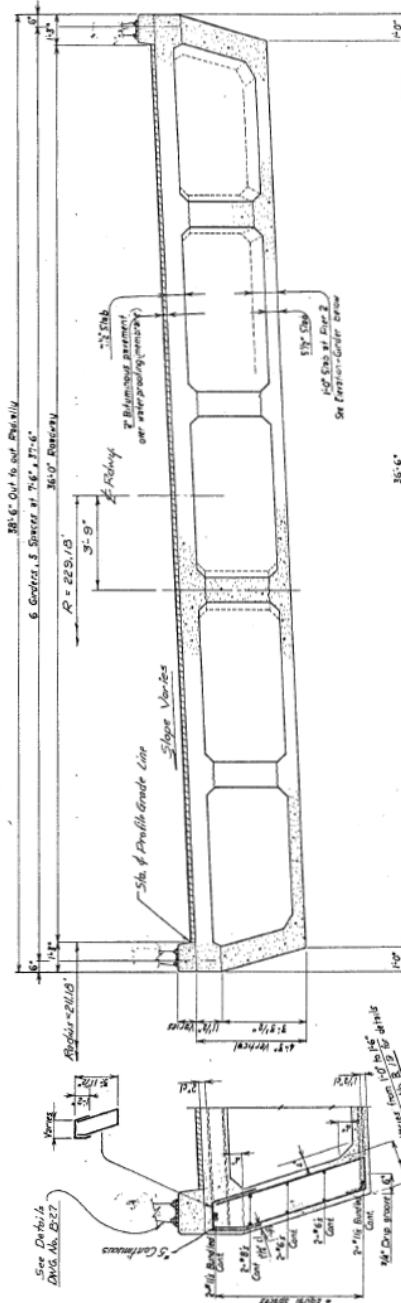
DEPARTMENT OF HIGHWAYS
STATE OF COLORADO
BRIDGE HYDRAULIC
INFORMATION
Big Thompson River
County Number 3 of 100
Drawn by [Signature]
Checked by [Signature]
Approved by [Signature]
Date, Sept. 2, 1971

STRUCTURE NO. C-16-02

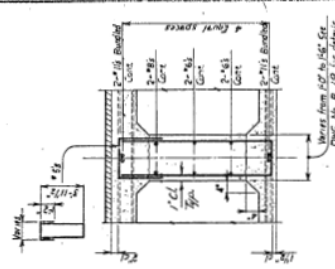


PERSONAL INFO	DIVISION	PICCOLA QD.	SHEET NO.	70-794 PAGE 8
<u>NAME</u>	<u>COLUMBO</u>	<u>FERO 106(13)</u>	<u>38</u>	
REVISIONS				

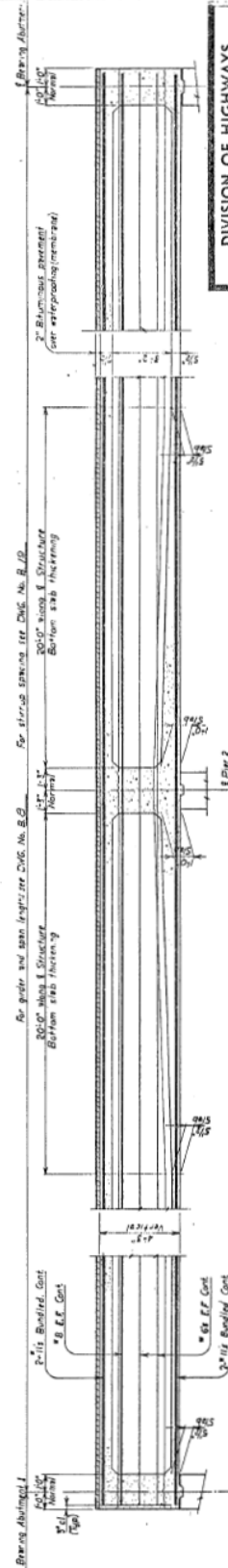
NO REVISIONS	5-23-80	REVISED		VOID	
AS CONSTRUCTED					



TYPICAL SECTION THRU EXTERIOR GIRDER
For Curb and Bridge Rail See DWG. No. B 27



TYPICAL SECTION THRU INTERIOR GIRDER



ELEVATION - GIBBS

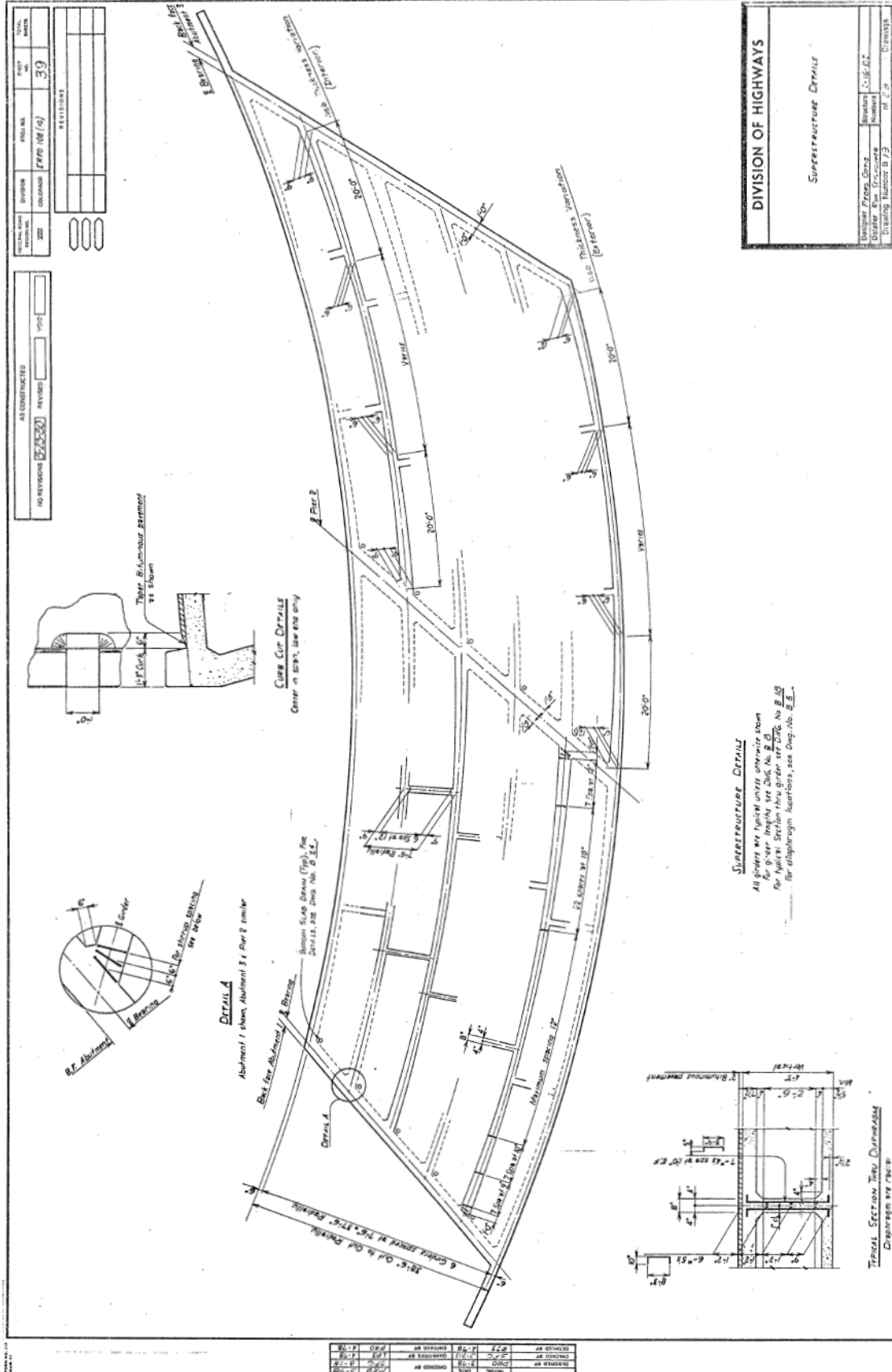
	1.0	1.1	1.2	1.3	1.4	1.5	1.6	1.7	1.8	1.9	2.0
$\frac{1}{100} \frac{d\sigma}{d\Omega} \frac{dN}{dE dA dt}$	0.00	0.012	0.018	0.024	0.030	0.044	0.061	0.070	0.08	0.098	0.10

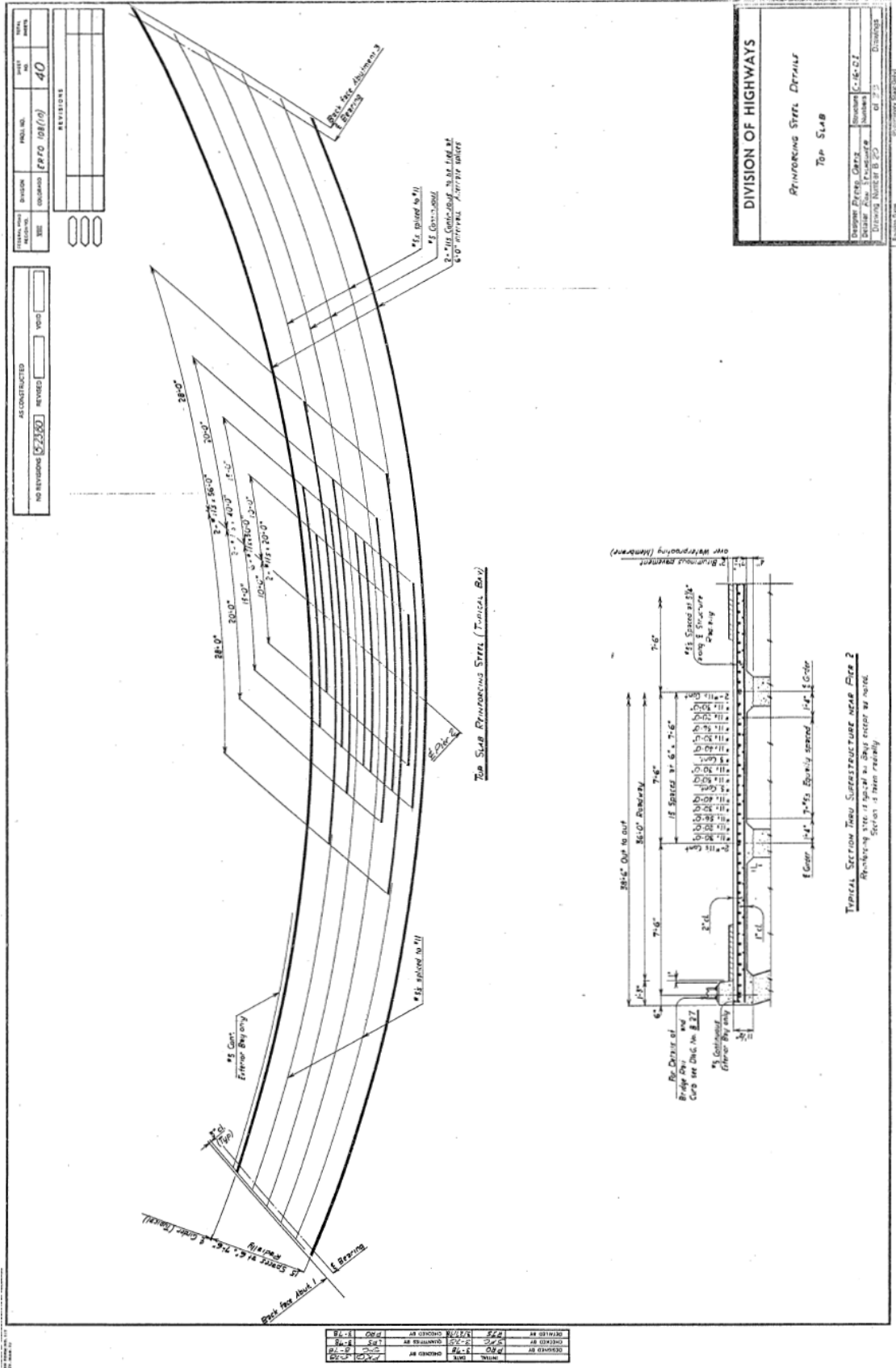
Symmetrical about Pier 2

DIVISION OF HIGHWAYS

SUBSTRUCTURE DETAILS

Disaster Prep. Cert. ☐ Structure Numbers ☐ C-10-D ☐ Drawings ☐





APPENDIX B. LOGNORMAL PARAMETERS FOR NEGATIVE MOMENT FRAGILITIES

Table 1. Lognormal parameters for negative moment fragilities

Bridge	Girder location	Parameters	
		λ	ξ
C-15-AM	Exterior	-1.029	0.794
	Interior	-0.903	0.781
C-15-AL	Exterior	-0.985	0.518
	Interior	-0.877	0.495
C-15-O	Exterior	-2.812	1.254
	Interior	-2.785	1.252
C-15-U	Exterior	4.765	2.586
	Interior	6.509	2.655
C-15-Y	Exterior	-1.393	0.427
	Interior	-1.365	0.415
C-15-C	Exterior	-3.016	2.068
	Interior	-3.003	2.083
C-15-AN	Exterior	-3.905	5.273
	Interior	-4.401	5.871
C-16-DI	Exterior	-6.141	3.161
	Interior	-5.967	3.148